Understanding modern and past sedimentary processes in selected lakes from the High Arctic and the Mediterranean realm

Inaugural-Dissertation

zur

Erlangung des Doktorgrades
der Mathematisch-Naturwissenschaftlichen Fakultät
der Universität zu Köln

vorgelegt von
Dipl. Geol. Alexander Francke
aus Duisburg

Berichterstatter	PD Dr. B. Wagner (Universität zu Köln)
(Gutachter)	Prof. Dr. Martin Melles (Unversität zu Köln)
	Dr. Laura Sadori (Università di Roma "La Sapienza")

Tag der mündlichen Prüfung: 14.04.2014

Abstract

Lacustrine sediment sequences can provide valuable archives of past environmental and climatological variability in terrestrial realms. In order to unravel the history of a lake and of a lake's catchment, a profound understanding of the sedimentary processes is required. This encompasses the supply of allochthonous organic matter, nutrients and clastic material to the lake, the subsequent redistribution within the lake as well as autochthonous organic matter and mineral deposition. These lake internal and external processes are closely linked to the environmental and climatological settings in the specific area and can be reconstructed by using geophysical and sedimentary data. Within the scope of this thesis, modern and past sedimentary processes of selected lakes from the High Artic (Lake El'gygytgyn, NE Siberia) and the Mediterranean Realm (lakes Dojran and Ohrid, Balkan Peninsula) were analyzed by using various datasets and analytical methods. The obtained information about variations in the lakes' internal and external processes were subsequently used for paleoenvironmental and -climatological reconstructions in the respective area.

At Lake El'gygytgyn, modern sedimentary processes were investigated by using geochemical, grain-size and mineralogical data from source rocks, inlet streams and surface sediments. The obtained information about modern sedimentary processes improved the understanding of hydro-acoustic and downhole logging data, as well as of variations in the granumoleric, geochemical and physical properties of core 5011-1 which covers the entire lacustrine succession of the 3.58 Ma year old Lake El'gygytgyn. Surface samples and downcore data were analyzed by using statistic methods such as Principal Component Analysis (PCA), Redundancy Analysis (RDA), Time Series Analysis and Cluster Analysis. At Lake Dojran, hydro-acoustic data and sediment properties (water content, OM, calcite ($CaCO_3$) content, sulfur content, grain-size, XRF scanning, $\delta^{18}O_{carb}$, $\delta^{13}C_{carb}$, $\delta^{13}C_{org}$) of a 7 m long sequence were used to untangle past sedimentary processes and environmental variations during the Late Glacial and Holocene period. Sediment (lithostratigraphic description, XRF scanning, water content, OM content, calcite content) and hydro-acoustic data were also used to characterize a 2 m thick Mass Wasting Deposit (MWD) in Lake Ohrid.

As various analytical and statistical methods were used to investigate modern and past sedimentary processes in the selected lakes, an evaluation of these methods is conducted within the scope of this thesis. It could be shown that information about modern sedimentary processes derived from lacustrine surface samples and from catchment samples can help to better understand past sedimentary processes as it provides insights into spatial variations in the deposition processes. Spatial variations of past sedimentary processes and the overall sediment architecture of lacustrine deposits can be analyzed using hydro-acoustic data. However, the vertical resolution of hydro-acoustic data is limited and the data commonly lacks a robust chronology. Chronostratigraphic well constrained and high resoluted information about past sedimentary processes can be derived from sedimentary properties of a sediment core. These properties include lithologic information such as sediment structure, grain-size, and inorganic and organic geochemistry. These proxy data can be obtained by visual core descriptions and laboratory analyses. However, certain proxies can commonly only be used to reconstruct a specific part of sedi-

mentary processes, for example grain-size data yields information about the transport energy during the deposition. Thus, a combination of multiple proxies is required to reconstruct the overall picture of sedimentary processes. If huge data sets are used for the reconstruction, statistic methods such as PCA, RDA, Time Series Analyses, and Cluster Analyses can help to simplify the data. However, it could be shown that mathematic methods can provide results that might lead to misinterpretations in a geological context.

In order to interpret sediment sequences for paleoenvironmental and -climatological variations in a temporal context, an age model is commonly established by using for example radiocarbon ages and chronological tie points derived from tephrostratigraphic or paleomagnetic data. Cross correlation to well dated sediment sequences or wiggle matching to orbital parameters can improve a chronostratigraphic modell. However, this involves the danger of misinterpretations or loss of information about the timing of geologic or climatic events.

Zusammenfassung

Seesedimente können als wertvolles Archiv der Klima- und Umweltgeschichte in terrestrischen Gebieten dienen. Um die Entwicklung eines Sees und dessen Einzugsgebietes anhand von lakustrinen Ablagerungen zu rekonstruieren bedarf es allerdings eines profunden Verständnisses der vorherschenden Sedimentationsprozesse. Diese Prozesse umfassen nicht nur den allochthonen Eintrag von organischem und klastischem Material und Nährstoffen, sondern auch die autochthone Ablagerung von Organik und Mineralen aus der Wassersäule. Dabei stehen diese internen und externen Prozesse im engen Zusammenhang zu den Umwelt- und Klimabedingungen in der Region und können mit Hilfe von geophysikalischen und sedimentologischen Methoden rekonstruiert werden. Im Rahmen dieser Arbeit wurden die Sedimentationsprozesse in ausgewählten Seen aus der Arktis (El'gygytgynsee, NO Sibirien) und dem Mittelmeerraum (Dojran- und Ohridsee, Balkanhalbinsel) mit Hilfe von verschiedenen Datensätzen und Methoden analysiert. Die gewonnenen Daten über Veränderungen der externen und internen Prozesse wurden anschließend zur Umwelt- und Klimarekonstruktion genutzt.

Am El'gygytgynsee wurden zunächst die rezenten Sedimentationsprozesse anhand von geochemischen, mineralogischen und granumolerischen Daten von anstehendem Gestein im Einzugsgebiet, sowie von Sedimentproben aus Zuflüssen und Oberflächenproben der lakustrinen Ablagerungen analysiert. Die gewonnenen Daten konnten anschließend für ein besseres Verständnis von hydroakustischen und "downhole logging" Daten sowie von Veränderungen der geochemischen, physikalischen und granumolerischen Zusammensetzung des Sedimentkerns 5011-1 aus dem 3.58 Millionen Jahre alten El'gygytgynsee genutzt werden. Die Auswertung der Oberflächenproben und Sedimentkerndaten erfolgte dabei mit Hilfe der statistischen Methoden der Hauptkomponentenanalyse (HKA), Redundanzanalyse (RDA), Zeitreihenanalyse und Clusteranalyse. Am Dojransee konnte die spätglaziale und holozäne Klima- und Umweltgeschichte anhand hydroakustischer Daten und den Sedimenteigenschaften (Wasser-, Kalzit-, Schwefel- und Organikgehalt, Korngröße, XRF-Daten, $\delta^{18}O_{carb}$, $\delta^{13}C_{carb}$, $\delta^{13}C_{org}$) eines 7 m langen Kernes rekonstruiert werden. Ebenso wurde anhand von sedimentologischen (Lithostratigraphie, XRF- Daten, Wasser-, Kalzit- und Organikgehalt) und hydroakustischen Daten ein 2 m mächtiger Rutschungskörper im Ohridsee untersucht.

Im Rahmen der an den ausgewählten Seen durchgeführten Untersuchungen zur Rekonstruktion von rezenten und vergangenen Sedimentationsprozessen wurden verschiedene analytische und statistische Auswertmethoden angewandt, die im Anschluß evaluiert und bewertet wurden. Es konnte gezeigt werden, dass Untersuchungen über rezente Sedimentationsprozesse anhand von lakustrinen Oberflächenproben sowie von Gesteins- und Sedimentproben aus dem Einzugsgebiet wichtige Informationen über räumliche Unterschiede der Ablagerungsbedingungen liefern können, was zum besseren Verständnis bei der Rekonstruktion der Sedimentationsgeschichte beitragen kann. Informationen über räumliche Veränderungen bei den Sedimentationsprozessen in der Vergangenheit, sowie über Sedimentstrukturen in lakustrinen Becken können auch anhand von hydroakustischen Daten gewonnen werden. Allerdings ist die vertikale Auflösung von hydroakustischen Daten begrenzt und eine genaue chronologische Einordnung ist oftmals nicht möglich. Hochauflösende und chronostratigraphisch eingrenzbare In-

formationen über frühere Sedimentationsprozesse können daher besser von den sedimentologischen Eigenschaften eines Sedimentkerns abgeleitet werden. Diese so genannten Proxy Daten beinhalten lithologische Informationen über Sedimentstruktur, Korngröße oder inorganische und organische Geochemie und können anhand von visuellen Beschreibungen oder analytischen Methoden erhoben werden. Da allerdings anhand bestimmter Proxys wie zum Beispiel der Korngrößenverteilung in der Regel nur ein Teil der Sedimentationsprozesse rekonstruiert werden kann, in diesem Falle die Strömungsenergie während der Ablagerung, sollten zur Erstellung eines Gesamtbildes der vorherschenden Prozesse mehrere Datensätze kombiniert werden. Dabei kann, wenn der gewählte Datensatz sehr umfangreich wird, die Anwendung von statistischen Methoden wie zum Beispiel der HKA, RDA, Zeitreihenanalyse oder auch der Clusteranalyse, hilfreich sein. Allerdings konnte im Rahmen dieser Arbeit gezeigt werden, dass die Ergebnisse solcher statistischer Methoden im geologischen Kontext schnell falsch interpretiert werden können.

Zur Umwelt- und Klimarekonstruktion anhand von Sedimentabfolgen im zeitlichen Kontext ist es nötig ein Altersmodell zu erstellen. Solche Altersmodelle werden in der Regel anhand von Radiokarbondatierungen sowie von chronostratigraphischen Informationen aus der Tephrostratigraphie und Paläomagnetik erstellt. So genanntes "wiggle matching" zu Erdbahnparametern oder auch "cross correlation" zu anderen, gut datierten Sedimentabfolgen kann die Qualität von Altersmodellen verbessern, birgt aber auch die Gefahr von Fehlinterpretationen sowie dem Verlust von Informationen über das genaue Timing von geologischen oder klimatischen Ereignissen.

Acknowledgment

First of all, I would like to give many thanks to my supervisor PD Dr. Bernd Wagner for giving me the opportunity to work on my Ph.D. thesis within the scope of the SCOPSCO project at the University of Cologne. He always supported me during my studies with fruitful discussions and gave me great motivation and guidance as well as the opportunity to participate on several field campaigns.

Many thanks also go to Prof. Dr. Martin Melles for giving me the opportunity to complete my studies with sample material from the "Lake El'gygytgyn Drilling Project" and for being my second referee.

For financial support of my thesis, of several field campaigns, and of a 3-week stay at the British Geological Survey (BGS) I would like to thank the German Research Foundation (DfG, grant no. WA 2109/11 and ME 1169/21), the German Federal Ministry of Education and Research (BMBF, grant no. 03G0642A), the International Continental Drilling Project (ICDP), and the Collaborative Research Centre (CRC) 806 "Our way to Europe".

Many thanks also go to Dr. Laura Sadori for being my third referee and to Prof. Dr. Frank Schäbitz for taking the chair of my examination committee.

In particular Dr. Volker Wennrich is acknowledged for the great support not only during the work for the "Lake El'gygytgyn Drilling Project", but also for many fruitful discussions and for acting as the assessor for my defenses.

Prof. Dr. Melanie Leng (University of Leicester, BGS, Nottingham) is acknowledged for giving me the opportunity to conduct my work on stable isotopes at the British Geological Survey in Nottingham and for the support with the scientific interpretation of the data.

Furthermore, I want to express my gratitude to my various co-authors, i.e. Dr. Catalina Gebhardt, Dr. habil. Norbert Nowaczyk, Prof. Dr. Janet Rethemeyer, and Prof. Dr. Julie Brigham-Grette.

I would like to thank my colleagues / ex- colleagues Dr. Daniela Sprenk, Dr. Anne Böhm, Dipl.-Geogr. Nicole Mantke, Dr. Sonja Berg, Dr. Janna Just, Dr. Finn Viehberg, Dr. Hendrik Vogel, and Dipl. Geol. Daniel Treu for their support.

I warmly thank Peter Schweinhage for editing the English of this manuscript as well as Darja Friesen and Andrea Lauss for the great support with Latex typsetting. Many thanks also go to Nadja Memmer, Raphael Gromig, and Niklas Leicher for final proof-reading.

Additionally, I would like to thank all colleagues from the Institute for Geology for a great time and experiences on both professional and personal level. In particular I would like to acknowledge Ascelina Hasberg, Daniela Sprenk, Linda Prinz, Sarah Esteban-Lopez, Marina Kemperle, Julia Diederich, Niklas Leicher, Benedikt Ritter, Raphael Gromig, Florian Boxberg, and Dominik Hofer.

Finally, I would like to thank my family and in particular my parents Irene and Jochen for the support and encouragement they gave me in the past! A special thank goes to Kristiana Balzer for wonderful help, support, and encouragement during my studies.

Contents

1 Introduction

1.1 Lake sediments as paleoenvironmental archive

The composition of lacustrine deposits is influenced by a variety of external and internal environmental factors. External influences, such as climate conditions, bedrock composition, vegetation cover, hydrogeologic conditions, and tectonic and volcanic activity predominantly affect the allochthonous sediment supply to a lake (Cohen, 2003). These external influences are highly interactive with lake internal factors such as aquatic biota, productivity, lake-internal current systems and bathymetry, all of those influencing the allochthonous and the autochthonous sedimentation (cf. Cohen, 2003). The dependency of the sediment compositions to these internal and external influences is the basis of the paleoenvironmental and paleoclimatological reconstruction using sedimentary, biogeochemical, geochemical and biological proxy data from lake sediments. Thereby, the interpretation of the lacustrine sediment archives requires a profound understanding of the sedimentary processes in the investigated lake system. Sedimentary processes can modify the recorded paleoenvironmental or paleoclimatological signal (Cohen, 2003). For example, intensive bioturbation can filter a climatic signal in terms of temporal resolution, or strong lake-internal currents might influence the deposition of pollen, diatoms or other biologic indicators. Moreover, event deposits, such as MWDs (mass wasting deposits), are deposited in a very short time period. Their sedimentation can commonly not be explained by climatological variations. More likely, they might be related to seismic activity or slope instability (e.g. Lindhorst et al., 2012; Sauerbrey et al., 2013).

Basic sediment properties, such as sediment structure, texture, grain-size distribution, and the amount of clastic and organic matter (OM) can give crucial information about sedimentary processes and catchment dynamics. Moreover, basic sediment properties can also directly be used for paleoenvironmental and paleoclimatological interpretations. For example, the grain-size distribution is linked to transport energy which can be interpreted in terms of lake level fluctuations, wave activity or contourite drift variations (e.g. Magny et al., 2007; Vogel et al., 2010a; Aufgebauer et al., 2012; Wagner et al., 2012). The amount of clastic material in the sediment could be explained by dilution with OM or variations of erosional processes in the catchment area. However, geological or geophysical data sets such as surface sediment samples, catchment samples, hydro-acoustic data, and sediment cores as well as analytical and statistical methods have their own potential and limits to unravel past sedimentary processes. Thus, a crictical evaulation of widly used methods, such as conducted within the scope of this thesis, can help to improve the use of sedimentary proxy data for paleoenvironmental and -climatological reconstruction. If sedimentary processes in a lake are well understood, lacustrine sediments can provide long lasting, high resoluted and continuous archives of paleoenvironmental and -climatological variability in terrestrial realms. Naturally, the temporal resolution depends on the sedimentation rate in the lake, and a continuous sediment sequence can be retrieved from lakes that did not experienced any extreme low stands of lake levels or desiccation events.

Together with ice cores from Greenland or Antarctica, loess sequences and speleothem records, lake sediments are the only terrestrial earth history records that provide such a combination of duration and resolution (cf. Cohen, 2003). A distinct benefit of lacustrine deposits is that lakes are widely distributed over terrestrial realms, which enables the selection of lakes in climatic sensitive areas. In the scope of this thesis, three lakes from the High Artic (Lake El'gygytgyn) and Mediterranean Realm (Lake Dojran and Lake Ohrid) have been investigated, as both regions are known to play an important role in the global climate system. The High Arctic region balances the surplus of solar energy of the tropics (Brigham-Grette et al., 2007), and global warming is predicted to be most pronounced in high latitude areas (ACIA, 2004; Serreze and Francis, 2006). The Mediterranean Region is located at the boundary of the atmospheric Hadley and Ferrel cells and is highly sensitive to variations in the mid-latitude and tropical climate systems (Giorgi and Lionello, 2008).

1.2 Studied lakes

The following sections provide a first overview about the studied lakes as well as about previous studies and available sediment cores at the respective sites. As this thesis is based on 6 individual publications, the reader is also referred to the according chapters for more detailed information about the lakes and projects. As only a brief overview about Lake Ohrid is presented in the publication of chapter 7, comprehensive information about Lake Ohrid are presented in chapter 1.2.3.

1.2.1 Lake El'gygytgyn

Lake El'gygytgyn is located in the central part of the Chukchi Peninsula in the Far East Russian Arctic, (67°30' N, 172°05' E, 492 m a.s.l. (above sea level), Fig. 1.1A). It has been formed within a meteorite impact crater (Fig. 1.1B, e.g. Dietz and McHone, 1977; Gurov et al., 1979), which was dated to about 3.58 Ma (Layer, 2000). The crater was filled with water a few thousand years after the impact (Brigham-Grette et al., 2013), and a continuous lacustrine sediment succession has been deposited until today (Melles et al., 2012; Brigham-Grette et al., 2013).

Lake El'gygytgyn is up to 175 m deep and it has a nearly circular shape with a diameter of about 12 km (Nolan and Brigham-Grette, 2007). Today, the water column is fully mixed with almost complete oxygen saturation during summer, but a thermal stratification occurs during winter (Cremer and Wagner, 2003). The lake is oligotrophic to ultra-oligotrophic as demonstrated by a low bioproductivity (Cremer and Wagner, 2003; Nolan and Brigham-Grette, 2007). Approximately 50 ephemeral inlet streams feed Lake El'gygytgyn, (see also Fig. 1.1, Nolan and Brigham-Grette, 2007), and deliver sediment in the order of about ca. 350 t/yr to the lake (Fedorov et al., 2013). The Envynman River drains the lake in southeastern direction.

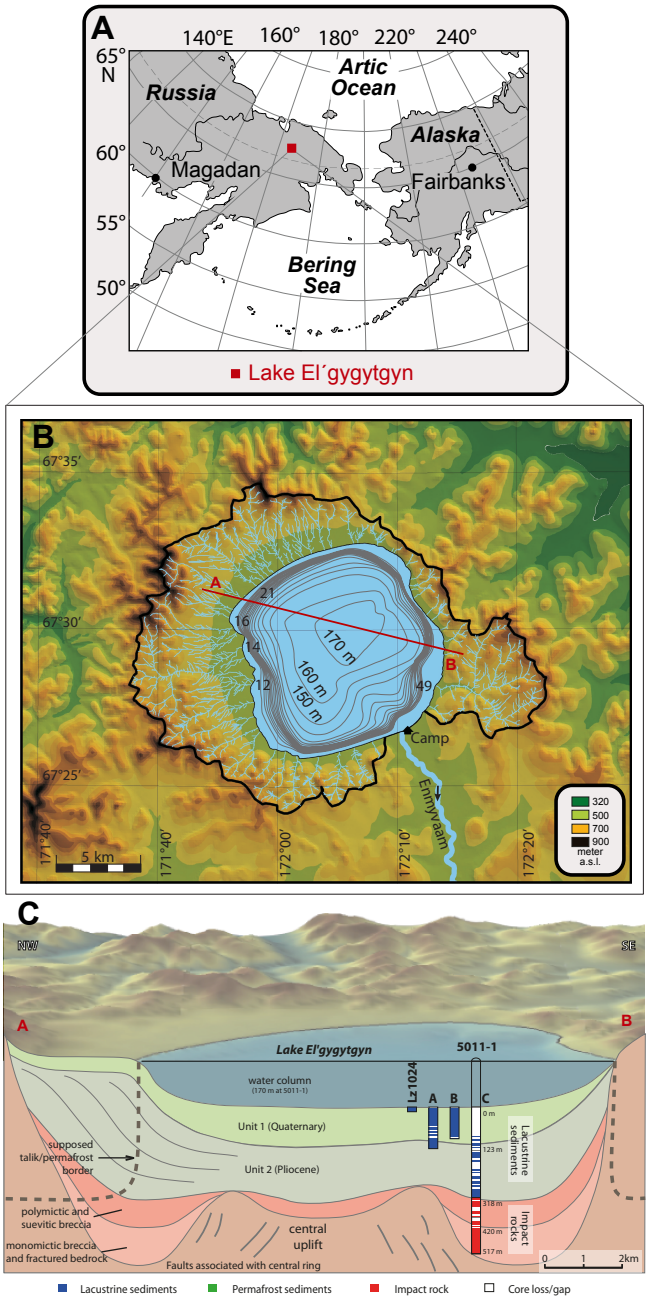

Figure 1.1: A: Location of Lake El'gygytgyn in the Far East Russian Artic, **B**: Bathymetric map of the lake and topographic map of the catchment area, including the approximately 50 inlet streams and the Enmyvaam River outlet. (Fedorov and Kupolov, 2005); red line: profile A to B. **C**: Schematic profile A to B with the locations of the pilot core Lz 1024 and the three holes (A, B and C) at ICDP site 5011-1 with the Pliocene/Pleistocene boundary penetrated at approximately 123 m, and the transition to the impact breccia at 318 m below lake floor (modified after Melles et al., 2011)

Lake El'gygytgyn is surrounded by continuous permafrost whose onset can presumably be traced back to the Late Pliocene (Glushkova and Smirnov, 2007) and which is assumed to have a thickness of about 330-360 m with an unfrozen talik underneath the lake (Mottaghy et al., 2013). The geomorphologic shape of the catchment area, which is confined by the almost circular crater rim measuring about 18 km in diameter, is modified by permafrost processes such as solifluction and cryogenic weathering (Glushkova and Smirnov, 2007).

Modern climate conditions at Lake El'gygytgyn correspond to a High Arctic climate with a mean annual air temperature of -10.4 °C and an annual precipitation between 70 and 200 mm measured between 2002 and 2008 (Nolan et al., 2013). Strong (up to 21 m/s) and very persistent winds (mean of 5.6 m/s in 2002) of north-northwestern and south-southeastern directions are dominant (Nolan and Brigham-Grette, 2007).

The long sediment core 5011-1 retrieved from central parts of the lake within the scope of an ICDP (International Continental Drilling Project) deep drilling campaign in 2009 covers the entire lacustrine succession and the upper about 200 m of the impact related bedrock (Fig. 1.1C). The core is the first continuous Pliocene/Pleistocene sediment record in the terrestrial Artic (Melles et al., 2012). Previously, paleoenvironmental and paleoclimatic records from the High Arctic were only available from ice cores from Greenland (NGRIP-members, 2004) which are limited to the last Glacial/Interglacial cycle, or from often discontinuously or temporally restricted archives from the marine realm and Arctic borderland (Thiede et al., 1998; Backman et al., 2005; Moran et al., 2006; Axford et al., 2009; Pienitz et al., 2009; Zech et al., 2011). Within the scope of several pre-site surveys for the deep drilling campaign, hydro-acoustic surveys were conducted and a set of lacustrine surface sampes, catchment samples, and sediment cores were recovered between 1998 and 2003.

1.2.2 Lake Dojran

Lake Dojran is located at the border of the Former Yugoslav Republic of Macedonia (FYROM) and Greece (Fig. 1.2A, 41°12' N, 22°44' E). It is considered to be a relict of the Plio-Pleistocene Peonic Lake, which was formed by volcanic and tectonic activities (Cvijic, 1911; Stojanov and Micevski, 1989).

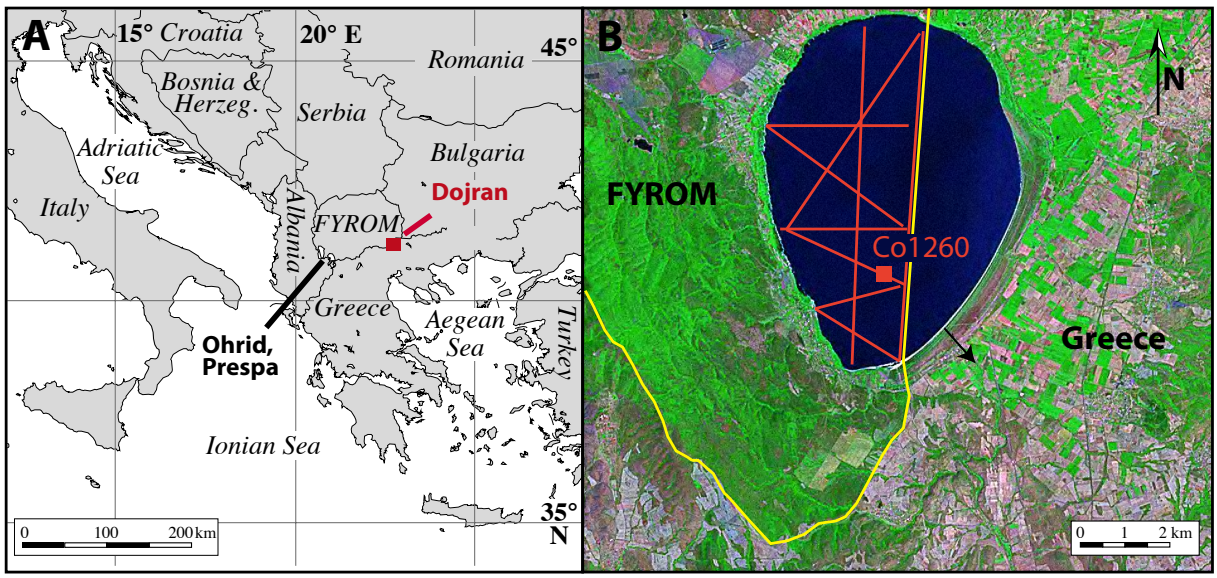

Figure 1.2: A: Location of Lake Dojran in the northeastern Mediterranean region at the border of the Former Yugoslav Republic of Macedonia (FYROM) and Greece. Marked are also lakes Ohrid and Prespa. **B**: Satellite image of Lake Dojran with the coring location Co1260 (red square) and the hydro-acoustic profiles. The black arrow indicates the position of the former outlet River Doiranitis, and the yellow line shows the border between FYROM and Greece.

Lake Dojran is located at 144 m a.s.l. in a carstic depression. Due to the carstic bedrock, the lake is bicarbonate- and chloride-rich, alkaline and productive (Stankovic, 1931; Griffiths et al., 2002). Thermal stratification of the water column occurs during the summer months (Zacharias et al., 2002), and it is presumed that lake water mixing occurs during winter, similar to Lake Prespa (Matzinger et al., 2006). Small rivers, creeks and probably an aquifer are feeding Lake Dojran in particular during winter and spring (Griffiths et al., 2002; Sotiria and Petkovski, 2004; Manley et al., 2008), and seasonal lake-level fluctuations resulted in floodings of littoral areas in the past (Manley et al., 2008). Today, the maximum lake level is controlled by the regulation of the channelized outlet River Doiranitis (Fig. 1.2B). Water supply to Lake Dojran also includes snowmelt from the Belisca Mountain range that is up to 1 870 m a.s.l. high. This high alpine terrain only covers about 18% of the catchment area (275 km^2) of Lake Dojran. Apart from that, the remaining catchment area does not exceed an elevation of 500 m a.s.l. (Sotiria and Petkovski, 2004).

The climate at Lake Dojran is influenced by typical Mediterranean conditions with monthly average summer and winter temperatures of +26.1 and +3.7 °C, respectively. The highest proportion of the annual precipitation (612 mm) falls during mild winters.

The sensitivity of sediments from Lake Dorjan to environmental variability was demonstrated by studies of surface sediments which recorded a lowering of the lake-level by about 6 m and an eutrophication in the past decades in chemical, biological and stable isotope data (Griffiths et al., 2002). Hence, Lake Dojran seems to provide a valuable record of environmental variability in the central eastern Mediterranean realm. Furthermore, Lake Dojran is relatively shallow (maximum water depth < 7 m) for a medium sized lake (Fig. 1.2B, surface area: 40 km^2). As shown by a comparison of records from lakes Prespa and Ohrid (location see Fig. 1.2), comparatively shallower lakes react often more sensitive to environmental change (Leng et al., 2010; Wagner et al., 2010). During a field campaign in 2011, a hydro-acoustic survey was conducted at the Macedonian part of the lake and a 7 m long sediment sequence (Co1260) was recovered from southern parts of the lake (Fig. 1.2).

1.2.3 Lake Ohrid

Lake Ohrid is located at the border of FYROM (Macedonia) and Albania (Fig. 1.2A, 40°70' N, 20°42' E) in a tectonic active, N-S trending graben. Chronostratigraphic interpretation of prominent cyclic patterns of hydro-acoustic data imply that the lake is about 2 Ma years old (Lindhorst et al., in press), which coincides with the minimum age derived from molecular clock analyses of DNA data from ancient lake species (summarized by Wagner and Wilke, 2011).

Lake Ohrid, comprising of about 358 km^2, is approximately 30 km long and 15 km wide (cf. Fig. 1.3). The lake is situated at 693 m a.s.l. and is surrounded by mountains up to 2 300 m a.s.l.. The maximum water depth is about 289 m with a relative simple tube-shape bathymetry and a mean water depth of 151 m (see Fig. 1.3, and summerized e.g. by Wagner et al., 2009; Vogel et al., 2010b). The main amount (55%) of the hydrologic input to Lake Ohrid originates from nutrient depleted carstic springs (Matzinger et al., 2006). 50% of this water originates from Lake Prespa, which is located about 150 m higher as Lake Ohrid (Fig. 1.3). Both lakes are connected via carst aquifers but they are topographically separated

by the Galicica Mountain Range (Fig. 1.3). River and surface inflow and direct precipitation cover the remaining 45% of the hydrologic input to Lake Ohrid (Matzinger et al., 2006). Including Lake Prespa, Lake Ohrid comprises a catchment area of 2 393 km^2. The only outflow of Lake Ohrid, the Crni Drim in northern parts of the lake, accounts for about 63% of the water loss of the lake. The remaining 37% are evaporated from the lake surface (Watzin et al., 2002; Matzinger et al., 2006). Due to the large water volume and to a low nutrient availability, Lake Ohrid is highly oligotrophic today (Stankovic, 1960; Matzinger et al., 2007; summarized by Vogel et al., 2010b). Enhanced productivity in the past is associated with more nutrient supply via the carst system during lake-level low-stands at Lake Prespa (Matzinger et al., 2006). Additionally, increased productivity is associated with a complete overturn of the entire water column. This mixing transfers dissolved phosphorous to the epilimnion (Wagner et al., 2009) and occurs approximately every 7 years (Matzinger et al., 2007). An overturn of the upper 200 m of the water column persists annually during wintertime and thermal stratification during the summer months (Matzinger et al., 2007).

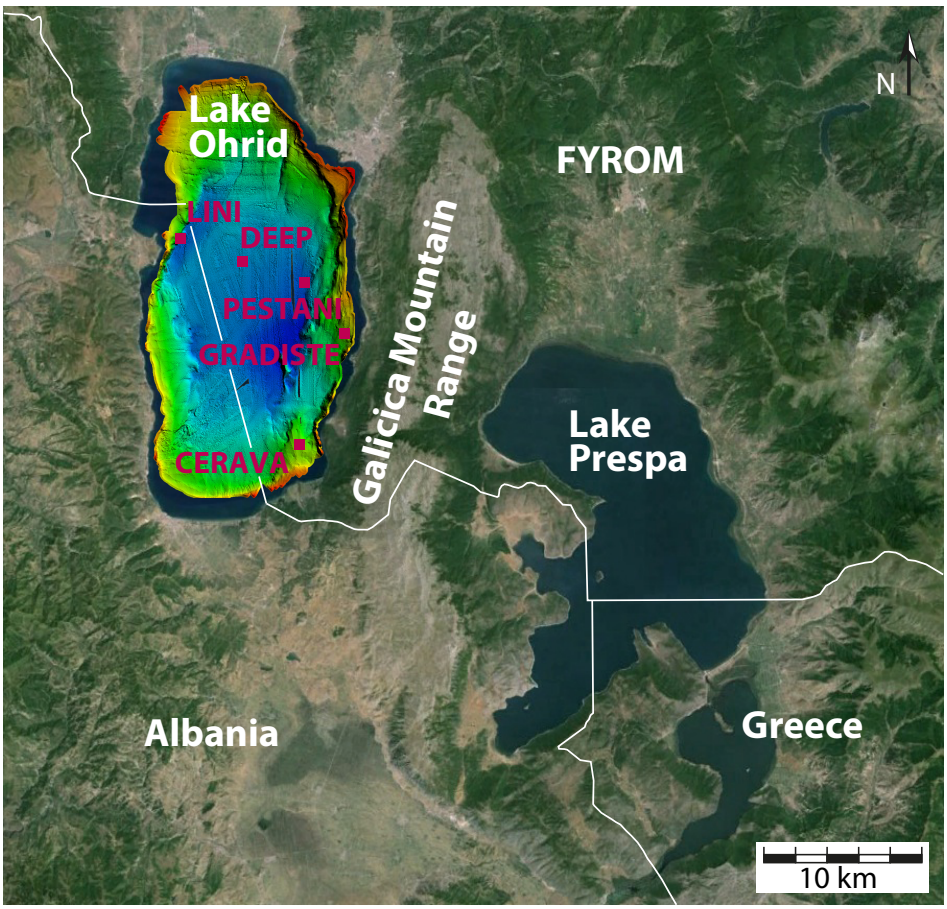

Figure 1.3: Lakes Ohrid and Prespa located at the borders of the Former Yugoslav Republic of Macedonia (FYROM), Albania and Greece, including a bathymetric map of Lake Ohrid (Lindhorst et al., 2012). Marked are the ICDP sites DEEP, CERAVA, GRADISTE, and PESTANI which were drilled in spring 2013. At LINI, a 10 m long sediment sequence was allready recovered in 2011. (map: google earth: © 2014 DigitalGlobe, © 2013 Google, Image Landsat).

The tectonic graben system of the Lake Ohrid valley is part of the Western Macedonian geotectonic zone of the Dinaric Alps (Hoffmann et al., 2010). Paleozoic metamorphic and magmatic rocks to the north and northeast, Triassic limestones and clastic sedimentary rocks to the northwest, east and southeast, and Jurassic to Cretaceous ultramafic rocks to the southwest and west form the bedrock in the surroundings of Lake Ohrid (Vogel et al., 2010b). In the plains to the north and to the south of the lake, the bedrock is overlain by Quaternary lacustrine and fluvial sediments (cf. Vogel et al., 2010b).

The climate at Lake Ohrid is influenced by both, continental and Mediterranean conditions, with maximum air temperatures below 31.5 °C, minimal temperatures above -5.7 °C, a mean annual air temperature of 11.1 °C, and an average annual precipitation of 800 to 900 mm between 1961 and 1990 (summarized by Vogel et al., 2010b). The prevailing wind directions are north and south.

A 568 m long sediment core (DEEP site) was retrieved from central parts of Lake Ohrid within the scope of the ICDP SCOPSCO project (Scientific Collaboration on Past Speciation Conditions in Lake Ohrid) in spring 2013 (Fig. 1.3). Preliminary data imply that the sequence covers the entire lacustrine sediment succession of the lake, promising to provide a valuable record of environmental variability and tephrostratigraphy in the Mediterranean Region. During the deep drilling campaign, long sediment cores were also recovered at CERAVA, GRADISTE, and PESTANI-site (Fig. 1.3). Previous studies on surface sediments (Vogel et al., 2010a) and sediment cores that cover the last glacial-interglacial cycle (Wagner et al., 2009; Vogel et al., 2010b) have already demonstrated the potential of Lake Ohrid deposits to record crucial information about modern and past sedimentary processes in the lake. These sedimentary processes could be linked to variations in the environmental settings and to the climatic conditions in the area (e.g. Wagner et al., 2009; Leng et al., 2010; Vogel et al., 2010b; Wagner et al., 2010), as well as to the deposition of tephralayers and cryptothephralayers (Wagner et al., 2008a; Caron et al., 2010; Sulpizio et al., 2010; Vogel et al., 2010c). In addition, multiple mass wasting deposits have been observed in Lake Ohrid (Wagner et al., 2008b; Lindhorst et al., 2010). In order to obtain more information about past sedimentary processes in Lake Ohrid, a 10 m long sediment sequence was recovered from western parts of Lake Ohrid close to the Lini Peninsula (LINI-site, Fig. 1.3), which is analyzed within the scope of this thesis.

1.3 Objectives

The main objective of this study is to improve the knowledge of sedimentary processes in lakes El'gygytgyn, Dojran and Ohrid as a basis for subsequent paleoenvironmental and -climatological reconstructions. The investigations are part of international research projects. The obtained sedimentary, geochemical and biogeochemical data were used to:

- provide information about external and internal sedimentary processes in the respective lake and lake's area, and to provide a basic sedimentary datasets for the studies of international research collaborators
- obtain information about paleoenvironmental and -climatoligical variability in the respective lake history
- discuss the potential and limits of the used proxy data, chronology, and statistic methods that were used in the individual publications.

Chapters 2 to 5 present the research at Lake El'gygytgyn which was conducted within the scope of the "Lake El'gygytgyn Drilling Project". In order to improve the knowledge about the deposition of clastic material in Lake El'gygytgyn as a basis for interpretations of the long sediment succession, modern sedimentary processes are investigated in chapter 2. For this purpose, multivariate statistic methods are applied to granumoleric, geochemical, biogeochemical and mineralogical data from lacustrine surface sediments, inlet streams and bedrock samples.

Chapter 3 presents the granumoleric data of the Quaternary sediment sequence of core 5011-1. Variations in the downcore grain-size data are interpreted in terms of variations in past sedimentary processes. A Principal Component Analysis (PCA) combined with time series analysis yield crucial information about the frequency in the data and the relative dominance of the oscillations during the Quaternary. These oscillations in the grain-size distribution can be explained by climate variability on glacial/interglacial time scales and by Northern Hemisphere insolation variations.

In chapter 4, the link of grain-size data and other parameters (color, magnetic susceptibility, biogenic silica, organic content, X-ray fluorescence (XRF) scanning data, pollen) to global climate variability is used to establish the chronology of core 5011-1. Paleomagnetic data indicating major reversals in the Earth's magnetic field provid initial tie points for the age model. The sediment parameters are subsequently tuned synchronously to Northern Hemisphere insolation variations and to the marine isotope stack LR04 (Lisiecki and Raymo, 2005).

Chapter 5 focuses on the petrophysical characterization of the Lake El'gygytgyn sediment sequence by using geophysical and chemical data. Seismic and downhole logging data are used to identify stratified and discontinuous parts in the sediment succession in order to detect mass movement deposits, and to characterize the transition from the bedrock to the lacustrine deposits. Physical and chemical parameters measured on the cores are used to divide the lacustrine sediment sequence into five different statistical clusters.

In Chapter 6, the sedimentary, environmental, and climatological history of Lake Dojran (Macedonia, Greece) during the Late Glacial and Holocene is investigated using hydro-acoustic data and sedimentary properties (water content, OM, calcite ($CaCO_3$) content, sulfur content, grain-size, XRF scanning, $\delta^{18}O_{carb}$, $\delta^{13}C_{carb}$, $\delta^{13}C_{org}$) of a 7 m long sediment core (Fig. 1.2B). The research of this study is incorporated into the CRC "Our way to Europe", which aims to capture the complex nature of chronology, regional structure, climatic, environmental and socio-cultural contexts of the dispersal of Modern Man from Africa to Western Eurasia, and particularly to Europe.

Chapter 7 focuses on probable triggers of the sedimentation of a MWD in Lake Ohrid (Macedonia, Albania), which is characterized using sediment (lithostratigraphic description, XRF scanning, water content, OM content, calcite content) and hydro-acoustic data. The MWD is temporally constrained by tephrostratigraphic tie points, radiocarbon dating, and cross correlation to existing cores. The research of this study contributes to the ICDP SCOPSCO project. The aims of this project are to (I) obtain more precise information about the age and origin of the lake, (II) unravel the seismotectonic history of the lake area including effects of major earthquakes and associated mass wasting events, (III) obtain a continuous record containing information on volcanic activities and climate changes in the central northern Mediterranean region, and (IV) better understand the impact of major geological/environmental events on general evolutionary patterns and shaping an extraordinary degree of endemic biodiversity as a matter of global significance.

In chapter 8, the potentials and the limits of the data and methods used in the previous chapters are discussed. In chapter 8.1, granumoleric and geochemistry data from lacustrine surface sediments and from catchment samples from inlet streams and source rocks are assessed for their potential to unravel modern sedimentary processes. Information about spatial variations of past to modern sedimentary processes can be investigated by using hydro-acoustic data, which is discussed in chapter 8.2. More detailed information about past sedimentary processes in a lake system can be obtained from sediment cores by analyzing their lithological properties, grain-size variability, and inorganic and organic geochemistry composition. The potential and limits of these data including systematical and analytical errors are assessed in chapter 8.3. Chapter 8.4 focuses on the age modeling of lacustrine sediment sequences and the consequences of different methods for the interpretations of sedimentary, paleoenvironmental and -climatologic variations in a temporal context. Finally, the utility of multivariate statistic methods such as the Principal Component Analyses (PCA) and the Redundancy Analyses (RDA) is evaluated in chapter 8.5.

2 Modern sedimentation patterns in Lake El'gygytgyn, NE Russia, derived from surface sediment and inlet streams samples

Journal article (2013):
Wennrich, V., Francke, A., Dehnert, A., Juschus, O., Leipe, T., Vogt, C., Brigham-Grette, J., Minyuk, P. S., Melles, M., and El'gygytgyn Science, P.: Modern sedimentation patterns in Lake El'gygytgyn, NE Russia, derived from surface sediment and inlet streams samples, Clim. Past, 9, 135-148, 10.5194/cp-9-135-2013, 2013.

Clim. Past, 9, 135–148, 2013
www.clim-past.net/9/135/2013/
doi:10.5194/cp-9-135-2013

Climate of the Past

Modern sedimentation patterns in Lake El'gygytgyn, NE Russia, derived from surface sediment and inlet streams samples

V. Wennrich[1], A. Francke[1], A. Dehnert[2], O. Juschus[3], T. Leipe[4], C. Vogt[5], J. Brigham-Grette[6], P. S. Minyuk[7], M. Melles[1], and El'gygytgyn Science Party

[1]University of Cologne, Institute for Geology and Mineralogy, Cologne, Germany
[2]Swiss Federal Nuclear Safety Inspectorate ENSI, Brugg, Switzerland
[3]Eberswalde University for Sustainable Development, Eberswalde, Germany
[4]Leibniz Institute for Baltic Sea Research Warnemuende, Marine Geology, Rostock, Germany
[5]University Bremen, Department of Geosciences, Crystallography/ZEKAM, Bremen, Germany
[6]University of Massachusetts, Department of Geosciences, Amherst, USA
[7]Russian Academy of Sciences, Northeast Interdisciplinary Scientific Research Institute, Magadan, Russia

Correspondence to: V. Wennrich (volker.wennrich@uni-koeln.de)

Received: 27 April 2012 – Published in Clim. Past Discuss.: 1 June 2012
Revised: 19 October 2012 – Accepted: 10 December 2012 – Published: 22 January 2013

Abstract. Lake El'gygytgyn/NE Russia holds a continuous 3.58 Ma sediment record, which is regarded as the most long-lasting climate archive of the terrestrial Arctic. Based on multi-proxy geochemical, mineralogical, and granulometric analyses of surface sediment, inlet stream and bedrock samples, supplemented by statistical methods, major processes influencing the modern sedimentation in the lake were investigated. Grain-size parameters and chemical elements linked to the input of feldspars from acidic bedrock indicate a wind-induced two-cell current system as major driver of sediment transport and accumulation processes in Lake El'gygytgyn. The distribution of mafic rock related elements in the sediment on the lake floor can be traced back to the input of weathering products of basaltic rocks in the catchment. Obvious similarities in the spatial variability of manganese and heavy metals indicate sorption or co-precipitation of these elements with Fe and Mn hydroxides and oxides. But the similar distribution of organic matter and clay contents might also point to a fixation to organic components and clay minerals. An enrichment of mercury in the inlet streams might be indicative of neotectonic activity around the lake. The results of this study add to the fundamental knowledge of the modern lake processes of Lake El'gygytgyn and its lake-catchment interactions, and thus, yield crucial insights for the interpretation of paleo-data from this unique archive.

1 Introduction

In spring 2009, the ICDP El'gygytgyn Drilling Project recovered the 318-m long lacustrine sediment record of Lake El'gygytgyn in Chukotka, NE Russia (Melles et al., 2011, 2012; Fig. 1). Long high-resolution lake sediment records are known to well document regional hydrologic and climatic responses to atmospheric changes (Brigham-Grette et al., 2007a), and therefore are valuable archives of climate and environmental changes (e.g. Allen et al., 1999; Gasse et al., 2011; Cohen, 2012). Given their often continuous sediment sequences, large and old lake basins play an important role in collecting sedimentological information providing a continental signature to couple with the marine realm. Thus, these lakes help to close gaps in the knowledge on land–ocean interactions through time. Nevertheless, the profound interpretation of proxy data derived from lake sediment records requires an in-depth knowledge of the lake-specific modern biological and sedimentological processes and their controlling factors (e.g. Vogel et al., 2010; Viehberg et al., 2012).

Lake El'gygytgyn represents a unique site, because it holds the most long-lasting climate archive of the terrestrial Arctic (Melles et al., 2011, 2012), reaching back to the time of meteorite impact event 3.58 Ma ago (Layer, 2000). Furthermore, the basin was never overcome by large Cenozoic continental ice-masses (Glushkova, 2001; Glushkova

Published by Copernicus Publications on behalf of the European Geosciences Union.

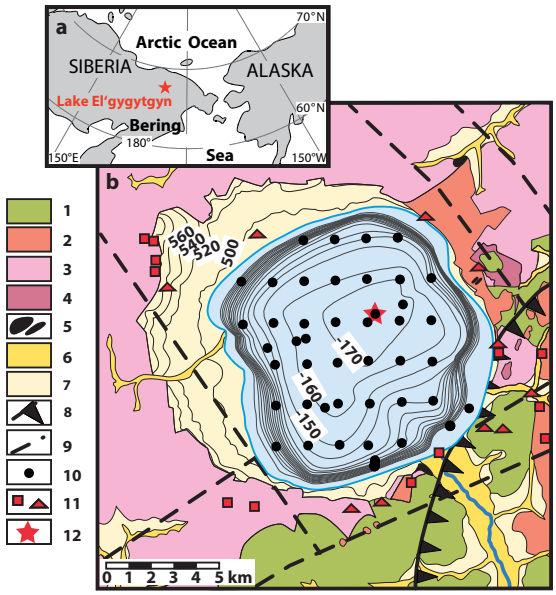

Fig. 1. **(a)** Map showing the location of Lake El'gygytgyn in the western Beringian Arctic, **(b)** geological map of the El'gygytgyn impact impact crater illustrating the major stratigraphic units (modified after Nowaczyk et al., 2002) and major fault systems (compiled after Belyi and Belaya, 1998; Belyi and Raikevich, 1994) in the lake catchment, bathymetric contour lines in the lake (modified after Belyi, 2001), and locations of lake floor and bedrock samples used in this study as well as of ICDP site 5011-1.; (1) Koekvun' Formation (basalt, andesite-basalt, tuff, tuff-breccia, sandstone, tuff-siltstone), (2) Ergyvaam Formation (ignimbrite, tuff), (3) Pykarvaam Formation (ignimbrite, tuff), (4) Voron'in Formation (ignimbrite, tuff), (5) dykes, stocks, and sills of subvolcanic rocks, (6) flood plain deposits, (7) terrace deposits, (8) boundary between the outer and inner OCVB zones, (9) major faults, (10) lake sediment surface samples, (11) bedrock samples (with squares referring to data from this study and triangles to data taken from Belyi and Belaya, 1998), (12) ICDP site 5011-1.

and Smirnov, 2007), resulting in widely time-continuous sedimentation. The lake is located in a region influenced by both Siberian and North Pacific oceanic air-masses (Barr and Clark, 2011; Yanase and Abe-Ouchi, 2007; Mock et al., 1998), making it very sensitive to regional atmospheric change. The high potential of Lake El'gygytgyn as a globally significant paleoclimate and environmental archive is confirmed by numerous studies on the lake sediments formed during the past three glacial/interglacial cycles (Brigham-Grette et al., 2007b; Lozhkin et al., 2007; Melles et al., 2007; Minyuk et al., 2007; Nowaczyk et al., 2007; Swann et al., 2010; Asikainen et al., 2007).

Within the framework of the pre-site survey research, modern climatological and hydrological processes in the lake surrounding and in the water column were intensively investigated (e.g. Cremer and Wagner, 2003; Cremer et al., 2005; Nolan and Brigham-Grette, 2007; Nolan et al., 2002; Fedorov et al., 2012), and a variety of modern to sub-recent sample sets were taken for study (Melles et al., 2005).

Here, we present the combined results of a multi-proxy and statistical approach to enhance the understanding of the modern sedimentation of Lake El'gygytgyn by analyzing a set of surface sediment and inlet streams samples, as well as hand samples from the surrounding bedrock. The major goal of this study is to provide information concerning the dominant sedimentation patterns in the lake controlled by climate-driven transport processes, bedrock geology, post-depositional processes, but possibly also influenced by tectonic activity. In combination with recent climatologic and hydrologic data (Nolan, 2012; Fedorov et al., 2012), these findings will enhance our understanding of fundamental in-lake processes, and thus, form an important basis for the interpretation of the Lake El'gygytgyn paleo-record extending to 3.58 Ma.

2 Study site

Lake El'gygytgyn (67°30′ N, 172°05′ E, 492 m a.s.l.; Fig. 1) is located within the Anadyr Mountain Range in central Chukotka/ Far East Russian Arctic. Today, the roughly circular lake has a diameter of ∼ 12 km and a maximum water depth of 175 m (Nolan and Brigham-Grette, 2007; Melles et al., 2007), filling the deepest part of the ∼ 18-km wide El'gygytgyn impact crater (Gurov et al., 2007). With a surface area of ∼ 110 km^2, the lake is fed by 50 ephemeral streams draining a watershed area of 293 km^2 defined by the crater rim (Nolan et al., 2002; Fig. 2a). The outlet stream, the Enmyvaam River at the south-eastern edge of the lake, flows into the Anadyr River, which eventually drains into the Bering Sea (Nolan and Brigham-Grette, 2007).

The climate in Chukotka is characterized by low mean winter and summer temperatures between −32 °C and −36 °C (January) and between +4° and +8 °C (July, August), respectively (Treshnikov, 1985), and a mean annual precipitation of ∼ 250 mm (Glotov and Zuev, 1995). In 2002, winter and summer temperature extremes of −40 °C and +26 °C, respectively, were recorded at Lake El'gygytgyn (Nolan and Brigham-Grette, 2007). Strong winds either from the north or south with a mean hourly wind speed of 5.6 ms^{-1} were punctuated by maximum values up to 21.0 ms^{-1} (Nolan and Brigham-Grette, 2007).

Lake El'gygytgyn is an oligotrophic to ultra-oligotrophic and cold-monomictic lake (Cremer and Wagner, 2003), with a yearly ice-cover lasting from mid-October until early to mid-July (Nolan et al., 2002). While thermal stratification of the water column is today established during the ice-covered season (Cremer et al., 2005), the lake becomes fully mixed by late summer after snowmelt and the initial ice break-up, triggered by the lateral movement of warmer shore-waters

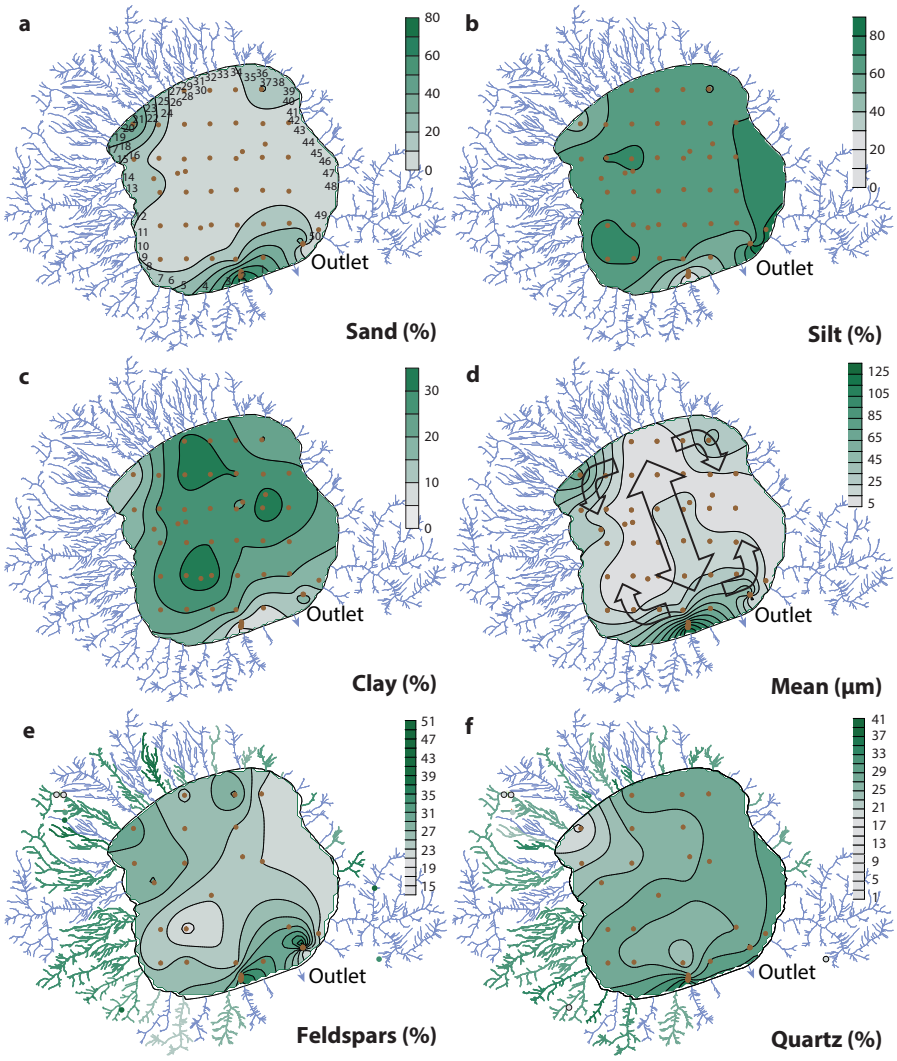

Fig. 2. Spatial distribution of volume percentages of **(a)** sand, **(b)** silt and **(c)** clay, **(d)** mean grain size, and proportions of **(e)** feldspars and **(f)** quartz in modern surface sediments (brown dots = sample location), inlet streams (coloured streams) and bedrock samples (coloured circles) of Lake El'gygytgyn. Numbers near the stream mouths in **(a)** refer to the creek numbering system of Nolan and Brigham-Grette (2007). Arrows in **(d)** indicate the near-surface circulation pattern, created by prevailing northern and southern wind directions (modified after Nolan and Brigham-Grette, 2007). Note that data of inlet stream and bedrock samples are only available for **(e)** and **(f)**.

and enhanced by strong winds (Nolan and Brigham-Grette, 2007). The residence time of the lake water was calculated to be ∼ 100 yr (Fedorov et al., 2012).

Geomorphological studies in the lake catchment have identified prominent lake terraces at 35–40 m, 9–11 m and 3–5 m above the modern lake level as remains of lake-level high-stands during the lake history (Glushkova and Smirnov, 2007; Schwamborn et al., 2008a, 2006). In addition, an ancient terrace 10 m below the modern water level points to a significant lake-level lowering, most likely during MIS 2 (Juschus et al., 2011). Although the existence of higher terraces 60 and 80 m above the recent lake level has been suggested (Gurov et al., 2007; Nekrasov, 1963), their lacustrine origin has not yet been finally confirmed (Glushkova and Smirnov, 2005; Juschus et al., 2011).

The El'gygytgyn impact crater was formed in Upper Cretaceous volcanic rocks of the Okhotsk–Chukchi Volcanic Belt (OCVB) (Gurov et al., 2007; Gurov and Gurova, 1979). The bedrock in the vicinity of the lake predominantly consists of ignimbrites, tuffs and andesite-basalts associated with the Pykarvaam, Voron'in, Koekvun' and Ergyvaam Formations (Belyi and Raikevich, 1994; Nowaczyk et al., 2002; Fig. 1b) dated to about 67–90 Ma (Kelley et al., 1999; Stone et al., 2009). The region of Lake El'gygytgyn is affected by continuous permafrost, presumably since the Late Pliocene (Glushkova and Smirnov, 2007). Erosion and detrital sediment transport of bedrock material into the lake basin are mainly triggered by permafrost related cryogenic weathering, as well as slope dynamics, and fluvial outwash in the lake surrounding (Schwamborn et al., 2008b, 2012; Fedorov et al., 2012). Thus, climate-driven variations in permafrost stability are believed to have a major influence on the lake sedimentation.

3 Material and methods

3.1 Field work

During a field campaign in summer 2003, a set of 55 surface sediment samples was collected from the floor of Lake El'gygytgyn (Fig. 1b). The samples were recovered from a floating platform using a gravity corer (UWITEC Corp., Austria) with plastic liners of 6 cm in diameter. Sample locations were determined according to a regular map grid, except for the shallowest parts of the lake, which were sampled along a transect at the southern shelf and at three sites along the southeastern shelf. This study is based on the uppermost 2 cm of the gravity cores, which represents roughly the past 150 years based on Holocene sedimentation rates (Fig. 3).

To investigate the influence of both fluvial sediment supply and bedrock geology on the modern sediments of Lake El'gygytgyn, an additional 30 sediment samples were taken from the major inlet streams entering the lake, and another 11 bedrock samples were collected from the lake catchment (Fig. 1b). The bedrock samples were supplemented by additional XRF data of bedrock samples taken from the literature (Belyi and Belaya, 1998).

3.2 Analytical work

Sediment samples from both the lake floor and inlet streams were freeze-dried in the lab and subsequently split into sample aliquots. Aliquots for geochemical and biogeochemical analyzes were ground to $< 63\,\mu$m and homogenized. Total nitrogen (TN) was measured with an elemental analyzer (vario EL III, elementar Corp.). The total organic carbon content (TOC) was measured using a METALYT CS 1000S analyzer (ELTRA Corp.), after pretreating the sediment with 10 % HCl to remove carbonates.

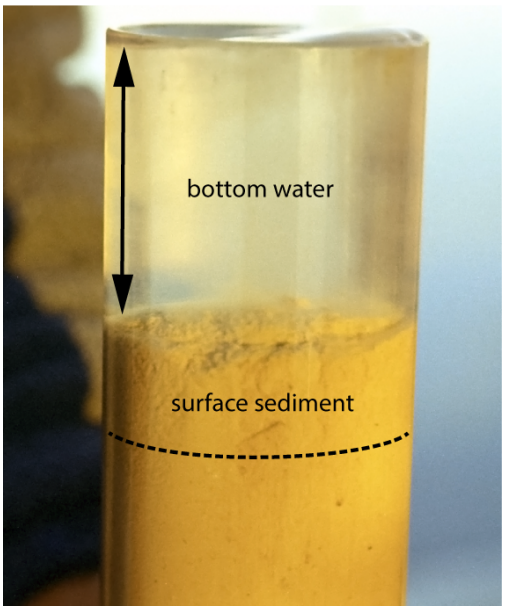

Fig. 3. Photograph of a gravity core taken near the northern shore of Lake El'gygytgyn from a water depth of 127.4 m. Surface samples used in this study comprise the uppermost 2 cm of the sediments (above the dotted line) representing roughly the past 150 yr based on Holocene sedimentation rates.

Major and trace elements were measured by ICP-OES (iCAP 6300 DUO, Thermo Scientific) after $HClO_4$/HF total digestions. Acid digestion was performed in closed Teflon vessels (PDS-6) heated for 6 h at 180 °C by treating 100 mg sample with 3 mL HF + 1 mL $HClO_4$. After digestion, acids were evaporated using a heated metal block (180 °C) and were re-dissolved and evaporated three times with 3 mL half-concentrated HCl, followed by re-dissolution with 2 vol% HNO_3 and dilution to 25 mL. Precision (1σ) and accuracy were checked by parallel analysis of international and in-house reference materials, leading to ≤ 2.8 to ≤ 2.6 % for major elements and ≤ 1.7 to ≤ 12.1 % for trace metals. Mercury was directly determined using 30–50 mg of dry homogenized sediment using a DMA-80 Direct Mercury Analyzer (MLS instruments). The analysis is based on combustion of the sample and pre-concentration of Hg at a gold trap (amalgam), re-heating and determination of Hg gas by atomic-absorption spectrometry (AAS). The detection limit of the analysis is very low ($< 1\,\mu g\,kg^{-1}$) and the reproducibility (precision) is ~ 5 % relative to the standard deviation from the average value.

The major and trace element composition of the bedrock samples was determined by wavelength-dispersive X-ray fluorescence (XRF) analysis using a sequential X-ray spectrometer (Phillips PW2400) calibrated with natural and synthetic

standards. Prior to analysis, powdered samples were heated for four hours at 105 °C before fusion with $Li_2B_4O_7$.

Bulk mineral contents of selected surface sediment ($n = 22$), stream ($n = 23$) and bedrock samples ($n = 7$) were determined by X-ray diffraction (XRD). XRD analyses were run on pressed powder pellets using a Philips PW 1820 diffractometer with CoKα radiation (40 kV, 40 mA), automatic divergence slit (ADS), graphite monochromator, and automatic sample changer. Scanning was performed from 3° to 100° 2theta with a step size of 0.02° 2theta and 1 seconds time per step. Mineral identifications were done by means of the Philips software X'Pert HighScore™ and sheet silicates were identified and quantified with the X-ray diffraction interpretation software MacDiff 4.25 (Petschick et al., 1996). Full quantification of the bulk mineral assemblage was carried out using the QUAX software package (Emmermann and Lauterjung, 1990) following the QUAX full pattern method (Vogt et al., 2002). The standard deviation for bulk mineral determination is ±2 % for quartz (Vogt, 1997) and ±5–10 % for feldspars and clay minerals (Vogt et al., 2002).

Grain-size analyses were performed on 1 g freeze-dried sediment. Prior to the measurement, samples were pretreated according to Francke et al. (2013) to remove organic matter (30 % H_2O_2, 50 °C, 18 h), vivianite nodules (0.5 M HNO_3, 50 °C, 5 h, 30 min shaking in between) and biogenic silica (0.5 M NaOH leaching, 90 °C, 2 × 30 min.). The results of the treatment steps were validated by biogeochemical analyses, Fourier Transform Infrared Spectroscopy (FTIRS), XRD, scanning electron microscopy (SEM) and optical microscopic investigations (Francke et al., 2013). Subsequently, the samples were mixed with $Na_4P_2O_7$ solution (0.05 % w/v) as a dispersant agent and finally measured by a Laser Particle Size Analyzer (DigiSizer 5200, Micromeritics Instrument Corp.). The laser-diffractometer uses a 1MB CCD-sensor and calculates 160 grain-size classes between 0.1 and 1000 μm with average values of three runs. One minute of ultrasonic treatment and flow rates of 10 L min^{-1} re-suspended the sediments prior to the analysis.

3.3 Statistics and interpolation

Calculations of grain-size parameters and statistics were performed using the program GRADISTAT (Blott and Pye, 2001). The statistical grain-size parameters were calculated according to the arithmetic method of moments.

To handle and simplify the element data of the surface sediments, and to visualize grain-size dependencies, both principal component analysis (PCA) and redundancy analysis (RDA) were carried out. Analyses were conducted using the Microsoft Excel add-in XLSTAT (Addinsoft SARL) with chemical element data as dependent response variables and various grain-size parameters (mean, mode, median, percentages of sand, mud, silt, clay, medium sand, fine sand, very fine sand, very coarse silt, coarse silt, medium silt, fine silt, very fine silt) as explanatory variables, respectively.

Interpolation and mapping of the surface sediment datasets were performed with the software Surfer 9 (Golden Software Inc.) using the Kriging method (Cressie, 1991; Oliver and Webster, 1990).

4 Results

4.1 Grain-size distribution

The surface sediments of Lake El'gygytgyn are silt dominated (Fig. 2b) with a mean grain-size ranging between 7.3 and 69.6 μm (Fig. 2d). The spatial distribution of the mean grain-size shows fine-grained sediments in the northern, eastern and western central lake basin, whereas coarser material is found at the southern, northwestern and northeastern edges of the lake (Fig. 2d). Coarse-grained areas with high sand content (> 63 μm) up to 73.8 % are located in the northwestern and northeastern corners of the lake and along the southern shore (Fig. 2a). Highest silt contents (2–63 μm) with maximum values up to 82.3 % (Fig. 2b) are observed at the southeastern edge of the basin near the mouth of creeks 49 and 50 (creek numbers according to Nolan et al., 2002; Fig. 2a). The clay content varies between 8.4 % at the southern shore and 33.6 % in the central lake basin (Fig. 2c).

Surprisingly, the center of the lake exhibits a tongue of sediments with higher mean grain sizes around 15–25 μm, extending from the southern shore towards the lake center (Fig. 2d). This feature is mainly due to a slight shift of the mean caused by an increase in very coarse silt (31–63 μm) of up to 17 %.

4.2 Bulk mineralogy

The bulk mineral composition of the surface sediments is dominated by a mixture of quartz, feldspars (plagioclase and K-feldspars), clay minerals and accessory minerals (Table 1). Although bedrock samples of the catchment contain fairly scattered amounts of quartz ranging from 2.9–27.7 %, the surface sediment and inlet stream samples show a rather heterogeneous quartz distribution with a clear enrichment (up to 34.3 %) at the southern and southeastern shore (Fig. 2f). Conversely, the northwestern shore is characterized by lowest quartz content.

Feldspars also exhibit high concentrations in the surface sediments at the southern and northeastern shores (max. 42.5 %) but differ from quartz due to the high concentration also found at the northwestern shore and a pronounced low in the central and eastern part of the lake (max. 22.8 %; Fig. 2e). These values fit within the concentration range of the inlet stream samples (25.4–40.0 %) and of the bedrock material (15.1–51.4 %; Fig. 2e). In the latter, feldspars occur as phenocrysts of orthoclase ($KAlSi_3O_8$) and plagioclase, mainly of oligoclase and

Table 1. Averaged bulk mineralogy composition of surface sediments, inlet stream and bedrock samples of Lake El'gygytgyn. For creek numbering see Fig. 2a.

	Material	*n*	quartz	plagioclase	K-feldspar	calcite	Mg-rich calcite	dolomite	ankerite	siderite	rhodocrosite	smectites & montmor.	mixed-layered clay minerals	illites & micas	kaolinite	chlorite	pyroxenes	amphibols	zeolites	magnetite	Fe-oxides, -hydroxides	barite
surface sediments	northern shelf	5	23.9	21.4	8.4	2.0	2.8	1.4	0.2	0.1	0.5	6.5	2.4	9.0	1.3	2.5	4.3	0.4	1.9	0.8	3.6	0.6
	southern shelf	15	29.3	27.4	6.9	1.2	2.2	1.3	0.2	0.1	0.8	4.2	2.6	11.0	1.3	2.2	3.8	0.3	2.6	0.6	1.8	0.3
	central basin	10	26.1	20.8	5.5	2.0	2.5	1.3	0.2	0.1	0.6	7.1	3.5	10.2	2.0	3.5	4.3	0.4	4.5	0.7	4.4	1.1
	southwestern shelf	6	28.0	24.2	6.0	1.0	2.1	1.0	0.2	0.1	0.7	5.7	3.0	12.8	3.0	3.8	3.7	0.1	4.7	0.6	1.3	0.6
streams inlet	S & W (creeks 1–18)	11	30.3	26.7	7.0	1.8	2.6	1.6	0.4	0.1	0.6	1.9	3.0	10.6	0.6	1.7	3.7	0.5	1.7	0.7	3.6	0.4
	N (creeks 19–37)	12	28.9	26.0	7.2	2.2	2.5	2.1	0.4	0.1	0.7	2.1	2.0	6.3	0.5	1.4	4.2	0.3	5.7	0.9	5.3	0.5
	E & SE (creeks 39–50)	3	26.2	26.7	8.9	2.1	1.9	1.6	0.3	0.1	0.6	4.7	2.9	6.0	1.2	2.1	4.2	0.3	3.9	1.2	4.0	0.7
bedrock samples	Pykarvaam Form.	5	18.5	26.1	5.2	1.6	3.2	1.2	0.3	0.1	0.7	2.8	1.9	21.7	0.6	1.1	3.4	0.2	2.7	0.7	3.1	0.5
	Koekvuum Form.	1	2.9	41.9	8.7	5.8	1.2	4.2	0.1	0.3	0.4	1.7	2.7	3.4	0.3	2.5	0.3	0.1	1.9	5.2	6.6	1.1
	Ergyvaam Form.	1	26.9	26.0	10.4	1.0	2.6	2.0	0.0	0.2	0.1	1.5	1.9	5.4	4.1	9.9	4.5	0.4	8.6	0.7	0.3	0.5

andesine ((Na,Ca)[Al(Si,Al)Si_2O_8]), in both the acid and andesitic volcanic rocks (Gurov et al., 2005; Belyi, 2010).

The clay mineral assemblage is composed of illite, smectite, chlorite, mixed layer clay minerals, and to a minor amount, kaolinite (Table 1), which concurs with earlier downcore clay mineral analyses from Lake El'gygytgyn (Asikainen et al., 2007). Furthermore, zeolites (up to 4.7 %), pyroxenes (up to 4.3 %) and Fe-oxides and -hydroxides (up to 4.4 %) occur in considerable amounts (Table 1), whereas carbonate phases, such as calcite ($CaCO_3$), Mg-rich calcite, siderite ($FeCO_3$) and rhodochrosite ($MnCO_3$), play only a minor role in surface sediments with contents < 3 % (Table 1). The accessory mineral assemblage resembles the composition of the inlet streams and bedrock samples.

4.3 Element composition

Based on the PCA results of the elemental concentrations in Lake El'gygytgyn surface sediments, three dominant element clusters can be defined. Group I, with high loadings on principle component (PC) 2 and low loadings on PC 1, includes Al_2O_3, Na_2O, CaO, K_2O, Ba and Sr (Fig. 4a). As illustrated in K_2O concentrations as high as 6.65 % (Fig. 5a), these elements are typically enriched close to the southern and northern shores but are rather depleted in the central lake basin. Lower K_2O concentrations are also indicated at the southeastern shore, but are represented only by a single value (Fig. 5a). Bedrock samples show a clear differentiation of group I elements in the different formations, with low K_2O concentrations of 1.2–2.2 % in the basaltic to andesitic rocks of the Koekvun' Formation, but distinctly higher values in the rhyolithic source rocks of the Pykarvaam (3.3–4.4 %) and Ergyvaam Formations (4.7 %; Fig. 5a). In contrast, the inlet stream samples show a rather homogeneous distribution of group I elements, with high K_2O concentrations ranging between 4.5 and 8.5 %.

Another cluster in the PCA results comprises the elements of group II, including Cr, Cu, Zr, TiO_2, Zn, V, Ni, Fe_2O_3, Co and Cd, showing high loadings of PC 1 and only low negative loadings of PC 2 (Fig. 4a). As shown for instance in the distribution plot of Cr (Fig. 5b), these elements are highly enriched in the southeastern part of Lake El'gygytgyn (up to 70.3 mg kg^{-1} Cr) and along the eastern shore, whereas the other parts of the basin show relatively low concentrations (6.3–30.5 mg kg^{-1} Cr). A similar heterogeneity in the distribution of group II elements is also valid for the bedrock and stream samples, with rather low values in most of the lake catchment but a clear enrichment in bedrock samples from the southeastern crater rim (up to 104 mg kg^{-1}Cr) and sediments from streams 48 to 50 (30.1–154.0 mg kg^{-1} Cr; Fig. 5b).

A third group of elements, characterized by medium negative loadings of PC1 and high negative loadings of PC2 in the PCA, contain typical heavy metals, such as Pb, Mo, MnO, As, but also P_2O_5, SO_2 and Hg (Fig. 4a). With the exception of arsenic, group III elements are typically elevated in the deepest part of the lake basin (e.g. MnO: 0.06–0.11 %), and are depleted in sediments along the coarse-grained northern and southern shores (e.g. MnO: 0.03–0.05 %; Fig. 5c). This spatial distribution significantly differs from bedrock and creek samples, showing a clear group III enrichment in the basaltic to andesitic rocks (MnO: 0.15–0.16 %) and stream samples (MnO: 0.07–0.09 %) of the southeastern crater rim.

Mercury is heterogeneously distributed in the recent sediments of Lake El'gygytgyn, in contrast to other group III elements. For major parts of the lake basin, Hg concentrations in the surface elements do not exceed 150 $\mu g\,kg^{-1}$ (Fig. 5d). In the northern central lake basin, in contrast, mercury exhibits a pronounced local maximum, with two sample locations yielding 4–5 times higher Hg contents (476 and 576 $\mu g\,kg^{-1}$) compared to all other lake sediment samples. Sediments from creeks 46 and 50 in the southeastern corner

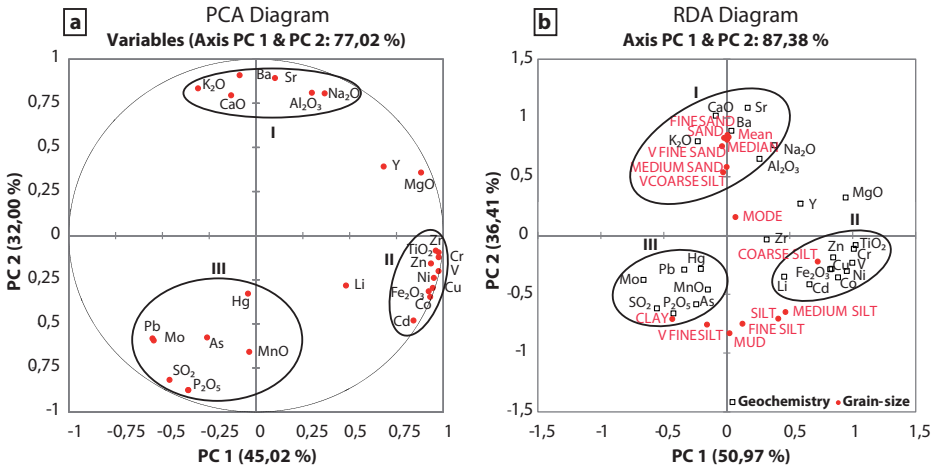

Fig. 4. Result of the **(a)** principal component analysis (PCA) of the inorganic geochemistry and **(b)** redundancy analysis (RDA) of the inorganic geochemistry and grain-size parameters (explanatory variables) in surface sediments of Lake El'gygytgyn.

of the basin yield Hg concentrations ranging between 182–1142 μg kg^{-1}, whereas mercury does not exceed 110 μg kg^{-1} at most of the other inlet streams (Fig. 5d).

5 Discussion

Lake El'gygytgyn surface sediments show a variety of distribution patterns based on grain-size parameters, element concentrations, bulk mineralogy, and organic parameters, which are controlled by transport processes, bedrock geology, early diagenetic processes and potential tectonic activity. Thus, these data have a direct impact on the interpretation of the paleoclimate record derived from sediment cores of Lake El'gygytgyn.

5.1 Sediment transport mechanisms within the water body

The grain-size distribution in the surface sediments of Lake El'gygytgyn and especially the mean grain size traces the general path of a two-cell wind induced current system in Lake El'gygytgyn (Fig. 2d), which appears to be triggered by strong winds from the north or south, as postulated by Nolan and Brigham-Grette (2007). Similar wind-driven two-cell current circulation systems are common features in Arctic lakes (e.g. Côté and Burn, 2002), often resulting in oriented lake bodies with an elliptical shape perpendicular to the main wind direction. Consistent with the occurrence of coarse-grained sediments found in the northwestern and northeastern corners of the lake and along the southern shore (Fig. 2a and d), maximum littoral drift at the edges of the lake, coincident with the highest erosional forces obviously prevents the deposition of fine-grained material (Nolan and Brigham-Grette, 2007).

The coarse-grained tongue extending from the southern shore towards the lake center cannot be of fluvial origin because large inlet streams as possible source do not exist along the southern shore. Furthermore, due to the low sand content within the area of the tongue (Fig. 2a) sediment transport from the southern, very sandy shelf by ice-rafting is also unlikely. Turbidity currents, whose deposits are typically characterized by graded bedding of the sediments with a coarse base and a fine silt/clay cap, are rather abundant in older sediments of Lake El'gygytgyn but have not been observed for the last 3200 uncal. ^{14}C years (Juschus et al., 2009; Sauerbrey et al., 2013). The lack of the typical structure in the modern sediments along the coarse tongue also rules out an origin from turbidity currents. Thus, the coarser sediment tongue is most likely the result of wave-induced re-suspension processes (Bloesch, 1995) with an erosion of fine-grained material from the shallow southern shelf (water depth < 10 m) during heavy storms with northerly wind directions and a subsequent northward transport by sub-surface currents. This suggestion is supported by the very coarse grain-size characteristically found on the southern shelf (Fig. 2a and d). The occurrence of such re-suspension processes was observed during a heavy storm from the north in August 2003. Wind velocities up to 16.8 ms^{-1} (Nolan, personal communication, 2012) and wave heights up to 1 m created a distinct northward reaching suspension cloud of ~ 1 km in length in front of the Enmyvaam river (Fig. 6), accompanied by a nearly shut off of the outlet by coarse sediment drift. The visible suspension cloud ended just at the shelf edge, implying a further transport and dispersion of the material into the deeper lake basin presumably via vertical lake currents or

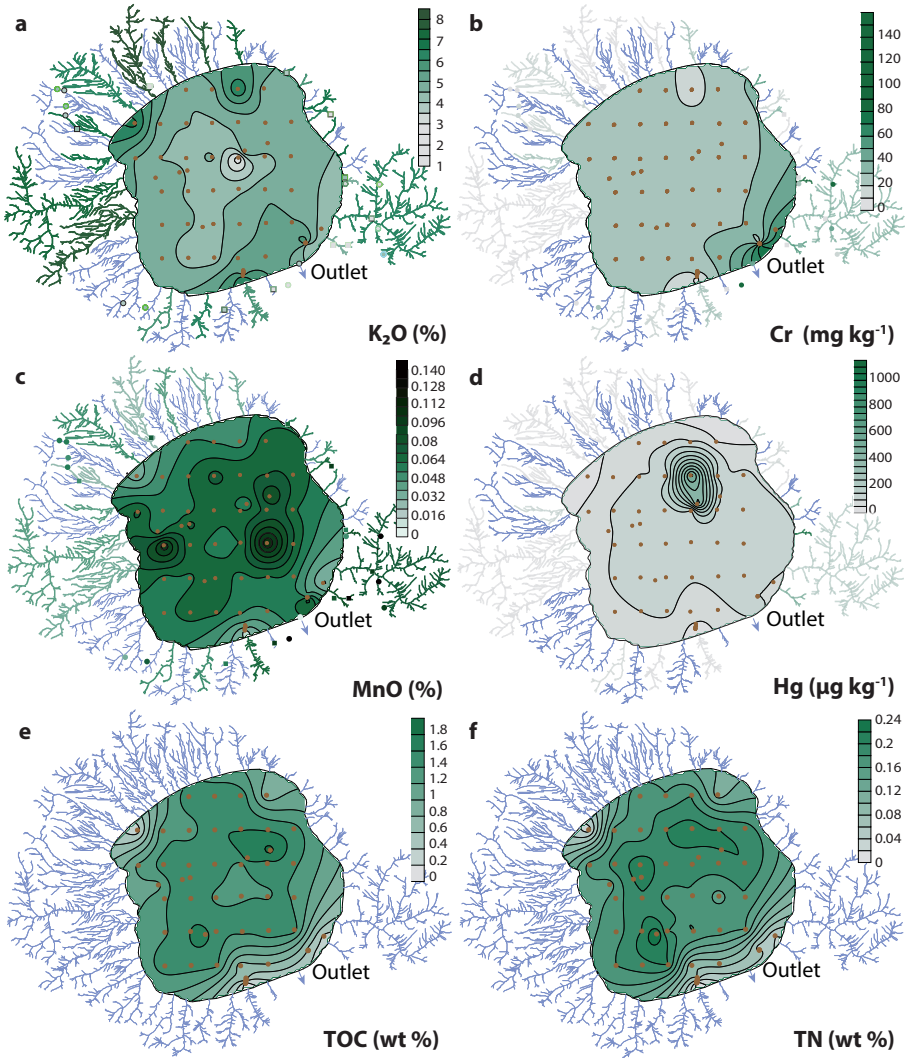

Fig. 5. Spatial distribution of concentrations of **(a)** K_2O [% wt/wt], **(b)** Cr [mg kg^{-1}], **(c)** MnO [% wt/wt], **(d)** Hg [$\mu g\,kg^{-1}$], **(e)** TOC [% wt/wt], and **(f)** TN [% wt/wt] in surface sediments (brown dots = sample location), inlet streams (coloured streams) and bedrock samples (coloured circles = this study; colored squares = taken from Belyi et al., 1998) of Lake El'gygytgyn. Note that no inlet stream and bedrock sample data are available for **(e)** and **(f)**.

hyperpycnal near bottom flows as described for Lake Michigan (Hawley and Lee, 1999) or Lake Malawi (Halfman and Scholz, 1993). Between 2001 and 2005, similar heavy storms with wind speeds exceeding 10 ms^{-1} and a duration of more than four hours were recorded at Lake El'gygytgyn between 9 (2001, 2004) and 26 (2002) times during the ice-free season (mid- July–mid-October; Nolan et al., 2002). The formation of a major suspension fan is likely amplified by the slightly triangular morphology of the southern shore line (Fig. 1b), focusing the wave activity at the southeastern edge just in front of the Enmyvaam outlet. Furthermore, similarities in the spatial pattern of the coarser-grained sediment tongue and a NE–SW oriented ridge structure indicated in the bathymetry (Fig. 1b) may imply a higher sedimentation rates along the suspension fan.

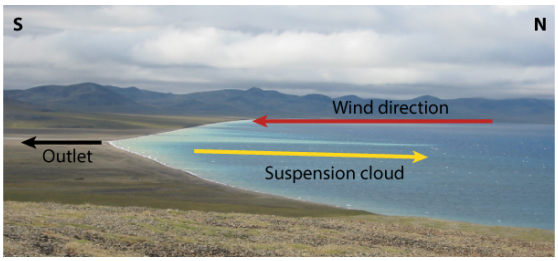

Fig. 6. Suspension cloud at the southern shelf of Lake El'gygytgyn, observed during a heavy storm with northerly winds in August 2003. View from the southeastern shore, also showing the Enmyvaam outlet stream exiting the lake to the left (distance ca. 1.5 km).

The bulk mineralogy clearly follows the general grain-size distribution with quartz showing some similarity with the pattern of silt content (Fig. 2b and e), and feldspar exhibiting a distinct similarity with the pattern of the sand content (Figs. 2a and f). The obvious enrichments of quartz in the silt and feldspar in the coarse fraction of the surface sediment can be directly traced back to cryogenic weathering processes within the active layer of the permafrost in the lake surrounding, which promote this grain-size dependent fractionation and accumulation (Konishchev, 1982; Schwamborn et al., 2008b).

The general patterns in mineralogy are also mirrored in the elemental composition, with group I elements exhibiting a distinct similarity to the distribution pattern of feldspars. Thus, group I elements can most likely be linked to the amount of plagioclase and K-feldspars (Fig. 2e) originating from the surrounding acidic volcanic rocks. The dominance of acidic volcanic rocks is also indicated by the relatively homogeneous distribution of group I elements in the sediments of the inlet streams and the source rocks surrounding the lake. Since carbonate rocks are very rare in the catchment of Lake El'gygytgyn, mostly occurring as vein fillings in the suevite below the lake sediments (Melles et al., 2011), the main sources for strontium can be attributed to Na-Ca-feldspars, replacing sodium or calcium (Cherniak and Watson, 1994), and to K-feldspars, with strontium and barium known to substitute potassium (El Bouseily and El Sokkary, 1975).

The apparent K_2O increase in the inlets and at the shelves of the northern and southern shore with respect to the respective source rocks implies an enrichment of potassium during cryogenic weathering and/or transport processes. This generally contradicts a higher grade of chemical weathering of the inlet stream deposits and surface sediments usually causing a depletion especially of Na, but also K and Ca (Nesbitt and Young, 1984). Furthermore, the RDA results of the element concentrations with grain-size parameters as explanatory variables show a clear correlation of the group I elements with the sand fraction (Fig. 4b). Consequently, elements of group I (e.g. K, Na, or Sr) might be used in sediment cores of Lake El'gygytgyn as indicators for coarser grain sizes (e.g. Wennrich et al., 2013).

5.2 Indications for sediment sources

The distinct clustering of group II elements in the east and southeast of the lake in combination with high concentrations of group II elements in the bedrock and inlet streams of the southeastern crater rim (Fig. 5b) suggest a bedrock source in the southeastern lake catchment. Especially Cr, Ni, Cu and Co, but also Fe_2O_3, were reported to have maximum values in the basaltic rocks (basalts, andesite-basalts) of the Koekvun' Formation (Belyi and Belaya, 1998) that pervasively outcrops along the southeastern section of the crater (Nowaczyk et al., 2002).

Simultaneously, the southeastern edge of the lake basin exhibits a pronounced silt maximum (Fig. 2b) that most likely can be traced back to the high flux of fluvial suspension from creek 49 (informally called "Lagerny Creek") as major inlet of Lake El'gygytgyn. During snow melt, Lagerny Creek produces the highest water and sediment discharge of all inlet streams in the range of 6.1 $m^3\ s^{-1}$ and 24.0 $g s^{-1}$, respectively (Fedorov et al., 2012).

A correspondence of group II elements and coarse silt (16–31 μm) and, to some degree, the medium silt (7–16 μm) and total silt fraction is not only supported by similarities in the spatial distribution patterns but also by the results of the RDA (Fig. 4b). Consequently, fluvial input of weathering products from the basaltic bedrock material via Lagerny Creek to the lake can be assumed as major source of group II elements. Nevertheless, group II elements exhibit a much more pronounced concentration gradient between the southeastern corner and the remaining lake basin compared to the silt content. This discrepancy most likely results from a very local source of group II elements, whereas the silt signal mirrors the general high input of silt-sized weathering products from the catchment into the lake that is further increased in the southeast by the high fluvial sediment input of Lagerny Creek.

The prevailing northward dispersion of this fluvial material along western lake shore (Figs. 2b and 5b) implies an anti-clockwise circulation pattern at the western lake shore, and thus, suggests northerly winds may be slightly dominant during the ice-free period as drivers of the current circulation system. But due to the poor sample resolution in this region this pattern may also be the result of interpolation artifacts.

According to down-core investigations on ICDP Site 5011-1 (Fig. 1) and pilot core PG1351 in the central part of Lake El'gygytgyn, Ti, Fe_2O_3, but also Cr and Ni typically are enriched during cold stages (Minyuk et al., 2007, 2011, 2013; Wennrich et al., 2013). Such sediments are usually characterized by low coarse silt to fine sand but higher clay and fine silt contents (Francke et al., 2013). This discrepancy implies a

fundamental change in the weathering and/or sedimentation settings in Lake El'gygytgyn under a perennial ice cover during glacial periods.

5.3 Indicators of post-depositional processes

The RDA results (Fig. 4b) as well as similarities in the distribution patterns of heavy metals, e.g. MnO, with those of clay, TOC and TN (Figs. 2c, 5c, e and f) strongly indicate group III elements in Lake El'gygytgyn surface sediments to follow the organic matter enriched fine fraction. The first suggests that group III elements are mainly bound to organic matter. Phosphorous and sulfur are typical components of lacustrine organic matter (Wetzel, 2001). Molybdenum as a catalyst for nitrogen fixation in living plants is generally accumulated in plant material (Bortels, 1930), but can also be fixed to the organic matter by early diagenetic processes (Robinson et al., 1993). But due to the high accordance of group III to clay, an incorporation of the heavy metals into crystal lattices of clay minerals (Lin and Puls, 2000; Tessier, 1992) has to be considered.

On the other hand, enhanced concentrations of heavy metals (Pb, As, Mo), but also P_2O_5, in the central basin of a fully-mixed Lake El'gygtygyn (Cremer et al., 2005) might partly be linked to the enhanced occurrence of Fe-oxides and -hydroxides (Table 1). In recent sediments from Lake Baikal and the San Francisco Bay, iron and manganese oxides have been shown to be a significant sink for P, Mo, Pb, As and other heavy metals by adsorption and co-precipitation (Lion et al., 1982; Müller et al., 2002).

Nevertheless, the occurrence of Fe-oxides and -hydroxides highlight the iron mineralogy at the sediment/water interface to clearly differ from those of Lake El'gygytgyn down-core sediments deposited during glacial periods, where higher Fe concentrations are linked to the diagenetic formation of vivianite ($(Fe)_3(PO_4)_2 \cdot 8\,H_2O$) under reducing pore-water conditions (Minyuk et al., 2007, 2013), with manganese incorporated as an impurity into the vivianite structure (Fagel et al., 2005).

5.4 Indicators of tectonic activity

In major parts of the Lake El'gygytgyn basin, mercury behaves like other group III elements and is positively correlated with the TOC content ($r^2 = 0.61$; Fig. 7). A similar coincidence of Hg and TOC was also observed in surficial sediments from Lake Baikal, with mercury as Hg^0 mainly absorbed onto organic matter (Gelety et al., 2005, 2007). This TOC-Hg analogy generally supports a scavenging of mercury by algae and/or suspended algal material as mentioned by Outridge et al. (2007) for lakes in the Canadian High Arctic.

An atmospheric source of mercury has been described for many remote lakes (e.g. Lorey and Driscoll, 1999; Cannon et al., 2003; Bindler et al., 2001) and might also contribute

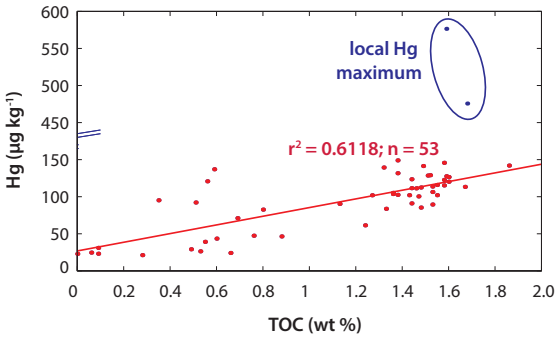

Fig. 7. Regression diagram of TOC [% wt/wt] vs. Hg [$\mu g\,kg^{-1}$] for surface sediment samples of Lake El'gygytgyn ($n = 55$). Linear regression line and coefficient of determination were calculated excluding the values of the local Hg maximum ($> 450 \mu g\,kg^{-1}$).

to the Hg budget of Lake El'gygytgyn. But the heterogeneous distribution of Hg in both the surface sediments and the tributaries with a very pronounced maximum in one region of the lake floor implies a local Hg source. The most likely source of the elevated mercury contents are volcanic formations especially of the outer zone of the OCVB outcropping around the lake, which are known not only for its gold and silver resources, but also for rich mercury ore deposits (Sidorov et al., 2011). Interestingly, the peak concentrations in the inlet streams of the southeastern catchment fit the result of a gas mercury survey in the lake catchment in 2003 yielding elevated Hg values in the soil air just in this region of the El'gygytgyn crater (Fedorov and Kupolov, 2005). These were initially interpreted as tracers of tectonic activity along a NW–SE striking major boundary within the OCVB and a fault system associated with the Malyi-Chaun graben zone along the southern shore. Similar fault-related mercury anomalies in soils have also been reported from the Baikal Rift Zone (Koval et al., 2006, 1999), and can presumably be traced back to tectonically-driven mercury mobilization as described for Hg deposits in Spain (e.g. Jébrak and Hernandez, 1995).

Although recent seismic activity is reportedly low for the El'gygytgyn region (Fujita et al., 2002), minor faults mapped within the lake sediment stratigraphy during seismic surveys (Niessen et al., 2007) indicate ongoing neotectonic activity. Such fault re-activation explains well the elevated Hg values in the inlet stream sediments. As no obvious transport process exists to explain the Hg maximum at two sites in the lake surface sediments, a tectonic origin of the mercury anomaly in the lake center cannot be excluded, even though the seismic surveys did not yield any active faults in the respective lake area. Thus, further research is necessary to reveal the mercury sources and its cycle in Lake El'gygytgyn and to validate the theory of tectonically triggered Hg mobilization. Nevertheless, detailed Hg downcore analyses of the

3.6 Ma record from the lake may have the potential to get new insights into the seismic history of this region, and/or the mechanisms that trigger mass movements.

6 Conclusions

A multi-proxy approach combining sedimentological, geochemical and mineralogical analyses with statistical methods was performed on a set of 55 surface sediment samples from Lake El'gygytgyn, NE Russia. The results of this study provide a detailed understanding of the major physical and chemical processes controlling modern sedimentation in this remote Arctic crater lake.

1. The spatial distribution of mean grain-size, sand and feldspar contents, and the concentration of group I elements (Ba, Sr, Al_2O_3, Na_2O, CaO, and K_2O) confirms the existence of a wind-induced two-cell current system triggering the surface-water circulation in the lake. Furthermore, mean grain-size strongly suggests transport of relatively coarse sediment from the southern shore towards the lake center as a result of the re-suspension of clay and silt-sized material during heavy storm events. High correlation of group I elements with the coarse fraction suggests that elements like sodium, calcium or strontium can be used as grain-size indicators in downcore samples of Lake El'gygytgyn.

2. Mafic rock related elements, such as Cr, Cu, Zn, V, Ni, and Co, can be directly linked to basaltic volcanic rocks in the southeastern quadrant of the crater, implying a significant source-rock effect controlling the spatial distribution of these elements. The largely northward dispersion of the silt-sized basaltic weathering products confirms the suggestion of a two-cell surface current system with a dominating anti-clock wise circulation at the southeastern shore.

3. The distribution of MnO and heavy elements like Pb, Mo, As and Hg, but also P_2O_5 and SO_2, correlates with the organic matter and clay contents, which are generally enriched in the deepest parts of the lake basin. This correlation might be indicative of the sorption or co-precipitation of these elements with Fe and Mn hydroxides and oxides, and an additional fixation to organic matter or clay minerals in the oxic surface sediment layer.

4. Ongoing tectonic activity along a NW–SE striking fault zone in the lake catchment is indicated by variable mercury concentrations in the inlet stream deposits, being distinctly elevated in the southeastern corner of the lake catchment. A local Hg maximum in the lake center is not yet understood, but might point to ongoing neotectonic activity within the lake area as well.

These results are of essential importance for deciphering the climatic and environmental history of the area since 3.6 Ma from the composition of the sediments drilled on ICDP Site 5011-1 within the scope of the international El'gygytgyn Drilling Project.

Acknowledgements. We thank Nicole Mantke (University of Cologne), K. Bienert and Sylvia Dorn (University Leipzig) and numerous students for her technical assistance in the laboratory, and Rita Fröhlking (AWI Bremerhaven) for performing the XRD analyses. Furthermore, we would like to thank our funding agencies, namely the International Continental Scientific Drilling Program (IPDP), German Federal Ministry of Education and Research (BMBF; grant 03G0642), US National Science Foundation (grants OPP 007122, 96-15768, and 0002643), Russian Academy of Sciences, Austrian Federal Ministry of Science and Research and all the participants of the International "El'gygytgyn Drilling Project" for support and collaborations. Financial support of the pre-site survey was provided by the German Federal Ministry for Education and Research (BMBF), grant no. 03G0586A, and the US National Science Foundation (NSF), OPP Award #96-15768, Atmospheric Sciences Award 99-05813, and OPP Award #00-02643, and the Russian Fund of Basic Research, and CRDF. Finally we appreciate the comments and suggestions of Denis-Didier Rousseau, Pierre Francus and an anonymous reviewer who helped to improve the manuscript.

Edited by: D.-D. Rousseau

References

Allen, J. R. M., Brandt, U., Brauer, A., Hubberten, H.-W., Huntley, B., Keller, J., Kraml, M., Mackensen, A., Mingram, J., Negendank, J. F. W., Nowaczyk, N. R., Oberhänsli, H., Watts, W. A., Wulf, S., and Zolitschka, B.: Rapid environmental changes in southern Europe during the last glacial period, Nature, 400, 740–743, doi:10.1038/23432, 1999.

Asikainen, C. A., Francus, P., and Brigham-Grette, J.: Sedimentology, clay mineralogy and grain-size as indicators of 65 ka of climate change from El'gygytgyn Crater Lake, Northeastern Siberia, J. Paleolimnol., 37, 105–122, doi:10.1007/s10933-006-9026-5, 2007.

Barr, I. D. and Clark, C. D.: Glaciers and climate in Pacific Far NE Russia during the Last Glacial Maximum, J. Quaternary Sci., 26, 227–237, doi:10.1002/jqs.1450, 2011.

Belyi, V.: Structure and formation of the El´gygytgyn Basin (Anadyr Mountains), Geomorphologia, 1, 31–41, 2001.

Belyi, V.: Impactite generation in the El'gygytgyn depression, northeast Russia, as a volcanic phenomenon. 2. On the petrography and geochemistry of the impactites, J. Volcanol. Seismol., 4, 149–163, doi:10.1134/s0742046310030012, 2010.

Belyi, V. and Belaya, B.: Late stage of the Okhotsk-Chukchi Volcanogenic Belt development (upstream of the Enmyvaam River), NEISRI FEB RAS, Magadan, Russia, 108 pp., 1998.

Belyi, V. and Raikevich, M. I.: The El'gygytgyn lake basin (geological structure, morphostructure, impactites, problems of investigation and preservation of nature), NEISRI FEB RAS, Magadan, 27 pp., 1994.

Bindler, R., Renberg, I., Appleby, P. G., Anderson, N. J., and Rose, N. L.: Mercury Accumulation Rates and Spatial Patterns in Lake Sediments from West Greenland:? A Coast to Ice Margin Transect, Environ. Sci. Technol., 35, 1736–1741, doi:10.1021/es0002868, 2001.

Bloesch, J.: Mechanisms, measurement and importance of sediment resuspension in lakes, Mar. Freshwater Res., 46, 295–304, 1995.

Blott, S. J. and Pye, K.: GRADISTAT: a grain size distribution and statistics package for the analysis of unconsolidated sediments, Earth Surf. Processes Land., 26, 1237–1248, doi:10.1002/esp.261, 2001.

Bortels, H.: Molybdän als Katalysator bei der biologischen Stickstoffbindung, Arch. Mikrobiol., 1, 333–342, doi:10.1007/bf00510471, 1930.

Brigham-Grette, J., Haug, G. H., and Climate Working Group: Climate Dynamics and Global Environments: A Community Vision for the Next Decade in ICDP, Continental scientific drilling: a decade of progress and challenges for the future, 53–94, 2007a.

Brigham-Grette, J., Melles, M., Minyuk, P., and Scientific Party: Overview and significance of a 250 ka paleoclimate record from El'gygytgyn Crater Lake, NE Russia, J. Paleolimnol., 37, 1–16, doi:10.1007/s10933-006-9017-6, 2007b.

Cannon, W. F., Dean, W. E., and Bullock, J. H.: Effects of Holocene climate change on mercury deposition in Elk Lake, Minnesota: The importance of eolian transport in the mercury cycle, Geology, 31, 187–190, doi:10.1130/0091-7613(2003)031<0187:eohcco>2.0.co;2, 2003.

Cherniak, D. J. and Watson, E. B.: A study of strontium diffusion in plagioclase using Rutherford backscattering spectroscopy, Geochim. Cosmochim. Ac., 58, 5179–5190, 1994.

Cohen, A. S.: Scientific drilling and biological evolution in ancient lakes: lessons learned and recommendations for the future, Hydrobiologia, 682, 3–25, doi:10.1007/s10750-010-0546-7, 2012.

Côté, M. M. and Burn, C. R.: The oriented lakes of Tuktoyaktuk Peninsula, Western Arctic Coast, Canada: a GIS-based analysis, Permafrost Periglac., 13, 61–70, doi:10.1002/ppp.407, 2002.

Cremer, H. and Wagner, B.: The diatom flora in the ultra-oligotrophic Lake El'gygytgyn, Chukotka, Polar Biol., 26, 105–114, doi:10.1007/s00300-002-0445-0, 2003.

Cremer, H., Wagner, B., Juschus, O., and Melles, M.: A microscopical study of diatom phytoplankton in deep crater Lake El'gygytgyn, Northeast Siberia, Algological Studies, 116, 147–169, 2005.

Cressie, N. A. C.: Statistics for spatial data, Wiley Series in Probability and Mathematical Statistics, John Wiley & Sons, 900 pp., 1991.

El Bouseily, A. M. and El Sokkary, A. A.: The relation between Rb, Ba and Sr in granitic rocks, Chem. Geol., 16, 207–219, 1975.

Emmermann, R. and Lauterjung, J.: Double X-ray analysis of cuttings and rock flour: a powerful tool for rapid and reliable determination of borehole lithostratigraphy, Scientific Drilling, 1, 269–282, 1990.

Fagel, N., Alleman, L. Y., Granina, L., Hatert, F., Thamo-Bozso, E., Cloots, R., and André, L.: Vivianite formation and distribution in Lake Baikal sediments, Global Planet. Change, 46, 315–336, 2005.

Fedorov, G. and Kupolov, A.: Gas Mercury Survey in the El'gygytgyn Crater, in: The Expedition El'gygytgyn Lake 2003 (Siberian Arctic), edited by: Melles, M., Minyuk, P., Brigham-Grette, J., and Juschus, O., Reports on Polar and Marine Research, 509, 69–70, 2005.

Fedorov, G., Nolan, M., Brigham-Grette, J., Bolshiyanov, D., Schwamborn, G., and Juschus, O.: Lake El'gygytgyn water and sediment balance components overview and its implications for the sedimentary record, Clim. Past Discuss., 8, 3977–4001, doi:10.5194/cpd-8-3977-2012, 2012.

Francke, A., Wennrich, V., Sauerbrey, M., Juschus, O., Melles, M., and Brigham-Grette, J.: Multivariate statistic and time series analyses of grain-size data in Quaternary sediments of Lake El'gygytgyn, NE Russia, Clim. Past Discuss., 9, 217–244, doi:10.5194/cpd-9-217-2013, 2013.

Fujita, K., Mackey, K. G., McCaleb, R. C., Gubina, L. V., Kovalev, V. N., Imaev, V. S., and Smirnov, V. N.: Seismicity of Chukotka, northeastern Russia, in: Tectonic Evolution of the Bering Shelf-Chukchi Sea-Arctic Margin and Adjacent Landmasses, edited by: Miller, L., Grantz, A., and Klemperer, S. L., Geol. S. Am. S., 360, 259–272, 2002.

Gasse, F., Vidal, L., Develle, A.-L., and Van Campo, E.: Hydrological variability in the Northern Levant: a 250 ka multi-proxy record from the Yammoûneh (Lebanon) sedimentary sequence, Clim. Past, 7, 1261–1284, doi:10.5194/cp-7-1261-2011, 2011.

Gelety, V., Gapon, A., Kalmychkov, G., Parkhomenko, I. Y., and Kostrova, S.: Mercury in the surficial bottom sediments of lake Baikal, Geochem. Int., 43, 220–226, 2005.

Gelety, V., Kalmykov, G., and Parkhomenko, I.: Mercury in the sedimentary deposits of Lake Baikal, Geochem. Int., 45, 170–177, doi:10.1134/s001670290702005x, 2007.

Glotov, V. Ye. and Zuev, S. A.: Hydrological characteristics of Lake El'gygytgyn, Kolyma, 3–4, 18–23, 1995.

Glushkova, O. Yu.: Geomorphological correlation of Late Pleistocene glacial complexes of Western and Eastern Beringia, Quaternary Sci. Rev., 20, 405–417, doi:10.1016/s0277-3791(00)00108-6, 2001.

Glushkova, O. Yu and Smirnov, V. N.: Highest Lake Terraces, in: The expedition El'gygytgyn Lake 2003 (Siberian Arctic), edited by: Melles, M., Minyuk, P., Brigham-Grette, J., and Juschus, O., Reports on Polar and Marine Research, 509, 85–88, 2005.

Glushkova, O. Yu. and Smirnov, V. N.: Pliocene to Holocene geomorphic evolution and paleogeography of the El'gygytgyn Lake region, NE Russia, J. Paleolimnol., 37, 37–47, doi:10.1007/s10933-006-9021-x, 2007.

Gurov, E. P. and Gurova, Ye.: Stages of shock metamorphism of silicic volcanic rocks in the El'gygytgyn meteorite crater, Chukotka, Dokl. Acad. Nauk SSSR.: Earth Science subsection, 249, 121–123, 1979.

Gurov, E. P., Koeberl, C., Reimold, W. U., Brandstätter, F., and Amare, K.: Shock metamorphism of siliceous volcanic rocks of the El'gygytgyn impact crater (Chukotka, Russia), Geol. S. Am. S., 384, 391–391, 2005.

Gurov, E. P., Koeberl, C., and Yamnichenko, A.: El'gygytgyn impact crater, Russia: Structure, tectonics, and morphology, Meteorit. Planet. Sci., 42, 307–319, 2007.

Halfman, J. D. and Scholz, C. A.: Suspended Sediments in Lake Malawi, Africa: A Reconnaissance Study, J. Great Lakes Res., 19, 499–511, 1993.

Hawley, N. and Lee, C.-H.: Sediment resuspension and transport in Lake Michigan during the unstratified period, Sedimentology, 46, 791–805, doi:10.1046/j.1365-3091.1999.00251.x, 1999.

Jébrak, M. and Hernandez, A.: Tectonic deposition of mercury in the Almadén district, Las Cuevas deposit, Spain, Miner. Deposita, 30, 413–423, doi:10.1007/bf00196401, 1995.

Juschus, O., Melles, M., Gebhardt, A. C., and Niessen, F.: Late Quaternary mass movement events in Lake El'gygytgyn, North-eastern Siberia, Sedimentology, 56, 2155–2174, doi:10.1111/j.1365-3091.2009.01074.x, 2009.

Juschus, O., Pavlov, M., Schwamborn, G., Preusser, F., Fedorov, G., and Melles, M.: Late Quaternary lake-level changes of Lake El'gygytgyn, NE Siberia, Quaternary Res., 76, 441–451, doi:10.1016/j.yqres.2011.06.010, 2011.

Kelley, S. P., Spicer, R. A., and Herman, A. B.: New Ar-40/Ar-39 dates for Cretaceous Chauna Group tephra, north-eastern Russia, and their implications for the geologic history and floral evolution of the North Pacific region, Cretaceous Res., 20, 97–106, 1999.

Konishchev, V. N.: Characteristics of Cryogenic Weathering in the Permafrost Zone of the European USSR, Arctic Alpine Res., 14, 261–265, 1982.

Koval, P. V., Kalmychkov, G. V., Gelety, V. F., Leonova, G. A., Medvedev, V. I., and Andrulaitis, L. D.: Correlation of natural and technogenic mercury sources in the Baikal polygon, Russia, J. Geochem. Explor., 66, 277–289, 1999.

Koval, P., Udodov, Y., San'kov, V., Yasenovskii, A., and Andrulaitis, L.: Geochemical activity of faults in the Baikal Rift Zone (Mercury, Radon, and Thoron), Dokl. Earth Sci., 409, 912–915, doi:10.1134/s1028334x06060171, 2006.

Layer, P. W.: Argon-40/argon-39 age of the El'gygytgyn impact event, Chukotka, Russia, Meteorit. Planet. Sci., 35, 591–599, 2000.

Lin, Z. and Puls, R. W.: Adsorption, desorption and oxidation of arsenic affected by clay minerals and aging process, Environ. Geol., 39, 753–759, doi:10.1007/s002540050490, 2000.

Lion, L. W., Altmann, R. S., and Leckie, J. O.: Trace-metal adsorption characteristics of estuarine particulate matter: evaluation of contributions of iron/manganese oxide and organic surface coatings, Environ. Sci. Technol., 16, 660–666, doi:10.1021/es00104a007, 1982.

Lorey, P. and Driscoll, C. T.: Historical Trends of Mercury Deposition in Adirondack Lakes, Environ. Sci. Technol., 33, 718–722, doi:10.1021/es9800277, 1999.

Lozhkin, A. V., Anderson, P. M., Matrosova, T. V., Minyuk, P. S., Brigham-Grette, J., and Melles, M.: Continuous Record of Environmental Changes in Chukotka during the Last 350 Thousand Years, Russ. J. Pac. Geol., 1, 550–555, doi:10.1134/s1819714007060048, 2007.

Melles, M., Minyuk, P., Brigham-Grette, J., and Juschus, O (Eds.).: The Expedition El´gygytgyn Lake 2003 (Siberian Arctic), Reports on Polar and Marine Research, 509, 139 pp., 2005.

Melles, M., Brigham-Grette, J., Glushkova, O. Yu., Minyuk, P. S., Nowaczyk, N. R., and Hubberten, H. W.: Sedimentary geochemistry of core PG1351 from Lake El'gygytgyn – a sensitive record of climate variability in the East Siberian Arctic during the past three glacial-interglacial cycles, J. Paleolimnol., 37, 89–104, doi:10.1007/s10933-006-9025-6, 2007.

Melles, M., Brigham-Grette, J., Minyuk, P., Koeberl, C., Andreev, A., Cook, T., Fedorov, G., Gebhardt, C., Haltia-Hovi, E., Kukkonen, M., Nowaczyk, N., Schwamborn, G., Wennrich, V., and and the El´gygytgyn Scientific Party: The Lake El'gygytgyn Scientific Drilling Project – Conquering Arctic Challenges through Continental Drilling, Scientific Drilling, 11, 29–40, 2011.

Melles, M., Brigham-Grette, J., Minyuk, P. S., Nowaczyk, N. R., Wennrich, V., DeConto, R. M., Anderson, P. M., Andreev, A. A., Coletti, A., Cook, T. L., Haltia-Hovi, E., Kukkonen, M., Lozhkin, A. V., Rosén, P., Tarasov, P., Vogel, H., and Wagner, B.: 2.8 Million Years of Arctic Climate Change from Lake El'gygytgyn, NE Russia, Science, 337, 315–320, doi:10.1126/science.1222135, 2012.

Minyuk, P. S., Brigham-Grette, J., Melles, M., Borkhodoev, V. Ya., and Glushkova, O. Yu.: Inorganic geochemistry of El'gygytgyn Lake sediments (northeastern Russia) as an indicator of paleoclimatic change for the last 250 kyr, J. Paleolimnol., 37, 123–133, doi:10.1007/s10933-006-9027-4, 2007.

Minyuk, P., Borkhodoev, V. Ya., and Goryachev, N.: Geochemical characteristics of sediments from Lake El'gygytgyn, Chukotka Peninsula, as indicators of climatic variations for the past 350 ka, Dokl. Earth Sci., 436, 94–97, doi:10.1134/s1028334x11010181, 2011.

Minyuk, P. S., Borkhodoev, V. Ya., and Wennrich, V.: Inorganic data from El'gygytgyn Lake sediments: stages 6–11, Clim. Past Discuss., accepted, 2013.

Mock, C. J., Bartlein, P. J., and Anderson, P. M.: Atmospheric circulation patterns and spatial climatic variations in Beringia, Int. J. Climatol., 18, 1085–1104, doi:10.1002/(SICI)1097-0088(199808)18:10<1085::AID-JOC305>3.0.CO;2-K, 1998.

Müller, B., Granina, L., Schaller, T., Ulrich, A., and Wehrli, B.: P, As, Sb, Mo, and Other Elements in Sedimentary Fe/Mn Layers of Lake Baikal, Environ. Sci. Technol., 36, 411–420, doi:10.1021/es010940z, 2002.

Nekrasov, I. A.: About the origin and history of the El'gygytgyn Lake basin, Geol. Geofiz., 1, 47–59, 1963.

Nesbitt, H. W. and Young, G. M.: Prediction of some weathering trends of plutonic and volcanic rocks based on thermodynamic and kinetic considerations, Geochim. Cosmochim. Ac., 48, 1523–1534, 1984.

Niessen, F., Gebhardt, A. C., Kopsch, C., and Wagner, B.: Seismic investigation of the El'gygytgyn impact crater lake (Central Chukotka, NE Siberia): preliminary results, J. Paleolimnol., 37, 49–63, doi:10.1007/s10933-006-9022-9, 2007.

Nolan, M.: Analysis of local AWS and NCEP/NCAR reanalysis data at Lake El'gygytgyn, and its implications for maintaining multi-year lake-ice covers, Clim. Past Discuss., 8, 1443–1483, doi:10.5194/cpd-8-1443-2012, 2012.

Nolan, M. and Brigham-Grette, J.: Basic hydrology, limnology, and meteorology of modern Lake El'gygytgyn, Siberia, J. Paleolimnol., 37, 17–35, doi:10.1007/s10933-006-9020-y, 2007.

Nolan, M., Liston, G., Prokein, P., Brigham-Grette, J., Sharpton, V. L., and Huntzinger, R.: Analysis of lake ice dynamics and morphology on Lake El'gygytgyn, NE Siberia, using synthetic aperture radar (SAR) and Landsat, J. Geophys. Res.-Atmos., 108, 8162, doi:10.1029/2001JD000934, 2002.

Nowaczyk, N. R., Minyuk, P., Melles, M., Brigham-Grette, J., Glushkova, O. Yu., Nolan, M., Lozhkin, A. V., Stetsenko, T. V., Andersen, P. M., and Forman, S. L.: Magnetostratigraphic results from impact crater lake El'gygytgyn, northeastern Siberia: a possibly 300 kyr long terrestrial paleoclimate record from the Arctic, Geophys. J. Int., 150, 109–126, doi:10.1046/j.1365-246X.2002.01625.x, 2002.

Nowaczyk, N. R., Melles, M., and Minyuk, P.: A revised age model for core PG1351 from Lake El'gygytgyn, Chukotka, based on magnetic susceptibility variations tuned to northern hemisphere insolation variations, J. Paleolimnol., 37, 65–76, doi:10.1007/s10933-006-9023-8, 2007.

Oliver, M. A. and Webster, R.: Kriging: a method of interpolation for geographical information systems, Int. J. Geogr. Inf. Syst., 4, 313–332, doi:10.1080/02693799008941549, 1990.

Outridge, P. M., Sanei, H., Stern, G. A., Hamilton, P. B., and Goodarzi, F.: Evidence for Control of Mercury Accumulation Rates in Canadian High Arctic Lake Sediments by Variations of Aquatic Primary Productivity, Environ. Sci. Technol., 41, 5259–5265, doi:10.1021/es070408x, 2007.

Petschick, R., Kuhn, G., and Gingele, F.: Clay mineral distribution in surface sediments of the South Atlantic: sources, transport, and relation to oceanography, Mar. Geol., 130, 203–229, 1996.

Robinson, C., Shimmield, G., and Creer, K.: Geochemistry of Lago Grande di Monticchio, S. Italy, in: Paleolimnology of European Maar Lakes, edited by: Negendank, J. and Zolitschka, B., Lecture Notes in Earth Sciences, Springer Berlin/Heidelberg, 317–332, 1993.

Sauerbrey, M., Juschus, O., Gebhardt, C., Wennrich, V., Nowaczyk, N., and Melles, M.: Mass movement deposits in the 3.6Ma sediment record of Lake El'gygytgyn, Chukotka, NE Siberia: classification, distribution and preliminary interpretation, Clim. Past Discuss., accepted, 2013.

Schwamborn, G., Meyer, H., Fedorov, G., Schirrmeister, L., and Hubberten, H.: Ground ice and slope sediments archiving late Quaternary paleoenvironment and paleoclimate signals at the margins of El'gygytgyn Impact Crater, NE Siberia, Quaternary Res., 66, 259–272, 2006.

Schwamborn, G., Fedorov, G., Schirrmeister, L., Meyer, H., and Hubberten, H. W.: Periglacial sediment variations controlled by late Quaternary climate and lake level change at Elgygytgyn Crater, Arctic Siberia, Boreas, 37, 55–65, doi:10.1111/j.1502-3885.2007.00011.x, 2008a.

Schwamborn, G., Förster, A., Diekmann, B., Schirrmeister, L., and Fedorov, G.: Mid- to Late-Quaternary Cryogenic Weathering Conditions at Elgygytgyn Crater, Northeastern Russia: Inference from Mineralogical and Microtextural Properties of the Sediment Record, Ninth International Conference On Permafrost, Fairbanks, 1601–1606, 2008b.

Schwamborn, G., Fedorov, G., Ostanin, N., Schirrmeister, L., Andreev, A., and the El'gygytgyn Scientific Party: Depositional dynamics in the El'gygytgyn Crater margin: implications for the 3.6 Ma old sediment archive, Clim. Past, 8, 1897–1911, doi:10.5194/cp-8-1897-2012, 2012.

Sidorov, A., Chekhov, A., Volkov, A., and Alekseev, V.: Metallogeny of the inner and outer zones of the Okhotsk-Chukotsk volcanogenic belt, Dokl. Earth Sci., 439, 949–954, doi:10.1134/s1028334x11060122, 2011.

Stone, D. B., Layer, P. W., and Raikevich, M. I.: Age and paleomagnetism of the Okhotsk-Chukotka Volcanic Belt (OCVB) near Lake El'gygytgyn, Chukotka, Russia, Stephan Mueller Special Publication Series, 4, 243–260, 2009.

Swann, G. E. A., Leng, M. J., Juschus, O., Melles, M., Brigham-Grette, J., and Sloane, H. J.: A combined oxygen and silicon diatom isotope record of Late Quaternary change in Lake El'gygytgyn, North East Siberia, Quaternary Sci. Rev., 29, 774–786, doi:10.1016/j.quascirev.2009.11.024, 2010.

Tessier, A.: Sorption of trace elements on natural particles in oxic environments, in: Environmental particles, edited by: Buffle, J. and van Leeuwen, H. P., Lewis Publishers, Chelsea, 425–453, 1992.

Treshnikov, A. F.: Atlas of the Arctic, Main Department of Geodesy and Cartography under the Council of Ministers of the USSR, Moscow, 1985.

Viehberg, F. A., Ülgen, U. B., Damcı, E., Franz, S. O., Ön, S. A., Roeser, P. A., Çağatay, M. N., Litt, T., and Melles, M.: Seasonal hydrochemical changes and spatial sedimentological variations in Lake Iznik (NW Turkey), Quaternary Int., 274, 102–111, doi:10.1016/j.quaint.2012.05.038, 2012.

Vogel, H., Wessels, M., Albrecht, C., Stich, H. B., and Wagner, B.: Spatial variability of recent sedimentation in Lake Ohrid (Albania/Macedonia), Biogeosciences, 7, 3333–3342, doi:10.5194/bg-7-3333-2010, 2010.

Vogt, C.: Regional and temporal variations of mineral assemblages in Arctic Ocean sediments as climatic indicator during glacial/interglacial changes, Reports on Polar Research, 251, 1–309, 1997.

Vogt, C., Lauterjung, J., and Fischer, R. X.: Investigation of the Clay Fraction ($< 2\,\mu$m) of the Clay Minerals Society Reference Clays, Clay. Clay Miner., 50, 388–400, 2002.

Wennrich, V., Minyuk, P., Borkhodoev, V., Francke, A., Ritter, B., Nowaczyk, N., Haltia-Hovi, E. M., Brigham-Grette, J., Melles, M., and El'gygytgyn Science Party.: Pliocene and Pleistocene climate and environmental history of Lake El'gygytgyn/ NE Russia based on high-resolution inorganic geochemistry data, Clim. Past, this issue, in prep., 2013.

Wetzel, R. G.: Limnology : lake and river ecosystems, 3. Edn., Elsevier Academic Press, San Diego, 1006 pp., 2001.

Yanase, W. and Abe-Ouchi, A.: The LGM surface climate and atmospheric circulation over East Asia and the North Pacific in the PMIP2 coupled model simulations, Clim. Past, 3, 439–451, doi:10.5194/cp-3-439-2007, 2007.

3 Multivariate statistic and time series analyses of grain-size data in Quaternary sediments of Lake El'gygytgyn, NE Russia

Journal article (2013):
Francke, A., Wennrich, V., Sauerbrey, M., Juschus, O., Melles, M., and Brigham-Grette, J.: Multivariate statistic and time series analyses of grain-size data in Quaternary sediments of Lake El'gygytgyn, NE Russia, Clim. Past, 9, 2459-2470, 10.5194/cp-9-2459-2013, 2013.

Clim. Past, 9, 2459–2470, 2013
www.clim-past.net/9/2459/2013/
doi:10.5194/cp-9-2459-2013

Climate of the Past
Open Access

Multivariate statistic and time series analyses of grain-size data in quaternary sediments of Lake El'gygytgyn, NE Russia

A. Francke[1], V. Wennrich[1], M. Sauerbrey[1], O. Juschus[2], M. Melles[1], and J. Brigham-Grette[3]

[1]University of Cologne, Institute for Geology and Mineralogy, Cologne, Germany
[2]Eberswalde University for Sustainable Development, Eberswalde, Germany
[3]University of Massachusetts, Department of Geosciences, Amherst, USA

Correspondence to: A. Francke (alexander.francke@uni-koeln.de)

Received: 14 December 2012 – Published in Clim. Past Discuss.: 14 January 2013
Revised: 20 September 2013 – Accepted: 3 October 2013 – Published: 5 November 2013

Abstract. Lake El'gygytgyn, located in the Far East Russian Arctic, was formed by a meteorite impact about 3.58 Ma ago. In 2009, the International Continental Scientific Drilling Program (ICDP) at Lake El'gygytgyn obtained a continuous sediment sequence of the lacustrine deposits and the upper part of the impact breccia. Here, we present grain-size data of the past 2.6 Ma. General downcore grain-size variations yield coarser sediments during warm periods and finer ones during cold periods. According to principal component analysis (PCA), the climate-dependent variations in grain-size distributions mainly occur in the coarse silt and very fine silt fraction. During interglacial periods, accumulation of coarser material in the lake center is caused by redistribution of clastic material by a wind-induced current pattern during the ice-free period. Sediment supply to the lake is triggered by the thickness of the active layer in the catchment and the availability of water as a transport medium. During glacial periods, sedimentation at Lake El'gygytgyn is hampered by the occurrence of a perennial ice cover, with sedimentation being restricted to seasonal moats and vertical conduits through the ice. Thus, the summer temperature predominantly triggers transport of coarse material into the lake center. Time series analysis that was carried out to gain insight into the frequency of the grain-size data showed variations predominately on 98.5, 40.6, and 22.9 kyr oscillations, which correspond to Milankovitch's eccentricity, obliquity and precession bands. Variations in the relative power of these three oscillation bands during the Quaternary suggest that sedimentation processes at Lake El'gygytgyn are dominated by environmental variations caused by global glacial–interglacial variations (eccentricity, obliquity), and local insolation forcing and/or latitudinal teleconnections (precession), respectively.

1 Introduction

The polar regions are known to play a crucial but not yet well understood role within the global climate system (Washington and Meehl, 1996; Johannessen et al., 2004), influencing both the oceanic and the atmospheric circulation. The recent global warming trend has been, and is predicted to be, most pronounced in the Arctic (ACIA, 2004; Serreze and Francis, 2006). However, rather little is known about the natural and environmental variability on geological timescales. Our current knowledge on the Cenozoic climate evolution of the Arctic has long been based on sparse, often discontinuous marine and terrestrial paleorecords of the Arctic Ocean and adjacent landmasses (Thiede et al., 1998; Moran et al., 2006; Axford et al., 2009; Pienitz et al., 2009; Zech et al., 2011).

The first continuous Pliocene–Pleistocene sediment record in the terrestrial Arctic was recovered in 2009 during a deep drilling campaign of the International Continental Scientific Drilling Program (ICDP) at Lake El'gygytgyn in the Far East Russian Artic (Fig. 1; Melles et al., 2011). Pilot studies on Lake El'gygytgyn sediments covering the last 2–3 glacial–interglacial cycles had already demonstrated the usability of this archive for paleoclimate reconstructions (e.g. Brigham-Grette et al., 2007; Melles et al., 2007; Niessen et al., 2007). Initial results from the upper part

Published by Copernicus Publications on behalf of the European Geosciences Union.

of the 318 m-long sediment record in central parts of the lake (ICDP site 5011-1) provided first details of Quaternary history, focusing on interglacial variability during the past 2.8 Myr (Melles et al., 2012).

Here, we present new results of granulometric analyses on ICDP core 5011-1 throughout the past 2.6 Myr. Grain-size data have extensively been used before as a paleoenvironmental and -climatological proxy on long terrestrial and lacustrine sedimentary records, including those from the Chinese Loess Plateau (e.g. An et al., 1991; Sun and Huang, 2006; Sun et al., 2006) and from lakes Baikal (Kashiwaya et al., 1998, 2001) and Biwa (Kashiwaya et al., 1987). At Lake El'gygytgyn, previous studies of grain-size variations are widely restricted to the sediments formed during the past 65 ka (Asikainen et al., 2007). During this period, particle-size variations were predominantly controlled by the regional climatic settings and their impacts on the physical properties in the lake and its catchment. Our grain-size investigations on ICDP core 5011-1 extend the results from this early research to the entire Quaternary. Furthermore, we incorporated more recent findings on the modern climatological, hydrological, and sedimentological settings (Fedorov et al., 2013; Nolan et al., 2013; Wennrich et al., 2013a). To better understand the sedimentological processes operating in Lake El'gygytgyn, we used principal component analysis (PCA) to detect dominating variations in the grain-size distributions, and we employed time series analysis to reveal oscillations in the granulometric data and their relative dominance over time.

2 Site information

Lake El'gygytgyn is located in the Far East Russian Arctic, in the central part of the Chukchi Peninsula (67°30′ N, 172°05′ E, 492 m a.s.l.; Fig. 1). It is formed within a meteorite impact crater (e.g. Dietz and McHone, 1977; Gurov et al., 1979) dated to about 3.58 Ma (Layer, 2000). The lake has a nearly circular shape with a diameter of about 12 km and a depth of about 175 m (Nolan and Brigham-Grette, 2007), whereas the catchment confined by the crater rim measures about 18 km in diameter (corresponding to 293 km^2). Today, the lake is not located in the center of the crater but slightly displaced to the southeast, resulting in an asymmetric catchment area (Fig. 1).

The El'gygytgyn crater region is part of the central Chukchi sector of the Okhotsk–Chukchi volcanic belt (Gurov and Gurova, 1979; Gurov et al., 2007). It is dominated by acid volcanic rocks, ignimbrites and tuffaceous clastic rocks of the late Cretaceous (e.g. Gurov et al., 2007; Stone et al., 2009). The lake is surrounded by continuous permafrost, whose onset can presumably be traced back to the late Pliocene (Glushkova and Smirnov, 2007), and which is assumed to have a thickness of about 330–360 m with an unfrozen talik underneath the lake today (Mottaghy et al., 2013). The recent geomorphologic shape of the lake

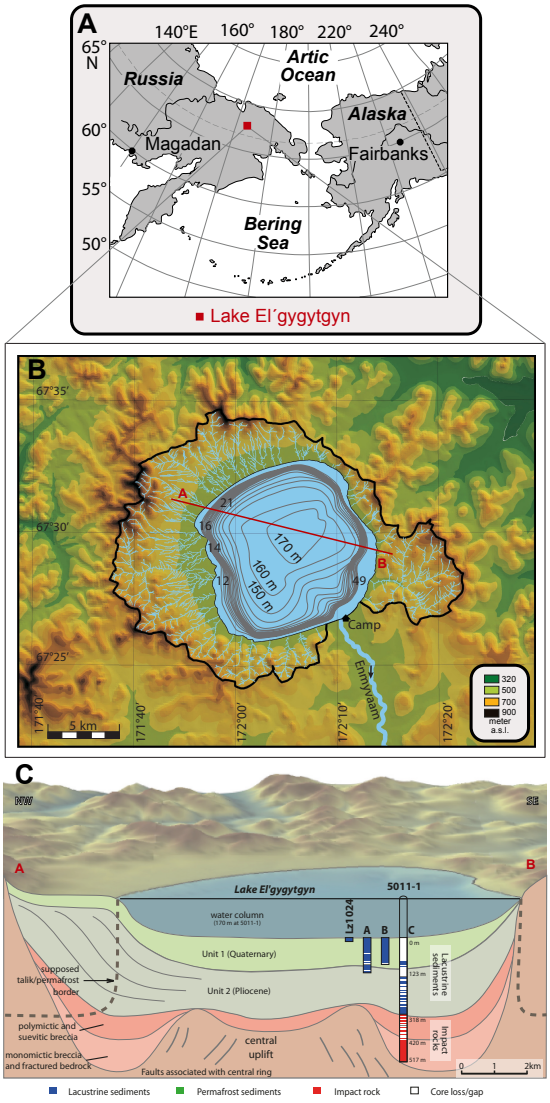

Fig. 1. (A) Location of Lake El'gygytgyn in the Far East Russian Artic; **(B)** bathymetric map of the lake and topographic map of the catchment area, including the approximately 50 inlet streams and the Enmyvaam River outlet (Fedorov and Kupolov, 2005); red line: profile A to B. **(C)** Schematic profile A to B with the locations of the pilot core Lz 1024 and the three holes (A, B and C) at ICDP site 5011-1 with the Pliocene–Pleistocene boundary penetrated at approximately 123 m, and the transition to the impact breccia at 318 m below lake floor (modified after Melles et al., 2011).

catchment is predominantly affected by permafrost processes such as solifluction and cryogenic weathering (Glushkova and Smirnov, 2007). In addition, distinct lake-level variations during the Middle Pleistocene to Holocene modified the geomorphic shape of the area and resulted in various

accumulative and erosional terraces at 35–40, 9–11 and 2.5–3.0 m above as well as 10 m below the modern lake level (Glushkova and Smirnov, 2007; Juschus et al., 2011).

The catchment of Lake El'gygytgyn is dissected by approximately 50 ephemeral inlet streams (see Fig. 1; Nolan and Brigham-Grette, 2007), which deliver sediment in the order of ca. 350 t yr^{-1} into the lake (Fedorov et al., 2013). In 2003, main sediment discharge occurred during snowmelt in spring and early summer, with highest values of 24 g s^{-1} in June and 0.33 g s^{-1} in August measured in creek 49 (cf. Fig. 1; Fedorov et al., 2013). Much of the sediment is trapped in coastal lagoons at the mouths of several inlet-streams, which are dammed by gravelly shore bars generated by ice floe pressure or storms (Glushkova and Smirnov, 2007; Nolan and Brigham-Grette, 2007; Fedorov et al., 2013). The lake is drained by the Enmyvaan River towards the south-east (Fig. 1), which was likely the only discharge during the lake's history (Glushkova and Smirnov, 2007; Nolan and Brigham-Grette, 2007).

The regional climate at Lake El'gygytgyn is cold, dry, and windy (Nolan and Brigham-Grette, 2007), with a mean annual air temperature of −10.4 °C and an annual precipitation between 70 and 200 mm measured between 2002 and 2008 (Nolan, 2013). Strong (up to 21 m s^{-1}) and very persistent winds (mean of 5.6 m s^{-1} in 2002) of north-northwestern and south-southeastern directions are dominant (Nolan and Brigham-Grette, 2007).

Lake El'gygytgyn is characterized as monomictic and oligotrophic to ultra-oligotrophic, with a low bioproductivity demonstrated by low diatom accumulation (Cremer and Wagner, 2003; Nolan and Brigham-Grette, 2007). Today, the water column is fully mixed with almost complete oxygen saturation during summer, but a thermal stratification occurring during winter (Cremer and Wagner, 2003). During peak glacial periods, in contrast, anoxic bottom water conditions prevailed, resulting from a perennial ice cover (Melles et al., 2007).

According to initial results from ICDP core 5011-1, the Quaternary sediments in the central basin of Lake El'gygytgyn can clearly be differentiated into three pelagic facies (Melles et al., 2012). Dark gray to black, finely laminated silt and clay with sporadic clasts are linked to peak glacial periods (facies A). In contrast, warm and peak warm ("super interglacial") interglacial conditions are reflected by olive gray to brownish, massive to faintly bedded silt (facies B) and laminated brownish silt (facies C), respectively. Beside these pelagic sediments, eight volcanic ash beds (cf. van den Bogaard et al., 2013) as well as numerous mass movement deposits (MMDs) of different type (turbdites, slumps, slides, grain flows, debrites) have been identified (Juschus et al., 2009; Sauerbrey et al., 2013).

3 Material and methods

Within the scope of this study, 1019 samples of Lake El'gygytgyn sediments originating from pelagic sediments in core composite of ICDP site 5011-1 (862 samples) and the pilot core Lz1024 (157 samples, locations see Fig. 1) have been analyzed for their grain-size distribution with a sampling resolution of 8 cm. Detailed descriptions about the lithostratigraphy, MMD's, and the creation of the composite profile are given by Melles et al. (2012), Sauerbrey et al. (2013), and by Nowaczyk et al. (2013) and Wennrich et al. (2013b), respectively. The age model of the Lake El'gygytgyn sediment sequence is primarily based on magnetostratigraphic data (Haltia and Nowaczyk, 2013). It is further improved by tuning of sediment proxies (including grain-size data) to the global marine benthic isotope stack of Lisiecki and Raymo (2005, LR04) and to local insolation patterns inferred from orbital parameters according to Laskar et al. (2004), Melles et al. (2012) and Nowaczyk et al. (2013).

Prior to the grain-size analyses, a multi-step chemical treatment procedure was developed to remove autochthonous sediment components without altering the clastic material. The results of each treatment step were subsequently validated by elemental analyses, Fourier-transformed infrared spectroscopy (FTIRS), X-ray diffraction (XRD), scanning electron microscopy (SEM) and optical microscopy. In a first step, approximately 0.75 g of dry sediment was treated with 15 mL H_2O_2 (30 % v/v, 50 °C, 18 h) to remove organic remains. Subsequently, authigenic precipitated vivianite ($(Fe)_3(PO_4)_2 \cdot 8\,H_2O$) was dissolved according to Asikainen et al. (2007) by treating the sediment with 15 mL HNO_3 (0.5 M, 50 °C, 5 h, 30 min shaking in between). Finally, biogenic silica (opal), whose content can exceed 50 % in Lake El'gygytgyn sediments (Vogel et al., 2013), was removed by adding 2 × 15 mL NaOH (1 M, 85 °C, 30 min) with manual shaking during the reaction. Between the single pre-treatment steps, the samples were centrifuged and neutralized with deionized (DI) water. The remaining sediment fraction was dispersed in 60 mL of demineralized and degassed water, mixed with $Na_4P_2O_7$ (m/v, 0.05 %) and shaken for 12 h. Prior to the analysis, samples were ultrasonified for one minute to remove air bubbles and to achieve redispersing. In a last step the sediment was sieved to 600 μm, as previous studies have shown that coarse sand- and gravel-sized particles only sporadically occur in Lake El'gygytgyn sediments (Asikainen et al., 2007). Single, coarse grains in the sediment produced big errors during grain-size analyses with the particle analyzer.

Grain-size analyses were performed using a Saturn DigiSizer 5200 laser particle analyzer, equipped with a Master Tech 52 autosampler (Micromeritics Co., USA). The analyzer is able to detect particle diameters between 0.1 and 1000 μm. For the measurement, the flow rate was set to 10 L min^{-1} and the obscuration was adjusted to 20 %. The

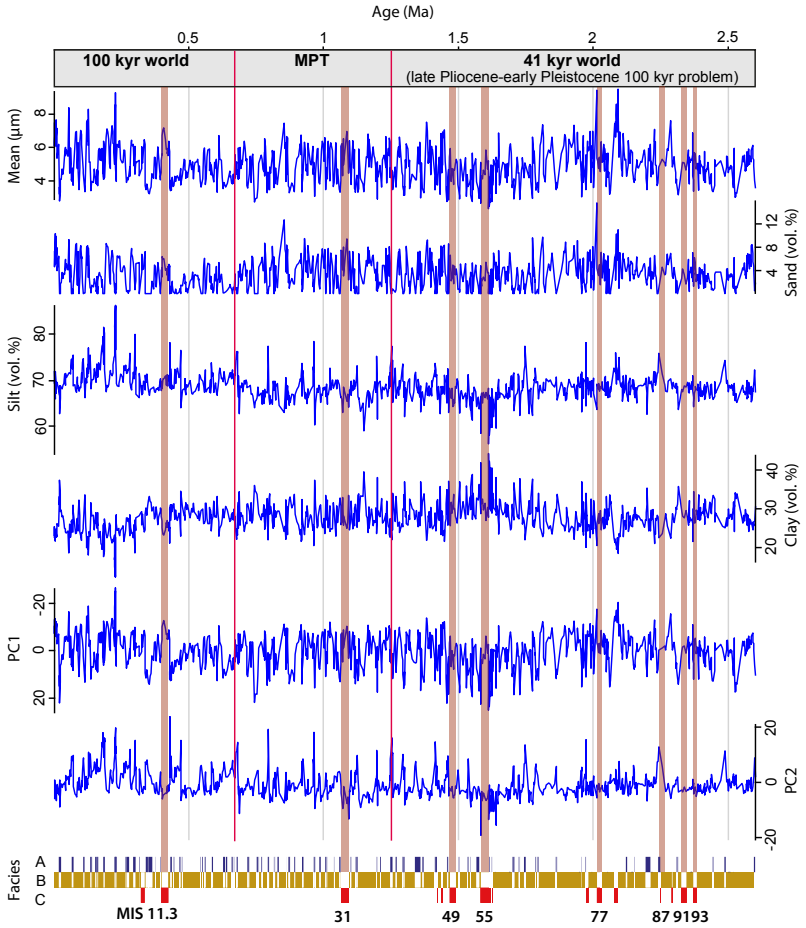

Fig. 2. Selected grain-size parameters (mean, sand, silt, clay) and sample scores of PC1 and PC2 in the Quaternary sediments of the core composite at ICDP site 5011-1 in central Lake El'gygytgyn. The timing of the Middle Pleistocene transition (MPT) from the 41 kyr world, including the Pliocene–early Pleistocene 100 kyr problem after Nie et al. (2008), to the 100 kyr world is derived from the time series analysis (cf. Fig. 6). Facies bar was modified from Melles et al. (2012); marine isotope stages of "super interglacial" facies C (after Melles et al., 2012) are labeled below.

grain-size distribution of three measurements was finally averaged.

Grain-size statistics were calculated with the software GRADISTAT version 8.0 (Blott and Pye, 2001), and are given according to the method by Folk and Ward (1957). Furthermore, a PCA was calculated with the software XLSTAT (Addinsoft Corp.). After an initial linear correlation test of the variables and standardization of the data, the PCA was carried out on the volume frequency of each grain diameter measured by the laser particle analyzer. The grain-size fractions as well as the mean, median and mode values were chosen as additional variables to simplify the visualization of the results.

For time series analysis of the PCA results, the bulk spectrum of the temporally unevenly spaced samples was calculated using the Fortran 90 program REDFIT by Schulz and Mudelsee (2002). Evolutionary spectra of the grain-size data and the benthic marine isotope stack LR04 (Lisiecki and Raymo, 2005) were plotted with the software package ESALAB (Weber et al., 2010).

4 Results

4.1 Grain-size data

Variations in the grain-size distributions are rather small, but still distinct (Fig. 2). The sand content does not exceed

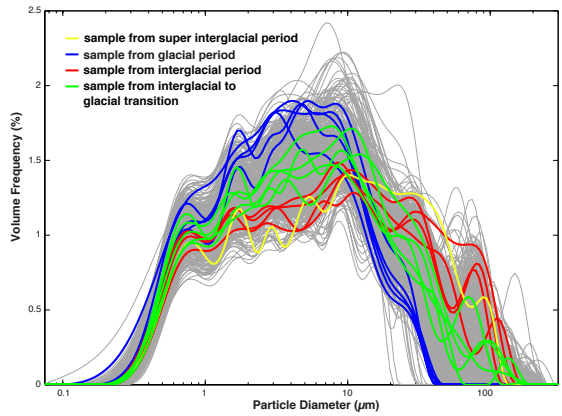

Fig. 3. Grain-size distributions of all analyzed samples from ICDP core 5011-1: blue: samples from glacial periods (facies A); green: samples from interglacial-to-glacial transitions; red: samples from interglacial periods (facies B); yellow: samples from super interglacial conditions (facies C).

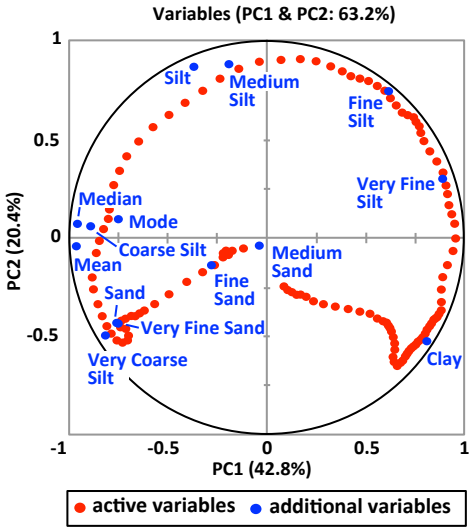

Fig. 4. Results of the PCA of the raw grain-size data (PC1 and PC2). Red dots (active variables) represent specific grain diameters measured by the laser particle analyzer. Selected grain-size fractions and parameters were chosen as additional variables (blue dots) for visualization of the results and are not directly included into the PCA calculations. PC1 (42.8 %) and PC2 (20.4 %) together comprise about 63.2 % of the total variance in the data set. The active variables clearly show a horseshoe pattern (for further explanations see text).

15.5 %, with medium sand being the coarsest grain-size fraction that occurs. The average silt and clay contents are about 69.2 and 27.7 %, respectively, showing minor fluctuations of not more than 15 % within both fractions. The mean values range between 2.5 and 9.3 μm (after Folk and Ward, 1957) and, thus, are classified as very fine (2–4 μm) to medium silt (8–16 μm). In general, this corresponds to earlier investigations on the grain-size distributions of the past 65 kyr in Lake El'gygytgyn (Asikainen et al., 2007).

Characteristic grain-size distribution patterns that describe the pelagic sediments of Lake El'gygytgyn at ICDP site 5011-1 are shown in Fig. 3. Samples from peak glacial periods (facies A) are fine-grained, do not contain any sand and mostly show a trimodal distribution, eventually including a double peak around 10 μm (Fig. 3, blue). Their grain-size distributions are commonly slightly asymmetric, which is caused by the lack of a normal tailing to coarse sediments and a coarse-skewed shoulder. Samples from interglacial (facies B) and super interglacial (facies C) periods are comparable (Fig. 3, red and yellow). Both sediment types comprise sand, are coarser than deposits from facies A, and are poorly sorted as indicated by the polymodal pattern of the grain-size distribution. A common feature of grain-size distributions from warm time periods is the lack of normal tailing but the occurrence of a peak or coarse-skewed shoulder at approximately 100 μm (Fig. 3). Sediments from climatic transitions (Fig. 3, green) are commonly finer than interglacial period deposits and coarser than glacial period deposits. The grain-size distributions can be comparable to typical patterns of glacial or interglacial sediments, but most transitional deposits appear polymodal and exhibit a peak or coarse-skewed shoulder at around 100 μm.

4.2 PCA

The PCA of the pelagic sediment yield 3 major principal components (PCs) explaining 75.4 % of the total variance in the grain-size data, with PC1, PC2 and PC3 covering variances of 42.8, 20.4, and 12.2 %, respectively. The plot of the active variables (PC1 vs. PC2; variance: 63.2 %; Fig. 4) clearly shows an arch spanning from clay to very coarse silt (Fig. 4), with highest negative factor loadings of PC1 revealing a grain diameter of 23.6 μm (coarse silt) and highest positives of 1.9 μm (clay to very fine silt). Grain diameters coarser than 44.5 μm (very coarse silt to medium sand) and finer than 0.6 μm (clay) focus to the origin of the diagram, which results in a horseshoe pattern (Fig. 4). The sample scores of PC1 (Fig. 2) show a high correlation to the mean ($R^2 = 0.93$) and the median values ($R^2 = 0.91$), whereas only a weaker correspondence to the mode values ($R^2 = 0.56$) is noticeable. In contrast, PC2 is highly correlated to medium silt ($R^2 = 0.83$) and PC3 is not correlated to any grain-size fraction.

4.3 Time series analysis

To gain insight into the frequency of the grain-size data, time series analyses of PC1 samples scores have been performed. The bulk spectrum yields three important peaks with

dominant oscillations at 98.5, 40.6, and 22.9 kyr, which exceed the significance level of 99 % χ^2 (Fig. 5).

As evolutionary power spectrum of PC1 sample scores (Fig. 6a) was carried with a window width of 240 ka and overlapping window segments were used for the calculations, the reported time period is between 2478 and 120 ka. During this period, the evolutionary power spectrum yields distinct variations in the relative power of the three dominate cycles (98.5, 40.6, and 22.9 kyr). The 98.5 kyr period is highly variable throughout the analyzed time period, with a strong relative power prior to 2300 and from 2100 to 1800 ka, from 1250 to 1000 ka, and after 800 ka, but a weak dominance in the periods 2200 to 2100 ka, 1800 to 1600 ka and 1000 to 800 ka. The 40.6 kyr cycle is more consistent with a strong relative power from 2400 to 1250 ka and from 950 to 670 ka, whereas a low signal occurs around 1750 ka and after 670 ka. The 22.9 kyr cycle occurs from 1900 to 1300 ka, from 1100 to 900 ka, and during two short time periods at 2250 and 130 ka.

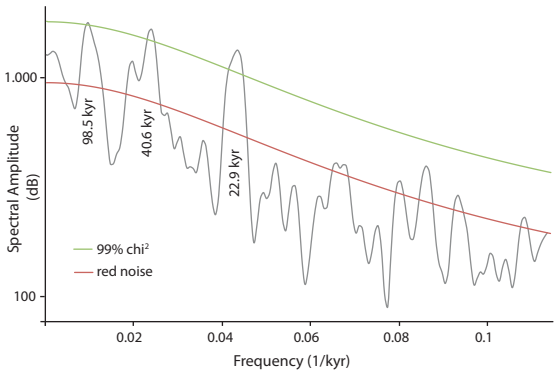

Fig. 5. Bias-corrected spectrum of sample scores of PC1 using the software REDFIT38, applying the Lomb–Scargle periodogram for unevenly spaced time series in combination with the Welch's overlapped segment averaging procedure (Mudelsee et al., 2009). Number of segments $n_{50} = 14$; window type: boxcar; red line: red noise level; green line: 99 % false-alarm level (χ^2). Significant cycles at 98.5, 40.6 and 22.9 kyr exceed both the red noise and the confidence level.

5 Discussion

5.1 Sedimentation processes at Lake El'gygytgyn

The Quaternary grain-size variability of core 5011-1 from Lake El'gygytgyn is strongly connected to climate variation, with coarse-grained, polymodal distributed sediments occurring during warm periods and fine-grained, trimodal distributed deposits during cold periods (Fig. 3). Grain-size distributions from samples deposited during a transition from interglacial to glacial periods appear mostly polymodal but are less coarse than samples from warm conditions (Fig. 3). The climate dependency of the grain-size distributions is also confirmed by a comparison of the mean grain size to other climate-dependent proxies of the Lake El'gygytgyn record (cf. Fig. 7). The Si/Ti ratio is a measure of the biogenic silica content (BSi) in the sediment and, thus, of the primary production by diatoms if grain-size effects by XRF scanning can be excluded (Melles et al., 2007, 2012; Vogel et al., 2013; Wennrich et al., 2013b). High Si/Ti ratios reflect a high content of BSi in the sediments, which is related to high primary production in the lake under warm climate conditions (Melles et al., 2007, 2012; Vogel et al., 2013; Wennrich et al., 2013b). For the analyzed data, the grain-size distribution is independent from the content of BSi in the sediment as diatoms were removed during sample pre-treatment for grain-size analyses. As both proxies show very similar variations, this supports the assumption of climate-dependent clastic sedimentation processes at Lake El'gygytgyn (Fig. 7).

As shown for modern conditions, the supply of clastic material to Lake El'gygytgyn is mainly restricted to spring and early summer, when snowmelt and warm temperatures result in the availability of fluvial discharge (cf. Fedorov et al., 2013). Additionally, the thickness of the active layer of the local permafrost should be linked to the availability of clastic material. During snowmelt, even pebble- to cobble-sized rocks as well as clumps of tundra are transported to the beach and close to the shoreline in the lake (cf. Asikainen et al., 2007; Nolan and Brigham-Grette, 2007). Coarse material may be filtered by the shore bars, explaining the lack of a normal tailing to coarse sediments in Lake El'gygytgyn deposits. Subsequently, sand-sized and finer sediments are redistributed by a wind-induced current pattern in the lake. The geochemical, mineralogical and sedimentological analyses of surface sediments from Lake El'gygytgyn, inlet streams, and source rocks have shown that clastic material that is transported to the lake is re-distributed by lake-internal currents (Wennrich et al., 2013a). These current systems are induced by strong wind conditions of predominantly northern or southern directions and result in the occurrence of a suspension cloud focused to the lake center (Wennrich et al., 2013a). In relation to the suspension cloud, a tongue of coarse-grained and poorly sorted sediments focused to the lake center can be observed in the surface sediments of Lake El'gygytgyn (cf. Wennrich et al., 2013a). Wind speed, current speed of the water body and transport energy for transportation of clastic material are very closely connected within this sedimentation system. Surface sediments from central parts of Lake El'gygytgyn exhibit comparable grain-size diameters and distribution patterns to sediments from interglacial periods. This implies that sedimentation processes described for the modern conditions persisted during interglacial periods throughout the entire Quaternary. In addition, no remarkable differences in the grain-size distributions from interglacial facies B and super interglacial

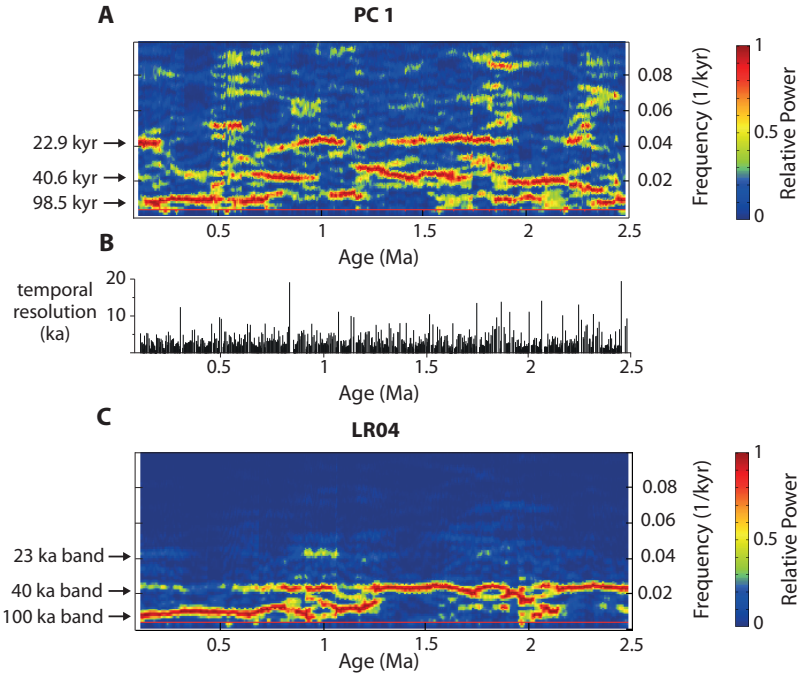

Fig. 6. **(A)** Evolutionary power spectrum of sample scores of PC1 from 120 to 2478 ka, resulting from the chosen window width of 240 ka (window type: boxcar). The used software ESALAB (Weber et al., 2010) is based on the same algorithms as REDFIT38. **(B)** Plot of the temporal resolution of the grain-size data versus time. The length of each bar represents the time period to the next sample below. **(C)** Evolutionary power spectrum of LR04 (Lisiecki and Raymo, 2005) applying the same settings as in **(A)**.

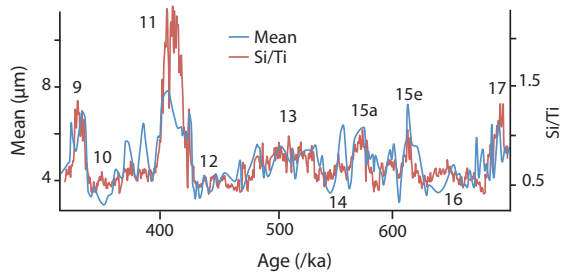

Fig. 7. Comparison of the mean values (after Folk and Ward, 1957) and the Si/Ti ratio as a proxy for bioproductivity in Lake El'gygytgyn between marine isotope stages 17 and 9. This short time period was exemplarily chosen to visualize grain-size and Si/Ti variability during several glacial–interglacial cycles including the super interglacial MIS11. The relationship is consistent over the entire record. Variations on a glacial–interglacial timescale but also of higher frequency are well reflected by the grain-size data. Grain-size distributions during MIS11 do not differ compared to other interglacials.

facies C could be observed (cf. Figs. 2, 3 and 7). Thus, the maximum transport energy during both interglacial periods was likely comparable. Variable transport energies during both types of interglacials could be indicated by the typical polymodal pattern of the grain-size distributions and the occurrence of the coarse-skewed shoulder or independent peak at $\sim 100\,\mu$m (cf. Fig. 3a). However, polymodal grain-size distributions could also be triggered by additional sedimentation processes, such as eolian or ice floe transportation. For modern conditions, eolian sediment input to Lake El'gygytgyn was estimated by measuring the particle concentration of the snow on the lake ice prior to the ice breakup. The amount of the eolian supply is calculated as 2 to 5 % of the total sediment deposition (Fedorov et al., 2013). After ice breakup, random ice floe transport of sediments of fluvial origin could have significantly contributed to the sediment supply of ICDP site 5011-1. Modern observations recorded sediment supply by inlet streams onto the ice cover during snowmelt, wherefrom the sediment is periodically flushed out when the temperatures are high enough (Fedorov et al., 2013). Sediment supply onto the ice cover and subsequent redistribution by ice floe transportation is also described for other seasonally ice-covered lakes, e.g. for Lake Baikal (Vologina et al., 2005).

Varying transport energies in the lake-water body, eolian supply and ice floe transportation can explain the coarse-grained, poorly sorted occurrence of interglacial grain-size distributions. The finer, better-sorted sediments from glacial periods, in contrast, suggest low transport energies and probably reduced eolian supply or ice floe transportation. Reduced eolian supply and ice floe transportation can be explained by a very short ice-free summer season or a perennial ice cover. An enhanced deposition of eolian deposits at the end of a long period with a perennial ice cover is not observed in the data, likely because of the low sample resolution. However, eolian sediment can be deposited despite a perennial ice cover during cold and dry periods (Asikainen et al., 2007; Melles et al., 2007). Material of eolian origin is able to move through the ice along grain boundaries and vertical conduits, whereby it might be compacted to 1–2 mm clasts (Nolan, 2013). These clasts are not observed in the grain-size data, likely because they are destroyed during the sample pretreatment. A perennial lake ice cover also excludes the redistribution of clastic material by a wind-induced current pattern. In general, sediment supply to Lake El'gygytgyn under such conditions is widely restricted to seasonal moats around the perennial lake ice, formed in late summer (Asikainen et al., 2007; Melles et al., 2007). The transportation of clastic material to the lake center likely depends on relatively weak lake-internal currents triggered by temperature differences between the seasonal moats with warmer water temperatures and deeper parts of Lake El'gygytgyn. The formation of a perennial lake-ice cover and the occurrence of seasonal moats predominantly depends on the summer temperature (Nolan, 2013). Summer temperature also triggers the thickness of the active layer of the permafrost and restricts the availability of water as a major transport medium for clastic material. A thin active layer and limited water availability hamper the supply of coarse material to the lake. Overall, the deposition of clastic material at ICDP site 5011-1 seems to be very sensitive to variations of the local summer temperature at Lake El'gygytgyn. Gradual transitions from warm to cold conditions on an interglacial–glacial timescale are well reflected by the mean grain size, and even higher amplitude variations (e.g. between MIS 11 and 10, Fig. 7) are present in the data. This implies gradual rather than abrupt changes of the sedimentation processes at Lake El'gygytgyn during such transitions.

5.2 PCA

Factor loadings of PC1 yield the most important grain diameter (fractions) contributing to the grain-size distribution (Fig. 4). High positive or negative factor loadings imply a high importance of the coarse silt or the very fine silt fraction, respectively. As variations in the grain-size data are primarily attributed to climate variability, sample scores of PC1 can be interpreted to represent climate variations. High negative PC1 scores are associated with warmer climate conditions with ice-free conditions during summer and enhanced sedimentation of coarse silt. In contrast, high positive PC1 scores are linked to glacial climate conditions and the enrichment of very fine silt. Silt, in particular medium silt, shows the weakest correlation to PC1 but high factor loading on PC2. The high correlation of medium silt to PC2 is apparently mainly triggered by the occurrence of the horseshoe pattern (Fig. 4). The horseshoe pattern is a mathematic artifact in PCA results (cf. Kendall, 1971; Gauch et al., 1977), which occurs if the analyzed data set is only influenced by one long gradient and each variable (inhere: grain diameter) is successively replaced by the next one, resulting in a unimodal response to the gradient (Swan, 1970; Gauch et al., 1977). Thus, PCA results substantiate the interpretation that grain-size variations of Lake El'gygytgyn sediments predominantly reflect variations in the sedimentary processes controlled by climate influences. Additional processes, such as lake-level variations or changes in the geomorphic shape of the catchment, have only limited influence on the grain-size distribution. In line with this result, a direct connection between the grain-size data and lake-level fluctuations recorded by the occurrence of lacustrine terraces in the area and in sediment cores from marginal parts of the lake (cf. Juschus et al., 2011) is not present.

5.3 Time series analysis

To distinguish between time periods, which are dominated by global glacial–interglacial or shorter-term variations, a time series analysis on PC1 sample scores was carried out. As the age model of core 5011-1 was derived by tuning sediment proxies with local insolation and the global marine isotope stack LR04 (Melles et al., 2012; Nowaczyk et al., 2013), the bulk spectrum (Fig. 5) yields dominant oscillations above the 99 % χ^2 confidence level at Milankovitch's eccentricity (98.5 kyr), obliquity (40.6 kyr) and precession oscillations (22.9 kyr). Despite the tuned age model of core 5011-1, the relative dominance of these three oscillations clearly differs from these of LR04 during the Quaternary (Fig. 6). Oscillations of higher frequency that exceed the red noise level (cf. Fig. 5) were not included in further analyses, as the temporal resolution of the grain-size data ranges between 0.02 and 19.79 ka (average: 2.56 ka, cf. Fig. 6b). Cycles of 98.5 and 40.6 ka are interpreted to be a result of global climate variability and variations of the global ice volume, as reflected by marine isotope stack LR04 (Lisiecki and Raymo, 2005; cf. Fig. 6c). In contrast, the 22.9 ka band is closely connected to local orbital precession forcing at the latitude of Lake El'gygytgyn, with coarser grain-size distributions associated with high insolation values. Consequently, ice-free summertime is extended during high insolation forcing, which is consistent with results of previous studies on the sedimentation pattern of Lake El'gygytgyns, e.g. magnetic susceptibility and TOC data (Melles et al., 2007; Nowaczyk et al., 2007). On the other hand, the strong precession cycle

in the Lake El'gygytgyn grain-size data could be a latitudinal teleconnection, as the precession cycle is rather weak in polar but stronger in equatorial regions (Berger and Loutre, 1991). Tropical to subtropical climate oscillations that are associated with variations on a precession cycle are the East Asian Monsoon (Sun et al., 2006) and the El Niño–Southern Oscillation (Tudhope et al., 2001). In transect from Lake El'gygytgyn to southern direction, winter monsoon variability on a precession cycle is recorded from the Chinese Loess Plateau (Sun et al., 2006).

During the early Pleistocene (2600 to 780 ka; see also Fig. 2), when global climate conditions were dominated by the 41 kyr band (e.g. Clark et al., 2006), similarities and dissimilarities between 5011-1 and LR04 occur (Fig. 6). The strong oscillation of the 41.7 kyr cycle in the grain-size data of 5011-1 well reflect global climate variability on the obliquity oscillation band. In contrast, the 98.5 kyr cycle in the grain-size data is more variable, with a strong response to climate forcing between 2450 and 2300 ka and between 2100 and 1800 ka, and a reduced power between 1800 and 1600 ka (Fig. 6). These findings partly agree with descriptions of Nie et al. (2008) about the 100 ka band during the early Pleistocene. Following their description of the "late Pliocene–early Pleistocene 100 kyr problem", there is a strong response of climate proxies between 3000 and 1800 ka, although forcing is strong between 2300 and 1300 ka. However, Lake El'gygytgyn grain-size data indicate only a weak 98.5 kyr cycle between 2300 and 2100 ka.

During the early Pleistocene, the 22.9 kyr precession band is strong around 2250 ka and between 1900 and 1300 ka when relative eccentricity or obliquity powers are low. Thus, the precession band at Lake El'gygytgyn mostly interplays with the eccentricity band and is therefore closely connected with the late Pliocene–early Pleistocene 100 kyr problem. The absence of the 23 ka band between 3000 and 1000 ka in global benthic isotope records (cf. Fig. 6) despite a strong precession cycle at all latitudes has been explained with an out-of-phase ice sheet growth and melt at each pole (Raymo et al., 2006). Grain-size data at Lake El'gygytgyn is not directly coupled to global ice-volume variability and, thus, shows the 23 ka precession band to be important for the climate conditions during specific time intervals. Variations on a 23 ka oscillation band during the early Pleistocene are also reported from the Chinese Loess Plateau (Sun et al., 2006) and African dust records (deMenocal, 1995).

The time periods of the Middle Pleistocene transition (MPT; see also Fig. 2) and the late Pleistocene are marked by the transition of the climate variability from the dominance of the obliquity oscillation to eccentricity oscillation (e.g. Clark et al., 2006). In our data set this transition is rather gradual with an initial onset of the 98.5 kyr cycle at 1250 ka, low power from 1000 to 800 ka and strong power afterwards until at least 130 ka. A weakening of the 100 ka eccentricity band around 1000 ka is also present in LR04 (Fig. 6c). At Lake El'gygytgyn, this period until 800 ka is characterized by an initially strong 22.9 kyr cycle and subsequent strong 40.6 kyr cycle. The decreasing relative power of the obliquity oscillation during the late Pleistocene implies that the MPT at Lake El'gygytgyn lasted from 1250 to 670 ka. Such a gradual transition is also described for LR04 with an initial onset at 1250 ka, a disturbance of the eccentricity cycle for 100 kyr around 1000 ka, and a completion of the transition to the 100 kyr world at 700 ka (Clark et al., 2006). The mechanism leading to the emergence of the 100 kyr band is hypothesized to have been triggered by a long-term cooling trend induced by decreasing pCO_2 (Berger et al., 1999; Tziperman and Gildor, 2003) and/or increasing ice sheet thickness due to exposure of high-friction crystalline bedrock (Clark and Pollard, 1998), whereas orbital forcing can be excluded (Clark et al., 2006).

6 Conclusions

Variations in the grain-size distribution of Lake El'gygytgyn sediments during the past 2600 ka have shown to be mainly influenced by summer temperature and thus, by global and regional climate conditions. Main factors triggering the clastic sedimentation in the lake are assumed to be the existence and duration of an annual lake-ice cover, the permafrost stability around the lake and the intensity of fluvial transport processes in the catchment. Studies on the modern sedimentation in the lake have shown that a wind-induced current pattern of different strengths triggers the occurrence of coarse-grained deposits at the center of the lake during ice-free periods (Wennrich et al., 2013a). Our data suggest that this process persisted throughout the entire Quaternary. Under glacial climate conditions, sediment supply to the lake is likely restricted to seasonal moats close to the shore and to vertical conduits in the ice.

Principal Component Analysis allowed identifying most important grain-size fractions attributed to variations in the data set. Coarse silt and very fine silt could be emphasized to be the major players in climate-dependent variations in the grain-size data, whereas medium silt does not show this climate dependency.

Time series analysis reveals major oscillation and their relative dominance in the grain-size data during the Quaternary. It can be concluded that duration of annual lake-ice cover and thickness of the active layer during summer are triggered by global glacial–interglacial cycles (98.5, 40.6 kyr) and by local insolation forcing and/or latitudinal teleconnections (precession band, 22.9 kyr). Early Pleistocene variations on a 98.5 kyr oscillation band partly agree with descriptions of the late Pliocene–early Pleistocene 100 kyr problem" by Nie et al. (2008). Additionally, our data suggest an interplay of the 98.5 and 22.9 kyr cycles during the early Pleistocene. Oscillations on the eccentricity band (98.5 kyr) likely reflect global climate variability at Lake El'gygytgyn, whereas

variations on the precession band (22.9 kyr) are probably connected with regional insolation variations or latitudinal climatic teleconnections. The MPT is well reflected by our data between 1250 and 670 ka.

Acknowledgements. Funding for the drilling at Lake El'gygytgyn was provided by the International Continental Scientific Drilling Program (ICDP), the US National Science Foundation (NSF), the German Federal Ministry of Education and Research (BMBF), Alfred Wegener Institute (AWI) and GeoForschungsZentrum Potsdam (GFZ), the Russian Academy of Sciences Far East Branch (RAS FEB), the Russian Foundation for Basic Research (RFBR), and the Austrian Federal Ministry of Science and Research (BMWF). The Russian GLAD 800 drilling system was developed and operated by DOSECC Inc., and LacCore, at the University of Minnesota, handled core curation. This study was financially supported by the BMBF (grant no. 03G0642A) and the German Research Foundation (DFG, grant nos. WA 2109/11 and ME 1169/21). The laboratory work was carried by out with the assistance of various students under the guidance of Nicole Mantke. Nicole Mantke also contributed together with Hendrik Vogel to the development of the pre-treatment steps prior to the grain-size analyses. Furthermore, we thank Nikolaos Tougiannidis and Michael Weber for providing the software ESALAB and assistance with the time series analyses. Conrad Kopsch is acknowledged for providing topographic data, which was used by Andreas Dehnert for the creation of Fig. 1b within the scope of a diploma thesis.

Edited by: T. Cook

References

ACIA: Impacts of a Warming Arctic-Arctic Climate Impact Assessment Cambridge and New York, Cambridge University Press, 144 pp., 2004.

An, Z. S., Kukla, G., Porter, S. C., and Xiao, J. L.: Late quaternary dust flow on the Chinese loess plateau, Catena, 18, 125–132, 1991.

Asikainen, C. A., Francus, P., and Brigham-Grette, J.: Sedimentology, clay mineralogy and grain-size as indicators of 65 ka of climate change from El'gygytgyn Crater Lake, Northeastern Siberia, J. Paleolimnol., 37, 105–122, doi:10.1007/s10933-006-9026-5, 2007.

Axford, Y., Briner, J. P., Cooke, C. A., Francis, D. R., Michelutti, N., Miller, G. H., Smol, J. P., Thomas, E. K., Wilson, C. R., and Wolfe, A. P.: Recent changes in a remote Arctic lake are unique within the past 200,000 years, P. Natl. Acad. Sci., 106, 18443–18446, doi:10.1073/pnas.0907094106, 2009.

Berger, A. and Loutre, M. F.: Insolation values for the climate of the last 10 million years, Quaternary Sci. Rev., 10, 297–317, doi:10.1016/0277-3791(91)90033-Q, 1991.

Berger, A., Li, X., and Loutre, M.: Modeling northern hemisphere ice volume over the last 3 Ma, Quaternary Sci. Rev., 18, 1–11, 1999.

Blott, S. J. and Pye, K.: GRADISTAT: A grain size distribution and statistics package for the analysis of unconsolidated sediments, Earth Surf. Proc. Land., 26, 1237–1248, 2001.

Brigham-Grette, J., Melles, M., and Minyuk, P.: Overview and significance of a 250 ka paleoclimate record from El'gygytgyn Crater Lake, NE Russia, J. Paleolimnol., 37, 1–16, 2007.

Clark, C. D. and Pollard, D.: Origin of the Middle Pleistocene transition by ice sheet erosion of regolith, Paleoceanography, 13, 1–9, 1998.

Clark, P. U., Archer, D., Pollard, D., Blum, J. D., Rial, J. A., Brovkin, V., Mix, A. C., Pisias, N. G., and Roy, M.: The middle Pleistocene transition: characteristics, mechanisms, and implications for long-term changes in atmospheric pCO_2, Quaternary Sci. Rev., 25, 3150–3184, doi:10.1016/j.quascirev.2006.07.008, 2006.

Cremer, H. and Wagner, B.: The diatom flora in the ultra-oligotrophic Lake El'gygytgyn, Chukotka, Polar Biol., 26, 105–114, doi:10.1007/s00300-002-0445-0, 2003.

deMenocal, P. B.: Plio-Pleistocene African Climate, Science, 270, 53–59, 1995.

Dietz, R. S. and McHone, J. F.: El'gygytgyn: Probably the world largest meteorite crater, Geology, 4, 391–392, 1977.

Fedorov, G. and Kupolov, A.: Gas Mercury Survey in the El'gygytgyn Crater, in: The Expedition El'gygytgyn Lake 2003 (Siberian Arctic), edited by: Melles, M., Minyuk, P., Brigham-Grette, J., and Juschus, O., Reports on polar and marine research, AWI, Bremerhaven, 69–70, 2005.

Fedorov, G., Nolan, M., Brigham-Grette, J., Bolshiyanov, D., Schwamborn, G., and Juschus, O.: Preliminary estimation of Lake El'gygytgyn water balance and sediment income, Clim. Past, 9, 1455–1465, doi:10.5194/cp-9-1455-2013, 2013.

Folk, R. L. and Ward, W. C.: Brazos River bar [Texas]; a study in the significance of grain size parameters, J. Sediment. Res., 27, 3–26, 1957.

Gauch, H. G., Whittaker, R. H., and Wentworth, T. R.: A comparative study of reciprocal averaging and other ordination techniques, J. Ecol., 65, 157–174, 1977.

Glushkova, O. Y. and Smirnov, V. N.: Pliocene to Holocene geomorphic evolution and paleogeography of the El'gygytgyn Lake region, NE Russia, J. Paleolimnol., 37, 37–47, doi:10.1007/s10933-006-9021-x, 2007.

Gurov, E. P. and Gurova, E. P.: Stages of shock metamorphism of volcanic rocks of siliceous composition – Examples from the El'gygytgyn crater (Chukotka), Doklady Academii Nauk UkrSSR, 249, 1197–1201, 1979.

Gurov, E. P., Gurova, E. P., and Rakitskaia, R. B.: Stishovite and coesite in shock-metamorphosed rocks of the El'gygytgyn crater in Chukotka, Akademiia Nauk SSSR Doklady, 248, 213–216, 1979.

Gurov, E. P., Koeberl, C., and Yamnichenko, A.: El'gygytgyn impact crater, Russia: Structure, tectonics, and morphology, Meteor. Planet. Sci., 42, 307–319, 2007.

Haltia, E. M. and Nowaczyk, N. R.: Magnetostratigraphy of sediments from Lake El'gygytgyn ICDP Site 5011-1: paleomagnetic age constraints for the longest paleoclimate record from the continental Arctic, Clim. Past Discuss., 9, 5077–5122, doi:10.5194/cpd-9-5077-2013, 2013.

Johannessen, O. M., Bengtsson, L., Miles, M. W., Kuzmina, S. I., Semenov, V. A., Alekseev, G. V., Nagurnyi, A. P., Zakharov, V. F., Bobylev, L. P., Pettersson, L. H., Hasselmann, K., and Cattle, P.: Artic climate change: observed and modelled temperature and sea-ice variability, Tellus A, 56, 328–341, 2004.

Juschus, O., Melles, M., Wennrich, V., Nowaczyk, N., Brigham-Grette, J., and Minyuk, P.: Sedimentation in Lake Elgygytgyn, NE Russia, during the past 340.000 years, AGU Fall Meeting Abstracts, 11, 1303, 2009.

Juschus, O., Pavlov, M., Schwamborn, G., Preusser, F., Fedorov, G., and Melles, M.: Late Quaternary lake-level changes of Lake El'gygytgyn, NE Siberia, Quaternary Res., 76, 441–451, doi:10.1016/j.yqres.2011.06.010, 2011.

Kashiwaya, K., Yamamoto, A., and Fukuyama, K.: Time variations of erosional force and grain size in Pleistocene lake sediments, Quaternary Res., 28, 61–68, doi:10.1016/0033-5894(87)90033-0, 1987.

Kashiwaya, K., Ryugo, M., Sakai, T., and Kawai, T.: Long-term climate-limnological oscillation during the past 2.5 million years in Lake Baikal sediments, Geophys. Res. Lett., 25, 659–662, 1998.

Kashiwaya, K., Ochiai, S., and Sakai, T.: Orbit-related long-term climate cycles revealed in a 12-Myr continental record from Lake Baikal, Nature, 410, 71–74, 2001.

Kendall, D. G.: Seriation from abundance matrices, in: Mathematics in the archeological and history siences, edited by: Hodson, F. R., Kendall, D. G., and Tautu, P., Edinburgh University Press, 215–252, 1971.

Laskar, J., Robutel, P., Joutel, F., Gastineau, M., Correia, A. C. M., and Levrard, B.: A long-term numerical solution for the insolation quantities of the Earth, Astron. Astrophys., 428, 261–285, doi:10.1051/0004-6361:20041335, 2004.

Layer, P. W.: Argon-40/argon-39 age of the El'gygytgyn impact event, Chukotka, Russia, Meteor. Planet. Sci., 35, 591–599, 2000.

Lisiecki, L. E. and Raymo, M. E.: A Pliocene-Pleistocene stack of 57 globally distributed benthic δ^{18}O records, Paleoceanography, 20, PA1003, doi:10.1029/2004pa001071, 2005.

Melles, M., Brigham-Grette, J., Glushkova, O. Y., Minyuk, P. S., Nowaczyk, N. R., and Hubberten, H. W.: Sedimentary geochemistry of core PG1351 from Lake El'gygytgyn – a sensitive record of climate variability in the East Siberian Arctic during the past three glacial-interglacial cycles, J. Paleolimnol., 37, 89–104, doi:10.1007/s10933-006-9025-6, 2007.

Melles, M., Brigham-Grette, J., Minyuk, P., Koeberl, C., Andreev, A., Cook, T., Fedorov, G., Gebhardt, C., Haltia-Hovi, E., Kukkonen, M., Nowaczyk, N., Schwamborn, G., Wennrich, V., and and the El'gygytgyn Scientific Party: The Lake El'gygytgyn Scientific Drilling Project – Conquering Arctic Challenges through Continental Drilling, Scientific Drill., 11, 29–40, 2011.

Melles, M., Brigham-Grette, J., Minyuk, P., Nowaczyk, N., Wennrich, V., Deconto, R., Andersen, P., Andreev, A. A., Coletti, A., Cook, T., Haltia-Hovi, E., Kukkonen, M., Lozhkin, A., Rosén, P., Tarasov, P., Vogel, H., and Wagner, B.: 2.8 Million Years of Arctic Climate Change from Lake El'gygytgyn, NE Russia, Science, 337, 315-320, doi:10.1126/science.1222135, 2012.

Moran, K., Backman, J., Brinkhuis, H., Clemens, S. C., Cronin, T., Dickens, G. R., Eynaud, F. D. R., Gattacceca, J. R. M., Jakobsson, M., Jordan, R. W., Kaminski, M., King, J., Koc, N., Krylov, A., Martinez, N., Matthiessen, J., McInroy, D., Moore, T. C., Onodera, J., O'Regan, M., Pälike, H., Rea, B., Rio, D., Sakamoto, T., Smith, D. C., Stein, R., St John, K., Suto, I., Suzuki, N., Takahashi, K., Watanabe, M., Yamamoto, M., Farrell, J., Frank, M., Kubik, P., Jokat, W., and Kristoffersen, Y.: The Cenozoic palaeoenvironment of the Arctic Ocean, Nature, 441, 601–605, 2006.

Mottaghy, D., Schwamborn, G., and Rath, V.: Past climate changes and permafrost depth at the Lake El'gygytgyn site: implications from data and thermal modeling, Clim. Past, 9, 119–133, doi:10.5194/cp-9-119-2013, 2013.

Mudelsee, M., Scholz, D., Röthlisberger, R., Fleitmann, D., Mangini, A., and Wolff, E. W.: Climate spectrum estimation in the presence of timescale errors, Nonlin. Processes Geophys., 16, 43–56, doi:10.5194/npg-16-43-2009, 2009.

Nie, J., King, J., and Fang, X.: Late Pliocene-early Pleistocene 100-ka problem, Geophys. Res. Lett., 35, L21606, doi:10.1029/2008GL035265, 2008.

Niessen, F., Gebhardt, A. C., Kopsch, C., and Wagner, B.: Seismic investigation of the El'gygytgyn impact crater lake (Central Chukotka, NE Siberia): preliminary results, J. Paleolimnol., 37, 49–63, doi:10.1007/s10933-006-9022-9, 2007.

Nolan, M.: Quantitative and qualitative constraints on hind-casting the formation of multiyear lake-ice covers at Lake El'gygytgyn, Clim. Past, 9, 1253–1269, doi:10.5194/cp-9-1253-2013, 2013.

Nolan, M. and Brigham-Grette, J.: Basic hydrology, limnology, and meteorology of modern Lake El'gygytgyn, Siberia, J. Paleolimnol., 37, 17–35, doi:10.1007/s10933-006-9020-y, 2007.

Nolan, M., Cassano, E. N., and Cassano, J. J.: Synoptic climatology and recent climate trends at Lake El'gygytgyn, Clim. Past, 9, 1271–1286, doi:10.5194/cp-9-1271-2013, 2013.

Nowaczyk, N., Melles, M., and Minyuk, P.: A revised age model for core PG1351 from Lake El'gygytgyn, Chukotka, based on magnetic susceptibility variations tuned to northern hemisphere insolation variations, J. Paleolimnol., 37, 65–76, doi:10.1007/s10933-006-9023-8, 2007.

Nowaczyk, N. R., Haltia, E. M., Ulbricht, D., Wennrich, V., Sauerbrey, M. A., Rosén, P., Vogel, H., Francke, A., Meyer-Jacob, C., Andreev, A. A., and Lozhkin, A. V.: Chronology of Lake El'gygytgyn sediments – a combined magnetostratigraphic, palaeoclimatic and orbital tuning study based on multi-parameter analyses, Clim. Past, 9, 2413–2432, doi:10.5194/cp-9-2413-2013, 2013.

Pienitz, R., Melles, M., and Zolitschka, B.: Results of recent sediment drilling activities in deep crater lakes, Pages News, 3, 117–118, 2009.

Raymo, M. E., Lisiecki, L. E., and Nisancioglu, K. H.: Plio-Pleistocene ice volume, Antarctic climate, and the global δ^{18}O record, Science, 313, 492–495, doi:10.1126/science.1123296, 2006.

Sauerbrey, M. A., Juschus, O., Gebhardt, A. C., Wennrich, V., Nowaczyk, N. R., and Melles, M.: Mass movement deposits in the 3.6 Ma sediment record of Lake El'gygytgyn, Far East Russian Arctic, Clim. Past, 9, 1949–1967, doi:10.5194/cp-9-1949-2013, 2013.

Schulz, M. and Mudelsee, M.: REDFIT: estimating red-noise spectra directly from unevenly spaced paleoclimatic time series, Comput. Geosci., 28, 421–426, 2002.

Serreze, M. and Francis, J.: The Artic Amplification Debate, Climatic Change, 76, 241–264, 2006.

Stone, D. B., Layer, P. W., and Raikevich, M. I.: Age and paleomagnetism of the Okhotsk-Chukotka Volcanic Belt (OCVB) near Lake El'gygytgyn, Chukotka, Russia, Stephan Mueller Special Publication Server, 4, 243–260, doi:10.5194/smsps-4-243-2009, 2009.

Sun, J. and Huang, X.: Half-precessional cycles recorded in Chinese loess: response to low-latitude insolation forcing during the Last Interglaciation, Quaternary Sci. Rev., 25, 1065–1072, doi:10.1016/j.quascirev.2005.08.004, 2006.

Sun, Y., Clemens, S. C., An, Z., and Yu, Z.: Astronomical timescale and palaeoclimatic implication of stacked 3.6-Myr monsoon records from the Chinese Loess Plateau, Quaternary Sci. Rev., 25, 33–48, doi:10.1016/j.quascirev.2005.07.005, 2006.

Swan, J. M. A.: An Examination of some ordination problems by use of simulated vegetation data, Ecology, 51, 89–102, 1970.

Thiede, J., Winkler, A., Wolf-Welling, T., Eldholm, O., Myhre, A., Baumann, K.-H., Henrich, R., and Stein, R.: Late Cenozoic history of the Polar North Atlantic: results from ocean drilling, Quaternary Sci. Rev., 17, 185–208, 1998.

Tudhope, A. W., Chilcott, C. P., McCulloch, M. T., Cook, E. R., Chappell, J., Ellam, R. M., Lea, D. W., Lough, J. M., and Shimmield, G. B.: Variability in the El Nino-Southern Oscillation Through a Glacial-Interglacial Cycle, Science, 291, 1511-1517, doi:10.1126/science.1057969, 2001.

Tziperman, E. and Gildor, H.: On the mid-Pleistocene transition to 100 kyr glacial cycles and the asymmetry between glaciation and deglaciation times, Paleoceanography, 18, 1001, doi:10.1029/2001PA000627, 2003.

van den Bogaard, C., Jensen, B. J. L., Pearce, N. J. G., Froese, D. G., Portnyagin, M. V., Ponomareva, V. V., Garbe-Schönberg, D., and Wennrich, V.: Volcanic ash layers in Lake El'gygytgyn: eight new regionally significant chronostratigraphic markers for western Beringia, Clim. Past Discuss., 9, 5977–6034, doi:10.5194/cpd-9-5977-2013, 2013.

Vogel, H., Meyer-Jacob, C., Melles, M., Brigham-Grette, J., Andreev, A. A., Wennrich, V., Tarasov, P. E., and Rosén, P.: Detailed insight into Arctic climatic variability during MIS 11c at Lake El'gygytgyn, NE Russia, Clim. Past, 9, 1467–1479, doi:10.5194/cp-9-1467-2013, 2013.

Vologina, E., Granin, N., Francus, P., Lomonosova, T., Kalashinkova, I., and Granina, L.: Ice transport of sand-silt material in southern lake Baikal, Russ. Geol. Geophys., 46, 186–192, 2005.

Washington, W. M. and Meehl, G. A.: High-latitude climate change in a global coupled ocean-atmosphere ice model with increasing atmospheric CO_2, J. Geophys. Res., 101, 12795–12801, 1996.

Weber, M. E., Tougiannidis, N., Kleineder, M., Bertram, N., Ricken, W., Rolf, C., Reinsch, T., and Antoniadis, P.: Lacustrine sediments document millennial-scale climate variability in northern Greece prior to the onset of the northern hemisphere glaciation, Palaeogeogr. Palaeocl., 291, 360–370, doi:10.1016/j.palaeo.2010.03.007, 2010.

Wennrich, V., Francke, A., Dehnert, A., Juschus, O., Leipe, T., Vogt, C., Brigham-Grette, J., Minyuk, P. S., Melles, M., and El'gygytgyn Science Party: Modern sedimentation patterns in Lake El'gygytgyn, NE Russia, derived from surface sediment and inlet streams samples, Clim. Past, 9, 135–148, doi:10.5194/cp-9-135-2013, 2013a.

Wennrich, V., Minyuk, P. S., Borkhodoev, V. Ya., Francke, A., Ritter, B., Nowaczyk, N., Sauerbrey, M. A., Brigham-Grette, J., and Melles, M.: Pliocene to Pleistocene climate and environmental history of Lake El'gygytgyn, Far East Russian Arctic, based on high-resolution inorganic geochemistry data, Clim. Past Discuss., 9, 5899–5940, doi:10.5194/cpd-9-5899-2013, 2013.

Zech, R., Huang, Y., Zech, M., Tarozo, R., and Zech, W.: High carbon sequestration in Siberian permafrost loess-paleosols during glacials, Clim. Past, 7, 501–509, doi:10.5194/cp-7-501-2011, 2011.

4 Chronology of Lake El'gygytgyn sediments - a combined magnetostratigraphic, palaeoclimatic and orbital tuning study based on multi-parameter analyses

Journal article (2013):
Nowaczyk, N., Haltia-Hovi, E., Ulbricht, D., Wennrich, R., Sauerbrey, M., Rosén, P., Vogel, H., Francke, A., Meyer-Jacob, C., Andreev, A. A., and Lozhkin, A.: Chronolgy of Lake El'gygytgyn sediments - a combined magnetostratigraphic, palaeoclimatic and orbital tuning study based on multi-parameter analyses, Clim. Past, 9, 2413-2432, doi:10.5194/cp-9-2413-2013, 2013.

Clim. Past, 9, 2413–2432, 2013
www.clim-past.net/9/2413/2013/
doi:10.5194/cp-9-2413-2013

Climate of the Past
Open Access

Chronology of Lake El'gygytgyn sediments – a combined magnetostratigraphic, palaeoclimatic and orbital tuning study based on multi-parameter analyses

N. R. Nowaczyk[1], E. M. Haltia[1,*], D. Ulbricht[1,], V. Wennrich[2], M. A. Sauerbrey[2], P. Rosén[3], H. Vogel[2,***], A. Francke[2], C. Meyer-Jacob[2,****], A. A. Andreev[2], and A. V. Lozhkin[4]**

[1]Helmholtz Centre Potsdam, GFZ German Research Centre for Geosciences, Section 5.2 – Climate Dynamics and Landscape Evolution, Telegrafenberg, 14473 Potsdam, Germany
[2]University of Cologne, Institute of Geology and Mineralogy, Zülpicher Straße 49A, 50674 Köln, Germany
[3]Umeå University, Climate Impacts Research Centre (CIRC), 981 07 Abisko, Sweden
[4]NEISRI, Russian Academy of Science, Magadan, 685000, Russia
[*]now at: University of Turku, Department of Geography and Geology, Section of Geology, 20014 Turku, Finland
[**]now at: Helmholtz Centre Potsdam, GFZ German Research Centre for Geosciences, Centre for Geoinformation Technology CeGIT, Telegrafenberg, 14473 Potsdam, Germany
[***]now at: Institute of Geological Sciences, University of Bern, Baltzerstraße 1+3, Bern, Switzerland
[****]now at: Umeå University, Ecology and Environmental Sciences, 981 07 Abisko, Sweden

Correspondence to: N. R. Nowaczyk (norbert.nowaczyk@gfz-potsdam.de)

Received: 15 May 2013 – Published in Clim. Past Discuss.: 7 June 2013
Revised: 18 September 2013 – Accepted: 26 September 2013 – Published: 1 November 2013

Abstract. A 318-metre-long sedimentary profile drilled by the International Continental Scientific Drilling Program (ICDP) at Site 5011-1 in Lake El'gygytgyn, Far East Russian Arctic, has been analysed for its sedimentologic response to global climate modes by chronostratigraphic methods. The 12 km wide lake is sited off-centre in an 18 km large crater that was created by the impact of a meteorite 3.58 Ma ago. Since then sediments have been continuously deposited. For establishing their chronology, major reversals of the earth's magnetic field provided initial tie points for the age model, confirming that the impact occurred in the earliest geomagnetic Gauss chron. Various stratigraphic parameters, reflecting redox conditions at the lake floor and climatic conditions in the catchment were tuned synchronously to Northern Hemisphere insolation variations and the marine oxygen isotope stack, respectively. Thus, a robust age model comprising more than 600 tie points could be defined. It could be shown that deposition of sediments in Lake El'gygytgyn occurred in concert with global climatic cycles. The upper ~ 160 m of sediments represent the past 3.3 Ma, equivalent to sedimentation rates of 4 to 5 cm ka^{-1}, whereas the lower 160 m represent just the first 0.3 Ma after the impact, equivalent to sedimentation rates in the order of 45 cm ka^{-1}. This study also provides orbitally tuned ages for a total of 8 tephras deposited in Lake El'gygytgyn.

1 Introduction

Lake El'gygytgyn in the Far East Russian Arctic (67.5° N, 172° E) with a diameter of 12 km is located off-centre in an 18 km wide impact crater formed 3.58 Ma ago (Layer, 2000). The 170 m deep lake has a bowl-shaped morphology, a surface area of 110 km^2, and a relatively small catchment of 293 km^2 (Nolan and Brigham-Grette, 2007). The bedrock in the crater catchment consists mainly of igneous rocks, lavas, tuffs, ignimbrites of rhyolites and dacites, rarely andesites and andesitic tuffs (Gurov and Koeberl, 2004), some of them with ages from 83.2 to 89.3 Ma (Layer, 2000) and 88 Ma (Kelley et al., 1999). Thus, they were emplaced during the Cretaceous normal polarity superchron (Ogg and Smith, 2004). In early 2009, the International Continental

Published by Copernicus Publications on behalf of the European Geosciences Union.

Scientific Drilling Program (ICDP) drilled through the whole 318 m thick sedimentary infill and further 199 m into the impact breccia of the El'gygytgyn crater (Melles et al., 2011). Three parallel sediment cores from ICDP Site 5011-1 (holes 1A, 1B, and 1C) from Lake El'gygytgyn were spliced to make a composite core. For the palaeo-climatic investigation mass movement deposits, like turbidites, and tephra layers were not included, but they are represented by gaps in the respective composite data records. In order to develop a high-resolution age model for the whole sedimentary sequence from Lake El'gygytgyn we used a multi-parameter approach. Major age constraints are provided from a comprehensive magnetostratigraphic investigation of the sediments recovered from holes 5011-1A, 1B, and 1C (Haltia and Nowaczyk, 2013). For refining the initial age model determined by the magnetostratigraphic results, nine additional stratigraphic parameters were synchronously tuned either to the benthic foraminiferal oxygen isotope (δ^{18}O) reference record for the last 5 Ma provided by Lisiecki and Raymo (2005), in general referred to as the LR04 stack, or to the Northern Hemisphere summer insolation according to orbital solutions of Laskar et al. (2004). From the data compilations of Nowaczyk et al. (2002), Nowaczyk et al. (2007), Frank et al. (2013) and the rock magnetic pilot study by Murdock et al. (2013) it became obvious that variations of total organic carbon (TOC) and magnetic susceptibility (MS) mostly reflect the redox conditions at the lake floor, with a predominant stratification (mixing) of the water body and anoxic (oxic) conditions during glacials (interglacials). These redox conditions are obviously controlled by insolation variations, mainly influenced by the 18 and 23 kyr precessional cycles, and, to a lesser extent, the 41 kyr obliquity cycle. Consequently, variations of TOC and MS, together with the intensity of the natural remanent magnetisation (NRM, which in Lake El'gygytgyn sediments, like the MS, mainly reflects the concentration of magnetic particles), were tuned to insolation variations. Since Lake El'gygytgyn is located within the Arctic permafrost region most sedimentary transport and bioproductivity takes place during summer, characterized by superficial thawing of permafrost soils, short vegetation periods in the catchment, and algal growth (mostly diatoms, but also *Botriococcus* and sometimes snow algae such as *Chlamidomonas*) in the water body. From mid-autumn to mid-spring all these processes come to a standstill. Thus, not only the intensity of insolation but also the length of the summer appears to be important for the possibility of sediment transport from the catchment into the lake. Therefore, we used the cumulative summer insolation from May to August for tuning. Variations in tree and shrub pollen percentage and biogenic silica (BSi) represent vegetation conditions in the (wider) area around the lake and bioproductivity within its water body, respectively. Sediment grain size, spectral colour, titanium (Ti) content, and Si / Ti ratio, the latter two parameters obtained from X-ray fluorescence (XRF) scanning, reflect mostly weathering and transport processes within and from the catchment, respectively, which in turn depend on climatic conditions. After initial age assignments using magnetic polarity stratigraphy, all these parameters together show striking similarities to global climate variability as expressed by the LR04 stack (Lisiecki and Raymo, 2005), which was therefore used as reference curve. The major environmental implications of the El'gygytgyn palaeoclimate record, occurrence of "super-interglacials" and the stepwise cooling of the Northern Hemisphere are discussed in Melles et al. (2012) and Brigham-Grette et al. (2013), respectively.

In general, age models derived from tuning may include several problems, such as circular reasoning or chronological uncertainties in both the reference record and the record to be tuned, when only restricted sets of data are consulted (Blaauw, 2012). However, wiggle matching can be further validated by using multi-proxy tuning (e.g. Bokhorst and Vandenberg, 2009; Prokopenko et al., 2006), as it was also performed in this study.

2 Material and methods

2.1 Data acquisition

For magnetostratigraphic investigation the upper $\sim$ 140 m of sediments were continuously subsampled with U-channels, whereas the remaining sequences were nearly exclusively analysed by using discrete samples, due to increasing stiffness of the sediments. Determination of the inclination of characteristic remanent magnetization (ChRM), which provides the polarity interpretation, is based on principle component analysis (Kirschvink, 1980) of results from stepwise and complete alternating field demagnetisation of all material. More detailed information on sampling strategy, data acquisition techniques, and methods of processing are given by Haltia and Nowaczyk (2013).

Magnetic (volume) susceptibility from cores PG1351 and Lz1024 were acquired with a Bartington MS2E sensor in combination with a MS2 control unit, integrated into the 1st generation GFZ split-core logger (scl-1.1). Magnetic susceptibility and colour information from sediments from ICDP Site 5011-1 cores were obtained every 1 mm using a 2nd generation split-core logger (scl-2.3), with its hardware and software designed and built at the Helmholtz Centre Potsdam, GFZ. Magnetic susceptibility was measured with a Bartington MS2E spot-reading sensor first attached to a MS2 control unit, which was later replaced by a technically improved MS3 control unit.

The response function of the MS2E sensor with respect to a thin magnetic layer is equivalent to a Gaussian curve with a half-width of slightly less than 4 mm (e.g. Fig. 4 in Nowaczyk, 2001). The amplitude resolution of the sensor is 10×10^{-6} in combination with the MS2 unit and 2×10^{-6} with the improved MS3 unit, both using an integration time of about a second. During data acquisition, after

every 10 measurements, the sensor is lifted about 4 cm above the sediment in order to take a blank reading in the air. This is done in order to monitor the shift of the sensor's background due to temperature drift. Subsequently, the air readings were linearly interpolated and subtracted from the readings on sediment.

A spectrophotometer (GretagMacbeth Spectrolino™) was applied with the scl-2.3 logger for acquiring a full colour spectrum from 380 nm to 720 nm at a physical resolution of 10 nm (i.e. providing 36 spectral lines for each measuring spot from ICDP Site 5011-1 cores). For sediments recovered within cores PG1351 and Lz1024 no colour information is available. The spectrophotometer integrates over a circular window of 4 mm in diameter (centre-weighted). In addition to the visible spectrum further colour information, derived from the spectral data, was transmitted by the instrument: the tristimulus values (X, Y, Z), defined by the International Commission on Illumination (CIE) in 1931, and vectors in the 1976 CIE (L^*, a^*, b^*) colour space. The tristimulus values of a colour are the amounts of the three colours the human eye can perceive (red, green, blue) in a three-component additive colour model (Fig. 2a). However, in order to reproduce a measured colour represented by (X, Y, Z) (e.g. on a TV or computer screen) a 3×3 matrix has to be applied to the (X, Y, Z) vector in order to obtain the required (R, G, B) values for display, as it is implemented in the split-core logger's controlling computer program. The elements of the matrix depend on type of illumination and observing angle, as well as on the (R, G, B) properties of the used hardware and/or computer operating system (or television system).

In the (L^*, a^*, b^*) colour space (Fig. 2b), the a^* coordinate represents variations in colour between red ($a^* > 0$) and green ($a^* < 0$), whereas the b^* coordinate represents variations in colour between yellow ($b^* > 0$) and blue ($b^* < 0$). The L^* component represents lightness (0 = black, 100 = white). In order to distinguish major colour changes of the sediments from Lake El'gygytgyn the hue angle (H) was also determined (Fig. 2b and c). It is calculated as $H = \text{atan2}\,(b^*, a^*)$, with $0° \leq H \leq 360°$. Hue values of major colours are red = 0°/360°, yellow = 60°, green = 120°, cyan = 180°, blue = 240°, magenta = 300°. An example of sediment colour, hue angle distribution, and individual colour spectra as obtained with the Spectrolino™ is shown in Fig. 3.

Since both the susceptibility and colour sensors need to be in full contact to the sediment surface, the scl-2.3 logger is additionally equipped with a third sensor, a high-precision mechanical micro-switch to scan the surface morphology first. This is achieved by moving the switch from a certain reference height downward onto the sediment where the switch triggers the termination of its own movement. Triggering force is in the range of 5 g. The distance moved by the switch is determined by the stepping motor control, thus supplying the information needed for subsequently lowering the susceptibility sensor and the spectrophotometer onto the sediment for data acquisition. During data acquisition core segments were covered by a thin and clear plastic foil in order to prevent all three sensors from being stained by the soft and moist sediments. Ideally, the foil is completely free of air bubbles and clinging to the sediment surface due to sediment moisture. However, the older the sediments are the lower their moisture content is. Thus, downward from about 200 m on, the foil was not always completely attached to the sediments and colour information got slightly biased with increasing drilling depth due to scattered light.

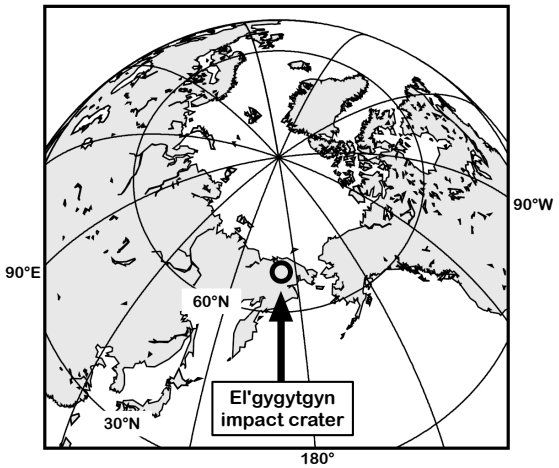

Fig. 1. Location of Lake El'gygytgyn in the Far Eastern Russian Arctic. The circle (not to scale) marks the site of the impact crater.

2.2 Further data used for tuning

Biogenic silica (BSi) contents were estimated at a sampling interval of 20 mm by using Fourier transform infrared spectroscopy (FTIRS). The method is described in detail by Vogel et al. (2008) and Rosén et al. (2010, 2011). Biogenic silica is mostly derived from diatoms, which are the major contributors to the intra-lake bioproduction (e.g. Cherapanova et al., 2007). Post-sedimentary dissolution of diatom frustules is negligible in sediments of Lake El'gygytgyn. Thus, the percentage of biogenic silica is taken as a proxy for bioproductivity in Lake El'gygytgyn. A detailed discussion on FTIRS results from ICDP Site 5011-1 is provided by Meyer-Jacob et al. (2013) and Vogel et al. (2013).

The content of total organic carbon (TOC) was determined every 20 mm using a Vario microCube elemental analyzer (Elementar, Germany). Elemental scans of major elements were performed with an ITRAX XRF (X-ray fluorescence) core scanner (Cox Analytical, Sweden), equipped with Cr- and Mo-tubes, respectively, which were set to 30 kV and 30 mA. The abundance of elements was determined at 2 mm resolution with an integration time of 10 s per measurement. The relative abundance of titanium (Ti) is taken as

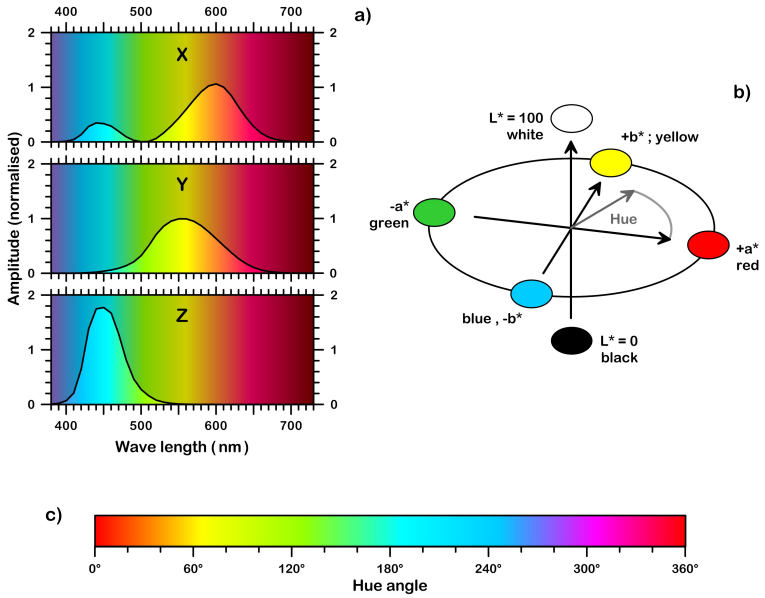

Fig. 2. Some basics in colour processing: **(a)** 2°-observer weighting functions for spectrum integration in order to obtain the tristimulus values (X, Y, Z), **(b)** $L^*a^*b^*$ colour space and definition of the hue angle as also shown in **(c)**, together with corresponding colours. Note that colours are more schematic rather than realistic.

a proxy of clastic lithogenic input, whereas silica (Si) represents the sum of both lithogenic and biogenic Si. Thus, the Si / Ti ratio reflects the variable contribution of biogenic silica against the clastic lithogenic background. For further details see Wennrich et al. (2013). Grain-size variability was estimated by principle component analysis (PCA) of granulometric analyses using a laser particle analyzer (Francke et al., 2013). For tuning of the ICDP-5011-1 composite record PC 1 (principle component 1) was used, with negative (positive) values representing coarse (fine) grained sediments. Pollen data is available every 8 cm, with lower resolution in the Pliocene section (see also Andreev et al., 2013 and Lozhkin and Andersen, 2013). Where available, the percentage of tree and shrub pollen was used as an additional environmental indicator with high (low) percentages representing warm (cold) conditions. Data from PG1351 are from Nowaczyk et al. (2002), data from Lz1024 are from Lozhkin et al. (2007).

2.3 Creation of a composite

For analysis of the Lake El'gygytgyn sedimentary succession a composite was created using data from core Lz1024, recovered in 2003, and from ICDP Site 5011-1, comprising only partly overlapping holes 1A, 1B, and 1C, recovered in 2009. From the 16.64-metre-long core Lz1024 data records of the upper 5.67 m were used to supplement the uppermost section of the composite that was not recovered with ICDP Site 5011-1 cores. According to initial data analyses, this depth interval is equivalent to marine oxygen isotope stages (MIS) 1 to 4 and most of MIS 5 (back to about 125 ka). Below 5.67 m, and until about 104.8 m composite depth, alternating sediment intervals from parallel holes 5011-1A and 1B were spliced together. Between 104.8 m and 113.4 m composite depth additional information from core 5011-1C could be used. Between 113.4 m and 145.7 m composite depth, cores 1A and 1C contributed to the composite. Below 145.7 m composite depth down to the sediment impact breccia interface at 318 m, only core 5011-1C, which has a mean recovery rate of only 50 % (Melles et al., 2011), could be used. However, at least the lowermost 38 m of the composite (280 to 318 m) is available with 90 to 99 % recovery.

Core intervals for the composite were selected mainly by visual inspection, using the better preserved/least disturbed sections from one of the records in cases of overlapping recovery. In general, tephra layers, turbidites, and mass movements were omitted leaving gaps within the composite data sets. Further details are described by Wennrich et al. (2013).

2.4 Tuning

Fixed age tie points for the ICDP Site 5011-1 composite record are provided by magnetostratigraphic investigation of sediments from this site by Haltia and Nowaczyk (2013). Ages for the documented major reversals were mainly assigned according to Lisiecki and Raymo (2005) as listed in Table 1. Between the tie points provided by

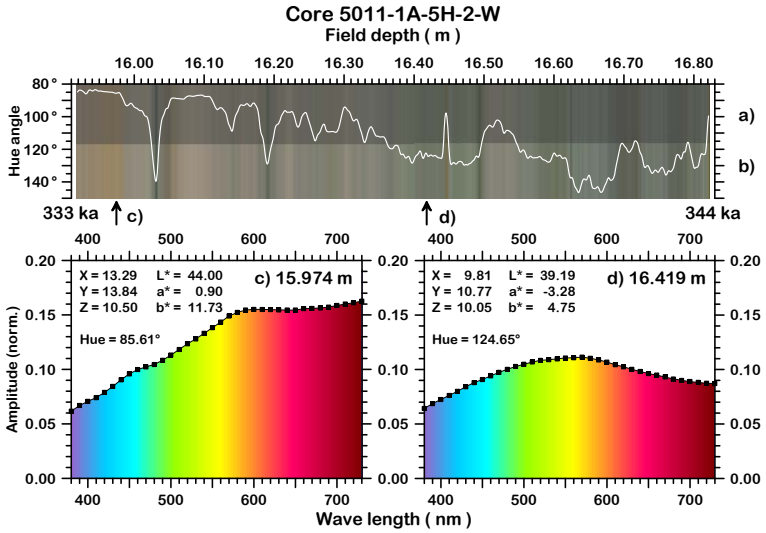

Fig. 3. Example for quantitative colour data acquisition from core 5011-1A-5H-W in field depth across Termination IV (time interval from 344 to 333 ka): **(a)** original and **(b)** contrast-enhanced down-core variation of colours measured with a GretagMacbeth Spectrolino™ spectrophotometer, together with hue angle (white curve), **(c)** and **(d)** two individual spectra including tristimulus values (X, Y, Z), (L^*, a^*, b^*) values, hue angle (see Fig. 2), and logging depth. The positions of the two measuring points are marked by arrows below **(b)**.

magnetostratigraphy, a synchronous tuning of nine additional data sets was performed using an interactive wiggle matching software. The **e**xtended **t**ool for **c**orrelation (**xtc**, Linux-based) is capable of loading all necessary data sets together into the memory of the computer (down-core data sets, reference data sets, age models, positions of tephras, scaling of axes). The (partly huge) sizes of the data sets used for tuning are listed in Table 2. In all, 1 mm spot-readings of magnetic susceptibility and TOC data, determined every 10 to 20 mm, were tuned to the Northern Hemisphere (67.5° N, El'gygytgyn latitude) cumulative spring–summer insolation (May to August) according to Laskar et al. (2004). Parallel to this, Ti as well as Si / Ti ratios based on 2 mm readings of X-ray fluorescence (XRF) counts, percentages of biogenic silica (BSi, opal) derived from Fourier transform infrared spectroscopy (FTIRS), determined every 20 mm, the hue angle determined every 1 mm, grain size PCA data, and tree pollen percentages (where available) were tuned to the LR04 marine oxygen isotope stack of Lisiecki and Raymo (2005). Jointly to the tuning of the ICDP Site 5011-1 data sets, age models for the Lake El'gygytgyn pilot cores were also developed (Lz1024) and refined (PG1351).

3 Results

The intention was to provide a sedimentary palaeoclimatic proxy-record that is cleaned of tephra layers, turbidites, slumps, and other disturbances, such as folded sediments. Therefore, these intervals were discarded for the creation of the ICDP Site 5011-1 composite. However, these sediment intervals can still provide useful information at least about the polarity of the geomagnetic field during their deposition. The expected dipole inclination for the site of Lake El'gygytgyn is 78.3°. Thus, folded layers with a tilt of, for example, 45° will still yield positive (negative) inclination during normal (reversed) polarity. It then depends on the angle between magnetization direction and tilting direction whether the disturbed direction is shallower or steeper than the undisturbed one. Also turbidites, although representing short depositional events on a geological timescale, should record a polarity if not an accurate palaeomagnetic direction at least in their upper fine-grained section. Therefore, in intervals close to reversals, the directional data of rejected intervals, such as the onset of the Olduvai subchron and reversals within the Gauss chron (see Haltia and Nowaczyk, 2013), were also taken into consideration when determining the polarity and localization of the major reversals.

3.1 Iterative tuning

The general strategy of tuning is demonstrated by data covering the time window from 740 ka to 1000 ka, comprising the Brunhes Matuyama reversal as well as the termination of the Jaramillo subchron (Fig. 4). Note that for reasons of clarity not all resulting correlation tie points within this interval are displayed. The major reversals of the earth's magnetic field, as incorporated in the official geomagnetic polarity timescale (GPTS, Ogg and Smith, 2004; Table 1), provide twelve 1st

Table 1. Ages of geomagnetic reversals from various authors, listed in the first row, and as inferred from multi-proxy tuning of ICDP Site 5011-1 sediments from Lake El'gygytgyn in this study, listed in the right column. Here, bold numbers indicate new/alternative ages, otherwise ages were adopted from Lisiecki and Raymo (2005).

Authors	Cande and Kent (1995)	Lourens et al. (1996)	Ogg and Smith (2004)	Lisiecki and Raymo (2005)	This study
Reversal			**Age**		
subchron					
cryptochron/excursion	Ma	Ma	Ma	Ma	Ma
Brunhes/Matuyama	0.780		0.781	0.780	0.780
Jaramillo (t)	0.990		0.988	0.991	0.991
intra-Jaramillo excursion (t)					**1.0142**
intra-Jaramillo excursion (o)					**1.0192**
Jaramillo (o)	1.070		1.072	1.075	1.075
Cobb-Mountain (t)	1.201		1.173		**1.1858**
Cobb-Mountain (o)	1.211		1.185		**1.1938**
Olduvai (t)	1.770	1.785	1.778	1.781	1.781
Olduvai (o)	1.950	1.942	1.945	1.968	1.968
Olduvai precursor (t)					**1.9782**
Olduvai precursor (o)					**1.9815**
La Réunion (t)	2.140	2.129	2.128		**2.1216**
La Réunion (o)	2.150	2.149	2.148		**2.1384**
Matuyama/Gauss	2.581	2.582	2.581	2.608	**2.588**
Kaena (t)	3.040	3.032	3.032	3.045	3.045
Kaena (o)	3.110	3.116	3.116	3.127	3.127
Mammoth (t)	3.220	3.207	3.207	3.210	3.210
Mammoth (o)	3.330	3.330	3.330	3.319	3.319
Gauss/Gilbert	3.580	3.596	3.596	3.588	3.588

Here: o – onset , t – termination.

order tie points (red dotted lines in Fig. 4) during the last 3.6 Ma for the age model, from which ten are very well defined in the El'gygytgyn sedimentary sequence. Only the top of the Kaena and the base of the Mammoth subchrons, both within the Gauss chron, are somewhat ambiguous, when only (cleaned) palaeomagnetic information are considered. Additional two 1st order tie points could be derived from the short Cobb Mountain event (Mankinen et al., 1978) within the Matuyama Chron, clearly linked to MIS 35 (Channell et al., 2008). Figure 4 comprises the Brunhes Matuyama reversal and the termination of the Jaramillo subchron as 1st order tie points. For the base of the lacustrine sediment section from Lake El'gygytgyn the age of the impact of 3.58 ± 0.04 Ma was adopted from Layer (2000) as another 1st order tie point.

After adopting this approach to convert depths into ages it became obvious that the morphology of the log(Si / Ti ratio) curve obtained from XRF scanning resembles the LR04 oxygen isotope reference curve from Lisiecki and Raymo (2005) quite well (Fig. 4b, d). The same is valid for the Ti content and the hue angle, when both plotted on an inverse axis (not shown in Fig. 4), and partly the record of biogenic silica obtained from Fourier transform infrared spectroscopy (FTIRS-BSi), which mainly resembles the so-called super-interglacials (Melles et al., 2012) from above a certain threshold level (Fig. 4a). This set of proxy records therefore was used to define 2nd order tie points (dark green short-dashed lines in Fig. 4) by interactive wiggle matching to the LR04 curve.

Compared to the LR04 stack, the Northern Hemisphere summer insolation shows a much stronger variability. Note that already the onsets of interglacials, MIS 19, 21, and 25, are linked to pronounced insolation maxima. In the further course of these interglacials one (MIS 19 and 25) or even two insolation minima occur (MIS 21). These minima and most of all other minima in insolation are obviously linked to lows in magnetic susceptibility and highs in TOC when applying 1st and 2nd order tie points for correlation. Figure 5 shows a simplified sketch of interdependencies of sedimentary properties versus insolation variations. Minima in insolation trigger anoxic conditions at the lake floor associated with severe dissolution of magnetic minerals (low magnetic susceptibility) but best preservation of organic matter (high TOC values). The termination of such phases coincide fairly well with the steepest gradient of increasing insolation after the preceding insolation minimum, and the beginning of intervals characterized by high susceptibility. Insolation maxima mark the beginning of periods with high bioproductivity. Nevertheless, due to dominating oxic bottom water

Table 2. Overview of stratigraphic data used for multi-proxy tuning of Lake El'gygytgyn sediments: number of obtained logger readings or individual determinations, with numbers in italics indicating raw data that was acquired on the full stratigraphic lengths of the respective cores. Scanning/sampling intervals are given below the parameter notation.

Data set	*5011-1A*	*5011-1B*	*5011-1C*	5011 comp.	Lz1024	PG1351	total
MS2E[a] 1 mm	*122 939*	*100 606*	*95 264*	143 752	16 026	11 050	489 637
colour[b] 1 mm	*122 988*	*101 074*	*99 060*	138 623	no	no	461 745
XRF[c] 2 mm	*61 357*	*50 132*	*46 464*	71 263	8273	186	237 675
NRM, ChRM[d] 2 (10–15) cm	*5806*	*4848*	*2113*	5883	607	476	19 733
biog. Silica[e] (1) 2 cm	*no*	*no*	*no*	5856	1657	229	7742
TOC[f] (1) 2 cm	*no*	*no*	*no*	6136	1658	334	7847
grain size 8 cm	*no*	*no*	*no*	1125	no	no	1125
Tree pollen[g] 5–6 (30–300) cm				392	184	124	556

[a] magnetic susceptibility, [b] full visible colour spectrum (36 lines), (X, Y, Z) tristimulus values, (L^*, a^*, b^*), hue angle, [c] X-ray fluorescence spectra, abundance of major elements [d] natural remenent magnetisation (NRM) and characteristic remanent magnetisation (ChRM) from U-channels, sampling interval for discrete samples in brackets, [e] from Fourier Transform Infrared Spectrocopy (FTIRS-BSi), sampling interval for Lz1024 in brackets, [f] total organic carbon, sampling interval for Lz1024 in brackets, [g] sampling interval for Pliocene interval in ICDP Site 5011-1 cores in brackets.

conditions, organic matter gets degraded (low TOC values), whereas magnetic minerals are being widely preserved, leading to high values in magnetic susceptibility, although the lithogenic contribution is lower than during glacials. During the super-interglacials (Melles et al., 2012), characterized by exceptional high biogenic silica values and high Si / Ti ratios – such as MIS 5, 9, 11, 17, 25 (see Fig. 4), 31, 47, and 49 (see also Supplement) – the high deposition rate of biogenic matter is the major controlling factor for modulating values of both magnetic susceptibility and TOC. The increased flux of organic matter into the sediment partly overwhelms degradation processes in oxic bottom waters, leading to intermediate values in both TOC and magnetic susceptibility. A fast oxygen consumption in the sub-bottom pore water has to be assumed which hampered a further sub-surface degradation of organic matter. Thus in total, a partial degradation of organic matter should have occurred so that the associated TOC peaks very likely give an underestimation of the primary bioproductivity (Nowaczyk et al., 2002, 2007). Magnetic susceptibility values are mostly controlled by the high primary bio-production and thus a by dilution of lithogenic compounds. Further on due to oxygen depletion in the pore waters, a partial dissolution of magnetic minerals has to be taken into account, since susceptibility values cannot be explained by dilution by biogenic compounds alone. Another special case is that of a glacial supposedly much moister than others (Melles et al., 2007). Due to increased snowfall and thus reduced light transmission, bioproductivity below the ice cover is significantly lower than during dry glacials. During dry glacials, Lake El'gygytgyn was supposed to be covered by clear ice, that is, with little to no snow on it, associated with a high light transmission, and thus better growing conditions for algae. Considering all these interdependencies, 3rd order tie points could be defined for fine-tuning (blue long-dashed lines in Fig. 4).

3.2 Chronostratigraphy and precision of age model

Figure 6 shows the most important parameters from ICDP Site 5011-1 composite record after synchronous tuning to the GPTS, the LR04 stack, and the Northern Hemisphere summer insolation. The parameters that were mainly tuned to the LR04 marine oxygen isotope stack (Fig. 6f) are plotted in the left section (Fig. 6a to e): grain size variations, hue angle (sediment colour), biogenic silica (FTIRS-BSi), Si / Ti ratio from XRF-scanning, and tree and shrub pollen percentages where available, including results from pilot cores PG1351 and Lz1024. The ChRM inclinations of the ICDP Site 5011-1 composite record (Fig. 6g) is plotted to the right of the LR04 stack. Geomagnetic field reversals can be recognized from flips between steep positive inclinations (normal polarity, grey background) and steep negative inclinations (reversed polarity, white background). Thus, the ICDP Site 5011-1 sedimentary record comprises the three geomagnetic chrons including Brunhes, Matuyama, and (most of the) Gauss (i.e. the last about 3.6 Ma). The right section of Fig. 6 relates variations of total organic carbon (TOC,

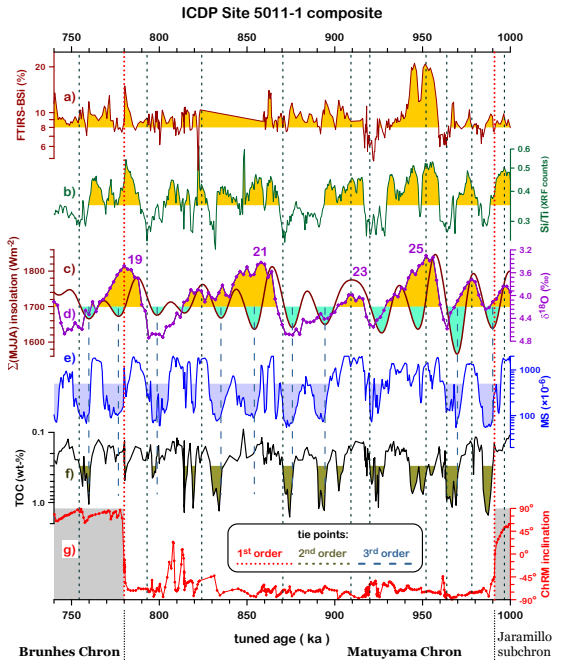

Fig. 4. Definition of 1st, 2nd, and 3rd order tie points of the age model: Chronostratigraphic plot for the time window 740 ka to 1000 ka of **(a)** biogenic silica (FTIRS-BSi), **(b)** Si / Ti ratio, with high (low) ratios indicating higher (lower) biogenic input with respect to lithogenic input, **(c)** cumulative summer (May to August) insolation for 67.5° N (according to Laskar et al., 2004), **(d)** LR04 oxygen isotope stack (δ^{18}O) from Lisiecki and Raymo (2005), **(e)** magnetic susceptibility (MS), **(f)** total organic carbon (TOC), and **(g)** ChRM inclination, with grey (white) indicating normal (reversed) polarity. Geomagnetic field reversals are defined as 1st order tie points of the age model. Correlation of Si / Ti ratio and biogenic silica to the LR04 stack define 2nd order tie points, and correlation of magnetic susceptibility and TOC to insolation patterns define 3rd order tie points. For further details, see text. FTIRS – Fourier transform infrared spectroscopy, XRF – X-ray fluorescence, ChRM – characteristic remanent magnetization.

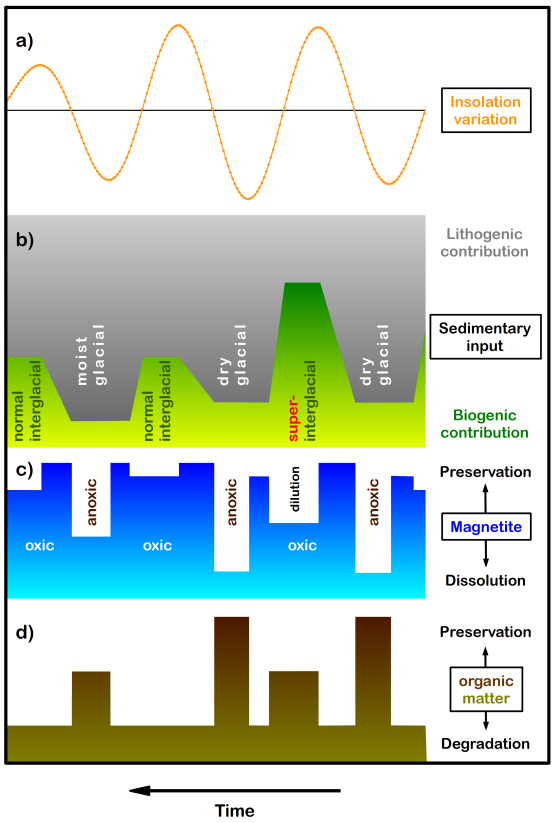

Fig. 5. Simplified sketch of interdependencies of Lake El'gygytgyn sedimentary properties with orbital forcing throughout the Pleistocene: **(a)** variation of summer insolation, **(b)** lithogenic versus biogenic sedimentary input, **(c)** magnetic susceptibility, and **(d)** concentration of organic matter. For detailed explanation see text.

Fig. 6h) and magnetic susceptibility (Fig. 6i) to the Northern Hemisphere insolation (cumulative, May to August, 67.5° N, Fig. 6j). The obtained age model of the ICDP 5011 composite is shown in Fig. 7 and age models for the pilot cores, PG1351 and Lz1024, are shown in Fig. 8. Mean sedimentation rates in Lake El'gygytgyn are in the range of 4 cm ka^{-1} for the last about 1.0 Ma. Going further back in time, sedimentation rates slightly increase to about 5 cm ka^{-1} roughly between 2.5 and 3.0 Ma, whereas the interval between 3.3 and 3.6 Ma is characterized by ten-fold higher sedimentation rates of about 45 cm ka^{-1}. This must be due to major environmental changes. In the marine LR04 oxygen isotope stack the oldest shift towards heavier values during the past 3.6 Ma, MIS M2 within the early Mammoth subchron, occurs around 3.3 Ma (see supporting online material for a more detailed display and labelling of data). This is parallelled by a drastic drop in tree and shrub pollen percentage down to 20 % in the sedimentary record of Lake El'gygytgyn. Furthermore, this actually substantiated the position of the onset of the Mammoth subchron in the ICDP Site 5011-1 record, since here the interpretation of palaeomagnetic data is hampered by numerous recovery gaps and low core quality.

In the first place, the precision of the age model(s) of Lake El'gygytgyn sediments is limited by the accuracy, precision and temporal resolution of the reference curves. The LR04 oxygen isotope stack for the last 5 Ma is provided in 1 kyr increments. Lisiecki and Raymo (2009) point out that especially the timing of glacial terminations documented in benthic oxygen isotope records from the Atlantic and the Pacific can already differ by up to 4 kyr. This problem accounts mainly for new marine benthic oxygen isotope records to be

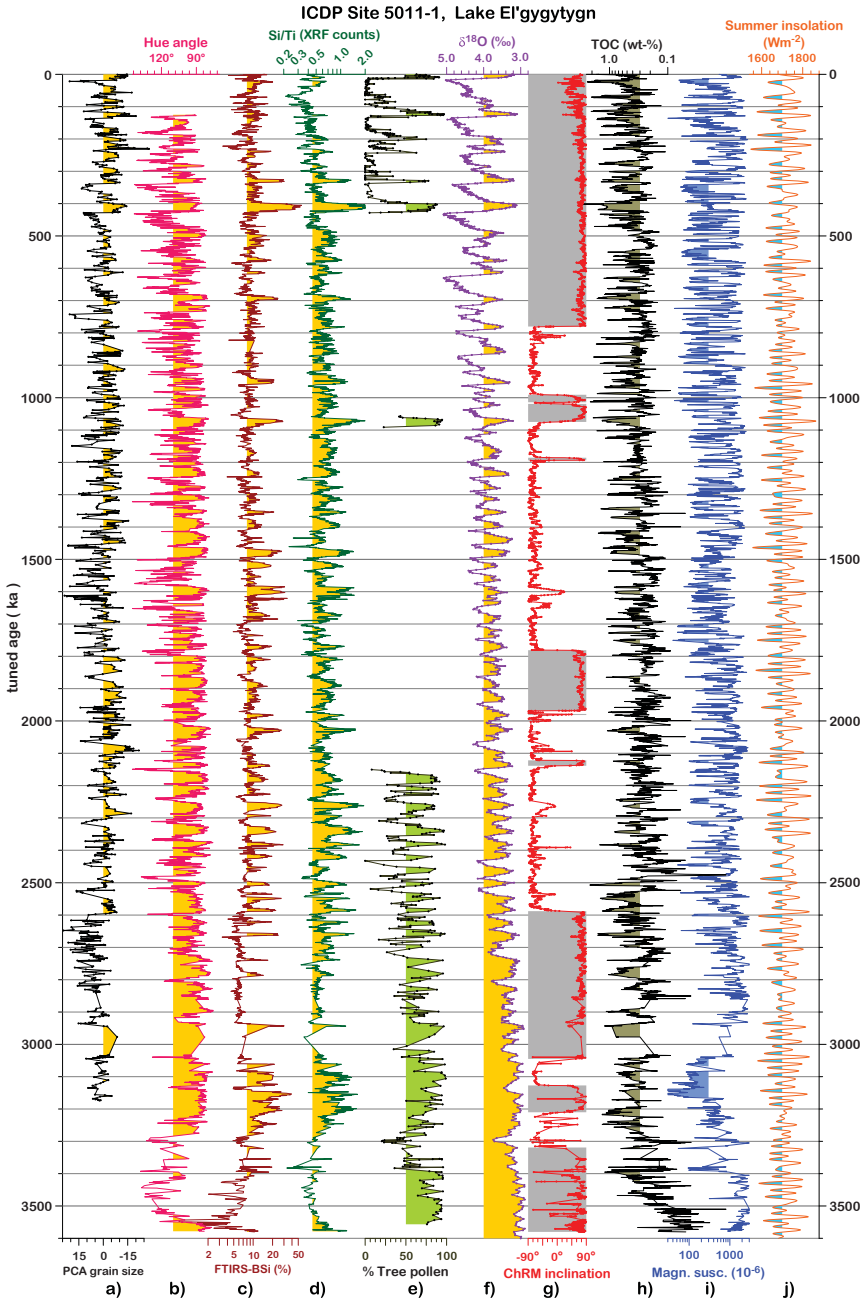

Fig. 6. Chrono-stratigraphic plot of main parameters used for developing the age model of the ICDP Site 5011-1 composite record from Lake El'gygytgyn: **(a)** grain size data from principle component analysis (PCA), with negative (positive) values representing coarse (fine) grained sediments, **(b)**, hue angle from photospectrometry (see Fig. 2), **(c)** biogenic silica from Fourier transform infrared spectroscopy (FTIRS-BSi), **(d)** Si / Ti ratio from X-ray fluorescence (XRF) scanning, **(e)** tree and shrub pollen percentages, **(f)** marine oxygen isotope stack (Lisiecki and Raymo, 2005), **(g)** inclination of the characteristic remanent magnetisation (ChRM), with grey (white) indication normal (reversed) polarity, **(h)** total organic carbon (TOC), **(i)** magnetic susceptibility, and **(j)** the cumulative Northern Hemisphere summer insolation (May to August), according to orbital solutions provided by (Laskar et al., 2004).

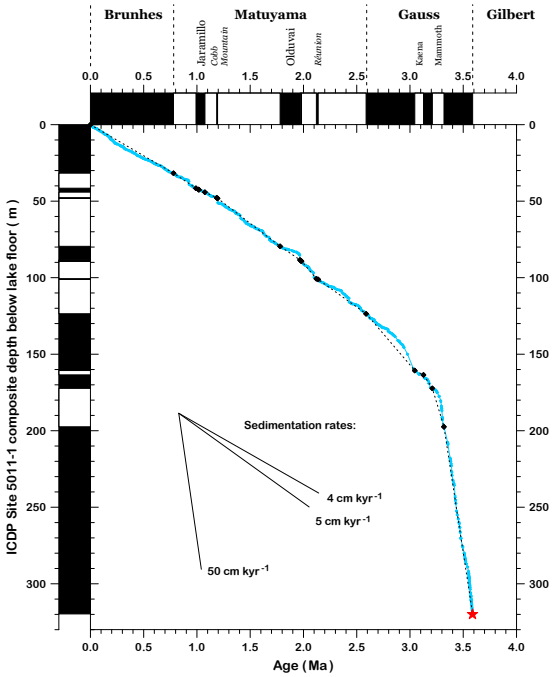

Fig. 7. Age depth model for the ICDP Site 5011-1 sedimentary composite record derived from tuning of physical, sedimentological, geochemical, and pollen records to the benthic oxygen isotope stack from Lisiecki and Raymo (2005) and the Northern summer insolation according to orbital solutions provided by (Laskar et al., 2004), respectively. Initial 1st order tie points (black diamonds) were provided by a comprehensive magnetostratigraphic investigation of ICDP Site 5011-1 cores (Haltia and Nowaczyk, 2013; see also Fig. 2). The red star marks the time of the impact inferred from $^{40}Ar/^{39}Ar$ dating (Layer, 2000) at 3.58 (±0.04) ka. Black (white) denote normal (reversed) polarity.

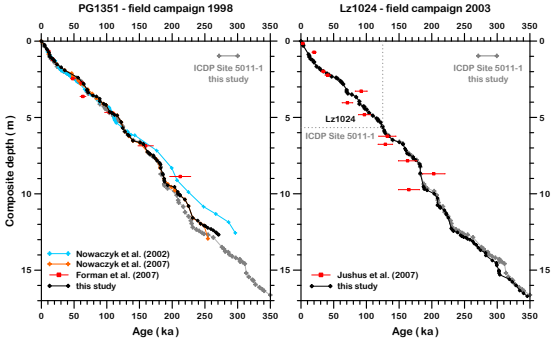

Fig. 8. Age depth models for pilot cores PG1351 (1998) and Lz1024 (2003) after synchronizing with ICDP Site 5011-1 age model (Fig. 7). Red squares with error bars mark results from infrared stimulated luminescence (IRSL) dating. The dotted line in the right graph mark the junction between Lz1024 and the ICDP Site 5011-1 composite record, assembled from cores 5011-1A, -1B, and -1C.

dated by correlation to a master record. However, the LR04 stack/master record is based on records with a global distribution, including the Atlantic and Pacific Oceans, so that stratigraphic correlation to it might introduce inaccuracies in dating in the range of several kyrs. The LR04 stack has been tuned to the 21 June insolation at 65° N according to orbital solutions of Laskar et al. (1993). Because of uncertainties in these solutions, Lisiecki and Raymo (2005) conclude that absolute ages in their LR04 stack might be offset by several kyrs, depending on time interval: up to 4 kyr from 0 to 1 Ma, up to 6 kyr from 1 to 3 Ma, up to 15 kyr from 3 to 4 Ma. In addition to usage of the LR04 stack as stratigraphic reference, we tuned magnetic susceptibility and TOC variations from Lake El'gygytgyn sediments to updated orbital solutions given in increments of 0.25 kyr and with an uncertainty of 0.1 % according to Laskar et al. (2004). Thus, tuning data with ages around 3 Ma might be offset by only 3 kyr. Therefore, absolute ages of El'gygytgyn sediments are possibly offset by up to about 3 kyr (considering Laskar et al., 2004) to 15 kyr (considering Lisiecky and Raymo, 2005) in the Pliocene, but relative age assignments to the reference records should have a precision of some 500 yr since many (3rd order) tie points were derived from the insolation reference record, which has a higher temporal resolution.

4 Discussion

4.1 Age of meteorite impact

The lowermost distinctly stratified sediments recovered from Lake El'gygytgyn clearly show normal polarity. Some intercalations of suevitic material in this section imply that these sediments must have been deposited shortly after the impact. The suevites are supposed to have been episodically washed in from the intra-crater catchment. Palaeomagnetic data from the underlying suevites show predominantly a normal polarity, too (Maharaj et al., 2013). Thus, it can be concluded, that the impact that created the El'gygytgyn Crater occurred definitely after the Gauss–Gilbert reversal (Table 1). However, it is not clear how long it took to form a permanent lake within the impact crater and when it came to a persistent deposition of sediments into it. Figure 9 shows the dating of the impact by Layer (2000) within the context of the geomagnetic polarity timescale(s). The 1σ error range of the dating (3.58 ± 0.04 Ma) crosses the Gauss-Gilbert reversal. Thus, the only conclusion that can be drawn is that the older (upper) limit for the age of the impact can be set to 3.588 Ma, when adopting the LR04 timescale, or to 3.596 Ma when using the Ogg and Smith (2004) GPTS. Unfortunately, no biogenic remnants (neither diatoms, nor pollen) that would

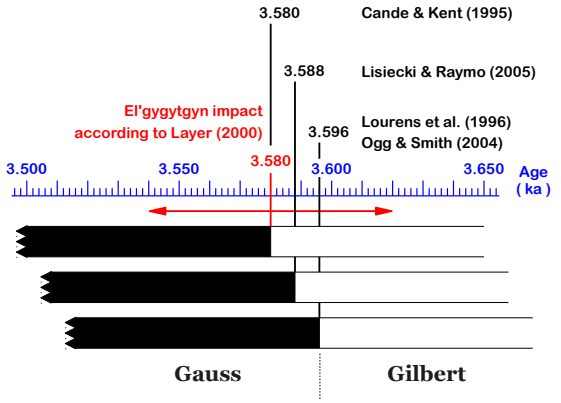

Fig. 9. Radiometric dating of the El'gygytgyn impact (Layer, 2000) in the context of currently used geomagnetic polarity timescales. Since the lowermost ICDP Site 5011-1 sediments show clear normal polarity directions, the impact must have occurred after the Gilbert Gauss reversal.

allow assignments to climate cycles are preserved within the lowermost about 25 m of sediments. Therefore, the younger (lower) limit of the impact age of 3.540 Ma is still defined by the 1σ error range of Layer (2000).

4.2 Polarity stratigraphy

In general, as listed in Table 1, our multi-proxy study of the Lake El'gygytgyn ICDP Site 5011-1 sedimentary record confirms ages of geomagnetic reversals within the past 3.6 Ma as given by Lisiecki and Raymo (2005). Table 1 lists also ages of known reversals provided in the geomagnetic polarity times scales (GPTS) of Cande and Kent (1995), Lourens et al. (1996), and Ogg and Smith (2004), since Lisiecki and Raymo (2005) do not provide ages for all of them. In addition to this, reversal ages listed in the various GPTSs slightly deviate from each other.

Palaeomagnetic data quality of the Gauss chron at ICDP Site 5011-1 is very heterogeneous since it is based mainly on a single core, ICDP 5011-1C (Haltia and Nowaczyk, 2013). Normal polarity in its earliest part is very well established. But between ~3.55 and ~2.95 Ma (290 and 145 m composite depth) directions are fairly scattered due to numerous recovery gaps and bad core quality, with at least some increase of data coverage around the middle Gauss normal polarity phase. Thus, the onset of the Mammoth and the termination of the Kaena reversed polarity subchrons are not clearly expressed. However, using the available data set of climate-proxy parameters a fairly robust age model could be achieved even for this interval. From ~2.95 Ma on (290 m composite depth) the ICDP 5011-1 composite is based on at least two cores and normal polarity within the upper Gauss chron is well expressed.

According to our study, the Matuyama Gauss reversal, consistently documented in cores ICDP Site 5011-1A and 1C (Haltia and Nowaczyk, 2013), occurred at 2.588 Ma, clearly within MIS 103 (Table 1, Fig. 6). Deino et al. (2006) provide an $^{40}Ar/^{39}Ar$-based age of 2.589 ± 0.003 Ma from two tephras, tightly bracketing the Matuyama Gauss reversal in the upper part of a diatomite of the fluvio-lacustrine sediments in the Chemeron Basin, Central Kenya Rift, Afrika. This would be in excellent agreement to our result. However, Deino et al. (2006) tune their radiometrically obtained age to an astronomically polarity timescale and shift this age to 2.610 Ma. This is close to the age of 2.608 Ma, given by Lisiecki and Raymo (2005). But, this would place the Matuyama Gauss reversal into MIS 104, a cold interval. This contradicts our stratigraphic results that only allow placement of the Matuyama Gauss reversal into the middle MIS 103 (Table 1, Fig. 6) (i.e. within a warm interval). This is also in agreement with findings by Prokopenko and Khursevich (2010) from Lake Baikal Site BDP-96. Thus, the Matuyama Gauss reversal at ICDP Site 5011-1, is definitely not recorded in MIS 104, but in MIS 103 at 2.588 Ma. The younger age of 2.581 Ma for this major reversal, given by Ogg and Smith (2004), places the Matuyama Gauss reversal into the late MIS 103 which also does not fit to results from Lake El'gygytgyn.

The reversed Matuyama chron is mainly interrupted by the prominent Olduvai and Jaramillo normal polarity subchrons, clearly expressed in the ICDP Site 5011-1 record. Besides these, there are three further, much shorter intervals of normal polarity, not listed in Lisiecki and Raymo (2005): the Réunion subchron (Chamalaun and McDougall, 1966; McDougall and Watkins, 1973), an Olduvai precursor (Channell et al., 2003), and the Cobb Mountain subchron (Mankinen et al., 1978). The ICDP Site 5011-1 derived age range for the Réunion subchron of 2.1216–2.1384 Ma is in good agreement with the GPTSs (Table 1) and radiometric dating results of 2.14 ± 0.03 Ma by Baksi et al. (1993), 2.137 ± 0.016 Ma by Singer et al. (2004), or 2.15 ± 0.02 Ma by Quidelleur et al. (2010). The results are also consistent with magnetostratigraphic data from North Atlantic ODP Site 981 (Feni Drift; Channell et al., 2003, Fig. 3), placing the Réunion subchron into MIS 80 and 81 (see Supplement). Magnetostratigraphic results from ICDP Site 5011-1 give an age range for the Olduvai precursor of 1.9782 to 1.9815 Ma (MIS 75, see Supplement). It is consistently documented in cores ICDP Site 5011-1A and 1B (Haltia and Nowaczyk, 2013). Evidence for this more excursional feature, nearly reaching a full normal polarity prior to the Olduvai normal polarity subchron, comes from sediments in the North Atlantic (Channell et al., 2003). In the ICDP Site 5011-1 record the Cobb Mountain subchron is covering the time interval from 1.1858 to 1.1938 Ma. This is equivalent to late MIS 34 and early MIS 35 (see Supplement), similar to findings from the North Atlantic at IODP Site U1308 by Channell et al. (2008). The obtained age range is also in broad agreement

with the GPTS (Table 1). Cores ICDP Site 5011-1A and 1B both show evidence for a short intra-Jaramillo excursion reaching reversed inclinations (Haltia and Nowaczyk, 2013). According to Channell et al. (2002), this short excursion occurred during MIS 30, a cold interval. Stratigraphic data from Lake El'gygytgyn, in contrast, only allows placing it into the younger warm interval of MIS 29 (Fig. 6) between 1.0142 and 1.0192 Ma with a duration of 5000 yr. A late Jaramillo reversed excursion was also found in Chinese loess (Guo et al., 2002).

Evidence for geomagnetic excursions during the Bruhnes chron (see e.g. Laj and Channel, 2007 for a review) is completely missing in Lake El'gygytgyn sediments. The main reason might be the comparatively low sedimentation rates. Shallow inclinations in the younger Brunhes chron sediments are mostly related to slightly disturbed core intervals from pilot core Lz1024.

4.3 Limnologic and climatic implications

Figure 10 illustrates the response of Lake El'gygytgyn sediments to climate variability throughout the past 3.6 Ma in more detail. The records of biogenic silica (FTIRS estimation), representing bioproductivity in the upper water layers of the lake, and TOC, representing mostly the efficiency of preservation of organic matter at the lake floor, are shown in Fig. 10a. The data is plotted in a way that both curves are superimposed in prominent anoxic intervals where a nearly complete preservation of organic matter is assumed, such as the glacial maxima of MIS 2 (∼ 24 ka), MIS 4 (∼ 65 ka), subglacial MIS 5b (∼ 110 ka), and several intervals of MIS 6 (∼ 135 ka, ∼ 160 ka, ∼ 180 ka). Otherwise, TOC values plot below the curve of biogenic silica, indicating a partial degradation of organic matter at the lake floor in the order of about 60 to 80 % (green area between both curves). This is in agreement with earlier findings from Lake El'gygytgyn pilot core PG1351 (Nowaczyk et al., 2007), using biogenic silica concentrations measured by wet digestion techniques, rather than estimates based on FTIRS, as it was done for ICDP Site 5011-1 core material. Thus, in Lake El'gygytgyn sediments, the amount of TOC, in general, does not represent the primary bioproduction.

Records of Ti content (XRF counts), taken as a proxy of lithogenic input from the catchment, and magnetic susceptibility (MS), representing preservation of magnetic particles during phases of oxygenated bottom waters, are shown in Fig. 10b. Curves were plotted in a way that MS superimposes Ti in time intervals when best preservation of magnetic particles can be assumed during dominating oxic conditions at the lake floor. However, in most cases the MS curve plots below the Ti curve, indicating far-reaching dissolution of up to 95 % of the magnetic fraction. There is even an anti-correlation between Ti content and magnetic susceptibility visible during longer sequences within the El'gygytgyn sedimentary record. Thus, magnetic susceptibility is anything but a proxy for the input of lithogenic material, although magnetic particles were very likely derived from the catchment inside the El'gygytgyn crater, bearing highly magnetic volcanic rocks (Haltia and Nowaczyk, 2013). The massive loss of magnetic particles of up to 95 % still allowed a clear detection of geomagnetic reversals (Haltia and Nowaczyk, 2013), but it definitely excludes a reliable estimation of relative geomagnetic palaeointensity variations (Nowaczyk et al., 2002, 2007). This is a major deficit of the El'gygytgyn sedimentary record, because correlation of palaeointensity variations to reference records, such as the PISO1500 stack (Channell et al., 2009) or the EPAPIS-3000 stack (Yamazaki and Oda, 2005, and further references therein), could have provided further geomagnetic tie points between the major reversals. This could have significantly substantiated the age model mainly derived from tuning Lake El'gygytgyn sedimentary climate proxies to the LR04 stack (Lisiecki and Raymo, 2005) and the Northern Hemisphere cumulative summer insolation, according to orbital solutions by Laskar et al. (2004). On the other hand, only the strict link between alternating redox conditions, leading to the alternating dissolution/preservation effects described above, and insolation variations enabled the definition of many tie points in the age model for ICDP Site 5011-1. Figure 10b also shows a clear anti-correlation between Ti and the LR04 stack. This indicates a dilution of the lithogenic fraction by biogenic components being larger (smaller) during warm (cold) phases. A good proxy for the varying ratio of bioproductivity, in Lake El'gygytgyn mostly biogenic (bio) silica from diatoms, to lithogenic (litho) input is the Si / Ti ratio (Melles et al., 2012; Wennrich et al., 2013), here obtained in high-resolution from XRF-scanning (Fig. 10c). Actually this ratio is $(Si_{bio} + Si_{litho}) / Ti_{litho}$. Thus, when Si_{bio} approximates zero the Si / Ti ratio approximates a certain value, depending on the average composition of the catchment rocks. The pure $(Si / Ti)_{litho}$ ratio might also change due to an increased (decreased) chemical alteration under anoxic (oxic) condition in cold (warm) phases at the lake floor (Minyuk et al., 2007). Nevertheless, the modulation of the Si / Ti ratio is obviously dominated by its varying biogenic contribution since the Si / Ti ratio resembles

Table 3. Positions and ages of tephra layers identified in Lake El'gygytgyn sediments. Core labels indicate: 1 – PG1351, 2 – Lz1024, A – 5011-1A, B – 5011-1B, C – 5011-1C.

Core	Index	5011-1 composite depth (m)	Age (ka)
1, 2	0	2.54–2.55	58
1, 2, A, B	1	7.88–7.89	177
A, B	2	27.52–27.52	674
A, B	3	36.41–36.47	918
A, B	4	60.79–60.80	1411
A, B	5	62.04–62.08	1434
A, B	6	79.25–79.26	1775
A, B, C	7	104.93–105.00	2225

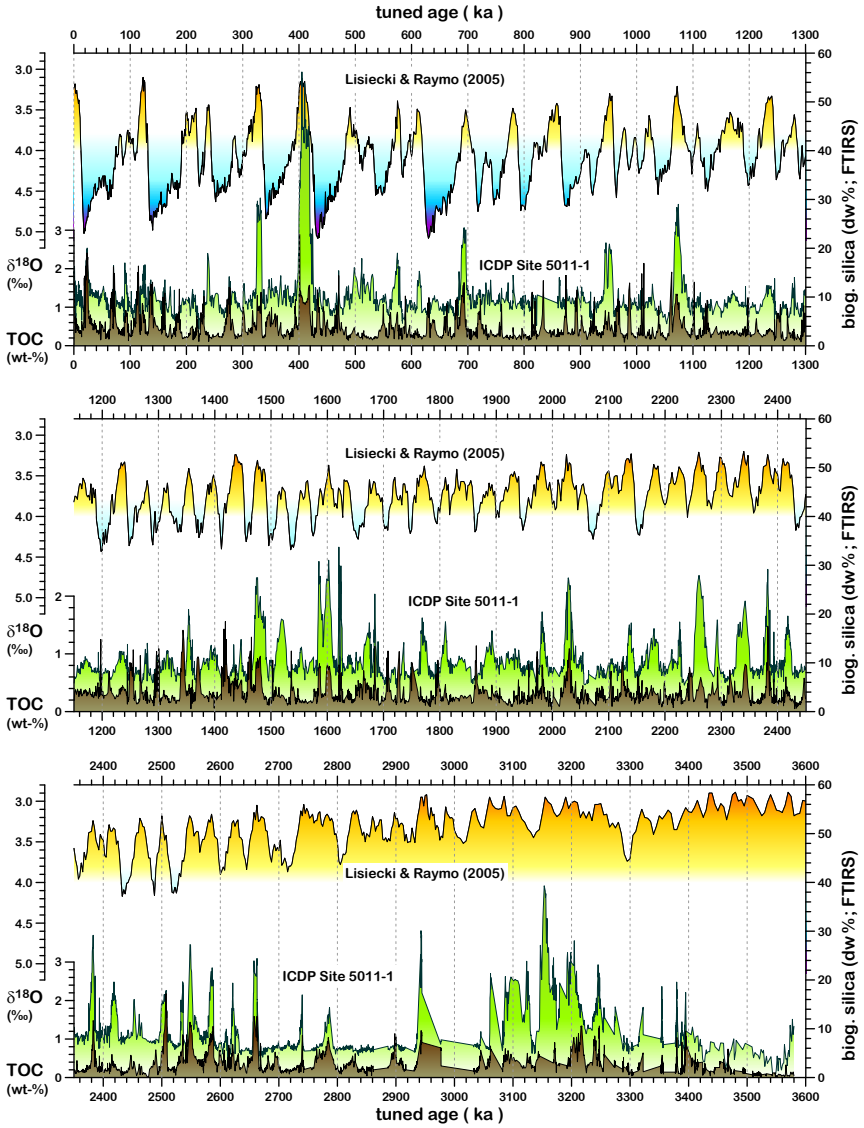

Fig. 10. Response of Lake El'gygytgyn (ICDP Site 5011-1) to climate variability as represented by the marine oxygen isotope (δ^{18}O) stack LR04 (Lisiecki and Raymo, 2005): Time series of **(a)** biogenic silica (FTIRS estimation), representing bioproductivity in the upper water layers of the lake, and total organic carbon (TOC), representing preservation of organic matter at the lake floor during phases of anoxic bottom waters, **(b)** Ti content (XRF counts), taken as a proxy of lithogenic input from the catchment, and magnetic susceptibility (MS), representing preservation of magnetic particles during phases of oxygenated bottom waters, **(c)** hue angle (colour) and Si / Ti ratio, both following global climate cycles. Curves in **(a)** and **(b)** were plotted in a way that TOC (MS) superimposes biogenic silica (Ti) in time intervals when best preservation of organic matter (magnetic particles) can be assumed during anoxic (oxic) conditions at the lake floor. Where the TOC curve lies below the biogenic silica curve in **(a)**, partial degradation (60 to 80 %) of organic matter is indicated (green area between both curves). Where the MS curve lies below the Ti curve in **(b)**, fairly massive dissolution (up to 95 %) of the magnetic fraction in the sediments is indicated (grey area between both curves). For further explanation see discussion in the text.

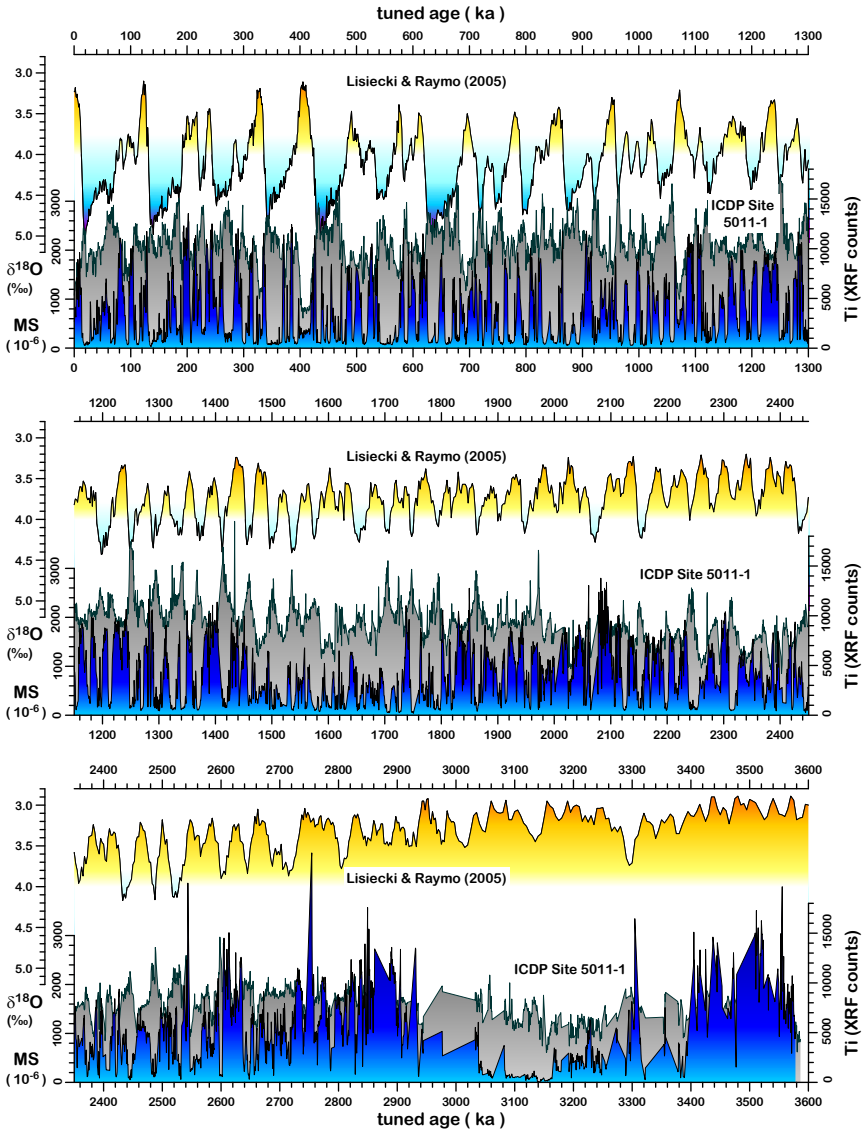

Fig. 10. Continued.

strongly the morphology of the FTIRS-BSi curve representing only biogenic silica (Fig. 6). The variations in Si / Ti ratio are also parallelled by changes in colour (hue angle) from yellowish brown (80°) to greenish grey (140°), also shown in Fig. 10c. According to an initial study on the time interval from MIS 8 to 12 (Wei et al., 2013), combining colour spectral data with mineralogical data from X-ray diffraction (XRD), colour changes mainly reflect physical weathering processes, with some additional chemical weathering, reflecting wet dry cyclicity. Thus, the hue angle turned out to be a very helpful parameter for tuning the ICDP Site 5011-1 sedimentary sequence and more detailed analyses of the full spectral colour information, from which the hue angle was derived, might give further information in the future. The percentages of tree & shrub pollen also vary in concert with variation in biogenic silica, Si / Ti ratio, colour (hue), and grain size (Fig. 6), but these aspects exceed the focus of this paper. Major environmental implications of the pollen record is published in Melles et al. (2012) and Brigham-Grette et al. (2013).

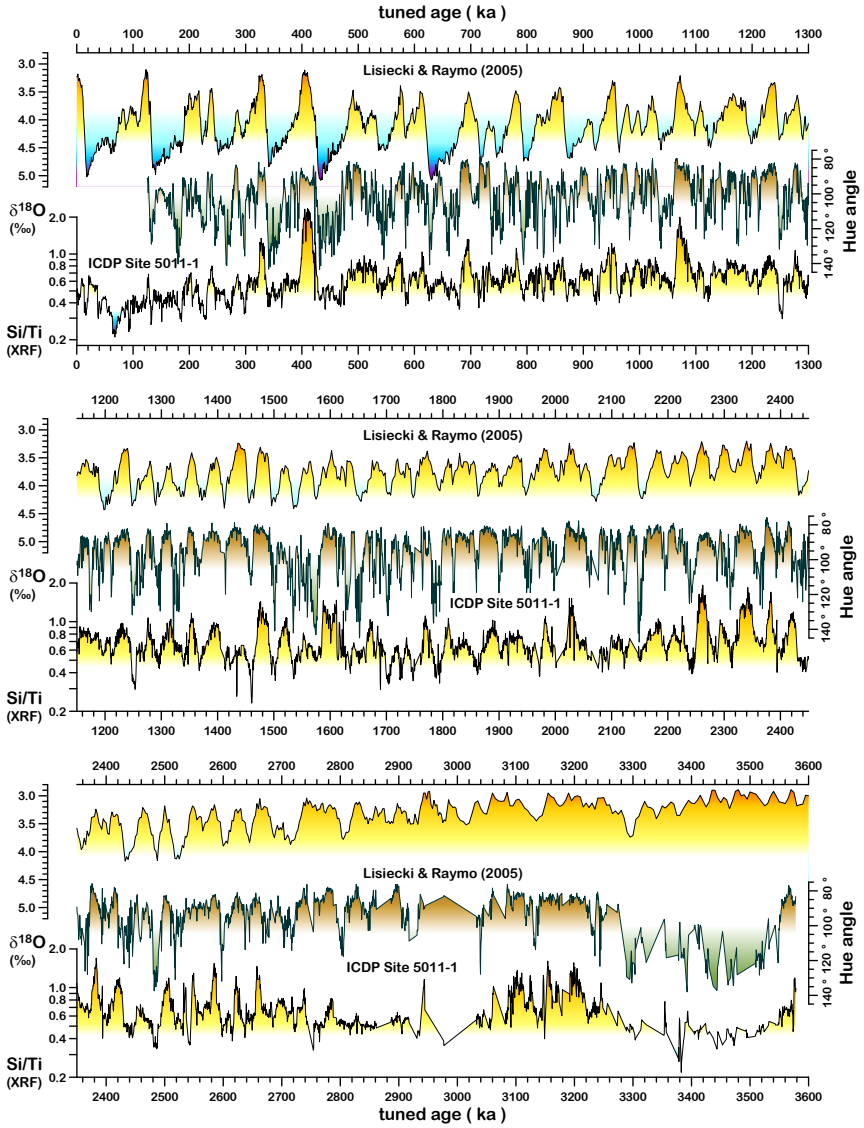

Fig. 10. Continued.

Data from Lake El'gygytgyn have been subjected to some wavelet time-series analysis (e.g. Torrence and Compo, 1997; Kumar and Foufoula-Georgiou, 1997). Wavelet analysis is the preferred method for a time-dependent frequency analysis, that is, in cases when non-stationary frequencies have to be confirmed in a time series. Actually it is a cross-correlation of a time series with a whole set of single base frequencies which are multiplied with a certain taper function (e.g. a Gaussian curve). Concerning the wavelet, the multiplication in the time domain is equivalent with a convolution of the spectral peak of the base frequency with the Fourier transform of the taper function in the frequency domain, which is a Gaussian curve in the case of a Gaussian curve (see Torrence and Compo, 1997). Thus, a wavelet is always sensitive to a whole frequency band centred by the base frequency of the wavelet. For analyses of Lake El'gygytgyn sediments a Morlet wavelet with a base frequency of 6 and a scale of 200 a was used (see Torrence and Compo, 1997), applying the PAST software (Hammer et al., 2001), Version 2.17. Prior to analyses data sets were re-sampled every 200 a.

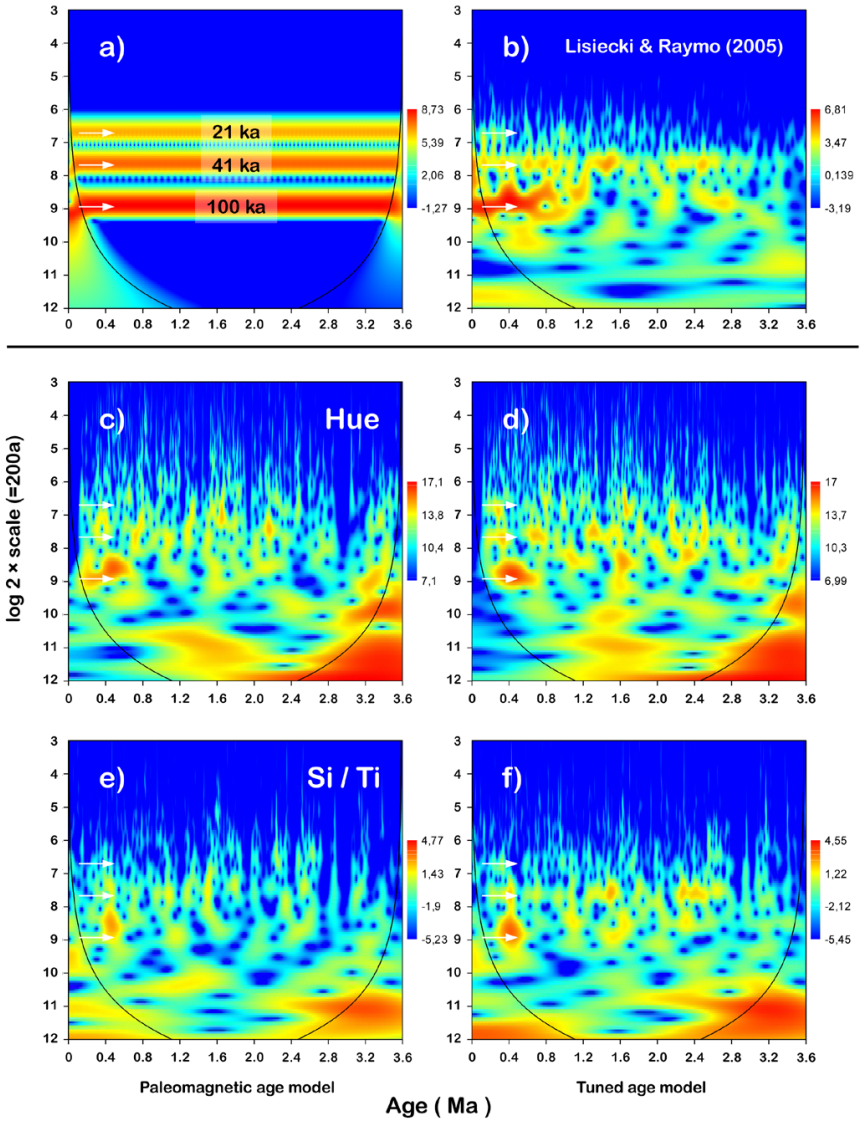

Fig. 11. Wavelet analyses using a Morlet wavelet with a base frequency of 6 and a scale of 200 a performed on some stratigraphic properties from Lake El'gygytgyn used for tuning: **(a)** persistent mono-frequency sine waves with periods of 21 ka (precession, at 6.7145), 41 ka (obliquity, at 7.6795), and 100 ka (eccentricity, at 8.9658) for reference, **(b)** the marine oxygen isotope stack by Lisiecki and Raymo (2005) that was used as one tuning reference curve, times series of **(c)** hue angle of sediment colour and **(e)** Si / Ti ratio from XRF scanning solely based on magnetostratigraphic dating and the same with fine-tuned age model **(d)** and **(f)**. White arrows always mark the positions of the major astronomical periods shown in **(a)**.

For illustration of the (limited) frequency resolution Fig. 11a shows the result from a superposition of three pure sine waves with periods of 21 ka (precession of earth's rotation axis), 41 ka (obliquity variations of earth's rotation axis), and 100 ka (eccentricity variations of earth's orbit), constantly persisting from 0 to 3.6 Ma. According to the theory of wavelet analysis, they are not represented by a single spectral line but a whole frequency band. The wavelet analysis of the LR04 stack in Fig. 11b reveals that the 100 ka cycle has been persisting only during the past about 800 ka. The 41 ka cycle can be clearly traced back to about 2.5 Ma. Figure 11c and d (11e and f) show the results from the hue (Si / Ti ratio)

on the basis of the palaeomagnetic age model only, and after fine-tuning to both the LR04 stack and the Northern Hemisphere summer insolation. The three astronomical periods shown in Fig. 11a, also indicated by white arrows, are less visible as in the LR04 stack, but nevertheless, a certain improvement can be seen, especially the 100 ka and the 41 ka frequency band. Finally, when considering Fig. 7, the pure palaeomagnetic age model already gave a fairly good estimate for the final fine-tuned age model. Thus, the deviations between the results from wavelet analysis in Fig. 11c (11e) and d (11f) cannot be large.

4.4 Tephra layers

Up to now, a total of eight tephra layers have been identified in Lake El'gygytgyn sediments. Currently, radiometric ages are not yet available. However, based on multi-proxy tuning of the sediments they are embedded in, tephra ages could be determined by chrono-stratigraphic means of this study. Their positions in composite depth and respective ages are listed in Table 3. Tephra 1 (177 ka) is described in some detail by Ponomareva et al. (2013). Large volcanic eruptions on Kamchatka listed by Bindemann et al. (2010) are potential sources of the tephras. Geochemical fingerprints worked out by van den Bogaard et al. (2013) shows that most of the tephras can be linked to the volcanic activity on Kamchatka. Only tephra 6 (1775 ka) should be related to the Aleutian volcanic arc. Thus, the origins of the tephras is sited more than 1000 km away from Lake El'gygytgyn, indicating that the observed tephras are marker layers of regional importance.

5 Conclusions

Despite the presence of more than 300 turbidites, mass movements of up to 1.2 m thickness (Sauerbrey et al., 2013), and poor core recovery in the lower section, a fairly detailed age model could be achieved for the about 320 m thick ICDP Site 5011-1 sedimentary composite record from Lake El'gygytgyn, Far Eastern Russian Arctic, covering the past 3.6 Ma. Reference ages of 14 reversals of the geomagnetic field, documented in the sediments, are provided by the timescales of Lisiecki and Raymo (2005) and Ogg and Smith (2004), respectively, showing slightly deviating ages for some of the reversals (Table 1). Within that range, reversal ages derived from chronostratigraphic analyses of Lake El'gygytgyn sediments are in a general agreement with these timescales. Thus, we suggest an age of 2.588 Ma for the Matuyama Gauss reversal. For the Réunion subchron a duration extending from 2.1384 to 2.1216 Ma could be derived. Our study confirms the existence of a short-term Olduvai precursor from 1.9815 to 1.9782 Ma, reaching full normal polarity, also documented in North Atlantic sediments (Channell et al., 2003). In ICDP Site 5011-1 sediments, the Cobb Mountain subchron is covering the time interval from 1.1938 to 1.1858 Ma. Our data also give evidence for an intra-Jaramillo excursion lasting from 1.0192 to 1.0142 Ma in MIS 29, which is younger than ages derived from other studies, placing it in MIS 30 (Channell et al., 2002). Despite recording of such short-term geomagnetic field features during the Matuyama chron no evidence for excursions within the Brunhes chron was found in Lake El'gygytgyn sediments. Repeatedly occurring perversive magnetite dissolution throughout the whole Pleistocene inhibited a reconstruction of geomagnetic palaeointensity variations. Nevertheless, in addition to the polarity stratigraphy, a synchronous tuning of 9 stratigraphic parameters to the LR04 marine oxygen isotope stack (Lisiecki and Raymo, 2005) and to the Northern Hemisphere cumulative summer insolation (May to August), according to orbital solutions by Laskar et al. (2004), respectively, led to a significant refinement of the age model by the definition of a total of about 600 tie points. The age model has some uncertainties towards the base of the (Pliocene) sediments between 2.94 and 3.54 Ma, mainly due to low sediment recovery during drilling. Here, pronounced variation in the percentages of tree pollen provided major clues for age assignments. Estimated sedimentation rates are in the range of 4 to 5 cm ka^{-1} for the past about 3.3 Ma, whereas the first 0.3 Ma after the impact that created the El'gygytgyn crater are characterised by about ten-fold higher sedimentation rates. This study also provides orbitally tuned ages for a total of eight remote tephras deposited in Lake El'gygytgyn which can act as marker layers in future studies.

Acknowledgements. Funding for this research was provided by the International Continental Scientific Drilling Program (ICDP), the US National Science Foundation (NSF), the German Federal Ministry of Education and Research (BMBF), Alfred Wegener Institute (AWI) and Helmholtz Centre Potsdam (GFZ), the Russian Academy of Sciences Far East Branch (RAS FEB), the Russian Foundation for Basic Research (RFBR), and the Austrian Federal Ministry of Science and Research (BMWF). The Russian GLAD 800 drilling system was developed and operated by DOSECC Inc., the down hole logging was performed by the ICDP-OSG, and LacCore, at the University of Minnesota, handled core curation. We like to thank all the participants of the expedition to Lake El'gygytgyn from January to May 2009 for their engagement during recovery of the ICDP Site 5011-1 cores. Numerous students helped during laboratory work. Wavelet analyses were performed using the PAST software package, Vers. 2.17, provided by Øyvind Hammer, Natural History Museum, University of Oslo (http://folk.uio.no/ohammer/past/index.html). This study was partly financed by BMBF grant no. 03G0642C – "Geochronology of the sediments in the El'gygytgyn crater".

The service charges for this open access publication have been covered by a Research Centre of the Helmholtz Association.

Edited by: B. Wagner

References

Andreev, A. A., Tarasov, P. E., Wennrich, V., Raschke, E., Herzschuh, U., Nowaczyk, N. R., Brigham-Grette, J., and Melles, M.: Late Pliocene and early Pleistocene environments of the north-eastern Russian Arctic inferred from the Lake El'gygytgyn pollen record, Clim. Past Discuss., 9, 4599–4653, doi:10.5194/cpd-9-4599-2013, 2013.

Baksi, A. K., Hoffman, K. A., and McWilliams, M.: Testing the accuracy of the geomagnetic polarity time-scale (GPTS) at 2–5 Ma, utilizing $^{40}Ar/^{39}Ar$ incremental heating data on whole-rock basalts, Earth Planet. Sc. lett., 118, 135–144, 1993.

Bindemann, I. N., Leonov, V. L., Izbekov, P. E., Ponomareva, V. V., Watts, K. E., Shipley, N. K., Perepelov, A. B., Bazanova, L. I., Jicha, B. R., Singer, B. S, Schmitt, A. K., Portnyagin, M. V., and Chen, C. H.: Large-volume silicic volcanism in Kamchatka: Ar-Ar, and U-Pb ages, isotopic, and geochemical characteristics of major pre-Holocene caldera-forming eruptions, Bull. Volc. Geotherm. Res., 189, 57–80, 2010.

Blaauw, M.: Out of tune: the dangers of aligning proxy archives, Quaternary Sci. Rev., 36, 38–49, 2012.

Bokhorst, M. P. and Vandenberghe, J.: Validation of wiggle matching using a multi-proxy approach and its palaeoclimatic significance, J. Quaternary Sci., 24, 937–947, 2009.

Brigham-Grette, J., Melles, M., Minyuk, P., Andreev, A., Tarasov, P., DeConto, R, Koenig, S., Nowaczyk, N., Wennrich, V., Rosén, P., Haltia, E., Cook, T., Gebhard, C., Meyer-Jacob, C., Snyder, J. and Herzschuh, U.: Pliocene warmth, polar amplification, and stepped Pleistocene cooling recorded in NE Arctic Russia, Science express, 340, 1421–1427, doi:10.1126/science.1233137, 2013.

Cande, S. C. and Kent, D. V.: Revised calibration of the geomagnetic polarity timescale for the late Cretaceous and Cenozoic, J. Geophys. Res., 100, 6093–6095, 1995.

Chamalaun, F. H. and McDougall, I.: Dating geomagnetic polarity epoches in Réunion, Nature, 210, 1212–1214, 1966.

Channell, J. E. T., Mazaud, A., Sullivan, P., Turner, S., and Raymo, M. E.: Geomagnetic excursions and paleointensities in the Matuyama Chron at Ocean Drilling Porgram Sites 983 and 984 (Iceland Basin), J. Geophys. Res., 107, EPM 1.1–EPM 1.14, doi:10.1029/2001JB000491, 2002.

Channell, J. E. T., Labs, J., and Raymo, M. E.: The Réunion subchronozone at ODP site 981 (Feni Drift, North Atlantic), Earth Planet. Sc. Lett., 215, 1–12, 2003.

Channell, J. E. T., Hodell, D. A., Xuan, C., Mazaud, A., and Stoner, J. S.: Age calibrated paleointensity for the last 1.5 Myr at ODP Site U1308 (North Atlantic), Earth Planet. Sc. Lett., 274, 59–71, 2008.

Channel, J. E. T., Xuan, C., and Hodell, D. A.: Stacking paleointensity and oxygen isotope data for the last 1.5 Myr (PISO-1500), Earth Planet. Sc. Lett., 283, 14–23, 2009.

Cherapanova, M. V., Snyder, J. A., and Brigham-Grette, J.: Diatom stratigraphy of the last 250 ka at Lake El'gygytgyn, northeast Siberia, J. Paleolimnol., 37, 155–162, 2007.

Deino, A. L., Kingston, J. D., Glen, J. M., Edgar, R. K., and Hill, A.: Precessional forcing of lacustrine sedimentation in the late Cenozoic Chemeron Basin, Central Kenya Rift, and calibration of the Gauss/Matuyama boundary, Earth Planet. Sc. Lett., 247, 41–60, 2006.

Francke, A., Wennrich, V., Sauerbrey, M., Juschus, O., Melles, M., and Brigham-Grette, J.: Multivariate statistic and time series analyses of grain-size data in Quaternary sediments of Lake El'gygytgyn, NE Russia, Clim. Past Discuss., 9, 217–244, doi:10.5194/cpd-9-217-2013, 2013.

Frank, U., Nowaczyk, N. R., Minyuk, P., Vogel, H., Rosén, P., and Melles, M.: A 350 ka record of climate change from Lake El'gygytgyn, Far East Russian Arctic: refining the pattern of climate modes by means of cluster analysis, Clim. Past, 9, 1559–1569, doi:10.5194/cp-9-1559-2013, 2013.

Guo, B., Zhu, R., Florindo, F., Ding, Z., and Sun, J. A.: A short, reverse polarity interval within the Jaramillo subchron: Evidence from the Jingbian section, northern China Loess plateau, J. Geophys. Res., 107, 10029–10040, 2002.

Gurov, E. P. and Koeberl, C.: Shocked rocks and impact glasses from the El'gygytgyn impact structure, Russia, Meteorit. Planet. Sci., 39, 1495–1508, 2004.

Haltia, E. M. and Nowaczyk, N. R.: Magnetostratigraphy of sediments from Lake El'gygytgyn ICDP Site 5011-1: paleomagnetic age constraints for the longest paleoclimate record from the continental Arctic, Clim. Past Discuss., 9, 5077–5122, doi:10.5194/cpd-9-5077-2013, 2013.

Hammer, Ø., Harper, D. A. T., and Ryan, P. D.: PAST: Paleontological Statistics Software Package for Education and Data Analysis, Palaeontol. Electron., 4, 9 pp., 2001.

Juschus, O., Preusser, F., Melles, M., and Radtke, U.: Applying SAR-IRSL methodology for dating fine-grained sediments from Lake El'gygytgyn, north-eastern Siberia, Quat. Geochronol., 2, 187–194, 2007.

Kirschvink, J. L.: The least-squares line and plane and the analysis of palaeomagnetic data, Geophys. J. Roy. Astr. S., 62, 699–718, 1980.

Kelley, S. P., Spicer, R. A., and Herman, A. B.: New $^{40}Ar/^{39}Ar$ dates for Cretaceous Chauna Group tephra, north-eastern Russia, and their implications for the geologic history and floral evolution of the North Pacific region, Cret. Res., 20, 97–106, 1999.

Kumar, P. and Foufoula-Georgiou, E.: Wavelet analysis for geophysical applications, Rev. Geophys., 35, 385–412, 1997.

Laj, C. and Channell, J. E. T.: Geomagnetic excursions, in: Treatise on Geophysics, Geomagnetism, edited by: Schubert, G., Bercovici, D., Dziewonski, A., Herring, T., Kanamori, H., Kono, M., Olson, P. L., Price, G. D., Romanowicz, B., Spohn, T., Stevenson, D., and Watts, A. B., Vol. 5. Elsevier, B.V., Amsterdam, 373–416, 2007.

Laskar, J., Robutel, F., and Boudin, F.: Orbital, precessional, and insolation quantities for the Earth from -20 Myr to $+10$ Myr, Astron. Astrophys., 270, 522–533, 1993.

Laskar, J., Robutel, P., Joutel, F., Gastineau, M., Correia, A. C. M., and Levrard, B.: A long-term numerical solution for the insolation quantities of the Earth, Astron. Astrophys., 428, 261–285, 2004.

Layer, P. W.: Argon-40/Argon-39 age of the El'gygytgyn impact event, Chukotka, Russia, Meteorit. Planet. Sci., 35, 591–599, 2000.

Lisiecki, L. E. and Raymo, M. E.: A Pliocene-Pleistocene stack of 57 globally distributed benthic $\delta^{18}O$ records, Paleoceanography, 20, PA1003, doi:10.1029/2004PA001071, 2005.

Lisiecki, L. E. and Raymo, M. E.: Diachronous benthic $\delta^{18}O$ responses during late Pleistocene terminations, Paleoceanography, 24, PA3210, doi:10.1029/2009PA001732, 2009.

Lourens, L. J., Antonarakou, A., Hilgen, F. J., Van Hoof, A. A. M., Vergnaud-Grazzini, C., and Zachariasse, W. J.: Evaluation of the Plio-Pleistocene astronomical timescale, Paleoceanography, 11, 391–413, 1996.

Lozhkin, A. V. and Anderson, P. M.: Vegetation responses to interglacial warming in the Arctic: examples from Lake El'gygytgyn, Far East Russian Arctic, Clim. Past, 9, 1211–1219, doi:10.5194/cp-9-1211-2013, 2013.

Lozhkin, A. V., Anderson, P. M., Matrosova, T. V., and Minyuk, P. S.: The pollen record from El'gygytgyn Lake: implications for vegetation and climate histories of northern Chukotka since the late middle Pleistocene, J. Paleolimnol., 37, 135–153, 2007.

Maharaj, D., Elbra, T., and Pesonen, L. J.: Physical properties of the El'gygytgyn impact structure, NE Russia, Meteorit. Planet. Sci., 48, 1130–1142, 2013.

Mankinen, E. A., Donelly, J. M., and Grommé, C. S.: Geomagnetic polarity event recorded at 1.1 m.y. B.P. on Cobb Mountain, Clear Lake volcanic field, California, Geology, 6, 653–656, 1978.

McDougall, I. and Watkins, N. D.:. Age and duration of the Réunion geomagnetic polarity event, Earth Planet. Sc. Lett., 19, 443–452, 1973.

Melles, M., Brigham-Grette, J., Glushkova, O. Y., Minyuk, P. S., Nowaczyk, N. R., and Hubberten, H.-W.: Sedimentary geochemistry of core PG1351 from Lake El'gygytgyn – a sensitive record of climate variability in the East Siberian Arctic during the past three glacial-interglacial cycles, J. Paleolimnol., 37, 89–104, 2007.

Melles, M., Brigham-Grette, J., Minyuk, P., Koeberl, C., Andreev, A., Cook, T., Fedorov, G., Gebhardt, C., Haltia-Hovi, E., Kukkonen, M., Nowaczyk, N., Schwamborn, G., Wennrich, V., and the El'gygytgyn Scientific Drilling Project – conquering Arctic challenges through continental drilling, Sci. Drilling, 11, 29–40, 2011.

Melles, M., Brigham-Grette, J., Minyik, P. S., Nowaczyk, N. R., Wennrich, V., DeConto, R. M., Anderson, P. M., Andreev, A. A., Coletti, A., Cook, T. L., Haltia-Hovi, E., Kukkonen, M., Lozhkin, A. V., Rosén, P., Tarasov, P., Vogel, H., and Wagner, B.: 2.8 Million years of Arctic climate change from Lake El'gygytgyn, NE Russia, Science, 337, 315–320, doi:10.1126/1222135, 2012.

Meyer-Jacob, C., Vogel, H., Melles, M., and Rosén, P.: Biogeochemical properties and diagenetic changes during the past 3.6 Ma recorded by FTIR spectroscopy in the sediment record of Lake El'gygytgyn, Far East Russian Arctic, Clim. Past Discuss., 9, 2489–2515, doi:10.5194/cpd-9-2489-2013, 2013.

Minyuk, P. S., Brigham-Grette, J., Melles, M., Borkhodoev, V. Y., and Glushkova, O. Y.: Inorganic geochemistry of El'gygytgyn Lake Sediments (northeastern Russia) as an indicator of paleoclimatic change for the last 250 kyr, J. Paleolimnol., 37, 123–133, 2007.

Murdock, K. J., Wilkie, K., and Brown, L. L.: Rock magnetic properties, magnetic susceptibility, and organic geochemistry comparison in core LZ1029-7 Lake El'gygytgyn, Russia Far East, Clim. Past, 9, 467–479, doi:10.5194/cp-9-467-2013, 2013.

Nolan, M. and Brigham-Grette, J.: Basic hydrology, limnology, and meteorology of modern Lake El'gygytgyn, Siberia, J. Paleolimnol., 37, 17–35, 2007.

Nowaczyk, N. R.: Logging of magnetic susceptibility, in: Tracking environmental change using lake sediments. Vol I: Basin analysis, coring, and chronological techniques, edited by: Last, W. M. and Smol, J. P., Kluwer Academic Publishers, Bortrecht, Netherlands, 155–170, 2001.

Nowaczyk, N. R., Minyuk, P., Melles, M., Brigham-Grette, J., Glushkova, O., Nolan, M., Lozhkin, A. V., Stetsenko, T. V., Anderson, P. M., and Forman, S. L.: Magnetostratigraphic results from impact crater Lake El'gygytgyn, northeastern Siberia: a 300 kyr long high-resolution terrestrial palaeoclimatic record from the Arctic, Geophys. J. Int., 150, 109–126, 2002.

Nowaczyk, N. R., Melles, M., and Minyuk, P.: A revised age model for core PG1351 from Lake El'gygytgyn, Chukotka, based on magnetic susceptibility variations tuned to northern hemisphere insolation variations, J. Paleolimnol., 37, 65–76, 2007.

Ogg, J. G. and Smith, A. G.: The geomagnetic polarity time scale, in: Gradstein, F., Ogg, J., and Smith, A., A Geological Timescale 2004, Cambridge University Press, 63–86, 2004.

Ponomareva, V., Portnyagin, M., Derkachev, A., Juschus, O., Garbe-Schönberg, D., and Nürnberg, D.: Identification of a widespread Kamchatkan tephra: a middle Pleistocene tie-point between Arctic and pacific paleoclimatic records, Geophys. Res. Lett., 40, 3538–3543, doi:10.1002/grl.50645, 2013.

Prokopenko, A. A. and Khursevich, G. K.: Plio-Pleistocene transition in the continental record from Lake Baikal: Diatom biostratigraphy and age model, Quaternary Int., 219, 26–36, 2010.

Prokopenko, A. A., Hinnov, L. A., Williams, D. F., and Kuzmin, M. I.: Orbital forcing of continental climate during the Pleistocene: a complete astronomically tuned climatic record from Lake Baikal, SE Siberia, Quaternary Sci. Rev., 25, 3431–3457, 2006.

Quidelleur, X., Holt, J. W., Salvany, T., and Bouquerel, H.: New K-Ar ages from La Montagne massif, Réunion Island (Indian Ocean), supporting two geomagnetic events in the time period 2.2–2.0 Ma, Geophys. J. Int., 182, 699–710, 2010.

Rosén, P., Vogel, H., Cunningham, L., Reuss, N., Conley, D. J., and Persson, P.: Fourier transform infrared spectroscopy, a new method for rapid determination of total organic and inorganic carbon and biogenic silica concentration in lake sediments, J. Paleolimnol., 43, 247–259, 2010.

Rosén, P., Vogel, H., Cunningham, L., Hahn, A., Hausmann, S., Pienitz, R., Zolitschka, B., Wagner, B., and Persson, P.: Universally applicable model for the quantitative determination of lake sediment composition using Fourier transform infrared spectroscopy, Environ. Sci. Technol., 45, 8858–8865, 2011.

Sauerbrey, M. A., Juschus, O., Gebhardt, A. C., Wennrich, V., Nowaczyk, N. R., and Melles, M.: Mass movement deposits in the 3.6 Ma sediment record of Lake El'gygytgyn, Far East Russian Arctic, Clim. Past, 9, 1949–1967, doi:10.5194/cp-9-1949-2013, 2013.

Singer, B. A., Brown, L. L., Rabassa, J. O., and Guillou, H.: $^{40}Ar/^{39}Ar$ chronology of Late Pliocene and Early Pleistocene geomagentic and glacial events in Southern Argentina, in: Channell, J. E. T., Kent, D. V., Lowrie, W., and Meert, J. G., Timescales of the Paleomagnetic Field, Geophys. Monograph Ser., 145, Amer. Geophys. Union, Washington, DC, 175–190, 2004.

Torrence, C. and Compo, G. P.: A practical guide to wavelet analysis, B. Am. Meteorol. Soc., 79, 61–78, 1997.

van den Bogaard, C., Jensen, B. J. L., Pearce, N. J. G., Froese, D. G., Portnyagin, M. V., Ponomareva, V. V., Garbe-Schönberg, D., and Wennrich, V.: Volcanic ash layers in Lake El'gygytgyn: eight new regionally significant chronostratigraphic markers for western Beringia, Clim. Past Discuss., 9, 5977–6034, doi:10.5194/cpd-9-5977-2013, 2013.

Vogel, H., Rosén, P., Wagner, B., Melles, M., and Persson, P.: Fourier transform infrared spectroscopy, a new cost-effective tool for quantitative analysis of biogeochemical properties in long sediment records, J. Paleolimnol., 40, 689–702, 2008.

Vogel, H., Meyer-Jacob, C., Melles, M., Brigham-Grette, J., Andreev, A. A., Wennrich, V., Tarasov, P. E., and Rosén, P.: Detailed insight into Arctic climatic variability during MIS 11c at Lake El'gygytgyn, NE Russia, Clim. Past, 9, 1467–1479, doi:10.5194/cp-9-1467-2013, 2013.

Wei, J., Finkelstein, D., Brigham-Grette, J., Castaneda, I., and Nowaczyk, N.: Sediment color reflectance spectroscopy as a proxy for wet/dry cycles at Lake El'gygytgyn, Far East Russia, during marine isotope stages 8 to 12, Sedimentology, in review, 2013.

Wennrich, V., Minyuk, P. S., Borkhodoev, V. Ya., Francke, A., Ritter, B., Nowaczyk, N., Sauerbrey, M. A., Brigham-Grette, J., and Melles, M.: Pliocene to Pleistocene climate and environmental history of Lake El'gygytgyn, Far East Russian Arctic, based on high-resolution inorganic geochemistry data, Clim. Past Discuss., 9, 5899–5940, doi:10.5194/cpd-9-5899-2013, 2013.

Yamazaki, T. and Oda, H.: A geomagnetic paleointensity stack between 0.8 and 3.0 Ma from equatorial Pacific sediment cores, Geochem. Geophy. Geosys., 6, Q11H20, doi:10.1029/2005GC001001, 2005.

5 Petrophysical characterization of the lacustrine sediment succession drilled in Lake El'gygytgyn, Far East Russian Arctic

Journal article (2013):

Gebhardt, A. C., Francke, A., KÃ$\frac{1}{4}$ck, J., Sauerbrey, M., Niessen, F., Wennrich, V., and Melles, M.: Petrophysical characterization of the lacustrine sediment succession drilled in Lake El'gygytgyn, Far East Russian Arctic, Clim. Past, 9, 1933-1947, 10.5194/cp-9-1933-2013, 2013.

Clim. Past, 9, 1933–1947, 2013
www.clim-past.net/9/1933/2013/
doi:10.5194/cp-9-1933-2013

Climate of the Past
Open Access

Petrophysical characterization of the lacustrine sediment succession drilled in Lake El'gygytgyn, Far East Russian Arctic

A. C. Gebhardt[1], A. Francke[2], J. Kück[3], M. Sauerbrey[2], F. Niessen[1], V. Wennrich[2], and M. Melles[2]

[1]Alfred Wegener Institute Helmholtz Centre for Polar and Marine Research, Columbusstraße, 27515 Bremerhaven, Germany
[2]University of Cologne, Institute of Geology and Mineralogy, Zülpicher Straße 49A, 50674 Cologne, Germany
[3]German Research Centre for Geosciences, Telegrafenberg, 14473 Potsdam, Germany

Correspondence to: A. C. Gebhardt (catalina.gebhardt@awi.de)

Received: 17 December 2012 – Published in Clim. Past Discuss.: 18 January 2013
Revised: 17 June 2013 – Accepted: 3 July 2013 – Published: 16 August 2013

Abstract. Seismic profiles of Far East Russian Lake El'gygytgyn, formed by a meteorite impact some 3.6 million years ago, show a stratified sediment succession that can be separated into subunits Ia and Ib at approximately 167 m below lake floor (=∼ 3.17 Ma). The upper (Ia) is well-stratified, while the lower is acoustically more massive and discontinuous. The sediments are intercalated with frequent mass movement deposits mainly in the proximal areas, while the distal region is almost free of such deposits at least in the upper part. In spring 2009, a long core drilled in the lake center within the framework of the International Continental Scientific Drilling Program (ICDP) penetrated the entire lacustrine sediment succession down to ∼ 320 m below lake floor and about 200 m farther into the meteorite-impact-related bedrock. Downhole logging data down to 390 m below lake floor show that the bedrock and the lacustrine part differ significantly in their petrophysical characteristics. The contact between the bedrock and the lacustrine sediments is not abrupt, but rather transitional with a variable mixture of impact-altered bedrock clasts in a lacustrine matrix. Physical and chemical proxies measured on the cores can be used to divide the lacustrine part into five different statistical clusters. These can be plotted in a redox-condition vs. input-type diagram, with total organic carbon content and magnetic susceptibility values indicating anoxic or oxic conditions and with the Si / Ti ratio representing more clastic or more biogenic input. Plotting the clusters in this diagram allows identifying clusters that represent glacial phases (cluster I), super interglacials (cluster II), and interglacial phases (clusters III and IV).

1 Introduction

The Arctic region is highly susceptible to global change and, at the same time, plays a major role in the global climate system through feedback processes in the oceans, the atmosphere, and the cryosphere. Accordingly it is important to understand past climate changes under different climate-forcing conditions in order to make accurate predictions about future climate development. Lakes of the higher latitudes are sparsely investigated even though they are highly sensitive to shifts in climatological and environmental conditions (e.g. temperature, precipitation, insolation, vegetation, ice coverage), and as such they are valuable tracers of climate change. This lack of investigation is mainly due to their remote locations and the logistical challenges of reaching these study sites. Lakes in the high Arctic are often characterized by long winters resulting in long periods of ice coverage, followed by a short open-water season. Furthermore, many lakes of the high Arctic are subject to glacial overprint and potentially do not contain long-term terrestrial paleoclimate records.

Lake El'gygytgyn (Fig. 1) provides a unique opportunity to investigate paleoclimate conditions of the Arctic realm reaching back 3.6 million years, approximately one million years prior to the first major glaciation of the Northern Hemisphere. The lake provides records of a reasonably high resolution for resolving climate fluctuations on orbital to centennial time scales (Melles et al., 2012). Until now, only a few terrestrial records with such a high temporal resolution are known from the Arctic realm (e.g. the Greenland ice cores, Dansgaard et al., 1993; Grootes et al., 1993; Svensson et al.,

Published by Copernicus Publications on behalf of the European Geosciences Union.

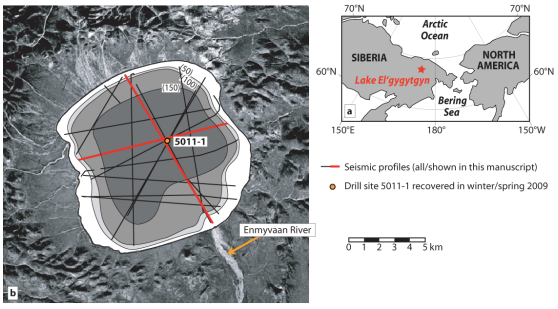

Fig. 1. Geographical map of the investigation area. **(a)** Location of Lake El'gygytgyn in NE Russia; **(b)** aerial photograph of the lake surroundings with lake bathymetry and seismic profiles. The profiles marked in red are shown in Figs. 2 and 3. The orange arrow marks the Enmyvaan River, the only outlet of the lake. Drill site ICDP 5011-1 is shown as an orange circle.

2011; NGRIP members, 2004), but none of them extends continuously to the onset of the Northern Hemisphere glaciation (Brigham-Grette et al., 2013). Marine records of the Arctic Ocean in general reach back much further in time, but show a lower temporal resolution (e.g. Lomonosov Ridge, Moran et al., 2006; Yermak Plateau, Myhre et al., 1995).

Lake El'gygytgyn is one of only a handful of lakes that formed inside a meteorite impact crater (Lerman et al., 1995). When the meteorite hit the target area 3.6 million years ago (Layer, 2000), the Northern Hemisphere was experiencing the rather constant, moderate to warm climate of the mid-Pliocene (Harris, 2005; Repenning and Brouwers, 1987). According to Harris (2005), the Arctic Ocean was unfrozen at that time, and Boreal cedar forests covered the landside along the Arctic Ocean coasts (Repenning and Brouwers, 1987). At around 3 million years before present, the Boreal forests were replaced by tundra around the Bering Strait and inland (Harris, 2005; Brigham-Grette et al., 2013). Herman and Hopkins (1980) reported a sharp change in the sedimentation regime as well as the first occurrence of ice-rafted debris (IRD) in the Arctic Ocean from about 2.53 Ma, and the onset of large-scale glaciation in Scandinavia (by means of a marked increase in IRD flux) was dated to 2.75 Ma by Fronval and Jansen (1996) and Jansen et al. (2000). Since then, the Arctic realm has experienced several advances and retreats of glaciers and ice sheets. A dropstone which was found in sediments as old as 45 Ma and the frequent occurrence of IRD since the early Miocene in a marine record from the Lomonosov Ridge show that the onset of the transition from a greenhouse world to colder climate with sea ice and icebergs might have begun much earlier than hitherto assumed (Moran et al., 2006).

The El'gygytgyn area has never been subjected to glacial overprint since its formation (Glushkova and Smirnov, 2007), and, thus, the lake contains an undisturbed climate record of approximately 3.6 million years, unique for the terrestrial Arctic realm. This record was drilled within the framework of the International Continental Scientific Drilling Program (ICDP). A permafrost core (ICDP site 5011-3) was retrieved from the eastern shoreline in late autumn 2008, and during winter/spring 2009 a 517 m-long drill core (ICDP site 5011-1) containing lacustrine sediments and the impact-related bedrock underneath was retrieved from the ice cover of the lake (Melles et al., 2011).

This paper aims to characterize the lacustrine part of core 5011-1 as well as the transitional zone between the lacustrine sediments and the impact-related bedrock by means of petrophysical parameters such as physical properties and downhole logging measurements. These findings are then compared to the facies description by Melles et al. (2007, 2012) and Brigham-Grette et al. (2013) and their interpretation contained therein.

2 General settings of the investigation area

2.1 Study area

Lake El'gygytgyn (67°30′ N, 172°05′ E) is located about 100 km north of the Arctic Circle in central Chukotka, NE Russia (Fig. 1). It was formed by a meteorite impact that was dated using $^{40}Ar/^{39}Ar$ to about 3.6 million years (Layer, 2000; Gurov et al., 1979a, b; Belyi, 1998). The lake's surface lies at about 490 m above sea level and the surrounding crater rim reaches elevations of ∼ 900 to 1000 m a.s.l.

The lake is roughly circular with a diameter of 12 km. Its catchment is limited to the crater rim with a total surface of 293 km^2 in total, including lake surface. About 50 small ephemeral creeks drain into the lake (Nolan and Brigham-Grette, 2007). The Enmyvaan River at the southern edge of the lake is its only outflow (Fig. 1a). The lake has a bowl-shaped form with a flat, central plain of 170 m water depth and flanks that are steepest in the north and northeast. A shelf of 10 to 12 m water depth has developed in the southeastern, southern, and southwestern to western areas of the lake (Fig. 1a).

The lake is presently ice-covered for 9–10 months annually with only a short period of completely open water (Nolan and Brigham-Grette, 2007). During the short summer season, the monomictic and ultra-oligotrophic lake gets mixed completely (Nowaczyk et al., 2002; Nolan and Brigham-Grette, 2007). The catchment vegetation consists mainly of moss tundra interspersed by few shrub willows; the modern tree line lies about 150 km further south and west (Nowaczyk et al., 2002). The current wind system exhibits a bipolar mode with winds approximately from north and south (Nolan and Brigham-Grette, 2007).

2.2 Lithological succession

In spring 2009, three drill cores were retrieved from the center of Lake El'gygytgyn (site 5011-1, cores 5011-1A, 1B, 1C) down to a maximum depth of 517.3 m below lake floor (b.l.f.). A detailed description of all drilling details is given by Melles et al. (2011). The cores were transported to the laboratory facilities at the University of Cologne, Germany, where they were opened and described. Based on the core description together with several measured paleoclimate proxies, a composite profile was defined (Melles et al., 2012; Nowaczyk et al., 2013). The composite sediment core consists mainly of highly variable silty–clayey pelagic sediments divided into different facies types by Melles et al. (2012) and Brigham-Grette et al. (2013), interfingered with mass movement deposits (Sauerbrey et al., 2013).

"Facies A" consists of fine clastic laminations of less than 5 mm thickness (average is ~ 0.2 mm). The sediments of facies type A are mainly dark gray to black in color. This suggests a stratified water column and anoxic bottom water conditions (Melles et al., 2012). The authors associate this facies type with peak glacial conditions and a perennial ice cover of the lake, with mean annual air temperatures of at least 4 (± 0.5) °C less than today. This facies was already described in pilot core PG1351 as subunits 3 ("cold & dry") and 4 ("cold & moist"), characterized by enhanced amounts of total organic carbon (TOC), medium to low biogenic silica content (Melles et al., 2007), and low magnetic susceptibility due to dissolution of magnetite by anoxic conditions (Nowaczyk et al., 2007). The cold & dry subtype is further referred to as A_d, the cold & moist subtype as A_m. Facies A sediments are limited to the younger part of the sediment record (Brigham-Grette et al., 2013), i.e. the uppermost ~ 124 m (< 2.6 Ma).

"Facies B" is the most abundant facies type in the composite profile and mainly consists of olive gray to brown, massive to faintly banded silt with greenish bands typically 1–3 cm thick. The sediments are characterized by a lack of sedimentary structures, indicating bioturbation and oxygenated bottom water (Melles et al., 2012). This implies warmer climate with ice-free summers and a mixed water column. This facies reflects a wide range of glacial to interglacial settings including the modern situation. TOC content is rather low in facies type B (0.83 ± 0.27 %) due to high organic matter decomposition in oxic bottom water conditions; biogenic silica values are intermediate to high due to enhanced primary productivity, and magnetic susceptibility is high reflecting good preservation of magnetite (Melles et al., 2012).

"Facies C" is the least common facies type found in the composite profile (Melles et al., 2012). It is irregularly distributed and consists of distinctly reddish-brown silt. Melles et al. (2012) suggest oxidation of bottom sediments by a well-ventilated water column as responsible for the distinct reddish color. This facies type was interpreted as representing "super interglacial" conditions e.g. during extraordinary warm MIS11 and 31, along with a number of earlier interglacials (Melles et al., 2012). Distinct laminae are found in facies type C, probably pointing at winter stratification and anoxic bottom water conditions under a seasonal ice cover. This is further supported by high TOC values. Biogenic silica content is also exceptionally high due to diatom blooms probably caused by enhanced nutrient influx from the catchment. Magnetic susceptibility is rather low both due to dilution of the magnetic susceptibility signal by the high biogenic silica content and partial dissolution of magnetite during periods (winters) with anoxic bottom water conditions.

"Facies D" is laminated similar to facies A, but its laminae are significantly thicker with an average thickness of up to ~ 1 cm. Laminae are characterized by distinct lower boundaries and a fining upward sequence from silt to clay with a higher total clay content than in facies A. Facies D is mostly gray but has some red and green hues in its oldest parts. The well-preserved laminations suggests a lack of bioturbation of the bottom sediment, and the characteristic fining upward sequences in each lamina suggest repeated pulses of sediment delivery to the lake, probably due to variations in fluvial input (Brigham-Grette et al., 2013). Facies D is limited to the Pliocene part of the record, with the youngest occurrence at ~ 141 m b.l.f. (≈ 2.9 Ma).

"Facies E" comprises the transition from the impact-altered bedrock to lacustrine sediments. This transition is more/less gradual with sediments composed of impact breccia and impact melt blocks in a matrix of lacustrine sediments, with the bedrock-related particles being dominant in the lower and the lacustrine sediments in the upper part (Koeberl et al., 2013; Raschke et al., 2012).

"Facies F" comprises a wide variety of mass movement deposits such as turbidites, debrites, slumps, slides and grain flows. A detailed description of the mass movement deposits and their distribution within the record is given by Sauerbrey et al. (2013). Only thin mass movement deposits (< 5 cm in thickness) were sampled in the composite profile of 5011-1, and thicker ones were omitted. These thinner mass movement deposits are almost exclusively turbidites.

3 Data acquisition and processing

3.1 Seismic data

Prior to deep drilling, two seismic site surveys were carried out in 2000 and 2003. In 2000, a single-channel survey was carried out using a Bolt 600B airgun (82 cm^3, 6 s shot interval resulting in approximately 8 m shot distance) with a 20-element single-channel hydrophone streamer (Geoacoustics AE5000) as receiver (Niessen et al., 2007). Single-channel reflection data were bandpass-filtered (100-150-350-450 Hz), and an AGC was used for display. In 2003, two single-channel and eight multi-channel profiles were acquired using a Mini-GI gun triggered in G-gun mode at a pressure of 110 bar (426 cm^3, 10 s shot interval resulting

in approximately 12 m shot distance). For the multi-channel profiles, a 14-channel streamer with an offset of 130 m and a hydrophone spacing of 10 m was used as receiving array (details are given in Niessen et al., 2007). Multi-channel data were processed in a standard sequence including bandpass filtering (70-90-240-300 Hz), velocity analysis, CMP stacking, and predictive deconvolution. Tracklines are shown in Fig. 1.

3.2 Core physical properties

Physical properties data of cores 5011-1A, 1B and 1C were acquired using a Geotek Multi-Sensor Core Logger (MSCL; Geotek Ltd., UK) both in the field laboratory during the drilling campaign in 2009 (magnetic susceptibility measurements on whole cores) and at the Alfred Wegener Institute (AWI) in Bremerhaven, Germany, between October 2009 and January 2011 (density measurements on split cores). The data were complemented with density and magnetic susceptibility data from pilot core Lz1024 which were measured at AWI in March 2004 on whole cores.

Magnetic susceptibility (MS) was measured in SI units using a Bartington MS-2 meter equipped with a loop sensor of 80 mm internal diameter. Data correction was done with respect to the specific core and loop sensor diameters according to the Bartington Manual (Geotek, 2000). Even though temperature inside the field lab container was sometimes variable due to opening and closing of the door, with inside temperatures around +20 °C and outside temperatures between −45 and −20 °C, no severe drifting of the temperature-sensitive sensor was observed. The small drifting that occurred was significantly lower than the lowest susceptibility readings and, thus, did not affect the data. Both magnetic susceptibility and density data were corrected for outliers, and composite profiles were spliced accordingly to the sampling scheme used for the discrete samples (Wennrich et al., 2013)

Gamma-ray density (GRAPE) was measured using a ^{137}Cs source mounted on the Geotek MSCL. For density calibration, standard core-size semi-cylinders consisting of different proportions of aluminum and water were logged prior to the cores according to the method described by Best and Gunn (1999) but modified for split cores. Split cores were only approximately 33 mm thick, which is too thin for the AWI Geotek MSCL to measure thickness reliably. To convert raw gamma ray attenuation counts to density, however, exact thickness measurements are required. Accordingly we used the surface scans that were measured by the ITRAX XRF core scanner (COX Analytical Systems, Sweden) at the University of Cologne (see Wennrich et al., 2013) in the course of the XRF measurements on the same split cores. These surface scans were calibrated for thickness using a semi-cylindrical piece with a radius of 33.15 mm to simulate a standard split core, and three pieces that were thicker (+10 mm, +20 mm) or thinner (−10 mm) than the standard to calibrate the entire range of possible sediment thicknesses. GRAPE was calculated using the standard method (Geotek, 2000).

3.3 Downhole logging data

While drilling hole 5011-1C, operations were stopped four times to allow for the acquisition of downhole logging data. All data presented here were acquired using slimhole probes manufactured by Antares (Germany). Operation of the probes under the extreme conditions of an Arctic winter drilling campaign went well overall but also took its toll in the damaging of two probes: the acoustic velocity and the caliper probe. For downhole logging sessions, the pipe was pulled out of the hole, except for the uppermost approximately 20 m where the casing was pushed into the sediment for stabilization, leaving a sufficiently stable borehole wall. After downhole logging sessions were finished, the pipes were redeployed, and drilling operations were resumed. For drilling operations, bentonite was used as drilling fluid. Downhole logging was carried out to a maximum depth of 394 m below lake floor. In order to fit the downhole logging depths to the composite profile depths, the entire downhole logging dataset was shifted downwards by 3 m. This results in an apparent discrepancy with depths used by the community working on the impact-related bedrock (e.g. Koeberl et al., 2013; Raschke et al., 2012); accordingly those depths were also shifted by 3 m downwards for comparison with the sediment section data. Both electrical resistivity and magnetic susceptibility data of the uppermost approximately 143 m could not be used as they were disturbed by the pipes of nearby abandoned holes 1A and 1B.

Electrical resistivity (ER) of the surrounding sediments/rock at two different lateral distances from the borehole wall (deep ∼ 60 cm and shallow ∼ 20 cm, with the actual penetration depending on rock porosity and the resistivity of fluid and rock) was measured using a dual laterolog probe. The probe has a vertical resolution of approximately 10 cm (electrode length: 8 cm), and typical logging speed was 12 m min^{-1}.

Borehole magnetic susceptibility (BMS) was measured using a probe that consists of a receiver coil and a transmitter coil that is located 20 cm above the former inside a non-magnetic pressure housing. The transmitter coil induces a 1 kHz alternating magnetic field. Magnetic susceptibility was corrected for the two different borehole diameters drilled during the Lake El'gygytgyn deep drilling project. Down to 274.33 m composite depth (i.e. 443 m below lake surface), a bit size of 124 mm was used; a correction factor of 1.4 was applied for this section. In the deeper part of the hole, a smaller bit size of 98 mm was used for drilling/coring, and accordingly a correction factor of 1.25 was used. The vertical resolution is approximately 20 cm (detector spacing), but relative variations can be identified with a resolution of about 5 cm. Penetration into the sidewall is ∼ 20 cm; typical logging speed was 8–10 m min^{-1}.

The total amount of naturally occurring radioactive radiation (GR) was measured using a total natural gamma ray probe. This GR probe was always run with other probes for depth corrections. One GR curve was chosen as the reference (Master-GR), and all other GR curves with their attached other measurements were shifted to fit the Master-GR. Vertical resolution is approximately 10 cm, and typical penetration into the rock is about 10 cm.

The spectrum of the naturally occurring radioactive radiation (SGR), i.e. uranium, thorium, and potassium, was measured using a natural gamma ray probe. Logging speed was slower than $2\,\mathrm{m\,min^{-1}}$ for the SGR probe to allow gathering of a reliable gamma ray spectrum. Vertical resolution is ~ 10 cm, and penetration into the rock is ~ 15 cm. Gamma rays penetrate steel casing; therefore both the GR and the SGR probes could be run in cased holes. Corrections were carried out for the casing as well as for the different diameters of the borehole. Th and K values are often used as a proxy for a first estimate and characterization of clay content in the sediments (e.g. Wonik, 2001; Ruffell and Worden, 2000; Schnyder et al., 2006), assuming that they are almost exclusively present in this grain-size fraction, and that K and Th are present in montmorillonite, illite, and kaolinite in different portions. To estimate the clay content in Lake El'gygytgyn sediments, we used the approaches given by Wonik (2001):

$$C_{\mathrm{cl}}(\mathrm{K}) = \frac{\mathrm{K} - \mathrm{K_{sand}}}{\mathrm{K_{clay}} - \mathrm{K_{sand}}}, \quad (1)$$

and

$$C_{\mathrm{cl}}(\mathrm{Th}) = \frac{\mathrm{Th} - \mathrm{Th_{sand}}}{\mathrm{Th_{clay}} - \mathrm{Th_{sand}}}, \quad (2)$$

with C_{cl} = clay content (%), $\mathrm{K_{sand}}$ and $\mathrm{Th_{sand}}$ = K and Th content of sand, and $\mathrm{K_{clay}}$ and $\mathrm{Th_{clay}}$ = K and Th content of clay. K and Th contents of sand are normally very low and were set to 0.1 % for K and 0.1 ppm for Th; K and Th contents of clay were set to the maximum K and Th values measured in the record, which are 4.5 % for K and 22.4 ppm for Th. K and Th in Eq. (1) and (2) are the actual readings from the SGR dataset. A third approach uses the GR data as follows (Wonik, 2001):

$$V_{\mathrm{cl}}(\mathrm{GR}) = 0.33 * \left(2^{2*\mathrm{GRI}} - 1\right), \quad (3)$$

$$\mathrm{GRI} = \frac{\mathrm{GR} - \mathrm{GR_{sand}}}{\mathrm{GR_{clay}} - \mathrm{GR_{sand}}}, \quad (4)$$

with V_{cl} = percentage of the volume of clay, $\mathrm{GR_{sand}}$ = 135 API and $\mathrm{GR_{clay}}$ = 10 API; GR in Eq. (4) is the actual reading from the GR dataset.

3.4 Si / Ti, TOC data

Silicium / titanium (Si / Ti) ratios were determined on core halves using an X-ray fluorescence (XRF) core scanner (ITRAX, Cox Ltd., Sweden). Details on the scanner settings and processing of the data are given in Wennrich et al. (2013). Total organic carbon (TOC) content was calculated as the difference between total carbon and total inorganic carbon using a DIMATOC 200 carbon analyzer (Dimatec Corp.) in aqueous suspension.

3.5 Statistical analyses

Statistical analyses were carried out in order to detect statistically differing groups of samples. In a second step, these clusters are then compared with their lithological description and, subsequently, their facies assignment. Due to the rather simple dataset, cluster rather than a PCA analysis was carried out using Matlab® and the implemented statistical toolbox (Mathworks Inc., Version 7.14.0.739). In a first step, downhole logging data (magnetic susceptibility, electrical resistivity, U counts, Th counts, K counts) were clustered into 3 groups (clusters 1 to 3) using k-mean clustering to allow for a first characterization of the entire record. Data < 143 m b.l.f. were omitted due to the disturbed magnetic susceptibility and electrical resistivity signal. In a second step, Si / Ti ratios, magnetic susceptibilities and TOC percentages measured on the composite core down to approximately 262 m composite depth were used for statistical clustering in 4 different groups (clusters I to IV), again the k-mean clustering method (please note that clusters 1 to 3 and I to IV are two different sets of clusters). For interpretation of the statistically derived clusters, the described facies type was assigned to all samples. Given that sampling occurred generally in 2 cm steps (Melles et al., 2012), we used the facies type at the mean depth of the sample as representative for the entire sample, neglecting that facies boundaries could also occur within a discrete sample.

4 Seismic and petrophysical description of the entire lithological succession

4.1 Seismic profiles

The impact crater shows internal geometries as expected for a crater of its size. A central uplift structure interpreted in the form of a central uplift ring structure was revealed by seismic refraction data; it is overlain by an impact breccia (suevite) (Gebhardt et al., 2006). The lacustrine sediments can be divided into two units by means of refraction data; the upper unit is characterized by a seismic velocity of $1550\,\mathrm{m\,s^{-1}}$ and a thickness of about 170 m, the lower unit by $1650\,\mathrm{m\,s^{-1}}$ and a variable thickness of 190 m on top of the uplift ring structure to 290 m in the surrounding basin (Gebhardt et al., 2006). For the description of the seismic sections, we follow the stratigraphic numbering introduced by Gebhardt et al. (2006). Unit I comprises all lacustrine sediments and is subdivided into subunits Ia and Ib. Units II and III are the underlying suevite layer and the brecciated bedrock that form

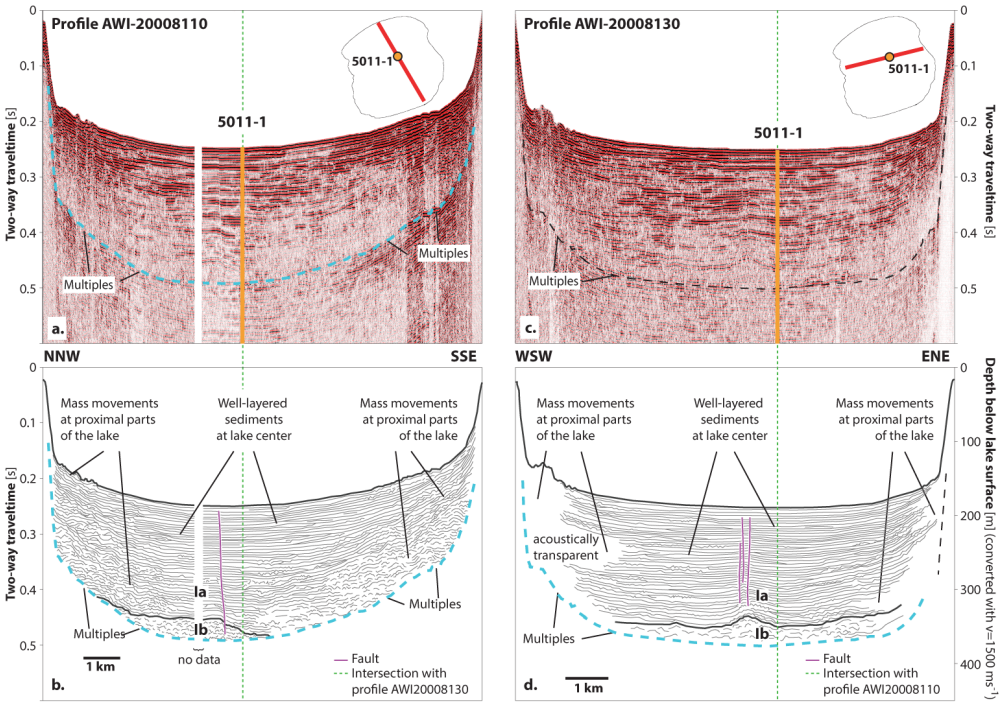

Fig. 2. Single-channel seismic reflection profiles AWI-20008110 and AWI-20008130 (acquired with a Bolt 600B airgun). Seismic profiles are shown in **(a)** and **(c)**; line drawings and interpretations in **(b)** and **(d)**. Green dashed line marks the intersection of the two lines that was chosen for drill site 5011-1; lilac lines show the faults that are likely related to the central uplift structure of the impact crater (see Gebhardt et al., 2006). Seismic profiles clearly show the boundary between subunits Ia and Ib. Units II and III are masked by the multiples.

the basement below the lake floor deformed by the impact. The subdivision of unit I into subunits Ia and Ib that was indicated by the refraction data by a shift in seismic velocities can also be observed in the reflection data. However, the larger part of Ib is masked by the multiple in the reflection data. Where observable, seismic reflection data exhibit that upper subunit Ia is well-layered, while lower subunit Ib is more chaotic and discontinuous (Fig. 2). The lake floor is relatively flat in large parts of the basin, but sometimes rough in the more proximal areas where mass movement deposits occur frequently in the upper layers of the sediments. Mass movement deposits are quite common mainly in the proximal parts of the lake in subunit Ia (e.g. Juschus et al., 2009; Niessen et al., 2007; Sauerbrey et al., 2013), and even in the lake center at the distal 5011-1 drill site, where they make up approximately one third of the entire sediment column (Sauerbrey et al., 2013). In the lower part of subunit Ia, mass movement deposits reach much farther toward the central part of the lake (Fig. 2), whereas in the upper layers they are almost entirely restricted to the proximal part of the lake. This is confirmed by the fact that only small mass movement deposits, mainly turbidites, were found in pilot cores PG1351 (~ 13 m length) (Melles et al., 2007) and Lz1024 (~ 16 m length) (Juschus et al., 2009). The turbidites were associated with distant debris flows in a conceptual model (Juschus et al., 2009), which was confirmed by the findings in the drill cores where debris flows are in most cases directly overlain by turbidites (Sauerbrey et al., 2013).

The wide shelf at the southeastern part of the lake is characterized by aggrading sequences; seismic data from the western and northwestern shelf are not available due to coarse sediments limiting acoustic penetration in these areas. Subunit Ia forms onlaps against the steep slope at the lake margins in a layer-cake manner (Fig. 2), gradually muting a formerly deeper surface with steeper relief (Niessen et al., 2007). Subunit Ia conformably overlies subunit Ib with a clear and distinct boundary between the two. Subunit Ib has a massive, acoustically chaotic character and rarely shows internal layering in the parts that are visible in the seismic profiles. Its upper boundary has a hummocky surface probably due to thick, chaotic mass movements in its uppermost parts (Fig. 2). Its lower boundary to unit II lies below the acoustic multiples and is therefore masked. However, refraction data showed that subunit Ib drapes the central uplift structure, which is characteristic for impact craters of this size (Gebhardt et al., 2006).

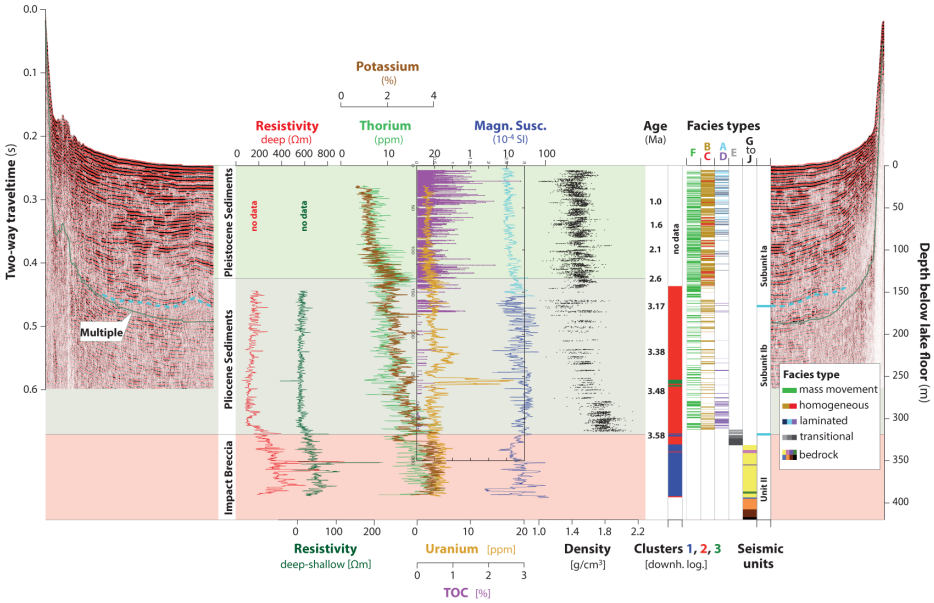

Fig. 3. Single-channel seismic reflection profile AWI-20008130 (acquired with a Bolt 600B airgun) with inset of downhole logging and core physical properties data. Note that the light-blue part of the magnetic susceptibility data derive from direct core measurements, while the dark blue part is from downhole logging measurements – i.e. exact values and amplitudes of the two datasets are not directly comparable. Dashed turquoise horizontal lines mark the boundaries of seismic subunits 1a and 1b; the boundary between units I and II is taken from Gebhardt et al. (2006). Sedimentary facies comprise mass movement deposits (facies F; green), massive interglacial sediments (facies B; ochre), laminated super interglacial sediments (facies C; red), laminated Quaternary glacial sediments representing "cold & dry" (facies A_d; light blue) and "cold & moist" climates (facies A_m; dark blue), laminated Pliocene sediments (facies D; lilac), and transitional sediments between impact breccia and lake sediments (facies E; gray). Facies types are used sensu Melles et al. (2007, 2012) and Brigham-Grette (2013). The impact breccia/suevite succession according to Koeberl et al. (2012) is given as follows: yellow: suevite; lilac: upper volcanic rock layer; violet: lower volcanic rock layer; green: ignimbrite. The clusters derived from k-mean clustering of downhole logging data are shown in blue for cluster 1, red for cluster 2 and green for cluster 3. Ages are taken from Nowaczyk et al. (2013).

Faults with a vertical offset of up to several meters were observed in the central part of the northern profiles in unit I. These show a decreasing offset toward the more recent sediment and are inactive in the upper meters of the lake sediments (Fig. 2); this was also observed in high-resolution sub-bottom profiles (Niessen et al., 2007). The faults are likely related to the later settling and subsidence of the central uplift structure (Gebhardt et al., 2006).

4.2 Physical properties from downhole and core measurements

Subunit Ia comprises the uppermost ∼167 m of the sediment column (Fig. 3), which corresponds to approximately 3.17 Ma (Nowaczyk et al., 2013). This also includes the Pliocene/Pleistocene transition at 123 m b.l.f. (2.6 Ma). Downhole logging data show that the Pleistocene sediments are characterized by relatively constant K and Th counts down to approximately 100 m b.l.f. (2.1 Ma, Nowaczyk et al., 2013); magnetic susceptibilities of the sediment core are highly variable, but fluctuate in a range between ∼ 15 and ∼ 200×10^{-4} SI (Fig. 3). Similar to magnetic susceptibility, density is highly variable throughout the entire record, but scatters around a mean value of approximately 1.5 g cm^{-3} in the sediments of subunit Ia (< 3.17 Ma). Lithologies and associated sedimentary facies are characterized by a rapid change between homogeneous (facies B) and laminated (facies A) layers that represent warm and cold phases, respectively (Melles et al., 2007), as well as occasional laminated sediments reflecting peak warm conditions (facies C). These hemipelagic sediments are intercalated by a large number of mass movement deposits of different types such as debris flows and turbidites (Sauerbrey et al., 2013) that become thicker toward the lower boundary of subunit Ia (Fig. 3). Below 100 m b.l.f., downhole logging K and Th counts show an increase with increasing depth, with the highest values exactly at the Pliocene/Pleistocene boundary and strongly decreasing values in the uppermost part of the Pliocene sediments. Magnetic susceptibility values of the Pliocene part of subunit Ia show a slight increase in amplitude in comparison to the Pleistocene data.

Subunit Ib comprises all lacustrine sediments between 167 m b.l.f. and the boundary to the underlying bedrock at ~320 m b.l.f. While magnetic susceptibility values of the Pleistocene part of subunit Ia originate from sediment core measurements (MS, light blue in Fig. 3), the values of the Pliocene section were measured in the borehole (BMS, dark blue). The two datasets are not completely comparable in terms of their exact values and amplitudes: it seems as if the lower part has much higher amplitudes; this however might be an artifact caused by the different measurement methods. Magnetic susceptibility seems to be more variable in long-term trends in the Pliocene part of the sediments; however, it is unclear if this is a real paleoclimate signal or just a scaling effect. Unfortunately, there is not enough overlap in between the two datasets to tune them to similar amplitudes. Nevertheless, it is obvious that magnetic susceptibility is much more variable between approximately 150 and 220 m b.l.f. than below (220 m corresponds to 3.38 Ma, Nowaczyk et al., 2013). Electrical resistivity is rather constant throughout the entire Pliocene sediment succession with exception of the lowermost approximately 20 m where a small maximum occurs at ~300 m b.l.f. Density shows an increase with increasing depth from mean values around 1.5 g cm^{-3} in the uppermost part of subunit Ib to mean values around 1.8 g cm^{-3} with values as high as > 2.0 g cm^{-3} in the lowermost part, i.e. in the transitional zone between lacustrine and impact-related units. Lithological description of subunit Ib is not as detailed as for subunit Ia due to lower core recovery and, thus, larger drilling-related gaps (for details on drillings operations, see Melles et al., 2011). As in the upper part, sediments alternate between laminated and homogeneous sediments, but the homogeneous facies B dominates the Pliocene part of the record. Only in the lowermost part, i.e. below ~270 m b.l.f. (3.48 Ma, Nowaczyk et al., 2013; Brigham-Grette et al., 2013), are laminated sediments more abundant. As in subunit Ia, mass movement deposits are intercalated frequently in the hemipelagic sediments.

Uranium values are rather constant throughout the entire record, with slightly higher values in the bedrock. Two strong exceptions however are observed in the lacustrine part: (a) between ~220 and ~244 m b.l.f., U values are slightly enhanced, and (b) a strong double peak is observed between ~251 and ~262 m b.l.f. The U peaks are confirmed by the independently measured total GR.

Electrical resistivity (deep and shallow), borehole magnetic susceptibility, and natural gamma ray counts of K, U and Th were used for cluster analyses to distinguish among different main units between 143 m and 394 m b.l.f. This includes the boundary between the lacustrine sediments and the brecciated bedrock. Three clusters could be distinguished: (1) cluster 1 is characterized by high electrical resistivity and enhanced K content values (Fig. 4 upper panel). Magnetic susceptibility is rather variable. (2) Cluster 2 is characterized by low electrical resistivity, variable magnetic susceptibility, and low U and K content. (3) Cluster 3 has

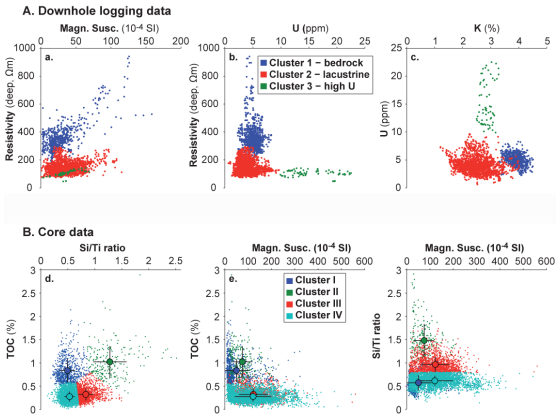

Fig. 4. Crossplots of clusters vs. geophysical and geochemical parameters. Upper panel: clusters 1 to 3 derived from k-mean clustering of downhole logging data (electrical resistivity (deep and shallow), magnetic susceptibility, U, Th, and K counts). Lower panel: clusters I to V derived from k-mean clustering of core data (TOC content, Si / Ti ratio, standardized magnetic susceptibility). In the lower panel, mean and standard deviation of parameters are shown for each cluster.

low electrical resistivity, high U and intermediate K values (Fig. 4 upper panel). It is clearly different from cluster 1 in almost all parameters, but coincides with cluster 2 in terms of low resistivity. Plotting these three clusters against depth (Figs. 3 and 5), it becomes obvious that cluster 1 clearly describes the bedrock. Cluster 2 comprises the main part of the lacustrine record. Cluster 3 is part of the lacustrine sediments but comprises only the section between 254.44 and 259.15 m b.l.f. and between 260.7 and 262.5 m b.l.f., where the strong U double peak is observed (Fig. 3).

Both pelagic sediments and mass movement deposits in Lake El'gygytgyn are part of clusters 2 and 3, which implies that these two sediment types do not differ in their petrophysical characteristics. This confirms that the mass movement deposits consist mainly of reworked lacustrine material (Sauerbrey et al., 2013). Enhanced U values in cluster 3 found in the borehole data could not be measured with the ITRAX XRF core scanner in the according core sections, probably due to the scanner's limited ability for measuring U. U is removed from the water column and buried in the sediment during oxic conditions (e.g. Anderson et al., 1989); this would probably point at high bottom water oxygen levels when these layers were accumulated. This, however, is not confirmed by the sediment description, which does not differ significantly from above or below these layers. Hence, it is more likely that U-rich rocks were eroded in the lake catchment during these periods and transported to the lake by fluvial/eolian rather than gravitational transport processes.

Natural gamma radiation is often measured and used as an indicator for clay content in sediments, based upon the fact

that K and Th are enriched in different clay minerals. This approach, however, does not work in Lake El'gygytgyn sediments where calculated clay values based upon K and Th measurements (Eqs. 1, 2, 3 and 4, respectively) do not correlate with conventionally measured clay contents. This can best be explained by the lake's location in a small catchment with short transport paths from the source rock to the accumulation site, which prohibits full weathering of all grains. K-bearing feldspar grains would normally weather into K-bearing clay, so K would be an indicator for clay solely. In the case of a very short distance from source to sink, K-bearing feldspar grains of probably fine sand or silt size would also end up in the sediment along with clay. This would in turn suggest that the assumption that sand does not contain K (see Eq. 1, Methods section) is wrong in our case.

4.3 Boundary between bedrock and lacustrine sediments

The most prominent change in the downhole logging data occurs at the boundary between lacustrine sediments and the underlying altered bedrock at ~320 m b.l.f. (Figs. 3 and 5). While sediments above ~313 m b.l.f. are clearly lacustrine with alternating homogeneous and laminated layers, intercalated with frequent mass movement deposits, sediments below ~313 m b.l.f. are a mixture between a sedimentary matrix and reworked impact breccia. The boundary between the lacustrine sediments and the underlying bedrock is thus rather a transitional zone than a sharp boundary. In the upper part of this transitional zone, i.e. ~313 and 319.8 m b.l.f. (transitional zone T1 in Fig. 5), lacustrine sediments form the dominant part of the record, while below 319.8 m b.l.f. (T2 and T3) the record contains mainly reworked impact breccia in a sedimentary matrix (Raschke et al., 2012). Therefore, the formal boundary between the lacustrine and the impact part of the drill core was defined at 319.8 m b.l.f., between drill runs 97Q and 98Q. Koeberl et al. (2013) subdivide the part of the transitional zone that lies below this boundary into two subunits, one from 319.8 to 323 (T2 in Fig. 5) and the second from 323 to 331 m b.l.f. (T3) (note that the original depth values from both Raschke et al. (2012) and Koeberl et al. (2013) were shifted downwards by 3 m to match the depth scale used by the lacustrine El'gygytgyn scientific community). Both subunits show similar lithologies with fine sand-sized grains mainly composed of glass fragments, intercalated with impact breccia and impact melt blocks. All three subunits of the transitional zone (T1 above, T2 and T3 below the formal boundary) are shown in light to dark gray tones of facies type E in Fig. 5. The boundary between the matrix-dominated (=lacustrine, T1) and the clast-dominated (=impact-related, T2 and T3) sections appears as a sharp boundary in the electrical resistivity and also in the magnetic susceptibility data. Nevertheless, cluster analyses shows that except for two small bands, the entire transitional zone exhibits characteristics that are more

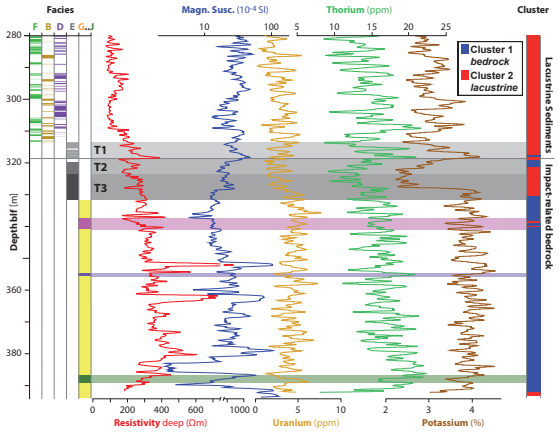

Fig. 5. Facies and downhole logging data of the transitional zone between impact-related bedrock and lake sediments. Facies description as in Fig. 3. Clusters derived from k-mean clustering of downhole logging data are shown in blue for cluster 1 (=bedrock) and red for cluster 2 (= lacustrine). The impact breccia/suevite succession according to Koeberl et al. (2012) is given as follows: yellow: suevite; lilac: upper volcanic rock layer; violet: lower volcanic rock layer; green: ignimbrite.

similar to the overlying lacustrine succession. Only below this transitional zone are the sediments clearly of bedrock affinity.

Chemical elements K and Th are enriched just above our formal bedrock–lake sediment boundary, but depleted below with exception of the lowermost part of the transitional zone. Below 331 m b.l.f., a long succession of suevite was described by Raschke et al. (2012) and by Koeberl et al. (2013). The suevite is obviously petrophysically heterogeneous with highly variable values in both electrical resistivity and magnetic susceptibility (Fig. 5). Two volcanic-like blocks (336.83 to 340 and 354 to 353 m b.l.f.), as well as an ignimbrite block (386 to 388.5 m b.l.f.) described by Koeberl et al. (2013) correspond to peaks in the electrical resistivity data (Fig. 5). Electrical resistivity shows a decreasing trend inside the upper volcanic block towards lower depths, while the opposite is observed in the ignimbrite layer. The former plots into the lacustrine cluster not because it is of lacustrine origin, but quite likely because it differs from the surrounding bedrock; the latter seems to be similar to the surrounding bedrock. Furthermore, electrical resistivity shows that the thick suevite layers have some pronounced internal layers of apparently different geophysical character.

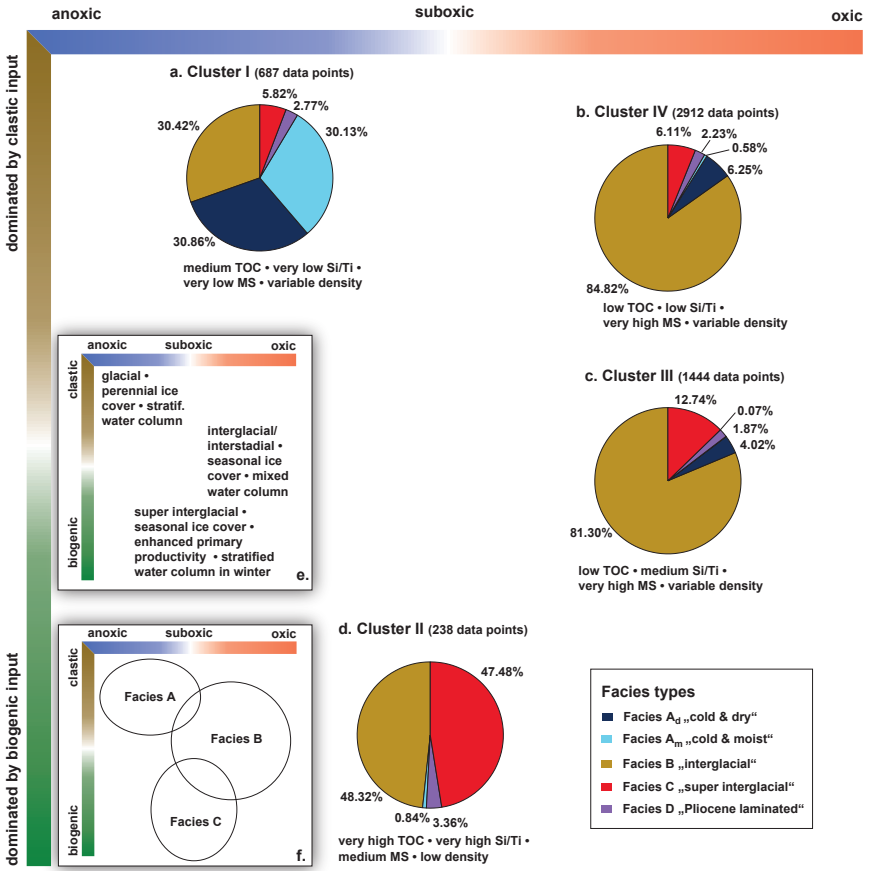

Fig. 6. Pie plots of core-data-derived clusters I to IV versus facies types known from core description. Facies colors correspond to those shown in Figs. 3 and 4. Clusters are distributed according to their redox conditions and clastic vs. biogenic input ratio. **(e)** shows where different paleoenvironmental conditions would plot in such a redox-condition vs. input-type diagram; **(f)** shows this for the Melles et al. (2007, 2012) and Brigham-Grette et al. (2013) facies types. Percentages in **(a)** to **(d)** are calculated for the facies distribution within each cluster.

5 Variability in the lacustrine succession

5.1 Description of the lacustrine succession

While electrical resistivity shows pronounced peaks in the bedrock and in the transitional zone, it is fairly constant with only very small peaks throughout the entire lacustrine section, exhibiting some smaller but smooth shifts only in the lowermost part (Figs. 3 and 5). This points at a rather uniform succession of sediments without abrupt changes, even though the sediments are highly variable and change rapidly between homogeneous and laminated layers and mass movement deposits (see facies column in Fig. 3). This is reflected in the fact that almost the entire lacustrine succession is represented by cluster 2, with only a very small part that has extraordinary high U values clustering separately into cluster 3 (Fig. 3). The apparent discrepancy between a highly variable sediment and yet quite similar petrophysical characteristics can also be best explained by the lake's location in a rather small catchment of only 293 km^2 including the lake's surface (Nolan and Brigham-Grette, 2007). This suggests that during warmer as well as during colder periods the same source rock is eroded, and thus almost all clastic grains that end up in the lacustrine sediments originate from the same provenance. However, there is a minor contribution to the sediment by eolian grains (Francke et al., 2013; Fedorov et al., 2012). In a large catchment, however, one could expect that different parts with different lithologies would experience e.g. variable cover by glaciers or vegetation, and thus result in differing erosion. Nevertheless, differing erosional processes, i.e. more physically dominated weathering during colder and more chemically dominated weathering during warmer periods, in the small hinterland as well as diatom blooms during warmer periods are strong enough to generate highly variable

Table 1. Amount of data points of the 6 facies types in the 4 clusters (mass movement deposit sediments and tephra were omitted in this table).

	Facies A_d	Facies A_m	Facies B	Facies C	Facies D	Total
Cluster I	212	207	209	40	19	708
Cluster II	0	2	115	113	8	238
Cluster III	58	1	1174	184	27	1444
Cluster IV	182	17	2470	178	65	2912
Total	452	227	3968	515	119	4769

sediment properties (cf. Minyuk et al., 2007) but with almost identical character in terms of petrophysical characteristics. Magnetic susceptibility, in turn, is highly variable in the lacustrine part, probably reflecting different weathering mechanisms and different modes of paleohydrological conditions (such as anoxia in the bottom water; see Melles et al., 2007, 2012) along with dilution effects by biogenic material.

In order to detect the variability within the lacustrine succession related to the different modes in paleoenvironmental conditions, we carried out clustering analyses on 5538 data points using similar parameters as in Melles et al. (2007, 2012). With Si / Ti ratio, TOC percentage and magnetic susceptibility from core measurements, we were able to identify four clusters (Tables 1 and 2): cluster I is defined by medium TOC percentages, very low Si / Ti ratios and very low magnetic susceptibility. Cluster II shows high TOC percentages along with high Si / Ti ratios and medium magnetic susceptibility. Cluster III has low TOC percentages and medium Si / Ti ratios along with high magnetic susceptibility. Cluster IV is defined by low TOC percentages and Si / Ti ratios combined with high magnetic susceptibility. Density does not vary significantly between clusters I, III and IV, but is considerably lower in cluster II.

5.2 Paleoclimate implications

Melles et al. (2007, 2012) used TOC percentage, Si / Ti content and magnetic susceptibility to identify the oxygenation state of the bottom water and, thus, whether the water column was mixed or stratified, which in turn gives evidence on the duration of an ice cover on the lake. During phases with a perennial ice cover, the water column could not mix, and depletion of oxygen in the bottom water led to enhanced preservation of organic material, while magnetite underwent dissolution, leading to reduced magnetic susceptibility values. In contrast, during times with seasonal ice cover, mixing of the water column was possible during summer months (as it is today; see Nolan and Brigham-Grette, 2007). Organic carbon was thus consumed in the oxic bottom water, and magnetic minerals were buried without alteration (Melles et al., 2007, 2012). Si / Ti ratios can be used to estimate the biogenic vs. clastic input to the lake (Melles et al., 2012; Wennrich et al., 2013; Brigham-Grette et al., 2013). Enhanced Si / Ti values suggest high biogenic silica contents, which in the case of Lake El'gygytgyn are produced by enhanced primary productivity, mainly diatoms, during warmer times with only seasonal ice cover. Low Si / Ti values indicate colder periods with perennial ice cover, thus limitation in light penetration necessary for photosynthesis, along with probably enhanced clastic input through the 50 small ephemeral inlets around the lake (Melles et al., 2007, 2012). During times with a perennial ice cover, clastic input is triggered by seasonal moats and vertical conduits in the ice, as is the case today when snow melt starts in late spring (Nolan et al., 2003; Asikainen et al., 2007; Francke et al., 2013).

Using this information, we can plot the clusters in a redox-condition vs. input-type diagram (Fig. 6). In such a diagram, the different modes of paleoenvironmental conditions known from earlier studies by Melles et al. (2007, 2012) can be visualized as shown in Fig. 6e and f: the glacial modes of facies A with perennial ice cover and a stratified water column plots into in the upper left corner (anoxic conditions, dominated by clastic input or by a relative dominance of clastic material due to the lack of biogenic input); the interglacial mode of facies B with seasonal ice cover and a mixed water column would show up in the right middle part (oxic conditions with variable, but intermediate contents of clastic and biogenic input), and facies C – the super interglacial mode – would be found in the lower middle with variably suboxic and oxic conditions and a dominance in biogenic input.

When plotting clusters I to IV into this diagram (Fig. 6), it becomes obvious that sediments of facies B, i.e. the interglacial sediments, plot into several clusters (Fig. 6a to d): a high portion of facies B sediments are found in cluster IV (62.25 % of all facies B data points), and another 29.59 % plot in cluster III. In clusters I and II, some minor percentage (5.27 % and 2.90 %) of facies B sediments are found. This supports the earlier study by Melles et al. (2012) that describes facies B sediments as highly variable.

Facies F, i.e. the mass movement deposits, also plots into all clusters with the majority in cluster IV (80.39 %). Almost equal percentages of 10.98 and 8.24 % plot into clusters III and II, and a negligible 0.39 % is found in cluster I. As facies F is not part of the hemipelagic sediments in Lake El'gygytgyn, it was omitted in the pie plots in Fig. 6 for better visualization of the distribution of facies types A to D in the different clusters. The fact that both facies F and facies B only have minor parts plotting into clusters I and II, along with the fact that these clusters only represent 13.01 and 4.51 % of all data points, suggests that these two clusters might represent sediment endmembers of Lake El'gygytgyn.

"Glacial" cluster I: cluster I (687 data points = 13.01 % of entire dataset, Fig. 6a) plots into a field where sediments of facies A and some of facies B would be assumed. It contains equal amounts (30.86 % and 30.13 %) of both cold & dry facies A_d and cold & moist facies A_m. Another 30.42 % of this cluster comprises sediments that were classified as facies B, i.e. sediments interpreted as accumulated during interglacials, and some 5.82 % were even described as being

Table 2. Mean and standard deviation (std dev) of total organic carbon (TOC), density, Si / Ti ratio and magnetic susceptibility (Magn. susc.) of clusters I to IV.

	TOC %		Density (g cm^{-3})		Si / Ti ratio		Magn. susc.	
	mean	std dev	mean	std dev	mean	std dev	mean	std dev
Cluster I	0.8354	0.2460	1.4791	0.1086	0.4927	0.1404	50.1806	55.4048
Cluster II	1.0216	0.3369	1.2735	0.1274	1.2826	0.3100	75.0329	41.8939
Cluster III	0.3215	0.1263	1.4385	0.0949	0.8362	0.1385	122.4036	61.3634
Cluster IV	0.2760	0.1076	1.4900	0.0962	0.5327	0.0934	120.7652	76.9754

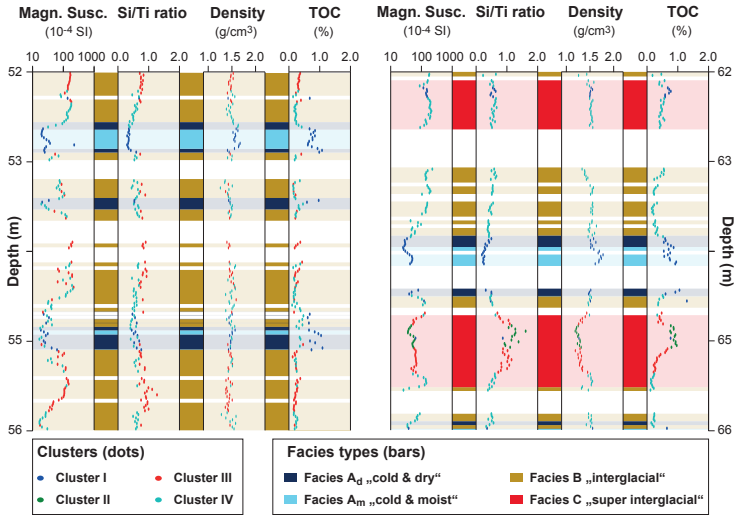

Fig. 7. Downcore distribution of facies types and clusters for 52 to 56 and 62 to 66 m b.l.f. Facies description as in Fig. 3. Clusters are superimposed on magnetic susceptibility, Si / Ti ratio, density and TOC content and are color-coded as in Fig. 4.

from super interglacials (facies C). This suggests that sediments of facies A show similar characteristics as a certain portion of facies B sediments, so they could not be statistically separated by means of cluster analysis. Nevertheless, the part of facies B data that plot into cluster I is only 5.27 % of all facies B data (Fig. 6a) and might even be negligible. In fact, samples used for this study are generally 2 cm thick, and we chose the facies type of their average composite depth as representative for the entire 2 cm, neglecting that facies boundaries might occur also within samples. Plotting facies types and clusters versus depth (Fig. 7) reveals that cluster I quite well captures the cold phases marked with light- and dark-blue bars in Fig. 7, for example at ∼ 52.5 to 52.9 m b.l.f., at ∼ 53.4 to 53.5 m b.l.f. and at 63.9 to 64.5 m b.l.f.

"Interglacial" clusters III and IV: cluster III (1444 data points = 27.34 % of entire dataset, Fig. 6c) as well as cluster IV (2912 data points = 55.15 % of the entire dataset, Fig. 6b) have very low TOC contents and high magnetic susceptibility values, pointing at oxic bottom water conditions during their deposition. While in cluster IV Si / Ti ratios are low, slightly higher Si / Ti ratios in cluster III suggest some biogenic input into the sediment. A high portion of cluster IV is composed of facies B sediment (84.82 %), and equal parts of 6.25 and 6.11 % consist of facies A_d and C, respectively. In cluster IV, which is the largest cluster and contains more than half of all data points, facies B is clearly dominant with 81.30 %, and 12.74 % are made up of facies C type sediments along with some 4.02 % of facies A_d. Both clusters contain the majority of all facies B data points and confirm that this facies type is rather variable yet similar being deposited under oxic conditions. The facies A_d sediments found in these two clusters, however, suggest that even during glacial times, oxic (or at least suboxic) conditions in the bottom water were sometimes encountered at least during periods with cold & dry conditions, and some biological production leading to enhanced Si / Ti ratios was possible. This is in good agreement with findings by Melles et al. (2007, 2012), who suggested that cold & dry facies A_d represents a perennial ice cover without snow cover. This would allow some light penetration and thus some primary productivity in the water column. In

contrast, cold & moist facies A_m was interpreted as representing a perennial ice cover covered by snow, inhibiting any light penetration into the water column, leading to only very limited photosynthetic life in the lake and thus low TOC values and Si / Ti ratios. This, in turn, is confirmed by only negligible 0.58 and 0.07 % of facies A_m in clusters III and IV, and 0.84 % in cluster II.

"Super interglacial" cluster II (238 data points = 4.51 % of the entire dataset; Fig. 6g): cluster II has significantly enhanced TOC and Si / Ti ratios and consists to almost equal parts of facies C and B sediments (47.48 and 48.32 %). The negligible remainder is 3.36 % facies D and 0.84 % facies A_m.

While density is rather variable in clusters I, III and IV, it is clearly lower than average in cluster II, which is in good agreement with a high content of biogenic silica. Even though approximately half of cluster II consists of facies C type sediments, only approximately one fifth of all facies type sediments plot into this cluster (21.94 %), while some 35.73 and 43.56 % plot into clusters III and IV. This might either point at a wider range of TOC percentages, Si / Ti ratio and magnetic susceptibility values within this facies type, or these samples are highly biased by facies changes within the distinct samples that led to a wrong assignment of facies type to a specific sample. When plotting facies and clusters together vs. depth (Fig. 7) it becomes obvious that only some parts of facies C (red bars) were captured by cluster II: between ∼ 62 and ∼ 62.7 m b.l.f., facies C sediments were visually described, but have rather low Si / Ti content and only slightly enhanced TOC values, so they were statistically gathered into clusters I and IV; these samples are part of the 5.82 % of facies C samples that were found in cluster I and 6.11 % in cluster IV. On the other hand, sediments of the thick facies C layer between ∼ 64.7 and ∼ 65.6 m b.l.f. show higher Si / Ti ratios and TOC content and were therefore gathered into clusters III and II. This would imply that even though facies C is easily detected by means of visual core description, its basic physical and geochemical properties might not always be significantly different from sediments of other facies types, notably from facies B. Nevertheless, this is in good agreement with findings by Melles et al. (2012) who report that while primary productivity was highest during these extraordinary phases, there are laminae found in the facies C sediments that suggest at least seasonally suboxic or anoxic conditions in the bottom waters. This could result in a wide variety of TOC percentages and magnetic susceptibility values in the resulting sediment and make it difficult to gather these sediments in one single cluster.

6 Conclusions

Seismic reflection profiles of Lake El'gygytgyn exhibit mostly well-stratified sediments with frequent mass movement deposits intercalated in the more proximal areas. The well-stratified acoustic layers correlate with the well-layered sediments of the drill core retrieved during winter/spring 2009 with highly variable facies types changing at high frequency in the core. The lacustrine sediment succession can be separated into two seismic subunits Ia and Ib. Whereas Ia is well-stratified, Ib is acoustically more chaotic and discontinuous. The sediment–bedrock boundary was identified earlier by Gebhardt et al. (2006) at around 320 to 330 m b.l.f. by means of a seismic-refraction-data-derived depth-velocity model. This was confirmed during drilling, with the first bedrock material found at approximately 320 m b.l.f.. Downhole logging data down to 394 m b.l.f., i.e. through the entire lacustrine column and some 74 m into the bedrock, show that the lacustrine and bedrock part clearly differ in their petrophysical characteristics: cluster analysis separates three clusters, two of which comprise the entire lacustrine succession, while the third contains the bedrock. The boundary between the impact-related bedrock and the lacustrine succession is not sharp, but rather a transitional zone with an upward increasing portion of lacustrine material. Potassium and resistivity values are enhanced in the bedrock section.

In the lacustrine succession, a prominent U peak of unknown origin is visible at around 255 m b.l.f., and slightly enhanced Th and K values mark the Pliocene/Pleistocene transition. The core could be clustered into four different clusters (I to IV) down to approximately 262 m composite depth. The clusters show significant differences in terms of their TOC percentage, Si / Ti ratio and magnetic susceptibility, and in some cases also density. This allows plotting the clusters into a redox-condition vs. input-type diagram. In comparison with earlier studies we could conclude that cluster I contains glacial sediments, III and IV sediments from interglacials, and II comprises the sediments from super interglacial intervals.

Acknowledgements. We thank all expedition members of the El'gygytgyn pre-site surveys in 2000 and 2003 as well as of the deep drilling campaign in winter/spring 2009 for their excellent cooperation and support during work at the lake. Funding for this research was provided by the International Continental Scientific Drilling Program (ICDP), the US National Science Foundation (NSF), the German Federal Ministry of Education and Research (BMBF), Alfred Wegener Institute (AWI) and GeoForschungsZentrum Potsdam (GFZ), the Russian Academy of Sciences Far East Branch (RAS FEB), the Russian Foundation for Basic Research (RFBR), and the Austrian Federal Ministry of Science and Research (BMWF). The Russian GLAD 800 drilling system was developed and operated by DOSECC Inc., the downhole logging was performed by the ICDP-OSG, and LacCore, at the University of Minnesota, handled core curation. Financial support for the laboratory analyses was provided by the German Ministry of Education and Research (BMBF grants no. 03G0586B and no. 03G0642B) and the Deutsche Forschungsgemeinschaft (DFG grant no. GE-1924/1-1).

Edited by: J. Brigham-Grette

References

Anderson, R. F., Fleisher, M. O., and LeHuray, A. P.: Concentration, oxidation state, and particulate flux of uranium in the Black Sea, Geochim. Cosmochim. Acta, 53, 2215–2224, 1989.

Asikainen, C. A., Francus, P., and Brigham-Grette, J.: Sedimentology, clay mineralogy and grain-size as indicators of 65 ka of climate change from El'gygytgyn Crater Lake, Northeastern Siberia, J. Paleolimnol., 37, 105–122, doi:10.1007/s10933-006-9026-5, 2007.

Belyi, V. F.: Impactogenesis and volcanism of the El'gygytgyn depression, Petrology, 6, 96–110, 1998.

Best, A. I. and Gunn, D. E.: Calibration of marine sediment core loggers for quantitative acoustic impedance studies, Mar. Geol., 160, 137–146, 1999.

Brigham-Grette, J., Melles, M., Minyuk, P. S., Andreev, A. A., Tarasov, P., DeConto, R. M., König, S., Nowaczyk, N. R., Wennrich, V., Rosén, P., Haltia-Hovi, E., Cook, T. L., Gebhardt, A. C., Meyer-Jacob, C., Snyder, J., and Herzschuh, U.: Pliocene warmth, polar amplification, and stepped Pleistocene cooling recorded in NE Russia, Science, 340, 1421–1427, doi:10.1126/science.1233137, 2013.

Dansgaard, W., Johnsen, S. J., Clausen, H. B., Dahl-Jensen, D., Gundestrup, N. S., Hammer, C. U., Hvidberg, C. S., Steffensen, J. P., Sveinbjoernsdottir, A. E., Jouzel, J., and Bond, G. C.: Evidence for general instability of past climate from a 250-kyr ice-core record, Nature, 364, 218–220, 1993.

Fedorov, G., Nolan, M., Brigham-Grette, J., Bolshiyanov, D., Schwamborn, G., and Juschus, O.: Lake El'gygytgyn water and sediment balance components overview and its implications for the sedimentary record, Clim. Past Discuss., 8, 3977–4001, doi:10.5194/cpd-8-3977-2012, 2012.

Francke, A., Wennrich, V., Sauerbrey, M., Juschus, O., Melles, M., and Brigham-Grette, J.: Multivariate statistic and time series analyses of grain-size data in Quaternary sediments of Lake El'gygytgyn, NE Russia, Clim. Past Discuss., 9, 217–244, doi:10.5194/cpd-9-217-2013, 2013.

Fronval, T. and Jansen, E.: Late Neogene paleoclimates and paleoceanography in the Iceland-Norwegian Sea. Evidence from the Iceland and Vøring Plateaus, in: Proceedings of the Ocean Drilling Program, Scientific Results, edited by: Thiede, J., Myhre, A. M., Firth, J. V., Johnson, G. L., and Ruddiman, W. F., College Station, Texas, USA, 455–468, 1996.

Gebhardt, A. C., Niessen, F., and Kopsch, C.: Central ring structure identified in one of the world's best preserved impact craters, Geology, 34, 145–148, doi:10.1130/G22278.1, 2006.

Geotek: Multi-Sensor Core Logger, available at: http://www.geotek.co.uk/, last access: 13 August 2013, Geotek, 127 pp., 2000.

Glushkova, O. Y. and Smirnov, V. N.: Pliocene to Holocene Geomorphic Evolution and Paleogeography of the El'gygytgyn Lake region, NE Russia, J. Paleolimnol. Special Issue, 37, 37–47, doi:10.1007/s10933-006-9021-x, 2007.

Grootes, P. M., Stuiver, M., White, J. W. C., Johnsen, S. J., and Jouzel, J.: Comparison of oxygen isotope records from the GISP2 and GRIP Greenland ice cores, Nature, 366, 552–554, 1993.

Gurov, E. P., Gurova, E. P., and Rakitskaya, R. B.: Stishovite and coesite in shock metamorphosed rocks of the El'gygytgyn crater in Chukotka, Doklady Academii Nauk USSR, 248, 213–216, 1979a (in Russian).

Gurov, E. P., Valter, A. A., Gurova, E. P., and Kotlovskaya, F. I.: El'gygytgyn impact crater, Chukotka: Shock metamorphism of volcanic rocks (abs.), Lunar and Planetary Science, 10, 479–481, 1979b.

Harris, S. A.: Thermal history of the Arctic Ocean environs adjacent to North America during the last 3.5 Ma and a possible mechanism for the cause of the cold events (major glaciations and permafrost events), Prog. Phys. Geogr., 29, 1–19, 2005.

Herman, Y. and Hopkins, D. M.: Arctic Ocean climate in late Cenozoic time, Science, 209, 557–562, 1980.

Jansen, E., Fronval, T., Rack, F., and Channel, J. E. T.: Pliocene-Pleistocene ice rafting history and cyclicity in the Nordic Seas during the last 3.5 Myr, Paleoceanography, 15, 709–721, 2000.

Juschus, O., Melles, M., Gebhardt, A. C., and Niessen, F.: Late Quaternary mass movement events in Lake El'gygytgn, North-eastern Siberia, Sedimentology, 56, 2155–2174, doi:10.1111/j.1365-3091.2009.01074.x, 2009.

Koeberl, C., Pitarello, L., Reimold, U., Raschke, U., Brigham-Grette, J., Melles, M., and Minyuk, P.: El'gygytgyn impact crater, Chukotka, Arctic Russia: Impact cratering aspects of the 2009 ICDP drilling project, Meteor. Planet. Sci., 48, 1108–1129, doi:10.1111/maps.12146, 2013.

Layer, P.: $^{40}Ar/^{39}Ar$ age of the El'gygytgyn crater event, Chukotka, Russia, Meteor. Planet. Sci., 35, 591–599, 2000.

Lerman, A., Imboden, D., and Gat, J.: Physics and Chemistry of Lakes, 2nd Edn., Springer, Berlin Heidelberg, 334 pp., 1995.

Melles, M., Brigham-Grette, J., Glushkova, O. Y., Minyuk, P. S., Nowaczyk, N. R., and Hubberten, H.-W.: Sedimentary geochemistry of a pilot core from Lake El'gygytgyn – a sensitive record of climate variability in the East Siberian Arctic during the past three climate cycles, J. Paleolimnol. Special Issue, 37, 89–104, doi:10.1007/s10933-006-9025-6, 2007.

Melles, M., Brigham-Grette, J., Minyuk, P. S., Koeberl, C., Andreev, A. A., Cook, T. L., Fedorov, G., Gebhardt, A. C., Haltia-Hovi, E., Kukkonen, M., Nowaczyk, N. R., Schwamborn, G., Wennrich, V., and the El'gygytgyn Scientific Party: The Lake El'gygytgyn scientific drilling project – conquering Arcric challenges through continental drilling, Sci. Drill., 11, 29–40, doi:10.2204/iodp.sd.11.03.2011, 2011.

Melles, M., Brigham-Grette, J., Minyuk, P. S., Nowaczyk, N. R., Wennrich, V., DeConto, R. M., Anderson, P. M., Andreev, A. A., Coletti, A., Cook, T. L., Haltia-Hovi, E., Kukkonen, M., Lozhkin, A. V., Rosén, P., Tarasov, P., Vogel, H., and Wagner, B.: 2.8 million years of Arctic climate change from Lake El'gygytgyn, NE Russia, Science, 337, 315–320, doi:10.1126/science.1222135, 2012.

Minyuk, P., Brigham-Grette, J., Melles, M., Borkhodoev, V. Y., and Glushkova, O. Y.: Inorganic geochemistry of El'gygytgyn Lake sediments (northeastern Russia) as an indicator of paleoclimatic change for the last 250 kyr, J. Paleolimnol. Special Issue, 37, 123–133, doi:10.1007/s10933-006-9027-4, 2007.

Moran, K., Backman, J., Brinkhuis, H., Clemens, S. C., Cronin, T., Dickens, G. R., Eynaud, F., Gattacceca, J., Jakobsson, M., Jordan, R. W., Kaminski, M., King, J. W., Koc, N., Krylov, A., Martinez, N., Matthiessen, J., McInroy, D., Moore, T. C., Onodera, J., O'Regan, M., Pälike, H., Rea, B., Rio, D., Sakamoto, T., Smith, D. C., Stein, R., St John, K., Suto, I., Suzuki, N., Takahashi, K., Watanabe, M., Yamamoto, M., Farrell, J., Frank, M., Kubik, P., Jokat, W., and Kristoffersen, Y.: The Cenozoic

palaeoenvironment of the Arctic Ocean, Nature, 441, 601–605, doi:10.1038/nature04800, 2006.

Myhre, A. M., Thiede, J., Firth, J. V., Ahagon, N., Black, K. S., Bloemendal, J., Brass, G. W., Bristow, J. F., Chow, N., Cremer, M., Davis, L., Flower, B., Fronval, T., Hood, J., Hull, D., Koç, N., Larsen, B., Lyle, M., McManus, J., O'Connel, S., Ostermann, L. E., Rack, F. R., Sato, T., Scherer, R., Spiegler, D., Stein, R., Tadross, M., Wells, S., Williamson, D., Witte, B., and Wolf-Welling, T.: Proceedings of the Ocean Drilling Program, Initial Reports, Leg 151, Ocean Drilling Program, College Station, Texas, 926 pp., 1995.

NGRIP members: High-resolution record of Northern Hemisphere climate extending into the last interglacial period, Nature, 431, 147–151, 2004.

Niessen, F., Gebhardt, A. C., Kopsch, C., and Wagner, B.: Seismic investigation of the El'gygytgyn impact crater lake (Central Chukotka, NE Siberia): preliminary results, J. Paleolimnol. Special Issue, 37, 49–63, doi:10.1007/s10933-006-9022-9, 2007.

Nolan, M. and Brigham-Grette, J.: Basic hydrology, limnology, and meteorology of modern Lake El'gygytgyn, Siberia, J. Paleolimnol. Special Issue, 37, 17–35, doi:10.1007/s10933-006-9020-y, 2007.

Nolan, M., Liston, G., Prokein, P., Brigham-Grette, J., Sharpton, B., and Huntzinger, R.: Analysis of lake ice dynamics and morphology on Lake El'gygytgyn, NE Siberia, using SAR and Landsat, J. Geophys. Res., 107, 8162, doi:10.1029/2001JD000934, 2003.

Nowaczyk, N. R., Minyuk, P., Melles, M., Brigham-Grette, J., Glushkova, O., Nolan, M., Lozhkin, A. V., Stetsenko, T. V., Andersen, P. M., and Forman, S. L.: Magnetostratigraphic results from impact crater Lake El'gygytgyn, northeastern Siberia: a 300 kyr long high-resolution terrestrial palaeoclimatic record from the Arctic, Geophys. J. Int., 150, 109–126, 2002.

Nowaczyk, N. R., Melles, M., and Minyuk, P.: A revised age model for core PG1351 from Lake El'gygytgyn, Chukotka, based on magnetic susceptibility variations correlated to northern hemisphere insolation variations, J. Paleolimnol. Special Issue, 37, 65–76, doi:10.1007/s10933-006-9023-8, 2007.

Nowaczyk, N. R., Haltia, E. M., Ulbricht, D., Wennrich, V., Sauerbrey, M. A., Rosén, P., Vogel, H., Francke, A., Meyer-Jacob, C., Andreev, A. A., and Lozhkin, A. V.: Chronology of Lake El'gygytgyn sediments, Clim. Past Discuss., 9, 3061–3102, doi:10.5194/cpd-9-3061-2013, 2013.

Raschke, U., Reimold, W., Zaag, P., Pitarello, L., and Koeberl, C.: Lithostratigraphy of the impactite and bedrock section in ICDP drill core D1c from the El'gygytgyn impact crater, Russia, Meteor. Planet. Sci., submitted, 2012.

Repenning, C. A. and Brouwers, E. M.: Mid-Pliocene to Late Pleistocene changes in the Arctic Ocean borderland ecosystem, Program with Abstracts, 251, INQUA, Ottawa, 1987.

Ruffell, A. and Worden, R.: Palaeoclimate analysis using spectral gamma-ray data from the Aptian (Cretaceous) of southern England and southern France, Palaeogeography Palaeoclimatology Palaeoecology, 155, 265–283, 2000.

Sauerbrey, M. A., Juschus, O., Gebhardt, A. C., Wennrich, V., Nowaczyk, N. R., and Melles, M.: Mass movement deposits in the 3.6 Ma sediment record of Lake El'gygytgyn, Far East Russian Arctic: classification, distribution and preliminary interpretation, Clim. Past Discuss., 9, 467–505, doi:10.5194/cpd-9-467-2013, 2013.

Schnyder, J., Ruffell, A., Deconinck, J.-F., and Baudin, F.: Conjunctive use of spectral gamma-ray logs and clay mineralogy in defining late Jurassic-early Cretaceous palaeoclimate change (Dorset, U. K.), Palaeogeogr.Palaeocli. Palaeoecol., 229, 303–320, doi:10.1016/j.palaeo.2005.06.027, 2006.

Svensson, A., Bigler, M., Kettner, E., Dahl-Jensen, D., Johnsen, S., Kipfstuhl, S., Nielsen, M., and Steffensen, J. P.: Annual layering in the NGRIP ice core during the Eemian, Clim. Past Discuss., 7, 749–773, doi:10.5194/cpd-7-749-2011, 2011.

Wennrich, V., Minyuk, P. S., Borkhodoev, V., Francke, A., Ritter, B., Raschke, U., Nowaczyk, N. R., Schwamborn, G., Brigham-Grette, J., Melles, M., and El'gygytgyn Scientific Party: Pliocene to Pleistocene climate and environmental history of Lake El'gygytgyn/NE Russia based on high-resolution inorganic geochemistry data, in preparation, 2013.

Wonik, T.: Gamma-ray measurements in the Kirchrode I and II boreholes, Palaeogeogr. Palaeocli. Palaeoecol., 174, 97–105, 2001.

6 A Late Glacial to Holocene record of environmental change from Lake Dojran (Macedonia, Greece)

Journal article (2013):
Francke, A., Wagner, B., Leng, M. J., and Rethemeyer, J.: A Late Glacial to Holocene record of environmental change from Lake Dojran (Macedonia, Greece), Clim. Past, 9, 481-498, 10.5194/cp-9-481-2013, 2013.

Clim. Past, 9, 481–498, 2013
www.clim-past.net/9/481/2013/
doi:10.5194/cp-9-481-2013

Climate of the Past
Open Access

A Late Glacial to Holocene record of environmental change from Lake Dojran (Macedonia, Greece)

A. Francke[1], B. Wagner[1], M. J. Leng[2,3], and J. Rethemeyer[1]

[1]University of Cologne, Institute for Geology and Mineralogy, Cologne, Germany
[2]University of Leicester, Department of Geology, Leicester, LE1 7RH, UK
[3]NERC Isotope Geosciences Laboratory, British Geological Survey, Nottingham, NG12 5GG, UK

Correspondence to: A. Francke (alexander.francke@uni-koeln.de)

Received: 12 November 2012 – Published in Clim. Past Discuss.: 21 November 2012
Revised: 31 January 2013 – Accepted: 4 February 2013 – Published: 28 February 2013

Abstract. A Late Glacial to Holocene sediment sequence (Co1260, 717 cm) from Lake Dojran, located at the boarder of the F.Y.R. of Macedonia and Greece, has been investigated to provide information on climate variability in the Balkan region. A robust age-model was established from 13 radiocarbon ages, and indicates that the base of the sequence was deposited at ca. 12 500 cal yr BP, when the lake-level was low. Variations in sedimentological (H_2O, TOC, $CaCO_3$, TS, TOC/TN, TOC/TS, grain-size, XRF, $\delta^{18}O_{carb}$, $\delta^{13}C_{carb}$, $\delta^{13}C_{org}$) data were linked to hydro-acoustic data and indicate that warmer and more humid climate conditions characterised the remaining period of the Younger Dryas until the beginning of the Holocene. The Holocene exhibits significant environmental variations, including the 8.2 and 4.2 ka cooling events, the Medieval Warm Period and the Little Ice Age. Human induced erosion processes in the catchment of Lake Dojran intensified after 2800 cal yr BP.

1 Introduction

Although several paleoenvironmental records spanning the entire Holocene already exist from the Balkan region (e.g., Bordon et al., 2009; Wagner et al., 2009; Vogel et al., 2010a; Peyron et al., 2011; Panagiotopoulos et al., 2012), some suffer from poor radiocarbon chronologies (Wagner et al., 2009; Vogel et al., 2010a), or are inconsistent in terms of spatial variability and short-term climate events (Magny et al., 2003, 2009; Tzedakis, 2007; Berger and Guilaine, 2009). Furthermore, significant anthropogenic impact at least since the late Holocene (e.g., Willis, 1994; Wagner et al., 2009; Aufgebauer et al., 2012; Panagiotopoulos et al., 2012) complicates the reconstruction of climate change in the Balkan region (Vogel et al., 2010a). Additional records with high-resolution sedimentary information from this region are needed to get a better understanding of Late Glacial to Holocene climatic variability and anthropogenic activity and their spatial variability. As shown by a comparison of records from lakes Prespa and Ohrid (Leng et al., 2010; Wagner et al., 2010), shallower lakes often react more sensitive to environmental change. Hence, we can assume that Lake Dojran with a maximum water depth < 7 m provides a valuable record of climatic change and anthropogenic impact at the Balkan region.

Lake Dojran is located at the boarder of the Former Yugoslav Republic of Macedonia (FYROM) and Greece (Fig. 1). A lake-level lowering of 6 m between 1955 and 2000 was mainly caused by irrigation and canalisation of the former outlet, River Doiranitis (Griffiths et al., 2002; Zacharias et al., 2002; Sotiria and Petkovski, 2004; Manley et al., 2008). This lake level decrease led to eutrophication and is well recorded in the chemical, biological and stable isotope data of the surface sediments (Veljanoska-Sarafiloska et al., 2001; Griffiths et al., 2002). Increasing anthropogenic influence at Lake Dojran from the mid to late Holocene has been inferred from pollen assemblages in sediment cores recovered close to the lakeshore (Athanasiadis et al., 2000). However, the sediments are poorly dated and there were likely variations in the sedimentation rates including major hiatuses, probably due to significant lake level changes, particularly in the lateral coring locations.

Published by Copernicus Publications on behalf of the European Geosciences Union.

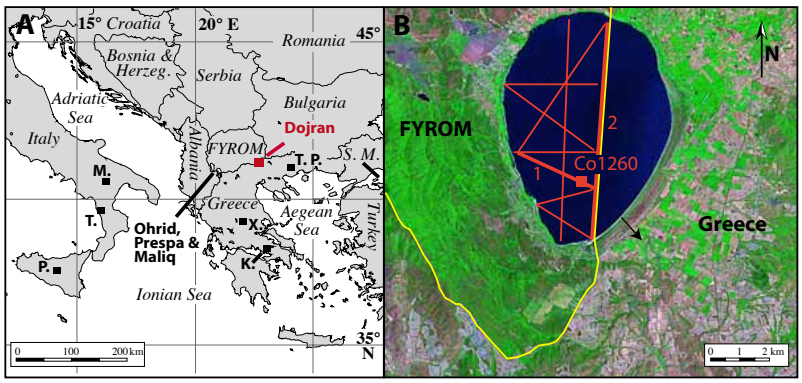

Fig. 1. (A) Locations of Lake Dojran in the northeastern Mediterranean region at the boarder of the Former Yugoslav Republic of Macedonia (FYROM) and Greece. Locations of other paleoclimate records in the region are lakes Ohrid, Prespa, and Maliq, Lake Xinias (X), Lake Kopais (K.), Lago Grande di Monticchio (M.), Lago di Trifoglietti (T.), Lago di Pergusa (P.), Tenaghi Philippon (T.P.), and the Sea of Marmara (S.M.). **(B)** Satellite image of Lake Dojran with the coring location Co1260 (red square) and the hydro-acoustic profiles. Numbers 1 and 2 mark the hydro-acoustic profiles shown in Fig. 2, the black arrow indicates the position of the former outlet River Doiranitis, and the yellow line shows the border between FYROM and Greece.

2 Site descriptions

Lake Dojran (Fig. 1, 41°12′ N, 22°44′ E) is considered to be a relict of the Plio-Pleistocene Peonic Lake, which was formed by volcanic and tectonic activities (Cvijic, 1911; Stojanov and Micevski, 1989). Lake Dojran is located at 144 m a.s.l. (above sea level) in a carstic depression formed by Paleozoic marble intercalated with phylites (Stojanov and Micevski, 1989). The lake catchment predominantly comprises Paleozoic mica gneiss, muscovite-gneiss and amphibolite, Tertiary volcanic and volcanic-sedimentary rocks, and Quaternary alluvial and limnic sediments (Stojanov and Micevski, 1989; Sotiria and Petkovski, 2004). Only 18 % of the total catchment area of 275 km^2 exceeds an elevation of 500 m a.s.l. The high-elevated regions are in the northeast of Lake Dojran, where the Belisca Mountain range is up to 1870 m a.s.l. high (Sotiria and Petkovski, 2004). Small rivers, creeks and groundwater drain the catchment area and feed Lake Dojran, particularly during winter and spring (Griffiths et al., 2002; Sotiria and Petkovski, 2004). The former outlet of Lake Dojran, River Doiranitis, which connected the lake to the Axios/Vardar River, is located some metres above the present lake-level. Current water loss from Lake Dojran is due to evaporation and probably to groundwater outflow.

The climate at Lake Dojran is influenced by the Mediterranean Sea via the connection of the Thessaloniki Plain, continental influences and local morphology, leading to a warmer climate with less days with frost compared to other regions in Macedonia (Sotiria and Petkovski, 2004). The mean annual air temperature was +14.3 °C between 1961 and 2000, with monthly average summer and winter temperatures of +26.1 and +3.7 °C, respectively (Sotiria and Petkovski, 2004). The highest proportion of the annual precipitation (612 mm) falls during mild winters (Sotiria and Petkovski, 2004), and dry conditions persist during warm summers.

In 2004, Lake Dojran had a lake water surface area of 40 km^2 with water depths between 3 and 4 m (Sotiria and Petkovski, 2004). However, there are seasonal and longer-term progressive changes that affected the surface area and water depth (cf. Athanasiadis et al., 2000; Manley et al., 2008). Thermal stratification occurs during the summer months (Zacharias et al., 2002), and it is presumed that lake water mixing occurs during winter, similar to Lake Prespa (Matzinger et al., 2006). Due to its location in the carstic depression, Lake Dojran is bicarbonate- and chloride-rich, alkaline and productive (Stankovic, 1931; Griffiths et al., 2002). Today, the littoral area of the lake comprises a fringe of up to 30 m wide reed beds.

3 Material and methods

3.1 Fieldwork

Fieldwork at Lake Dojran was carried out in June 2011. A hydro-acoustic survey (Innomar SES-2000 compact, 10 kHz) on the Macedonian part of the lake (Fig. 1) was used to provide more detailed information on the lake bathymetry and the sediment architecture. At coring location Co1260 (41°11.703′ N, 22°44.573′ E) undisturbed, horizontal bedded sediments and a water depth of ∼6.6 m were observed (Fig. 2). Core Co1260 was recovered from a floating platform using a gravity corer for undisturbed surface sediments and a percussion piston corer for deeper sediments (both UWITEC Co., Austria). After recovery, the overlapping 300 cm long sediment cores were cut into (and up to)

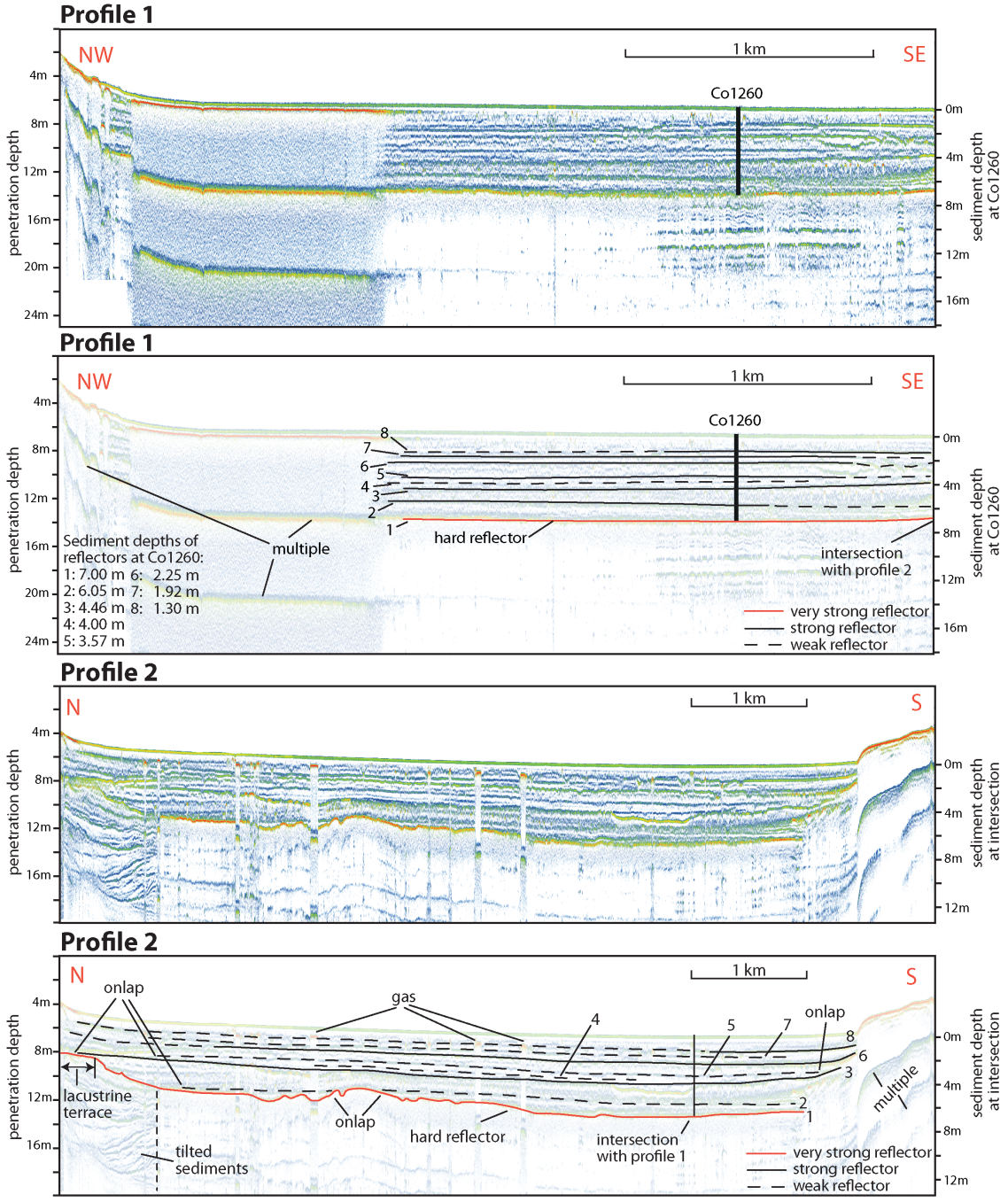

Fig. 2. Un-interpreted and interpreted hydro-acoustic profiles 1 and 2. For location see Fig. 1. The bars to the left indicates depths below lake surface, those to the right depths below sediment surface at the coring location Co1260 (profile 1) or the intersection (profile 2) between the two profiles. The length of the black bar at the coring location Co1260 corresponds to the core length.

100 cm long sections. Core catcher samples were transferred at 2 cm resolution in plastic vials.

3.2 Analytical work

In the laboratory, the cores were split into two halves and one half was sealed airtight for archiving. On the other half, X-Ray Fluorescence (XRF) scanning was carried out in 2 mm resolution with an ITRAX core scanner (Cox Analytical Systems, Sweden), equipped with a Cr-tube and a Si-drift detector in combination with a multi-channel analyser. Voltage and amperage were set to 30 kV and 30 mA, respectively. The measured count rates can be used as semi-quantitative estimates of relative concentrations of the detected elements (Croudace et al., 2006). Inaccuracies in comparison to conventional XRF analyses rise due to different resolutions and variations in grain-size, porosity, water content and surface structure of the core.

The sediments were then subsampled in 2 cm intervals and half of each sample, including those from the core catchers, was freeze-dried. The water content was calculated from the weight loss after freeze-drying. Approximately 1 g of the dry sediment was treated with hydrochloric acid (HCl), hydrogen peroxide (H_2O_2), sodium hydroxide (NaOH), and $Na_4P_2O_7$ for grain-size analysis (8 cm resolution) of terrigenous clastic material. Grain-size measurements were carried out with a Saturn DigiSizer 5200 laser particle analyser and a Master Tech 52 multisampler (Micromeritics Co., USA) after one minute of ultrasonic treatment. The data processing of each sample was based on three runs and the GRADISTATv8 programme (Blott and Pye, 2001).

An aliquot of the freeze-dried samples was ground to $< 63\,\mu$m and homogenised for biogeochemical analysis (2 cm resolution). Total nitrogen (TN) and total sulfur (TS) were determined with a Vario Micro Cube combustion CNS elemental analyser (ELEMENTAR Co., Germany). Total carbon (TC) and total inorganic carbon (TIC) were measured with a DIMATOC 200 (DIMATEC Co., Germany). The calcite content ($CaCO_3$) was calculated by multiplying the TIC with 8.33 and total organic carbon (TOC) was determined by subtracting TIC from TC.

Isotope studies included modern lake and spring waters (O, H, C isotopes) and wet sediment samples (O, C isotopes) at 4 cm resolution. For O isotope composition of modern lake and spring water, the water was equilibrated with CO_2 using an Isoprep 18 device for oxygen isotope analysis with a VG SIRA mass spectrometry. A EuroPyrOH-3110 system based on an on-line Cr reduction method was used for hydrogen isotope analysis. For C isotope analysis of total dissolved inorganic carbon (TDIC), the inorganic carbon was precipitated during the field work from ca. 85 mL water using ca. 15 mL of NaOH-$BaCl_2$. In the laboratory, the precipitated barium carbonate ($BaCO_3$) was washed with deionized water. For isotope analyses, CO_2 was extracted from $BaCO_3$ with anhydrous phosphoric acid (H_3PO_4) under vacuum and the isotopes were analysed using a VG Optima dual inlet mass spectrometer.

For inorganic carbon and oxygen isotope analysis of endogenic calcite, horizons with more than 1 % TIC were bleached with sodium hypochlorite (NaOCl), neutralised and sieved to 80 μm. After the $< 80\,\mu$m fraction was ground, the extraction of gaseous CO_2 and the subsequent measurement followed that described above for TDIC.

Samples for organic carbon isotope analysis were treated with HCl to remove $CaCO_3$, neutralised, filtered to 20 μm and the supernatant was dried at 50 °C. After the $> 20\,\mu$m fraction was ground and homogenised, it was combusted by an Elemental Analyzer (Costech Co., USA) on-line to a VG TripleTrap and Optima dual-inlet mass spectrometer. $CaCO_3$ adjusted TOC content was determined by the elemental analyser. Modern water and sediment isotopic ratios are reported as per mill (‰) deviations from the VSMOW (O and H water) and VPDB (O, C barium carbonate, calcites; C organics) scales.

Radiocarbon dating on bulk sediment samples, terrestrial plant material, charcoal and biogenic carbonates were carried out by accelerator mass spectrometry (AMS) at the University of Cologne Centre for AMS (Germany) and the ETH Laboratory of Ion Beam Physics in Zurich (Switzerland). Previously, sample pre-treatment and graphitisation was carried out according to Rethemeyer et al. (2013). Organic carbon from bulk sediment, terrestrial plant material and charcoal samples was chemically extracted by acid-alkali-acid extraction (AAA). The alkali extraction was omitted for small samples sizes to avoid loss of sample material. Combustion and graphitisation was carried out with a Vario Micro Cube elemental analyser (ELEMENTAR Co., Germany) coupled to a graphitisation system, where the CO_2 is converted to graphite with hydrogen over iron as catalyst. The surface of biogenic carbonates was leached with 1 M H_2SO_4 and the carbonate sample was subsequently converted to CO_2 by hydrolysis with 99 % H_3PO_4 under He. CALIB 6.1.1 (Stuiver and Reimer, 1993) and the IntCal09 dataset (Reimer et al., 2009) were used for conversion of the conventional radiocarbon ages into calendar ages (cal yr BP) on an uncertainty level of 2σ. Based on the calibrated ages a polynomial age model was established and sedimentation rates were calculated.

4 Results and discussion

4.1 Hydro-acoustic survey

From the hydro-acoustic survey, profiles 1 and 2 were selected to show the bathymetry and sediment architecture of Lake Dojran (Fig. 2). The bottom morphology of Lake Dojran is relatively simple, with a mean water depth of ca. 6.6 m and slightly inclining slopes towards the shores (Fig. 2).

The maximum penetration depth of the hydro-acoustic signal only sporadically exceeds 7 m sediment depth. One of the spots with deeper penetration is close to the northern shore, where onlap structures and tilted sedimentation below ca. 7 m sediment depth suggest tectonic activity (Fig. 2, profile 2). In the central basin, a hard reflector occurs at 7 m. This reflector is close to the surface multiple, but has a more undulated shape, particularly in the northern part of the basin. In addition, the multiple in the central basin is slightly deeper, as observed in spots, where hyperbolic reflections with transparent areas underneath indicate the occurrence of gas. At coring location Co1260, parallel, but somewhat undulated reflectors particularly below 7 m imply sediment thickness of at least ∼ 13.4 m and do not indicate underlying bedrock. Below this depth, the reflectors are too weak or are overlain by multiples (Fig. 2). The undulated shape of the hard reflector at 7 m (reflector 1) and the weaker reflections below suggest somewhat disturbed sedimentation as it might have occurred during a lake level lowstand. A terrace in the northern part of the lake (Fig. 2, profile 2) probably represents a paleo-shoreline. The hard reflector at coring location Co1260 is overlain by reflector 2 at 6.05 m sediment depth, which indicates onlap structures to the hard reflector in the central to northern part of the lake and close to the terrace (profile 2, Fig. 2). Reflector 3 (4.46 m) indicates onlap structures only at the terrace close to the northern shore (Fig. 2). Reflector 4 (4.00 m) pinches out in central areas of the lake and suggests minor lake level fluctuations or the occurrence of lake internal currents, such as observed in Lake Prespa (Wagner et al., 2012). Reflectors 5 (3.57 m) and 6 (2.25 m) span almost the entire lake basin and were likely formed when the lake level was higher. Reflector 7 (1.92 m) pinches out again, whilst reflector 8 (1.30 m) can be observed in marginal parts of the lake and, thus, indicates a somewhat higher lake-level.

4.2 Lithostratigraphy and biogeochemistry

Based on visual core description, XRF data and water content, the correlation of the overlapping segments of core Co1260 led to a composite profile of 717 cm length, which has been subdivided into four lithofacies (Fig. 3).

Lithofacies 1 (717 to 658 cm) is grey, has a low water content and a crumbly structure due to a high abundance of clay clasts. The sediment is poorly sorted, mainly with coarse silt with sporadic drop stones. Aquatic or terrestrial macrophyte remains are not apparent, and the amount of finely dispersed organic material (OM) is low, as indicated in TOC < 1 % and TS < 0.5 %. TOC/TN varies between 3 and 12 and suggests that OM is mainly of aquatic origin, however, ratios < 4 can be associated with selective decomposition of TOC (Leng et al., 1999). A high TOC/TS in the lowermost 17 cm of lithofacies 1 indicates well-oxygenated bottom water conditions and surface sediments (cf. Müller, 2001; Wagner et al., 2009). The $CaCO_3$ content of lithofacies 1 varies between 5 and 20 %, and is mainly derived from endogenic calcite, as shown by SEM (Fig. 4). Additional sources of $CaCO_3$ include ostracodes and shells or shell fragments of bivalves, such as at ∼ 664 cm depth. Post-sedimentary dissolution of calcite can be excluded at least for the upper part of lithofacies 1 (ca. 682–658 cm), because the sediments contain well-preserved ostracodes (determined F. Viehberg). Potassium (K) and iron (Fe) counts from XRF analyses, which can be associated with clastic sediment supply (Cohen, 2003; Arnaud et al., 2005), are low, but might be an artifact of the crumbly structure of the core surface. The lowermost section of lithofacies 1, where $CaCO_3$ is < 9 % and the mean grain size is highest (Fig. 3), corresponds to the hard reflector (reflector 1) in the hydro-acoustic profiles at 7 m sediment depth.

Lithofacies 2 (658 to 520 cm) is grey to olive grey, has an increasing water content and a massive structure. The grain-size composition is dominated by medium to very coarse silt, which indicates high transport energy due to low water depths or high inflow. Sporadic fine sand lenses are interpreted as ice rafted detritus (IRD). Lithofacies 2 has been sub-divided into lithofacies 2a (658 to 590 cm) with fine-grained sediments, relatively high OM and TOC/TN and lithofacies 2b (590 to 520 cm) with coarser sediments, lower OM and TOC/TN. Similar patterns of TOC and TS suggest that TS derives mainly from OM, however, a low TOC/TS and a good correlation between TOC/TS and Fe throughout lithofacies 2 suggest that TS is partly derived from pyrite (Wagner et al., 2006, 2009). Plant remains or carbonate fossils are not apparent in lithofacies 2a and 2b. The transition of lithofacies 2a to 2b likely corresponds to reflector 2 (6.05 m) in the hydro-acoustic profiles.

Lithofacies 3 (520 to 265 cm) is olive grey, has a water content between 55 and 70 %, and a massive or marbled structure. Grain-size is dominated by medium and coarse silt. A TOC increase from around 1 % at the base to ca. 3 % at the top implies decreasing decomposition or increasing lake productivity, which is, however, only partly reflected in small variations in TOC/TN. Increasing lake productivity is better indicated in $CaCO_3$ of up to 40 %, which anti-correlates with K and Fe counts. The variations in $CaCO_3$, K, and Fe counts form the sub-division of lithofacies 3 (Fig. 3). Lithofacies 3a (520 to 401 cm) is massive or marbled and has high $CaCO_3$ and low K counts. Shell fragments and well-preserved *Dreissena* bivalves occur sporadically between 505 and 404 cm and are more common at 503 and 404 cm (Fig. 3). In the lower part of lithofacies 3a (520 to 460 cm) TS increases to 1 %. SEM analyses showed a high abundance of pyrite (Fig. 4), although this does not correlate with Fe counts, which probably indicates that Fe is bound in other chemical compounds above and below the TS increase. Lithofacies 3b (401 to 390 cm) is massive, has minimum $CaCO_3$, which is anti-correlated with K and Fe counts, and has a maximum in grain-size distribution. In lithofacies 3c (390 to 265 cm), which is also massive, $CaCO_3$ increases to around 40 % at 350 cm, before it drops to negligible values at the

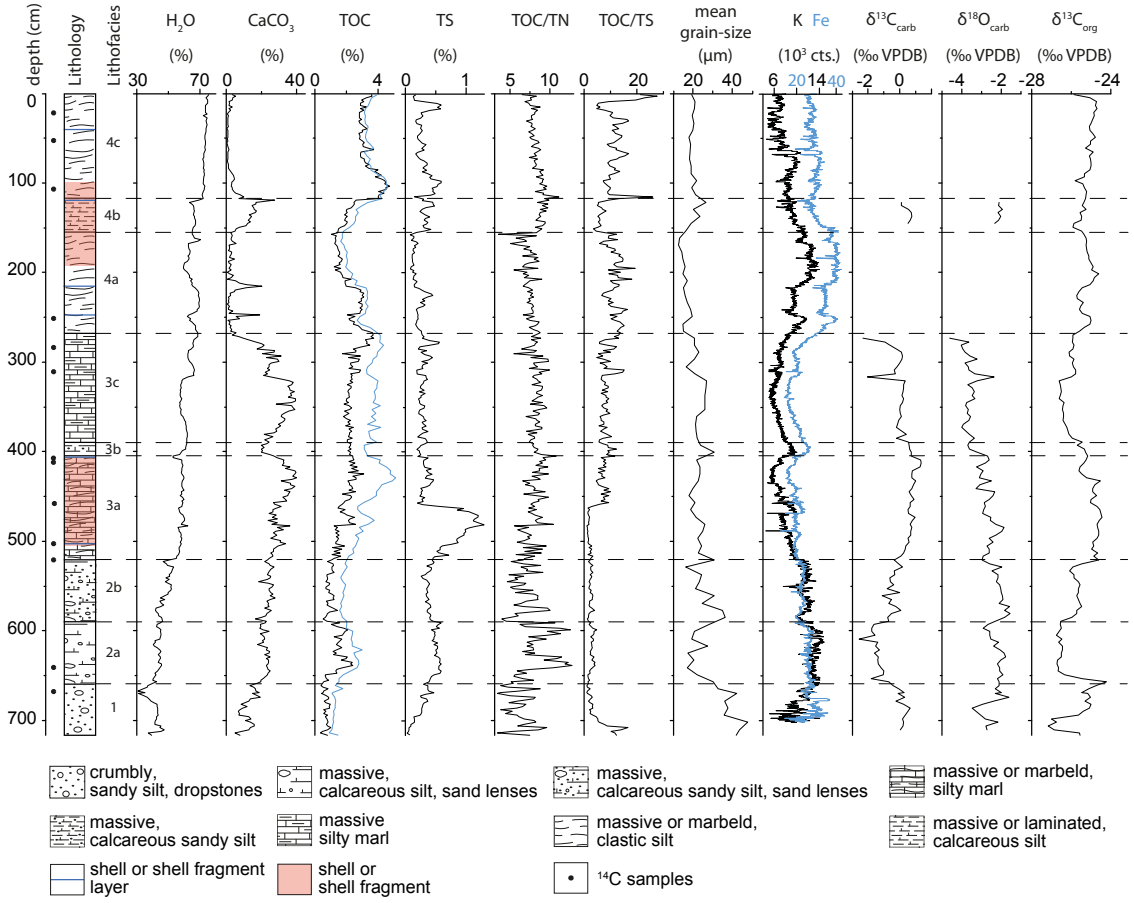

Fig. 3. Positions of ^{14}C samples (black dots), lithology, lithofacies, water content, calcite ($CaCO_3$), TOC (black line) and $CaCO_3$ adjusted TOC (blue line), TS, TOC/N, TOC/TS, mean grain-size, Potassium (K, black line) and Iron (Fe, blue line) counts, $\delta^{13}C_{carb}$, $\delta^{18}O_{carb}$ and $\delta^{13}C_{org}$ of core Co1260.

top. Although the $CaCO_3$ content is similar to lithofacies 3a, shell and shell fragments are absent. The decrease of $CaCO_3$ at the top of this sub-lithofacies correlates with increasing K and Fe counts and a decrease of the mean grain-size from ca. 310 cm. The change in sedimentary characteristics in lithofacies 3 are also reflected in the hydro-acoustic data, as reflector 3 (4.46 m) corresponds with the upper limit of the TS peak, and reflectors 4 (4.00 m) and 5 (3.57 m) represent distinct change in mean grain size (Fig. 3).

Lithofacies 4 (265 to 0 cm) is dark olive brown to dark olive black, has a water content of 60 to 76 % and a massive, marbled, or laminated structure. Medium and coarse silt dominate the grain-size composition. A high abundance of shell fragments and some well-preserved *Dreissena* bivalves occur between 195 and 100 cm. $CaCO_3$ is in general low, but shows some distinct peaks, where shells or shell fragments occur (Fig. 3). The occurrence of these shell layers seems to be irregular, as a layer of well-preserved *Dreissena* bivalves was found at 32 cm in one core segment, but did not occur in the overlapping segment. Variations in sediment structure, colour, associated $CaCO_3$ and OM allow a sub-division of lithofacies 4. Lithofacies 4a occurs between 265 and 152 cm, is characterised by a massive or marbled structure, a dark olive brown colour, a low $CaCO_3$, and decreasing trends in TOC content and TOC/TN. The mean grain size is the lowest for the entire sequence, whereas K and Fe reach maximum counts. This suggests pelagic sedimentation and a low productivity, or dilution by relatively high clastic input. Low productivity is confirmed by low TS and high TOC/TS, implying good mixing of the water column and potentially additional decomposition of OM. $CaCO_3$ dissolution can be excluded, as ostracodes are well preserved. Lithofacies 4b, from 152 to 116 cm, is massive or irregularly laminated, has a dark olive grey to very dark

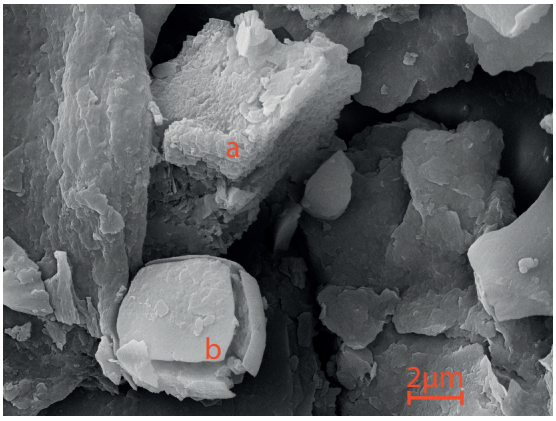

Fig. 4. SEM photos of bulk sediment from 137 cm depth in core Co1260 showing endogenic calcite ($CaCO_3$, **a**) and pyrite (FeS_2, **b**). The broken structure of the pyrite is probably due to sample pre-treatment and heating to 50 °C.

brown colour, a relatively high $CaCO_3$, TS and TOC/TN, mean grain size and a relatively low TOC/TS. TOC increases throughout lithofacies 4b. Lithofacies 4c comprises the uppermost 116 cm of core Co1262 and is massive, with a dark olive brown colour. Some faint black laminations occur between 18 and 8 cm, where a peak in TS occurs. While $CaCO_3$ is negligible, TOC is the highest of the entire core. The mean grain size is constant around 20 μm, but K and Fe counts show some distinct fluctuations in the uppermost ca. 60 cm. Distinct change in sedimentological characteristics of lithofacies 4 can be correlated with the reflectors in the hydroacoustic profile (Fig. 2). Reflector 6 (2.25 m) coincides with a broad maximum in TOC and water content, reflector 7 (1.92 m) is, where the maximum in K and Fe counts can be observed and reflector 8 (1.3 m) marks the maximum in mean grain size and $CaCO_3$.

The overall massive to marbled structure of the entire sediment succession suggests bioturbation. This is confirmed by a relatively high abundance ostracodes in the sediments. The occurrence of the ostracode *Darwinula stevensoni* (determined F. Viehberg), which was observed in sandy groundwater-influenced sediments (Meisch, 2000), substantiates that Lake Dojran is influenced by an aquifer.

4.3 Isotope record

$\delta^{18}O_{water}$ and δD_{water} of samples from springs, which enter Lake Dojran, plot close to the global meteoric water line (GMWL, Fig. 5, Table 1). $\delta^{18}O_{water}$ and δD_{water} of modern lake water have higher values and plot on a local evaporation line (LEL). The isotope data also show that the evaporation of the lake water was lower in 2011 compared to 1997 (cf. Griffiths et al., 2002), which corresponds with an increasing lake-level in the last few years. Because the present lake level of Lake Dojran is below the outlet, the data also imply that aquifers play an important role in the water balance. Similarly to the water isotopes (O, D), $\delta^{13}C_{TDIC}$ of total dissolved inorganic carbon (TDIC) in the lake has higher values than the marginal springs (Table 1), most likely due a long residence time enabling the dissolved bicarbonates to exchange with isotopically heavier atmospheric CO_2. This is a common feature in lakes, in which the water isotope geochemistry is dominated by evaporation (Leng and Marshall, 2004; Leng et al., 2012).

In core Co1260, the sediments from lithofacies 1 and 4 with TIC < 1 % could not be analysed for carbon isotopic composition (Fig. 3). The rest of core Co1260 shows moderate fluctuations in $\delta^{18}O_{carb}$ between −4.6 and −1.2 ‰. These moderate values with relatively low variability (ca. 3 ‰) suggest that the lake has not experienced complete hydrologic closure during the deposition of these sequences (cf. Roberts et al., 2008). Variations in $\delta^{18}O_{carb}$ can be caused by changes in the isotopic composition of precipitation (linked to source and/or temperature variation), in the precipitation/evaporation (P/E) ratio, or in the lake water residence time (cf. Roberts et al., 2008; Leng et al., 2012). $\delta^{13}C_{carb}$ varies between −3.2 and +1.4 ‰, with the lowest values in lithofacies 2a and at the top of lithofacies 3c. These low values are probably due the greater contribution of soil derived CO_2 or decomposition of OM relative to the amount of carbon from the carst and the atmosphere (cf. Leng et al., 2010).

The pattern of $\delta^{13}C_{org}$, with values between −27.1 to −24.2 ‰, corresponds only partly with $\delta^{13}C_{carb}$. Therefore, TDIC cannot be the only carbon pool for OM in the Lake Dojran sediments, which suggests that variations in $\delta^{13}C_{org}$ could also derive from change in allochthonous versus autochthonous OM deposition.

4.4 Chronology

The age model for core Co1260 is based on 13 radiocarbon ages and cross correlation with other lacustrine sediment cores from the Balkan region (Table 2, Fig. 6).

Seven samples, composed of terrestrial plant material and charcoal, provide a robust basis for the age model. However, there is an age reversal in samples COL 1320.1.1 (460.9 cm, 10 820 ± 420 cal yr BP) and COL 1321.1.1 (521.9 cm, 10 660 ± 440 cal yr BP, Table 2). Both samples are of terrestrial plant material and originate from the same core section, but sample COL 1320.1.1 was probably dislocated during opening of the cores, as it was found on the surface of the core halves. In contrast, sample COL 1321.1.1 was from the inner part of one of the core halves and is, therefore, considered to provide the accurate age.

In addition to the terrestrial plant samples, 2 bulk organic carbon and 3 carbonate samples were used for the establishment of the age-depth model. Bulk organic carbon,

Table 1. Modern isotope data of spring and lake water as standard deviations from VSMOW (O, H isotopes) and VPDB (TDIC), collected in June 2011 (own data) and in September 1997 (Griffiths et al., 2002).

location	collection	$\delta^{18}O_{water}$ (‰ VSMOW)	δD_{water} (‰ VSMOW)	$\delta^{13}C_{TDIC}$ (‰ VPDB)
spring	June 2011	−9.51	−62.8	−11.6
spring	June 2011	−8.08	−50.5	−13.0
lake center	June 2011	−0.91	−13.0	−5.9
lake margin	June 2011	−0.86	−13.3	−4.7
lake margin	June 2011	−0.86	−13.1	−4.8
spring	September 1997	−7.9	−50.4	−7.9
lake center	September 1997	+2.0	+1.1	+0.2
lake margin	September 1997	+2.1	+1.9	+0.6

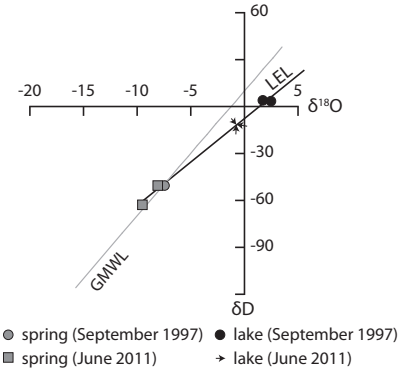

Fig. 5. The modern isotope composition ($\delta^{18}O_{water}$ and δD_{water}) from water of Lake Dojran and from marginal springs. The samples were collected in September 1997 (Griffiths et al., 2002) and in June 2011 (see also Table 1). Arrows mark the lake water samples from June 2011 because they plot very close to each other in the *x*-*y* plot. The lake water samples fall away from the Global Meteoric Water Line (GMWL) and plot on a Local Evaporation Line (LEL).

carbonate and terrestrial plant material samples can be influenced by reservoir effects, i.e., incorporation of fossil/old organic matter from bedrocks or other sources not in equilibrium with atmospheric $^{14}CO_2$ (Cohen, 2003 and references therein; Ramsey, 2008 and references therein). Terrestrial plant material in general is regarded to provide most reliable ages, as it is not or only marginally affected by the incorporation of aquatic carbon. However, in the record from Tenaghi Philippon pollen grains and peat indicated a significant reservoir effect (Pross et al., 2009). Bulk organic carbon and carbonate shell samples are more influenced by reservoir effects and have to be regarded more critically, particularly because reservoir effects can vary over time. This was also shown in the records from lakes Prespa and Ohrid (Vogel et al., 2010b; Aufgebauer et al., 2012). A low reservoir effect is suggested by the small age difference of COL 1312.1.1 (bulk organic carbon: 140 ± 140 cal yr BP) at 16.5 cm depth, a terrestrial plant residue from 53.3 cm (COL 1324.1.1: 410 ± 110 cal yr BP), and the sediment surface. Samples from 502.9 cm (ETH 449571.1, carbonate: 11 250 ± 60 cal yr BP) and 521.9 cm depth (COL 1321.1.1, terrestrial plant: 10 660 ± 440 cal yr BP) suggest a reservoir effect of several hundred years. The large difference between bulk organic C and carbonate ages at 635 and 682 cm depth (ETH 46615.1.1: 11 920 ± 310 cal yr BP and ETH 44958.1.1: 32 830 ± 650 cal yr BP) could indicate an even higher reservoir effect. On the other hand, a high TOC/TN of sample ETH 46615.1.1 indicates a predominantly terrestrial origin and suggest that the age of this sample could be reliable and that sample ETH 44958.1.1 is probably re-deposited. Redeposition can also be assumed for the shell fragment sample at 404.9 cm (ETH 44956.1.1; 7350 ± 80 cal yr BP). This sample is significantly younger than the 2 cm underlying terrestrial plant fragment COL 1319.1.1 (8960 ± 440 cal yr BP) and there was no lithological indication for a hiatus or a distinct change in sedimentation rates. However, the age of sample COL 1319.1.1 is also somewhat questionable, as this sample has a very low carbon weight (0.28 mg), and the calendar age is located on a ^{14}C plateau. A small reservoir effect can also not be excluded, as a minimum in $CaCO_3$ at 397 cm depth in core Co1260 likely corresponds with the 8.2 ka cooling event, such as observed in nearby lakes Prespa and Ohrid (Wagner et al., 2009, 2010; Vogel et al., 2010a; Aufgebauer et al., 2012).

For the polynomial interpolation of the age depth model of core Co1260, the sediment surface was adjusted to −61.5 cal yr BP and 6 terrestrial plant material samples, the charcoal sample, the two bulk organic carbon samples, and the cross-correlation point at the 8.2 ka cooling event were included (Table 2, Fig. 6). The calculated age model of core Co1260 yields a basal age of ca. 12 500 cal yr BP. According to the established age model, the sedimentation rate of core Co1260 is high at the bottom and the top of the core and low between 390 and 330 cm sediment depth (Fig. 6).

Table 2. Radiocarbon and calendar ages from core Co1260. The calibration of radiocarbon ages into calendar ages is based on Calib 6.1.1 (Stuiver and Reimer, 1993) and INTCAL09 (Reimer et al., 2009) and on a 2σ uncertainty.

AMS Lab ID	core depth (cm)	material	C weight (mg)	^{14}C age (yr BP)	calendar age (cal yr BP)
COL 1312.1.1	16.5	bulk organic C	0.44	140 ± 35	140 ± 140
COL 1324.1.1	53.3	terrestrial plant	0.45	360 ± 70	410 ± 110
COL 1314.1.1	111.3	terrestrial plant	0.32	840 ± 70	790 ± 120
COL 1194.1.1	253.0	terrestrial plant	1.00	2430 ± 30	2520 ± 170
COL 1316.1.1	287.3	terrestrial plant	1.00	3080 ± 30	3290 ± 80
COL 1317.1.1	309.1	charcoal	1.00	3560 ± 40	3850 ± 130
ETH 44956.1.1	404.9	carbonate	1.01	6410 ± 40	7350 ± 80
COL 1319.1.1	406.4	terrestrial plant	0.28	8020 ± 150	8960 ± 440
COL 1320.1.1	460.9	terrestrial plant	0.63	9520 ± 160	10 820 ± 420
ETH 44957.1.1	502.9	carbonate	1.00	9840 ± 40	11 250 ± 60
COL 1321.1.1	521.9	terrestrial plant	0.90	9330 ± 160	10 660 ± 440
ETH 46615.1.1	635.0	bulk organic C	1.00	10 220 ± 70	11 920 ± 310
ETH 44958.1.1	682.0	carbonate	0.48	28 570 ± 170	32 830 ± 650

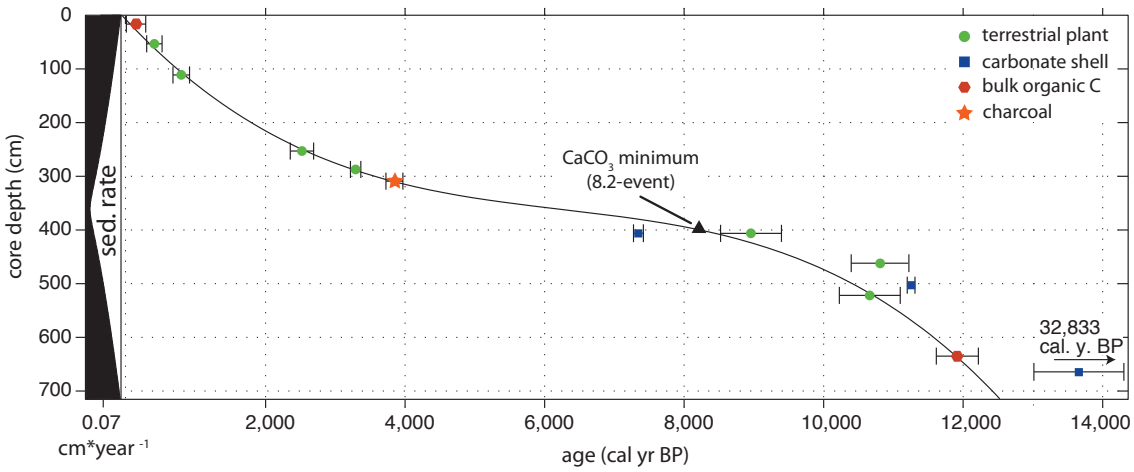

Fig. 6. Age-depth model of core Co1260 based on 13 calibrated radiocarbon ages derived from terrestrial plant material, charcoal, carbonates and bulk organic C samples. Additionally, the 8.2 ka cooling event described from lakes Ohrid and Prespa (Wagner et al., 2009, 2010; Vogel et al., 2010a; Aufgebauer et al., 2012) was correlated with the minimum in $CaCO_3$ at 397 cm depth (see Fig. 3). Sample ETH 44958.1.1 from 682.0 cm depth, which has an age of 32 830 ± 650 cal yr BP, was most likely re-deposited. The sedimentation rate was calculated from the polynomial age-depth model.

5 Interpretation

5.1 Late Glacial (12 500 to 11 500 cal yr BP)

The Late Glacial part of core Co1260 is represented by deposits of lithofacies 1 and 2a (717–590 cm) and covers the period between 12 500 and 11 500 cal yr BP (Figs. 3 and 7).

The deposits of lithofacies 1 between 717 and 658 cm represent the period 12 500 to 12 100 cal yr BP. The high abundance of clay clasts, which are most likely formed under subaerial conditions, implies that the deposits were formed to a certain amount from redeposited lacustrine material. This is confirmed by the undulated morphology of reflector 1, which corresponds to the lower 17 cm of lithofacies 1, and by the occurrence of the shell fragment with an age of 32 830 ± 650 cal yr BP at 682 cm depth. Low lake level, redeposition, and intensive wave action are also indicated by a high mean grain-size and the overall poor sorting. The poor sorting is enhanced by the occurrence of drop stones from ice floe transport. As drop stones do not occur in the surface sediments of Lake Dojran and the modern lake is only occasionally covered by ice (Zacharias et al., 2002), winter temperatures during the deposition of lithofacies 1 must have been lower than today. Lower temperatures are also

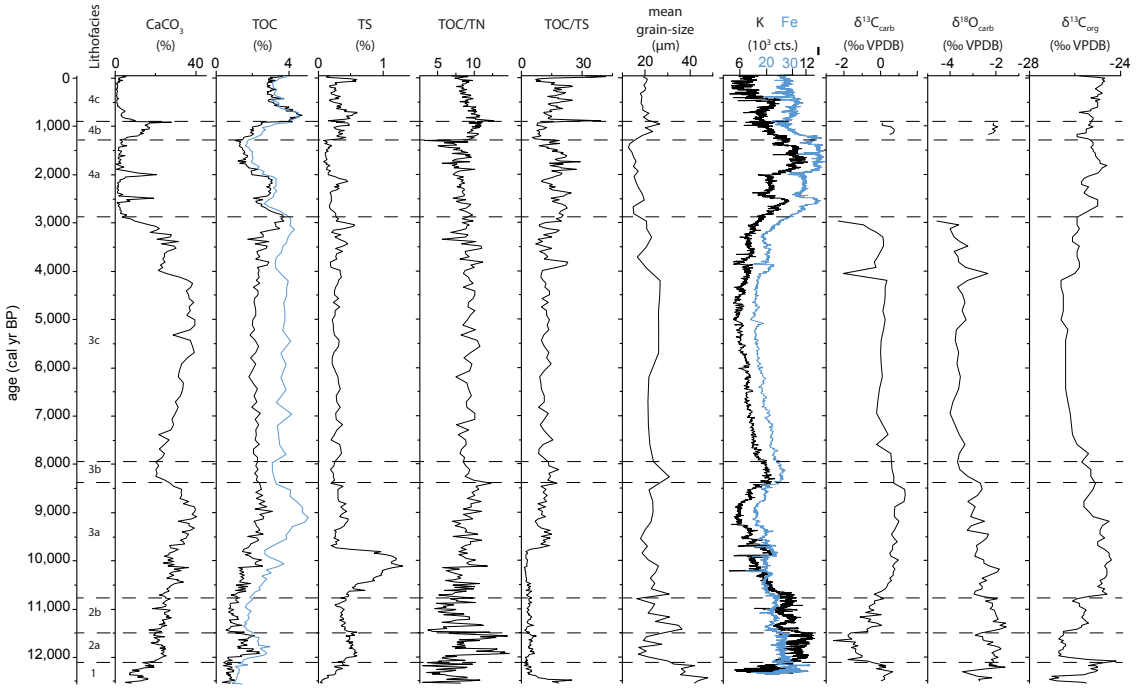

Fig. 7. Lithofacies, calcite ($CaCO_3$), TOC (black line) and $CaCO_3$ adjusted TOC (blue line), TS, TOC/N, TOC/TS, mean grain-size, Potassium (K, black line) and Iron (Fe, blue line) counts, $\delta^{13}C_{carb}$, $\delta^{18}O_{carb}$, and $\delta^{13}C_{org}$ of core Co1260 plotted versus age.

suggested by the relatively low OM and $CaCO_3$. In the modern lake, low lake levels during relatively warm conditions correspond with periods of algal blooms and eutrophication (cf. Griffiths et al., 2002). Intensive macrophyte growth, such as often occurs during low lake levels (cf. Coops et al., 2003; Beklioglu et al., 2006), is also not evident in lithofacies 1. However, there are some smaller fluctuations in OM and $CaCO_3$, which indicate minor variations in local temperatures or lake level. A minimum of $\delta^{13}C_{org}$ and a maximum in TOC/TN suggest increased allochthonous OM input at this time. A low lake level could have promoted the degradation of OM, particularly in the lowermost 17 cm of lithofacies 1, where a high TOC/TS indicates higher oxygen supply to the surfaces sediments. Relatively low $\delta^{18}O_{carb}$ values until 12 250 cal yr BP and subsequent higher values at the top of lithofacies 1 imply increased evaporation and correspond to a subtle finer grain-size distribution. A higher lake level could reduce the wave action at Co1260 and enlarge the surface area of the lake water, while the water volume would only increase marginally due to the flat-bottomed nature of Lake Dojran. Greater surface area promotes more evaporation of the lake water. Overall, the sedimentary characteristics imply cold and dry conditions between 12 500 to 12 100 cal yr BP.

The deposits of lithofacies 2a from 658 to 590 cm depth represent the period 12 100 to 11 500 cal yr BP. The environmental conditions during this period are difficult to disentangle. The absence of clay clasts and a lower mean grain size imply less re-deposition, low wave action, and a higher lake level. A slightly higher lake level is confirmed by the onlap structures of reflector 2 (Fig. 2). Fine sand lenses, which are interpreted as IRD, indicate that the lake was still ice covered during winter. A relatively high sediment supply, probably from increased inflow by rivers or creeks, is indicated by increased K and Fe counts between 12 100 and 11 500 cal yr BP. Enhanced erosion and input of soil derived CO_2 is also suggested by low $\delta^{13}C_{carb}$, as a low TOC/TS suggests that oxidation of OM was negligible. Higher OM and $CaCO_3$ content during this period indicate enhanced productivity and slightly higher summer temperatures and more humid conditions. Unstable environmental conditions between 12 100 and 11 500 cal yr BP are indicated by two maxima in OM and TOC/TN and slight minima in $\delta^{13}C_{org}$ at 11 900 and 11 560 cal yr BP, which are probably caused by increased allochthonous nutrient supply. The interspersed minimum in OM between 11 800 and 11 600 cal yr BP corresponds to low TOC/TN and implies a short period of less allochthonous nutrient supply and reduced water inflow from rivers or creeks. The $\delta^{18}O_{carb}$ decrease between 11 800 and 11 500 cal yr BP probably corresponds with an isotopic depletion at the end of the Younger Dryas, which is described

from various lacustrine isotope records from the Mediterranean region and indicates increasing humidity (Roberts et al., 2008 and references therein).

Overall cold and dry climate between 12 500 and 11 500 cal yr BP at Lake Dojran can be attributed to the Younger Dryas, when 6 °C lower temperatures and arid conditions with 50 % less annual precipitation compared to modern conditions are reported from the northern Aegean region (Kotthoff et al., 2008a, 2011), the Sea of Marmara (Valsecchi et al., 2012), and from other terrestrial records in Italy (Allen et al., 2002), Macedonia (Bordon et al., 2009; Panagiotopoulos et al., 2012), and Greece (Digerfeldt et al., 2000; Lawson et al., 2004). However, the cold and dry climate during the Younger Dryas is barely visible in geochemical and hydrological data from lakes Prespa and Ohrid (Fig. 8). This is probably due to the long lake water residence time in Ohrid (Leng et al., 2012) and lower winter temperatures and moisture deficits, which have only minor effects on lake internal processes (Vogel et al., 2010a; Aufgebauer et al., 2012; Panagiotopoulos et al., 2012). Lake Dojran with its low volume to large surface area is likely more sensitive to hydrological change. The transition from a low lake level and low temperatures during the formation of lithofacies 1 towards higher a lake level and warmer temperatures during the sedimentation of lithofacies 2a at Lake Dojran around 12 100 cal yr BP corresponds well with marine records from the western Mediterranean Sea and the North Atlantic, and with terrestrial archives from the Iberian Peninsula and northwest Europe (Cacho et al., 2001 and references therein). Furthermore, the transition might correspond to a decrease in salinity in the Levantine Basin and the Ionian Sea after 12 000 cal yr BP (cf. Emeis et al., 2000). However, a separation in two phases such as indicated by Co1260 is not evident in other terrestrial records from Greece or in marine pollen records from the Aegean Sea and the Sea of Marmara (Rossignol-Strick, 1993; Digerfeldt et al., 2000; Lawson et al., 2004, 2005; Kotthoff et al., 2008a, 2011; Valsecchi et al., 2012). At least the particular dry phase described from the northern Aegean region around 11 800 cal yr BP (Kotthoff et al., 2008a, 2011) corresponds with the low OM content and low TOC/TN ratios in Co1260 between 11 800 and 11 600 cal yr BP.

5.2 Early Holocene (11 500 to 7900 cal yr BP)

The deposits of lithofacies 2b, 3a and 3b (590–390 cm) in core Co1260 represent the early Holocene between 11 500 and 7900 cal yr BP (Figs. 3 and 7).

Lithofacies 2b (590–520 cm) covers the period 11 500 to 10 700 cal yr BP. The sporadic occurrence of sand lenses indicates that the winter temperatures at Lake Dojran remained low. Low winter temperatures during the early Holocene are also reported from Lake Ohrid and are explained by southward movement of cold polar air during winter seasons (Vogel et al., 2010a; Wagner et al., 2010).

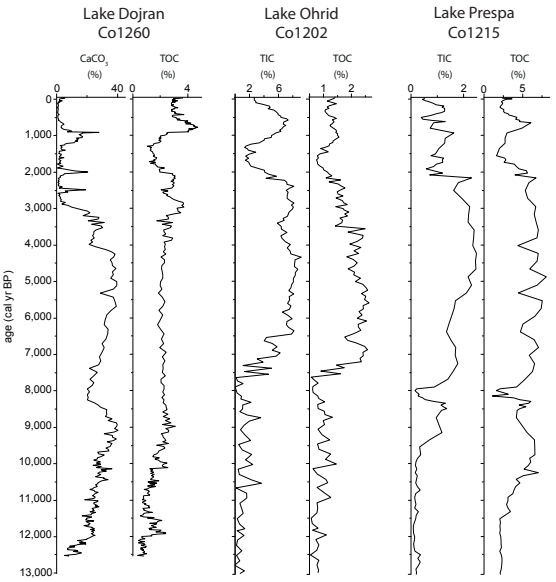

Fig. 8. $CaCO_3$ and TOC of core Co1260 from Lake Dojran in comparison to $CaCO_3$ and TOC content from lakes Ohrid (Vogel et al., 2010a) and Prespa (Aufgebauer et al., 2012) during the last 13 000 cal yr BP.

Although the occurrence of the sand lenses leads to distinct variations in grain-size distribution, the overall coarser sediments suggest relatively high transport energy at coring location Co1260. The high transport energy is most likely due to stronger inflow and not triggered by a lake-level low stand, because clay clasts are absent and there is no indication for a very low lake level in the hydro-acoustic profile (Fig. 2). A constant $CaCO_3$ along with lower allochthonous clastic and organic sediment input, indicated by lower K, Fe, TOC/TN, and higher $\delta^{13}C_{org}$, implies somewhat lower productivity in the lake, which corresponds with lower TOC. Thereby, the higher $\delta^{13}C_{org}$ are probably rather a result of less allochthonous OM than of more productivity. The discrepancy between relatively high inflow and low erosion can be explained by the development of a dense vegetation cover in the catchment, such as observed around lakes Prespa and Maliq to the west (Bordon et al., 2009; Aufgebauer et al., 2012; Panagiotopoulos et al., 2012) and the Aegean region to the south and southeast (Kotthoff et al., 2008a). Extensive reed beds in the littoral areas of Lake Dojran could have also restrained allochthonous clastic supply by filtering and organic sediment supply by nutrient consumption (cf. Yin and Lan, 1995; Wang et al., 2002). This could have limited the productivity in the lake center although temperatures increased rapidly in the Mediterranean region during the early Holocene (Allen et al., 1999; Bordon et al., 2009; Kotthoff et al., 2011). Despite more humid conditions as

indicated by our data, the low TOC/TS implies oxygen depletion in the bottom waters and stratification of the lake during summer. Summer stratification was probably promoted by higher summer temperatures in the early Holocene, such as reported from various records in the central and eastern Mediterranean region (e.g., Allen et al., 1999; Lawson et al., 2004; Kotthoff et al., 2008a; Vogel et al., 2010a; Peyron et al., 2011; Aufgebauer et al., 2012). Increased humidity in the early Holocene conflicts with the high $\delta^{18}O_{carb}$ values, which would normally be interpreted as indicating a low P/E ratio. Enhanced evaporation, however, is enabled by a higher lake level when this is accompanied by an increasing lake water surface area especially in lakes like Dojran, which is located in a flat-bottomed basin (cf. Leng et al., 2005; Hernández et al., 2008). A large surface area also promotes greater exchange of TDIC with atmospheric CO_2 and, therefore, tends to lead to both higher $\delta^{13}C_{TDIC}$ and $\delta^{13}C_{carb}$ as seen in lithofacies 2b.

In lithofacies 3a (520–401 cm), which covers the period 10 700 to 8300 cal yr BP, the grain-size distribution is dominated by medium and coarse silt, but is less variable due to the lack of fine sand lenses. The lack of the sand lenses indicates that the lake was not significantly covered by ice during winter. The decreasing $\delta^{18}O_{carb}$ after 10 200 cal yr BP could be associated with a greater through flow due to further increasing humidity. This corresponds with increasing moisture in southern Italy until 9400 cal yr BP (Joannin et al., 2012), but in particular with increasing $\delta^{18}O_{carb}$ after 9400 cal yr BP at Lake Prespa, which was explained by increasing summer wetness (Leng et al., 2010). Despite this increasing humidity during the early Holocene, which incidentally coincides partly with the formation of sapropel 1a between ca. 10 000 and 8200 cal yr BP in the Mediterranean Sea (Emeis et al., 2000; Mercone et al., 2000; Kotthoff et al., 2008b; Schmiedl et al., 2010), K and Fe imply decreasing catchment erosion until 9000 cal yr BP. Less input from the catchment could be due to denser vegetation in the littoral areas and catchment, which while filtering clastic material might cause greater delivery of more allochthonous OM to the lake, as indicated by increasing TOC/TN. Another explanation for increasing allochthonous OM supply could be as a result of lake level increase and flooding of the shallow, reed bed-covered littoral parts of the lake. This is indicated by reflector 3 in the seismic data, which is the oldest reflector that covers the lacustrine terrace in the northern part of profile 2 (Fig. 2). The flooded shallow lake parts would have formed suitable habitats for Mollusca, which probably explains the high abundance of shells and shell fragments in lithofacies 3a. The increase in lake surface and volume was apparently correlated with a distinct change in redox conditions, such as indicated in the TS peak and the shift of TOC/TS. The larger surface could have led to higher wind fetch and, thus, a better mixing of the water column after 9500 cal yr BP. More nutrient and allochthonous OM supply from the flooded parts likely promoted productivity in the lake, and can be inferred from a minimum of $\delta^{13}C_{org}$ and maxima in $CaCO_3$ adjusted TOC and $CaCO_3$ around 9000 cal yr BP. Decreasing $CaCO_3$ and $CaCO_3$ adjusted TOC contents after 8700 cal yr BP suggests decreasing lake productivity, which goes along with increasing erosion, such as indicated by increasing K and Fe.

In lithofacies 3b from 401 to 390 cm, which covers the period 8300 to 7900 cal yr BP, the coarser grain-size distribution implies relatively high transport energy. Increased transport energy is probably due to a lower lake level and increased wave action, which is indicated by the pinching out of the hydro-acoustic reflector 4 in the central area of the lake. A low lake level implies dry conditions at Lake Dojran, which is, however, inconsistent with low $\delta^{18}O_{carb}$. Potential explanations for the lower $\delta^{18}O_{carb}$ are a smaller surface area, which reduces evaporation, or increasingly lower $\delta^{18}O$ of rainfall from the Atlantic (Zanchetta et al., 2007a) or eastern Mediterranean origin (cf. Develle et al., 2010). Despite the presumed arid conditions, high K and Fe imply enhanced clastic sediment supply and erosion in the catchment, which is probably associated with a less dense vegetation cover in the catchment. Less dense vegetation could have reduced the availability and supply of allochthonous OM to the lake as suggested by low TOC/TN and high $\delta^{13}C_{org}$, and could also be triggered by lower temperatures. This is also suggested by subtly lower TS and higher TOC/TS, indicating less pronounced thermal stratification and improved oxygen supply to the surface sediments. Furthermore, low $CaCO_3$ and $CaCO_3$ adjusted TOC contents in lithofacies 3b imply low productivity, such as also reported from lakes Prespa and Ohrid (Wagner et al., 2009, 2010; Vogel et al., 2010a; Aufgebauer et al., 2012). The low temperatures are most likely associated with the 8.2 ka cooling event, which covers a broad period in Mediterranean paleoclimate records varying between 8500 and 8000 cal yr BP (e.g., Magny et al., 2003 and references therein; Rohling and Palike, 2005; Berger and Guilaine, 2009 and references therein). The 8.2 ka cooling is associated with an interruption of the sapropel 1 formation in the Mediterranean Sea (e.g., Kotthoff et al., 2008b; Schmiedl et al., 2010; Siani et al., 2012) and a hydrological tripartition of Europe. Whilst wet conditions have predominated between 43 to 50° N, dry conditions persisted north and south of this corridor (Magny et al., 2003), which is in line with low lake level and dry conditions at Lake Dojran. Pollen analyses from Lake Maliq (Bordon et al., 2009) and Tenaghi Philippon (Peyron et al., 2011) suggest that the dryness is predominantly due to restricted winter precipitation.

5.3 Mid-Holocene (7900 to 2800 cal yr BP)

The deposits of lithofacies 3c from 390 to 265 cm of core Co1260 represent the mid-Holocene between 7900 and 2800 cal yr BP (Figs. 3 and 7).

The finer and relatively stable grain-size distribution at least until 4300 cal yr BP implies lower wave action, a high

lake level, and humid conditions with only minor fluctuations and more inflow. A relatively high lake level between 7900 and 4300 cal yr BP is also suggested by reflector 5 (3.57 m, around 6000 cal yr BP) in the hydro-acoustic data (Fig. 2). The onlap structures to reflector 3 in the lateral parts of the lake imply that the lake level did not exceed that of the early Holocene. A high lake level until around 6000 cal yr BP could correlate with the formation of S1b (Emeis et al., 2000; Mercone et al., 2000; Kotthoff et al., 2008b; Schmiedl et al., 2010). The broad maxima in $CaCO_3$ and mean grain-size between ca. 6000 and 4300 cal yr BP correlates with a minimum in K and Fe and suggests slightly increased productivity, slightly reduced lake level and lower supply of clastic material. This is likely correlated to warmer temperatures and more arid conditions during the mid-Holocene, such as observed in other paleoclimate records in the Mediterranean region (e.g., Wick et al., 2003; Kotthoff et al., 2008a,b; Roberts et al., 2008; Wagner et al., 2009; Leng et al., 2010; Vogel et al., 2010a; Aufgebauer et al., 2012; Joannin et al., 2012). The shift from more humid to more arid conditions at Lake Dojran was only moderate, as OM, TS, TOC/TS, TOC/TN, $\delta^{13}C_{org}$, and $\delta^{18}O_{carb}$ in core Co1260 are relatively stable between 7900 and 4300 cal yr BP. In addition, the stable $\delta^{18}O_{carb}$ during this period suggests that the atmospheric circulation pattern was relatively stable and that there was no distinct shift in the origin of rainfall. Low and stable $\delta^{18}O_{carb}$ during the mid-Holocene is a common feature in central Mediterranean isotope lake sediment records, although there are some differences in the exact timing (e.g., Zanchetta et al., 2007b; Roberts et al., 2008; Develle et al., 2010; Leng et al., 2012 and references therein).

Between 4300 and 2800 cal yr BP, more fluctuations and a distinct change in some of the proxies suggest greater instability during a period of gradual environmental change at Lake Dojran. A minimum in mean grain-size and a peak in $\delta^{18}O_{carb}$ around 4000 cal yr BP suggest low inflow, dry conditions and/or ^{18}O enriched rainfall for a short period. This period coincides with low lake productivity, as indicated by $CaCO_3$ adjusted TOC and $CaCO_3$. Low productivity is likely caused by low temperatures, as low TOC/TS imply less intensive thermal stratification. Restricted nutrient availability is less likely, as increasing K and Fe counts imply increasing clastic supply and erosion in the catchment. The short period of low temperatures and arid conditions around 4000 cal yr BP is most likely associated with the 4.2 ka cooling event, which has been described in other records from the Mediterranean region (e.g., Bar-Matthews et al., 1999; Weiss and Bradley, 2001; Magny et al., 2009; Wagner et al., 2009; Vogel et al., 2010a). The 4.2 ka cooling event in the Mediterranean region corresponds to low lake levels in North Africa and the Near East, which is explained by a weak African monsoon (Kotthoff et al., 2008a and references therein; Magny et al., 2009). In addition, a positive NAO (North Atlantic Oscillation) index favours cold and dry conditions in the Mediterranean region by reduced moisture availability of Atlantic origin and cold polar air outbreaks from the Siberian high (Lamy et al., 2006; Magny et al., 2009). Subsequent to the 4.2 ka cooling event, increasing K and Fe and a higher mean grain size imply higher erosion in the catchment, stronger inflow and more humid conditions. More humid conditions between 3950 and 3800 cal yr BP are also reported from the central and western Mediterranean regions (Magny et al., 2009). Erosion processes could also have been promoted by human induced deforestation, as pollen analyses indicate first permanent settlements at Lake Dojran during this period (Athanasiadis et al., 2000). The anthropogenic deforestation was probably intensified until ca. 2800 cal yr BP as indicated by increasing K and Fe and decreasing $\delta^{13}C_{carb}$, the latter one is a proxy for enhanced soil derived CO_2 or enhanced remineralisation of OM in the lake. The enhanced clastic sedimentation coincides with decreasing $CaCO_3$. Comparable human-induced modifications of the environmental setting and the sedimentological properties around the same time are also reported from Lake Prespa (Aufgebauer et al., 2012; Panagiotopoulos et al., 2012) and Lake Ohrid (Wagner et al., 2009; Vogel et al., 2010a, Fig. 8).

5.4 Late Holocene (2800 cal yr BP to present)

The deposits of lithofacies 4 (265–0 cm) in core Co1260 represent the late Holocene between 2800 cal yr BP and today (Figs. 3 and 7).

In lithofacies 4a (265 to 152 cm), which covers the period 2800 to 1200 cal yr BP, the decreasing mean grain-size indicates declining inflow and a decreasing lake level. A decreasing lake level is also suggested by the hydro-acoustic data, where reflector 6 (2.25 m) occurs in lateral parts of the lake, whereas the overlaying reflector 7 (1.92 m) pinches out in these parts (Fig. 2). Relatively arid conditions in the Mediterranean region during the late Holocene are also reported from other records, including Lake Prespa (Schilman et al., 2001; Roberts et al., 2008 and references therein; Joannin et al., 2012; Leng et al., 2012; Siani et al., 2012). A lower lake level at Lake Dojran could have resulted in a relative enlargement of shallow lake areas covered by reed beds. The reed beds likely restricted the productivity in the lake (low TOC, $CaCO_3$ and TS), as they retain the supply of allochthonous OM and nutrients (decreasing TOC/TN, high $\delta^{13}C_{org}$). The reed beds, however, did not lead to less supply of clastic material (high K, Fe and sedimentation rates), probably because human-induced wood clearance and anthropogenic impact in the catchment increased (cf. Athanasiadis et al., 2000), as it is also reported from other records in the eastern and northeastern Mediterranean region (Willis, 1994; Denèfle et al., 2000; Kotthoff et al., 2008a; Bordon et al., 2009; Panagiotopoulos et al., 2012; Valsecchi et al., 2012). A lower lake level could also have promoted the occurrence of shells and shell redeposition (Bially and Macisaac, 2000) by greater exposure of the shell beds to wave action. This assumption is supported

by high abundances of shells or shell fragments in upper parts of lithofacies 4a. The low lake level is also indicated in a distinct shift of sedimentation rates in a sediment core from the lateral parts of the lake (Athanasiadis et al., 2000). This shift is likely caused by a hiatus, when lateral parts of the lake became sub-aerially exposed. Despite the anthropogenic overprint, the period between 2800 to 1200 cal yr BP apparently was characterised by a slight cooling, which resulted in reduced thermal stratification as suggested by relatively high TOC/TS.

In lithofacies 4b (152 to 116 cm), which covers the period from 1200 to 900 cal yr BP, the coarser mean grain-size implies higher transport energy, which is probably associated with more inflow and humid conditions and a higher lake level. The higher lake level is also indicated by the occurrence of the hydro-acoustic reflector 8 in lateral parts of Lake Dojran. A lower proportion of reed likely covered the lateral parts of the lake leading to a reduced filter effect and enhanced supply of allochthonous OM, as seen in high TOC/TN and lower $\delta^{13}C_{org}$. Flooding of reed-covered areas would have enlarged the surface area of the lake, which would again promote the exchange of TDIC with atmospheric CO_2, such as suggested by the high $\delta^{13}C_{carb}$. The enlarged surface area also intensified summer evaporation, as indicated by high $\delta^{18}O_{carb}$. The gradual increase of OM and $CaCO_3$ is likely due to higher lake productivity, and could be additionally caused by declining anthropogenic activities, less erosion and supply (dilution) of clastic material from the catchment. A similar observation was made at Lake Prespa and explained by a denser vegetation cover between 1500 and 600 cal yr BP (Aufgebauer et al., 2012). Lake productivity was likely promoted by a warmer climate associated with the Medieval Warm Period (cf. Crowley and Lowery, 2000), which resulted in an intensification of the thermal stratification during summer and in high TS, low TOC/TS and the faintly laminated structures in lithofacies 4b.

In lithofacies 4c (116 to 0 cm), which covers the period from 900 cal yr BP until today, the subtle finer grain-size distribution suggests lower transport energy, inflow and lake level. Significant lake level fluctuations, such as that reported from lakes Prespa and Ohrid (Matzinger et al., 2006; Wagner et al., 2009; Vogel et al., 2010a; Aufgebauer et al., 2012), are not recorded in Lake Dojran. We can assume that anthropogenic impact affected the lake hydrology and the catchment dynamics of Lake Dojran significantly during this period. Nevertheless, reduced precipitation of $CaCO_3$ along with high OM implies high productivity, but low temperatures subsequent to the Medieval Warm Period. Low temperatures are also indicated by high TOC/TS in lithofacies 4c, which implies restricted thermal stratification during summer. The colder temperatures after the Medieval Warm Period are also observed in other records from the Balkan areas and are commonly attributed to the Little Ice Age (Wagner et al., 2009; Vogel et al., 2010a; Aufgebauer et al., 2012). The lake level lowstand of Lake Dojran about 2–3 decades ago, when the maximum water depths was < 4 m, is not obvious in the sediment record. The only hint for the lake level lowstand could come from a sub-surface peak in TS. The lake level lowstand was likely caused by a combination of dry climate and by high water use for irrigation, which likely promoted the eutrophication, as shown by the increasing TOC and $CaCO_3$ in the upper few centimetres of core Co1260 and confirmed by other surface sediment cores (Griffiths et al., 2002).

6 Conclusions

The investigation of the sediment architecture of Lake Dojran and sediment properties of core Co1260 provides valuable information on climate variability and human impact in the Balkan region. As Lake Dojran is a relatively shallow lake for its size, paleoclimatic change and human interactions seem to have had a significant impact on lake hydrology, allochthonous supply of OM and clastic material, and lake productivity. The shallow morphology of Lake Dojran causes greater evaporation of the lake water when lake levels are relatively high and supports that reed beds in littoral areas of the lake are apparently crucial for in-lake processes, as these reed beds consume nutrients from the catchment and reduce lake internal productivity. The following interpretations, based on analysis of the data presented here, for climate variability and human impact from the Lake Dojran sediment sequence can be drawn for the Late Glacial and Holocene:

Cold and dry conditions with low productivity and a low lake-level persisted between 12 500 to 12 100 cal yr BP and are followed by slightly higher temperatures and more humid conditions with subtle enhanced productivity and a higher lake level until 11 500 cal yr BP. This entire period is attributed to the Younger Dryas. Similarly to the western, contrasting findings from the eastern Mediterranean region and the northern high latitudes, the Younger Dryas can be separated into an early cold and dry early period followed by a warmer and more humid later period.

During the early Holocene (11 500 to 8300 cal yr BP), temperatures increased, though nutrient availability and productivity in the lake were restricted until 10 700 cal yr BP. This is likely due to the impact of filtering of the inflow through littoral reed beds. More humid conditions and higher lake level coincide with the formation of sapropel 1 (S1a) in the marine realm and improved the nutrient supply to the lake by more runoff and smaller reed beds. Highest productivity occurred around 9000 cal yr BP and implies a thermal maximum in the region. Lake level lowering and lower productivity between 8300 and 7900 cal yr BP implies a return to drier conditions and lower temperatures during the 8.2 ka cooling event.

Stable conditions between 7900 and 4300 cal yr BP suggest that the more arid conditions after the formation of sapropel 1 (S1b) had only minor impact on hydrology and productivity of Lake Dojran. More unstable

conditions and gradual environmental change occurred between 4300 and 2800 cal yr BP. Dry and cold conditions around 4000 cal yr BP are correlated with the 4.2 ka cooling event, whereas increasing erosion is most likely associated with human induced wood clearance of the catchment of Lake Dojran.

Intensive anthropogenic impact occurs during the late Holocene (2800 cal yr BP to today) as seen by intensive erosion and enhanced nutrient supply. Despite this anthropogenic overprinting, the sediment characteristics of Co1260 clearly indicate temperature variations associated with the Medieval Warm Period and the Little Ice Age.

Acknowledgements. This study was funded by the German Research Foundation (DfG) and is part of the project SCOPSCO: Scientific Collaboration on Past Speciation Conditions in Lake Ohrid of the DfG priority programme 1006 "International Continental Drilling Programme (ICDP)" Germany and of the project B2 of the Collaborative Research Centre (CRC) 806 "Our way to Europe – Cultural – Environmental Interaction and Human Mobility in the Late Quaternary". We would like to thank Anne Böhm, Daniel Treu, Frank Schäbitz and Konstantinos Panagiotopoulos for their contributions on the fieldtrip in June 2011. The authors thank Nicole Mankte, Ulrike Patt, Lana König (all University of Cologne), Christopher Kendrick (NIGL), Jonathan Lewis (NIGL) and various students from the University of Cologne for assistance with the laboratory work. Finn Viehberg and Ascelina Hasberg are acknowledged for the determination of the ostracodes in core Co1260. Volker Wennrich contributed with numerous fruitful discussions.

Edited by: M. Magny

References

Allen, J. R. M., Brandt, U., Brauer, A., Hubberten, H.-W., Huntley, B., Keller, J., Kraml, M., Mackensen, A., Mingram, J., Negendank, J. F. W., Nowaczyk, N. R., Oberhänsli, H., Watts, W. A., Wulf, S., and Zolitschka, B.: Rapid environmental changes in southern Europe during the last glacial period, Nature, 400, 740–743, doi:10.1038/23432, 1999.

Allen, J. R. M., Watts, W. A., McGee, E., and Huntley, B.: Holocene environmental variability-the record from Lago Grande di Monticchio, Italy, Quatern. Int., 88, 69–80, doi:10.1016/s1040-6182(01)00074-x, 2002.

Arnaud, F., Revel, M., Chapron, E., Desmet, M., and Tribovillard, N.: 7200 years of Rhone river flooding activity in Lake Le Bourget, France: a high-resolution sediment record of NW Alps hydrology, Holocene, 15, 420–428, doi:10.1191/0959683605hl801rp, 2005.

Athanasiadis, N., Tonkov, S., Atanassova, J., and Bozilova, E.: Palynological study of Holocene sediments from Lake Doirani in northern Greece, J. Paleolimnol., 24, 331–342, 2000.

Aufgebauer, A., Panagiotopoulos, K., Wagner, B., Schaebitz, F., Viehberg, F. A., Vogel, H., Zanchetta, G., Sulpizio, R., Leng, M. J., and Damaschke, M.: Climate and environmental change in the Balkans over the last 17 ka recorded in sediments from Lake Prespa (Albania/F.Y.R. of Macedonia/Greece), Quatern. Int., 274, 122-135, doi:10.1016/j.quaint.2012.02.015, 2012.

Bar-Matthews, M., Ayalon, A., Kaufman, A., and Wasserburg, G. J.: The Eastern Mediterranean paleoclimate as a reflection of regional events: Soreq cave, Israel, Earth Planet. Sc. Lett., 166, 85–95, doi:10.1016/s0012-821x(98)00275-1, 1999.

Beklioglu, M., Altinayar, G., and Tan, C. O.: Water level control over submerged macrophyte development in five shallow lakes of Mediterranean Turkey, Arch. Hydrobiol., 166, 535–556, doi:10.1127/0003-9136/2006/0166-0535, 2006.

Berger, J.-F. and Guilaine, J.: The 8200 cal BP abrupt environmental change and the Neolithic transition: A Mediterranean perspective, Quatern. Int., 200, 31–49, doi:10.1016/j.quaint.2008.05.013, 2009.

Bially, A. and Macisaac, H. J.: Fouling mussels (Dreissena spp.) colonize soft sediments in Lake Erie and facilitate benthic invertebrates, Freshwater Biol., 43, 85–97, doi:10.1046/j.1365-2427.2000.00526.x, 2000.

Blott, S. J. and Pye, K.: GRADISTAT: A grain size distribution and statistics package for the analysis of unconsolidated sediments, Earth Surf. Proc. Land., 26, 1237–1248, 2001.

Bordon, A., Peyron, O., Lézine, A.-M., Brewer, S., and Fouache, E.: Pollen-inferred Late-Glacial and Holocene climate in southern Balkans (Lake Maliq), Quatern. Int., 200, 19–30, doi:10.1016/j.quaint.2008.05.014, 2009.

Cacho, I., Grimalt, J. O., Canals, M., Sbaffi, L., Shackleton, N. J., Schönfeld, J., and Zahn, R.: Variability of the western Mediterranean Sea surface temperature during the last 25,000 years and its connection with the Northern Hemisphere climatic changes, Paleoceanography, 16, 40–52, doi:10.1029/2000pa000502, 2001.

Cohen, H.: Paleolimnology: The History and Evolution of Lake Systems, Oxford University Press, 2003.

Coops, H., Beklioglu, M., and Crisman, T. L.: The role of water-level fluctuations in shallow lake ecosystems – workshop conclusions, Hydrobiologia, 506–509, 23–27, doi:10.1023/b:hydr.0000008595.14393.77, 2003.

Croudace, I. W., Rindby, A., and Rothwell, R. G.: ITRAX: description and evaluation of a new multi-function X-ray core scanner, New Tech. Sediment Core Anal., 267, 51–63, 2006.

Crowley, T. J. and Lowery, T. S.: How Warm Was the Medieval Warm Period?, Ambio, 29, 51–54, doi:10.1579/0044-7447-29.1.51, 2000.

Cvijic, J.: L'ancien Lac Egéen, Annales de Géographie, 20, 233–259, 1911.

Denèfle, M., Lézine, A.-M., Fouache, E., and Dufaure, J.-J.: A 12,000-Year Pollen Record from Lake Maliq, Albania, Quaternary Res., 54, 423–432, doi:10.1006/qres.2000.2179, 2000.

Develle, A.-L., Herreros, J., Vidal, L., Sursock, A., and Gasse, F.: Controlling factors on a paleo-lake oxygen isotope record (Yammouneh, Lebanon) since the Last Glacial Maximum, Quaternary Sci. Rev., 29, 865–886, doi:10.1016/j.quascirev.2009.12.005, 2010.

Digerfeldt, G., Olsson, S., and Sandgren, P.: Reconstruction of lake-level changes in lake Xinias, central Greece, during the last 40 000 years, Palaeogeogr. Palaeocl., 158, 65–82, doi:10.1016/s0031-0182(00)00029-8, 2000.

Emeis, K.-C., Struck, U., Schulz, H.-M., Rosenberg, R., Bernasconi, S., Erlenkeuser, H., Sakamoto, T., and Martinez-Ruiz, F.: Temperature and salinity variations of Mediterranean Sea surface waters over the last 16,000 years from records of planktonic stable oxygen isotopes and alkenone unsaturation ratios, Palaeogeogr. Palaeocl., 158, 259–280, doi:10.1016/S0031-0182(00)00053-5, 2000.

Griffiths, H. I., Reed, J. M., Leng, M. J., Ryan, S., and Petkovski, S.: The recent palaeocology and conservation status of Balkan Lake Dojran, Biol. Conserv., 104, 35–49, 2002.

Hernández, A., Bao, R., Giralt, S., Leng, M. J., Barker, P. A., Sáez, A., Pueyo, J. J., Moreno, A., Valero-Garcés, B. L., and Sloane, H. J.: The palaeohydrological evolution of Lago Chungará (Andean Altiplano, northern Chile) during the Lateglacial and early Holocene using oxygen isotopes in diatom silica, J. Quaternary Sci., 23, 351–363, doi:10.1002/jqs.1173, 2008.

Joannin, S., Brugiapaglia, E., de Beaulieu, J.-L., Bernardo, L., Magny, M., Peyron, O., Goring, S., and Vannière, B.: Pollen-based reconstruction of Holocene vegetation and climate in southern Italy: the case of Lago Trifoglietti, Clim. Past, 8, 1973–1996, doi:10.5194/cp-8-1973-2012, 2012.

Kotthoff, U., Müller, U. C., Pross, J., Schmiedl, G., Lawson, I. T., van de Schootbrugge, B., and Schulz, H.: Lateglacial and Holocene vegetation dynamics in the Aegean region: an integrated view based on pollen data from marine and terrestrial archives, Holocene, 18, 1019–1032, doi:10.1177/0959683608095573, 2008a.

Kotthoff, U., Pross, J., Müller, U. C., Peyron, O., Schmiedl, G., Schulz, H., and Bordon, A.: Climate dynamics in the borderlands of the Aegean Sea during formation of sapropel S1 deduced from a marine pollen record, Quaternary Sci. Rev., 27, 832–845, doi:10.1016/j.quascirev.2007.12.001, 2008b.

Kotthoff, U., Koutsodendris, A., Pross, J., Schmiedl, G., Bornemann, A., Kaul, C., Marino, G., Peyron, O., and Schiebel, R.: Impact of Lateglacial cold events on the northern Aegean region reconstructed from marine and terrestrial proxy data, J. Quaternary Sci., 26, 86–96, doi:10.1002/jqs.1430, 2011.

Lamy, F., Arz, H. W., Bond, G. C., Bahr, A., and Pätzold, J.: Multicentennial-scale hydrological changes in the Black Sea and northern Red Sea during the Holocene and the Arctic/North Atlantic Oscillation, Paleoceanography, 21, PA1008, doi:10.1029/2005pa001184, 2006.

Lawson, I., Frogley, M., Bryant, C., Preece, R., and Tzedakis, P.: The Lateglacial and Holocene environmental history of the Ioannina basin, north-west Greece, Quaternary Sci. Rev., 23, 1599–1625, doi:10.1016/j.quascirev.2004.02.003, 2004.

Lawson, I. T., Al-Omari, S., Tzedakis, P. C., Bryant, C. L., and Christanis, K.: Lateglacial and Holocene vegetation history at Nisi Fen and the Boras mountains, northern Greece, Holocene, 15, 873–887, 2005.

Leng, M. J., Roberts, N., Reed, J. M., and Sloane, H. J.: Late Quaternary palaeohydrology of the Konya Basin, Turkey, based on isotope studies of modern hydrology and lacustrine carbonates, J. Paleolimnol., 22, 187–204, doi:10.1023/a:1008024127346, 1999.

Leng, M. J. and Marshall, J. D.: Palaeoclimate interpretation of stable isotope data from lake sediment archives, Quaternary Sci. Rev., 23, 811–831, doi:10.1016/j.quascirev.2003.06.012, 2004.

Leng, M. J., Metcalfe, S., and Davies, S.: Investigating Late Holocene Climate Variability in Central Mexico using Carbon Isotope Ratios in Organic Materials and Oxygen Isotope Ratios from Diatom Silica within Lacustrine Sediments, J. Paleolimnol., 34, 413–431, doi:10.1007/s10933-005-6748-8, 2005.

Leng, M. J., Baneschi, I., Zanchetta, G., Jex, C. N., Wagner, B., and Vogel, H.: Late Quaternary palaeoenvironmental reconstruction from Lakes Ohrid and Prespa (Macedonia/Albania border) using stable isotopes, Biogeosciences, 7, 3109–3122, doi:10.5194/bg-7-3109-2010, 2010.

Leng, M. J., Wagner, B., Boehm, A., Panagiotopoulos, K., Vane, C. H., Snelling, A., Haidon, C., Woodley, E., Vogel, H., Zanchetta, G., and Baneschi, I.: Understanding past climatic and hydrological variability in the Mediterranean from lake sediment isotope and geochemical data, Quaternary Sci. Rev., doi:10.1016/j.quascirev.2012.07.015, in press, 2012.

Magny, M., Bégeot, C., Guiot, J., and Peyron, O.: Contrasting patterns of hydrological changes in Europe in response to Holocene climate cooling phases, Quaternary Sci. Rev., 22, 1589–1596, doi:10.1016/s0277-3791(03)00131-8, 2003.

Magny, M., Vannière, B., Zanchetta, G., Fouache, E., Touchais, G., Petrika, L., Coussot, C., Walter-Simonnet, A.-V., and Arnaud, F.: Possible complexity of the climatic event around 4300–3800 cal. BP in the central and western Mediterranean, Holocene, 19, 823–833, doi:10.1177/0959683609337360, 2009.

Manley, R., Spirovska, M., and Andovska, S.: Water balance model of Lake Dojran, BALWOIS Conference Publications, Ohrid, FYROM, 27–31 May 2008.

Matzinger, A., Jordanoski, M., Veljanoska-Sarafiloska, E., Sturm, M., Müller, B., and Wüest, A.: Is Lake Prespa Jeopardizing the Ecosystem of Ancient Lake Ohrid?, Hydrobiologia, 553, 89–109, doi:10.1007/s10750-005-6427-9, 2006.

Meisch, C.: Freshwater Ostracoda of Western and Central Europe, Süßwasserfauna von Mitteleuropa, edited by: Schwoerbel, J. and Zwick, P., Akademischer Verlag Spektrum, Heidelberg, 2000.

Mercone, D., Thomson, J., Croudace, I. W., Siani, G., Paterne, M., and Troelstra, S.: Duration of S1, the most recent sapropel in the eastern Mediterranean Sea, as indicated by accelerator mass spectrometry radiocarbon and geochemical evidence, Paleoceanography, 15, 336–347, doi:10.1029/1999pa000397, 2000.

Müller, A.: Late- and Postglacial Sea-Level Change and Paleoenvironments in the Oder Estuary, Southern Baltic Sea, Quaternary Res., 55, 86–96, doi:10.1006/qres.2000.2189, 2001.

Panagiotopoulos, K., Aufgebauer, A., Schäbitz, F., and Wagner, B.: Vegetation and climate history of the Lake Prespa region since the Lateglacial, Quatern. Int., doi:10.1016/j.quaint.2012.05.048, in press, 2012.

Peyron, O., Goring, S., Dormoy, I., Kotthoff, U., Pross, J., de Beaulieu, J.-L., Drescher-Schneider, R., Vannière, B., and Magny, M.: Holocene seasonality changes in the central Mediterranean region reconstructed from the pollen sequences of Lake Accesa (Italy) and Tenaghi Philippon (Greece), Holocene, 21, 131–146, doi:10.1177/0959683610384162, 2011.

Pross, J., Kotthoff, U., Müller, U. C., Peyron, O., Dormoy, I., Schmiedl, G., Kalaitzidis, S., and Smith, A. M.: Massive perturbation in terrestrial ecosystems of the Eastern Mediterranean region associated with the 8.2 kyr B.P. climatic event, Geology, 37, 887–890, doi:10.1130/g25739a.1, 2009.

Ramsey, B. C.: Radiocarbon Dating: Revolutions in Understanding, Archaeometry, 50, 249–275, doi:10.1111/j.1475-4754.2008.00394.x, 2008.

Reimer, P. J., Baillie, M. G. L., Bard, E., Bayliss, A., Beck, J. W., Blackwell, P. G., Ramsey, C. B., Buck, C. E., Burr, G. S., Edwards, R. L., Friedrich, M., Grootes, P. M., Guilderson, T. P., Hajdas, I., Heaton, T. J., Hogg, A. G., Hughen, K. A., Kaiser, K. F., Kromer, B., McCormac, F. G., Manning, S. W., Reimer, R. W., Richards, D. A., Southon, J. R., Talamo, S., Turney, C. S. M., van der Plicht, J., and Weyhenmeyer, C. E.: IntCal09 and Marine09 Radiocarbon Age Calibration Curves, 0–50,000 Years cal BP, Radiocarbon, 51, 1111–1150, 2009.

Rethemeyer, J., Fülöp, R. H., Höfle, S., Wacker, L., Heinze, S., Hajdas, I., Patt, U., König, S., Stapper, B., and Dewald, A.: Status report on sample preparation facilities for ^{14}C analysis at the new CologneAMS center, Nucl. Instrum. Meth. Phys. Res. B, 294, 168–172, doi:10.1016/j.nimb.2012.02.012, in press, 2013.

Roberts, N., Jones, M. D., Benkaddour, A., Eastwood, W. J., Filippi, M. L., Frogley, M. R., Lamb, H. F., Leng, M. J., Reed, J. M., Stein, M., Stevens, L., Valero-Garcés, B., and Zanchetta, G.: Stable isotope records of Late Quaternary climate and hydrology from Mediterranean lakes: the ISOMED synthesis, Quaternary Sci. Rev., 27, 2426–2441, doi:10.1016/j.quascirev.2008.09.005, 2008.

Rohling, E. J. and Palike, H.: Centennial-scale climate cooling with a sudden cold event around 8,200 years ago, Nature, 434, 975–979, doi:10.1038/nature03421, 2005.

Rossignol-Strick, M.: Late Quaternary climate in the Eastern Mediterranean Region, Paléorient, 19, 135–152, doi:10.3406/paleo.1993.4588, 1993.

Schilman, B., Bar-Matthews, M., Almogi-Labin, A., and Luz, B.: Global climate instability reflected by Eastern Mediterranean marine records during the late Holocene, Palaeogeogr. Palaeocl., 176, 157–176, doi:10.1016/s0031-0182(01)00336-4, 2001.

Schmiedl, G., Kuhnt, T., Ehrmann, W., Emeis, K.-C., Hamann, Y., Kotthoff, U., Dulski, P., and Pross, J.: Climatic forcing of eastern Mediterranean deep-water formation and benthic ecosystems during the past 22 000 years, Quaternary Sci. Rev., 29, 3006–3020, doi:10.1016/j.quascirev.2010.07.002, 2010.

Siani, G., Magny, M., Paterne, M., Debret, M., and Fontugne, M.: Paleohydrology reconstruction and Holocene climate variability in the South Adriatic Sea, Clim. Past Discuss., 8, 4357–4399, doi:10.5194/cpd-8-4357-2012, 2012.

Sotiria, K. and Petkovski, S.: Lake Doiran – An overview of the current situation, Greek Biotope/Wetland Centre (EKBY), Society for the Investigation and Conservation of Biodiversity and the Sustainable Development of Natural Ecosystems (BIOECO), Thermi, 1–117, 2004.

Stankovic, S.: Sur les particularités limnologiques des lacs égéens, Verhandlungen der internationalen Vereinigung für theoretische und angewandte Limnologie, 5, 138–146, 1931.

Stojanov, R. and Micevski, E.: Geology of Lake Doiran and its surrounding, Contributions of the Macedonian Academy of Sciences and Arts, Section of Biological and Medical Sciences, 10, 37–52, 1989.

Stuiver, M. and Reimer, P. J.: Extended (super 14) C data base and revised CALIB 3.0 (super 14) C age calibration program, Radiocarbon, 35, 215–230, 1993.

Tzedakis, P. C.: Seven ambiguities in the Mediterranean palaeoenvironmental narrative, Quaternary Sci. Rev., 26, 2042–2066, doi:10.1016/j.quascirev.2007.03.014, 2007.

Valsecchi, V., Sanchez Goñi, M. F., and Londeix, L.: Vegetation dynamics in the Northeastern Mediterranean region during the past 23 000 yr: insights from a new pollen record from the Sea of Marmara, Clim. Past, 8, 1941–1956, doi:10.5194/cp-8-1941-2012, 2012.

Veljanoska-Sarafiloska, E., Stafilov, T., and Jordanoski, M.: Distribution of DDT Metabolites in the sediment and muscle fish tissue from agriculturally impacted Lake Dojran (Macedonia/Greece), Fresenius Environ. Bull., 20, 2027–2035, 2001.

Vogel, H., Wagner, B., Zanchetta, G., Sulpizio, R., and Rosén, P.: A paleoclimate record with tephrochronological age control for the last glacial-interglacial cycle from Lake Ohrid, Albania and Macedonia, J. Paleolimnol., 44, 295–310, doi:10.1007/s10933-009-9404-x, 2010a.

Vogel, H., Zanchetta, G., Sulpizio, R., Wagner, B., and Nowaczyk, N.: A tephrostratigraphic record for the last glacial-interglacial cycle from Lake Ohrid, Albania and Macedonia, J. Quaternary Sci., 25, 320–338, doi:10.1002/jqs.1311, 2010b.

Wagner, B., Melles, M., Doran, P. T., Kenig, F., Forman, S. L., Pierau, R., and Allen, P.: Glacial and postglacial sedimentation in the Fryxell basin, Taylor Valley, southern Victoria Land, Antarctica, Palaeogeogr. Palaeoecl., 241, 320–337, doi:10.1016/j.palaeo.2006.04.003, 2006.

Wagner, B., Lotter, A. F., Nowaczyk, N., Reed, J. M., Schwalb, A., Sulpizio, R., Valsecchi, V., Wessels, M., and Zanchetta, G.: A 40,000-year record of environmental change from ancient Lake Ohrid (Albania and Macedonia), J. Paleolimnol., 41, 407–430, doi:10.1007/s10933-008-9234-2, 2009.

Wagner, B., Vogel, H., Zanchetta, G., and Sulpizio, R.: Environmental change within the Balkan region during the past ca. 50 ka recorded in the sediments from lakes Prespa and Ohrid, Biogeosciences, 7, 3187–3198, doi:10.5194/bg-7-3187-2010, 2010.

Wagner, B., Aufgebauer, A., Vogel, H., Zanchetta, G., Sulpizio, R., and Damaschke, M.: Late Pleistocene and Holocene contourite drift in Lake Prespa (Albania/F.Y.R. of Macedonia/Greece), Quatern. Int., 274, 112–121, doi:10.1016/j.quaint.2012.02.016, 2012.

Wang, W., Wang, D., and Yin, C.: A Field Study on the Hydrochemistry of Land/Inland Water Ecotones with Reed Domination, Acta Hydrochim. Hydrobiol., 30, 117–127, 2002.

Weiss, H. and Bradley, R. S.: What Drives Societal Collapse?, Science, 291, 609–610, doi:10.1126/science.1058775, 2001.

Wick, L., Lemcke, G., and Sturm, M.: Evidence of Lateglacial and Holocene climatic change and human impact in eastern Anatolia: high-resolution pollen, charcoal, isotopic and geochemical records from the laminated sediments of Lake Van, Turkey, Holocene, 13, 665–675, doi:10.1191/0959683603hl653rp, 2003.

Willis, K. J.: The vegetational history of the Balkans, Quaternary Sci. Rev., 13, 769–788, doi:10.1016/0277-3791(94)90104-x, 1994.

Yin, C. and Lan, Z.: The nutrient retention by ecotone wetlands and their modification for Baiyangdian lake restoration, Water Sci. Technol., 32, 159–167, doi:10.1016/0273-1223(95)00616-8, 1995.

Zacharias, I., Bertachas, I., Skoulikidis, N., and Koussouris, T.: Greek Lakes: Limnological overview, Lakes Reserv. Res. Manage., 7, 55–62, doi:10.1046/j.1440-1770.2002.00171.x, 2002.

Zanchetta, G., Drysdale, R. N., Hellstrom, J. C., Fallick, A. E., Isola, I., Gagan, M. K., and Pareschi, M. T.: Enhanced rainfall in the Western Mediterranean during deposition of sapropel S1: stalagmite evidence from Corchia cave (Central Italy), Quaternary Sci. Rev., 26, 279–286, doi:10.1016/j.quascirev.2006.12.003, 2007a.

Zanchetta, G., Borghini, A., Fallick, A., Bonadonna, F., and Leone, G.: Late Quaternary palaeohydrology of Lake Pergusa (Sicily, southern Italy) as inferred by stable isotopes of lacustrine carbonates, J. Paleolimnol., 38, 227–239, doi:10.1007/s10933-006-9070-1, 2007b.

7 Possible earthquake trigger for 6th century mass wasting deposit at Lake Ohrid (Macedonia/Albania)

Journal article (2012):
Wagner, B., Francke, A., Sulpizio, R., Zanchetta, G., Lindhorst, K., Krastel, S., Vogel, H., Rethemeyer, J., Daut, G., Grazhdani, A., Lushaj, B., and Trajanovski, S.: Possible earthquake trigger for 6th century mass wasting deposit at Lake Ohrid (Macedonia/Albania), Clim. Past, 8, 2069-2078, 10.5194/cp-8-2069-2012, 2012.

Clim. Past, 8, 2069–2078, 2012
www.clim-past.net/8/2069/2012/
doi:10.5194/cp-8-2069-2012

Climate of the Past

Possible earthquake trigger for 6th century mass wasting deposit at Lake Ohrid (Macedonia/Albania)

B. Wagner[1], A. Francke[1], R. Sulpizio[2], G. Zanchetta[3], K. Lindhorst[4], S. Krastel[4,5], H. Vogel[1], J. Rethemeyer[1], G. Daut[6], A. Grazhdani[7], B. Lushaj[7], and S. Trajanovski[8]

[1]Institute of Geology and Mineralogy, University of Cologne, Zülpicher Str. 49a, 50674 Cologne, Germany
[2]Dipartimento di Scienze della Terra e Geoambientali, University of Bari, Italy
[3]Dipartimento di Scienze della Terra, University of Pisa, Italy
[4]Helmholtz Centre for Ocean Research, GEOMAR, Kiel, Germany
[5]Institute of Geosciences, University of Kiel, Germany
[6]Institute of Geography, University of Jena, Germany
[7]Institute of Geosciences & Energy, Water & Environment, Polytechnic University of Tirana, Albania
[8]Hydrobiological Institute Ohrid, 6000 Ohrid, Macedonia

Correspondence to: B. Wagner (wagnerb@uni-koeln.de)

Received: 10 August 2012 – Published in Clim. Past Discuss.: 7 September 2012
Revised: 20 November 2012 – Accepted: 12 December 2012 – Published: 20 December 2012

Abstract. Lake Ohrid shared by the Republics of Albania and Macedonia is formed by a tectonically active graben within the south Balkans and suggested to be the oldest lake in Europe. Several studies have shown that the lake provides a valuable record of climatic and environmental changes and a distal tephrostratigraphic record of volcanic eruptions from Italy. Fault structures identified in seismic data demonstrate that sediments have also the potential to record tectonic activity in the region. Here, we provide an example of linking seismic and sedimentological information with tectonic activity and historical documents. Historical documents indicate that a major earthquake destroyed the city of Lychnidus (today: city of Ohrid) in the early 6th century AD. Multichannel seismic profiles, parametric sediment echosounder profiles, and a 10.08 m long sediment record from the western part of the lake indicate a 2 m thick mass wasting deposit, which is tentatively correlated with this earthquake. The mass wasting deposit is chronologically well constrained, as it directly overlays the AD 472/AD 512 tephra. Moreover, radiocarbon dates and cross correlation with other sediment sequences with similar geochemical characteristics of the Holocene indicate that the mass wasting event took place prior to the onset of the Medieval Warm Period, and is attributed it to one of the known earthquakes in the region in the early 6th century AD.

1 Introduction

Lake Ohrid (40°54′–41°10′ N, 20°38′–20°48′ E, Fig. 1) is a transboundary lake located on the Balkan Peninsula and shared between the Republics of Macedonia and Albania. The lake is about 30 km long, 15 km wide and has an area of 360 km^2 (Stankovic, 1960). According to geological and biological age estimations the lake formed about 2–5 Ma ago (summarised in Albrecht and Wilke, 2008). The lake is situated in a tectonically active, N–S trending graben (Burchfiel et al., 2008; Hoffmann et al., 2010), which results in a relatively simple bathtub-shaped morphology, with steep slopes along the western and eastern sides and less inclined slopes in the northern and southern part. The average water depth is 150 m and the maximum water depth is 293 m (new data from seismic survey). The current lake level is at 693 m above sea level (a.s.l.) and the lake is surrounded by the Mokra Mountains to the west (1514 m a.s.l.) and the Galicica Mountains to the east (2265 m a.s.l.; Fig. 1).

Several studies on up to ca. 15 m long sediment sequences have shown that Lake Ohrid is a valuable archive of climatic and environmental changes over the last glacial/interglacial cycle (e.g., Wagner et al., 2009, 2010; Vogel et al., 2010a). Moreover, tephrostratigraphic studies revealed that Lake Ohrid and neighboring Lake Prespa are important distal

Published by Copernicus Publications on behalf of the European Geosciences Union.

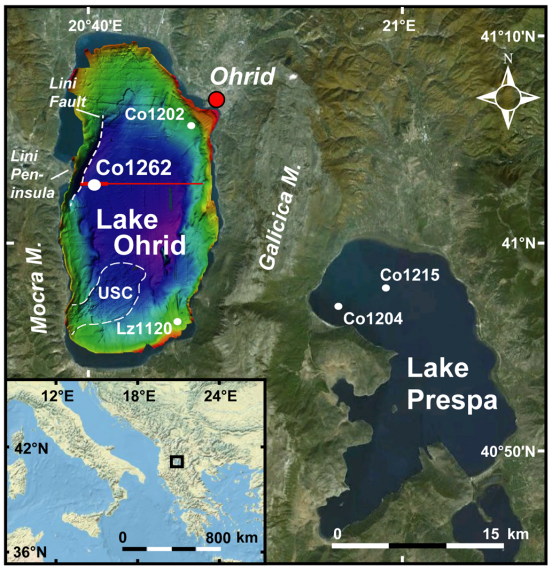

Fig. 1. Map of the northern Mediterranean region showing the location of lakes Ohrid and Prespa. White dots indicate coring locations Lz1120 and Co1202 from field campaigns in 2005 and 2007 in the southeastern and northeastern part of Lake Ohrid, and the new coring location Co1262 in the western part of the lake, as well as coring locations Co1204 and Co1215 from former field campaigns at Lake Prespa (Wagner et al., 2010, 2012). The red line in Lake Ohrid indicates the location of the multichannel seismic (entire line) and hydro-acoustic (thick line) profiles shown in Figs. 2 and 3. White dashed lines in Lake Ohrid indicate the location of the Lini Fault and the Udenisht Slight Complex (USC). The red dot indicates the approximate location of the city of Ohrid.

archives of explosive eruptions from Italian volcanoes (summarised in Sulpizio et al., 2010a; Caron et al., 2010; Vogel et al., 2010b, Damaschke et al., 2012). Hiatuses and disturbed sedimentation in some of the studied sediment sequences from Lake Ohrid can probably be explained by tectonic activity in the region triggering several landslides (e.g., Wagner et al., 2009; Vogel et al., 2010a). These mass wasting deposits and associated fault structures are also recorded in seismic profiles from the lake and occur mainly in the marginal parts of the lake basin (Wagner et al., 2008a; Reicherter et al., 2011). A detailed morphological mapping of the floor of Lake Ohrid by means of an ELAC 1180 Seabeam system revealed that most of the southwestern part of the lake is affected by a large mass failure event, the so-called Udenisht Slide Complex (Fig. 1; Lindhorst et al., 2012). Though some of the mass wasting deposits may be triggered by distinct lake level fluctuations (Lindhorst et al., 2010), most of them likely formed due to tectonic activity (Reicherter et al., 2011). As Lake Ohrid is located within the Korca-Ohrid Earthquake Source Zone, several medium to large earthquakes have occurred within the last 2000 yr (e.g., Aliaj et al., 2004). For example, recent earthquakes occurred on 6 June 2012 ($M = 4.4$), on 6 September 2009 ($M = 5.6$), and on 23 November 2004 ($M = 5.4$) (European-Mediterranean Seismological Centre, EMSC, 2012). More destructive earthquakes in the younger history are recorded in 1963 close to capital city of Macedonia, Skopje ($M = 6.1$, Suhadolc et al., 2004), or in 1911 at Lake Ohrid with a Magnitude of 6.7 (Ambraseys and Jackson, 1990; Mucço et al., 2002). Unfortunately, the database is less well constrained for historical times. According to Aliaj et al. (2004), a major earthquake destroyed the cities of "Lychnidus" (today: city of Ohrid) and "Scupi" (today: city of Skopje), which is located ca. 120 km towards the northeast of Ohrid, at 518 AD. This data can also be found in most public reports. In contrast, Ambraseys (2009) reports that this earthquake rather affected the city of Scupi, whilst the city of Lychnidus was destroyed 9 yr later at 527 AD. This data could correspond with the data indicated in Reicherter et al. (2011, and references therein), according to which the city of Lychnidus was destroyed in late May 526 AD, by a magnitude $M > 6$ earthquake. Despite these uncertainties, it seems unquestionable that at least one major earthquake affected the Ohrid region in the beginning of the 6th century AD.

Here we combine seismic, sedimentological, climatic, tephrostratigraphic, and historical information in order to trace back the possible signature of 6th century earthquakes on the Lake Ohrid sediment record. In light of the available data, we furthermore evaluate the potential of Lake Ohrid for paleoseismicity investigations, as it was proposed by Reicherter et al. (2011) and demonstrated in other lacustrine (e.g., Schnellmann et al., 2002) or marine basins (e.g., Beck et al., 2012).

2 Material and methods

Hydro-acoustic surveys were carried out in Lake Ohrid between 2004 and 2009 in order to obtain information on the lake's bathymetry and sedimentary architecture. Multichannel seismic surveys were carried out in 2007 and 2008 using a Mini GI Gun (0.25 L in 2007 and 0.1 L in 2008) and a 16-channel 100 m long streamer. In addition, a multibeam survey was carried out in 2009 using an ELAC 1180 Seabeam system. These surveys have shown prominent faults and half-graben structures along the western and eastern margins of the lake, which were also indicated in parametric sediment echosounder profiles (SES-96 light in 2004 and SES 2000 compact in 2007 and 2008, Innomar Co.). In front of the Lini Peninsula at the western margin of the lake (Fig. 1), where a succession of mass wasting deposits was indicated in the multichannel seismic surveys (Reicherter et al., 2011; Fig. 2), also parametric echosounder profiles were obtained. The parametric sediment echosounder transducer was mounted on the side of a small research vessel. The effective frequency

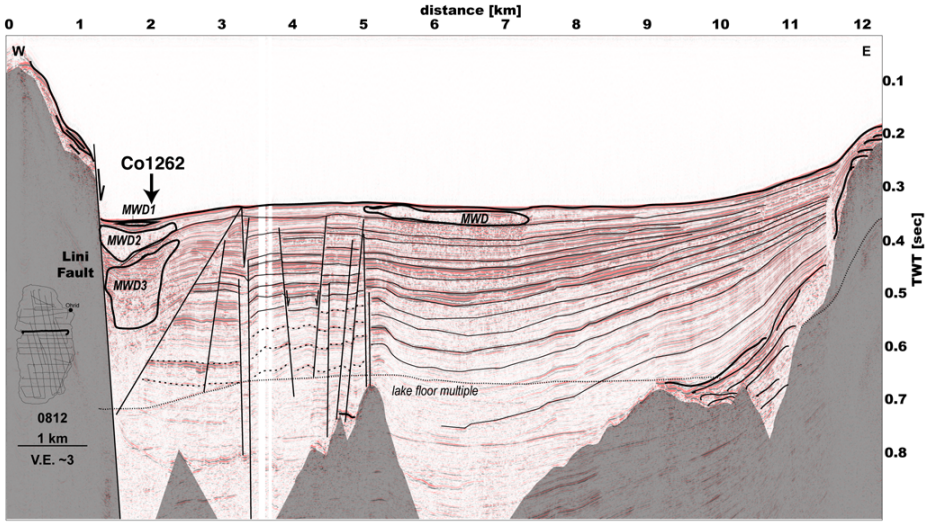

Fig. 2. Interpreted multichannel seismic profile taken by a Mini GI Gun across Lake Ohrid with the Lini Fault in the west. Grey parts indicate bedrock. The arrow indicates coring location Co1262. Transparent sediment bodies indicate mass wasting deposits (MWD1-3).

of the echosounder was set to 10 kHz in order to obtain the optimum settings ranging from deep penetration to high resolution. The sound velocity in the water was set to 1440 m s^{-1}. Post-processing was carried out with the INNOMAR software tool ISE 2.9.2. The theoretical vertical resolution of the two types of seismic data can be estimated to ca. 1 m for the Mini GI gun and 0.2 m for the Innomar data.

Based on the hydro-acoustic surveys, a coring location in front of the Lini Peninsula (41°03′56.9″ N, 020°40′21.9″ E) at 260 m water depth was selected for the study of mass wasting deposits and their relation to earthquakes. A 10 m long sediment sequence (Co1262) was recovered in June 2011 from a floating platform using a gravity corer and a 2 m long percussion piston corer (UWITEC Co. Austria) for deeper sediments. For the recovery of the piston cores, a reentry cone was positioned on the lake floor. Extension rods of 2 m length controlled the exact release of the piston during the individual continuous coring process. Core recovery was in the order of 100 % including core catcher samples. Core loss or disturbance of sediment between the individual 2 m segments can therefore be regarded as low (< 6 cm). After recovery, the 2 m long sediment cores were cut into ca. 1 m long segments and stored in the dark at 4 °C until further processing.

In the laboratory at the University of Cologne, the core segments were opened and one core half was described macroscopically and subjected to high-resolution X-ray fluorescence (XRF) scanning. XRF scanning was performed using an ITRAX core scanner (COX Ltd., Sweden), which was equipped with a Cr-tube set to 30 kV and 30 mA, and a Si-drift chamber detector. Core Co1262 was scanned with a resolution of 2 mm and a scanning time of 10 s per measurement. Ca, K, and Sr were selected of the measured elements, as they are indicators for carbonate precipitation, the input of clastic material, and the occurrence of potential tephras and cryptotephras in sediment sequences from Lake Ohrid (Vogel et al., 2010a, b). Total carbon (TC) and total inorganic carbon (TIC) were determined with a DIMATOC 200 (DIMATEC Co.). Total organic carbon (TOC) was calculated by the difference between TC and TIC.

Tephrostratigraphy, radiocarbon dating, and cross correlation with other sediment cores from lakes Ohrid and Prespa were used to provide a chronological framework for core Co1262. Samples from horizons with peaks in K and Sr were selected for tephrostratigraphic work. Volcanic ejecta from these horizons were analysed with respect to their geochemical composition according to previous work on sediment cores from Lake Ohrid (Sulpizio et al., 2010a; Vogel et al., 2010b). Energy-dispersive spectrometry (EDS) of glass shards and micro-pumice fragments was performed using an EDAX-DX micro-analyser mounted on a Philips SEM 515 (operating conditions: 20 kV acceleration voltage, 100 s live time counting, 200–500 nm beam diameter, 2100–2400 shots s^{-1}, ZAF correction). Details about analytical precision, ZAF correction and inter-laboratory comparison can be found in Sulpizio et al. (2010a, b) and Vogel et al. (2010b). Radiocarbon dating on core Co1262 was carried out by accelerator mass spectrometry (AMS) at the University of Cologne Centre for AMS on five samples of terrestrial plant remains and on one sample of fish remains. Sample pre-treatment and graphitisation was carried out according to Rethemeyer et al. (2013). Other macrofossils were not found in core Co1262 and previous studies have shown that

bulk organic matter dating on Lake Ohrid sediments provided erroneous ages (Wagner et al., 2008a; Vogel et al., 2010a). CALIB 6.1.1 (Stuiver and Reimer, 1993) and the IntCal09 dataset (Reimer et al., 2009) were used for conversion of the conventional radiocarbon ages into calendar ages (cal yr BP) on an uncertainty level of 2σ. Cross correlation with other sediment cores from lakes Ohrid and Prespa concentrated on carbonate content (TIC and Ca; Lake Ohrid) and organic matter content (TOC; Lake Prespa), as former studies have shown that these proxies sensitively recorded climatic and environmental changes during the Holocene (Wagner et al., 2009, 2010; Vogel et al., 2010a; Aufgebauer et al., 2012). Significant fluctuations in these proxies could have been attributed to significant events, such as the 8.2 cooling event, the Medieval Warm Period (MWP) or Little Ice Age (LIA) and were constrained by tephrostratigraphy and radiocarbon dating on macrofossil remains. Similar fluctuations in core Co1262 are assumed to represent the same events.

3 Results

3.1 Hydro-acoustic survey

The multichannel seismic survey revealed a succession of three mass wasting events in front of the Lini Peninsula (Fig. 2), where one of the most active faults of the Lake Ohrid graben system is located (cf. Reicherter et al., 2011). The topmost two mass wasting events (MWD1 and MWD2, Fig. 2) are also imaged in the parametric sediment echosounder profile perpendicular to the Lini Peninsula as transparent and partly chaotic seismic units (Fig. 3). Whilst the thickness of MWD2 exceeds 10 m (Fig. 2), the parametric sediment echosounder profile indicates that the thickness of MWD1 is about 2 m at the coring location Co1262 (Fig. 3). Between MWD2 and MWD1 and on top of MWD1, parallel to subparallel continuous reflections with low to medium amplitudes indicate widely undisturbed well-stratified sediments. A significant erosional unconformity at the base of MWD1 cannot be detected in the parametric sediment echosounder line at the coring location, probably because MWD1 pinches out only a few hundred meters to the east of the coring location and a potential erosion decreased with increasing distance from the steep slope (Fig. 3).

3.2 Sediment core

The geochemical characteristics of the 1008 cm long sediment sequence Co1262 correlate well with the parametric sediment echosounder data and with sediment cores previously recovered from Lake Ohrid. Overall, core Co1262 is mainly formed by relatively homogenous clayey to silty mud of greyish to olive colour. The sediments appear massive, probably as a result of bioturbation, as it was also observed in other sediment sequences from Lake Ohrid at least throughout the Holocene (Wagner et al., 2009; Vogel et al., 2010a). Some weak colour changes are probably due to distinct changes in the content of carbonate, which is represented by TIC and Ca, and organic matter, which is represented by TOC (Fig. 4). Significant changes in these constituents were also recorded in other sediment sequences from Lake Ohrid throughout the Holocene (Wagner et al., 2009; Vogel et al., 2010a). The lowermost meter of core Co1262 contains some gravel grains, which were interpreted as ice-rafted debris in other cores from lakes Ohrid and Prespa (Wagner et al., 2009; Vogel et al., 2010a; Aufgebauer et al., 2012). Some changes in grain size composition are correlated with minima in water content and likely represent mass wasting deposits. For example, a 15 cm thick horizon between 980 and 965 cm has low, but increasing water content and a fining upward trend in grain size composition from fine sand at its base to fine silt and clay at the top. This is interpreted as a distal turbidite of a mass wasting deposit (Schnellmann et al., 2005). Smaller mass wasting deposits are also indicated at depths of 548 and 350 cm, but they are < 4 cm thick and too small to be visible in the seismic data. A significant change of the sedimentological and geochemical characteristics occurs at 320 cm depth, where a 1–2 cm thick sandy horizon overlays a thin greyish band of 1 mm thickness (Fig. 5). On top of this sand layer, the sediment is very homogenous until 121 cm depth. Significant changes in carbonate or organic matter content do not occur and the water content is low, but increases slightly upwards. This homogenous horizon between 320 and 121 cm depth corresponds with MWD1 in the parametric sediment echosounder data. An erosional discordance at the basis of MWD1 is not distinct in the sediment core (Fig. 5) and matches with the parametric sediment echosounder data. The uppermost 121 cm of core Co1262 are characterised by silty to clayey mud of greyish to olive colour, relatively high water content, and some distinct fluctuations of TIC and TOC, and likely represent undisturbed pelagic sedimentation.

4 Chronology of core Co1262 and the mass wasting deposit

The occurrence of three well-dated tephras, six radiocarbon ages, and the significant patterns of TIC and Ca allow good chronological control of the entire core and, specifically, of MWD1 between 320 and 121 cm depth.

Overall, the occurrence of ice-rafted debris, low Ca and TIC at the core base imply that the core reaches back into the Late Pleistocene, when carbonate precipitation in Lake Ohrid was restricted or carbonates were not preserved and when the lake was at least partly ice covered during winter (Wagner et al., 2009; Vogel et al., 2010a). In several studied cores from lakes Ohrid and Prespa, the onset of carbonate precipitation and preservation was correlated with the Pleistocene/Holocene transition (Wagner et al., 2009, 2010; Vogel et al., 2010a; Aufgebauer et al., 2012). However,

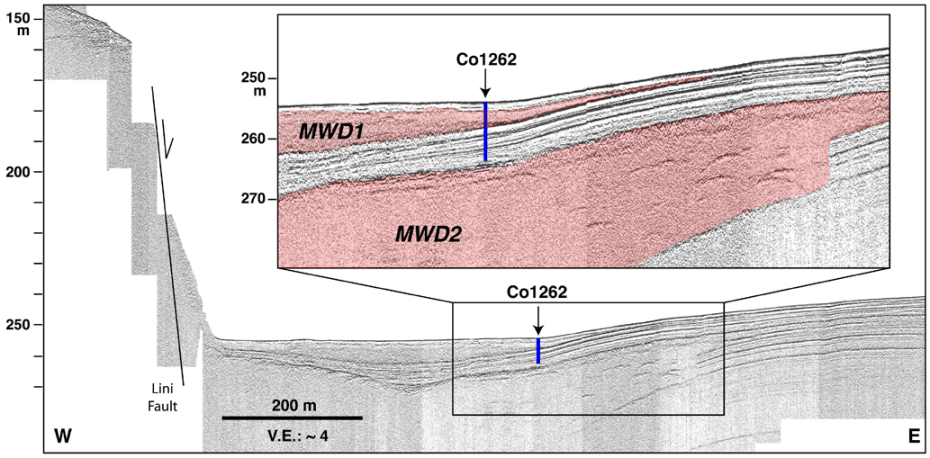

Fig. 3. Uninterpreted and interpreted (insert) hydro-acoustic profile in front of the Lini peninsula (see Fig. 1 for exact location). The profile was obtained with an Innomar transducer. The blue bar indicates the coring location Co1262 and transparent sediment bodies (red coloured in the interpreted insert) indicate mass wasting deposits (MWD1 and MWD2).

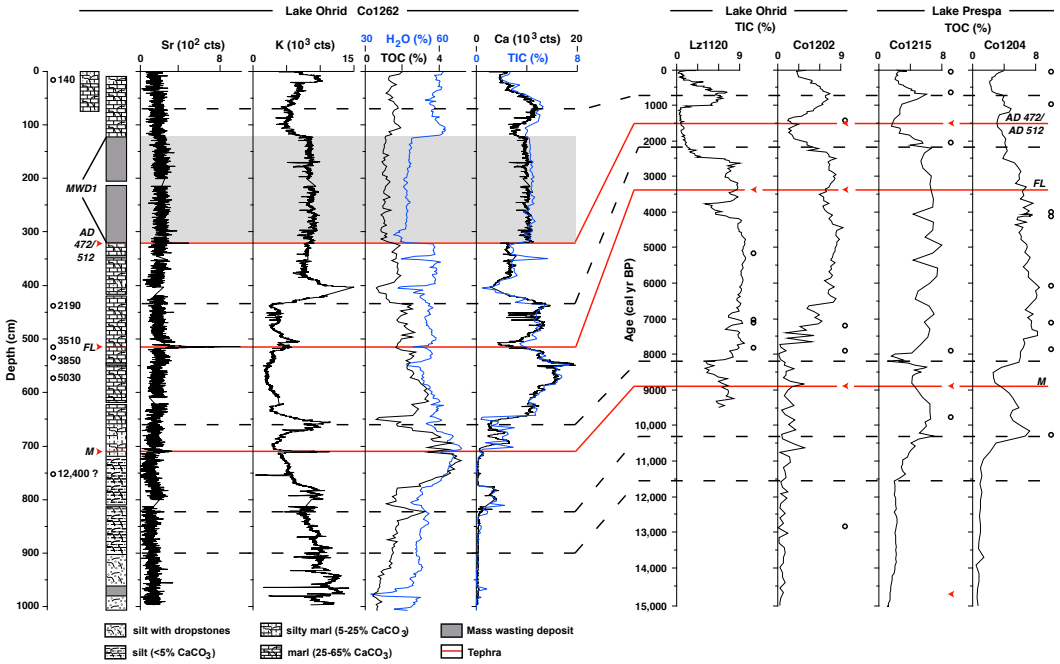

Fig. 4. Lithology, water content, and geochemical composition of core Co1262 from Lake Ohrid. Note that the entire sediment succession appears massive due to bioturbation. The gaps in XRF scanning data (Sr, K, and Ca counts) are due to non-overlapping cores. These gaps are smaller in water content, TIC, and TOC, as core catcher samples are included. The cross correlation with cores Lz1120 and Co1202 from Lake Ohrid and cores Co1215 and Co1204 from Lake Prespa (black dashed lines) can be used for an age estimation of core Co1262. Red arrows and lines indicate tephras and cryptotephras (AD 472/512, FL eruption, and M = Mercato). Black circles indicate radiocarbon dated horizons in cores from lakes Ohrid and Prespa (ages in core Co1262 are calibrated ages from Table 1).

Table 1. Radiocarbon and calendar ages from core Co1262. The calibration of radiocarbon ages into calendar ages is based on Calib 6.1.1 (Stuiver and Reimer, 1993) and INTCAL09 (Reimer et al., 2009) and on a 2σ uncertainty.

AMS Lab ID	Core depth (cm)	Material	C weight (mg)	^{14}C age (yr BP)	Calendar age (cal yr BP)
COL 1251.1.1	17	terrestrial plant	1.00	164 ± 20	140 ± 145
COL 1735.1.1	442	terrestrial plant	0.74	2176 ± 46	2190 ± 140
COL 1736.1.1	520	terrestrial plant	0.99	3280 ± 45	3510 ± 110
COL 1737.1.1	537	terrestrial plant	0.93	3581 ± 40	3850 ± 130
COL 1738.1.1	574	terrestrial plant	1.00	4370 ± 44	5030 ± 190
COL 1243.1.1	754	fish bone	0.53	$10{,}492 \pm 37$	$12\,400 \pm 190$

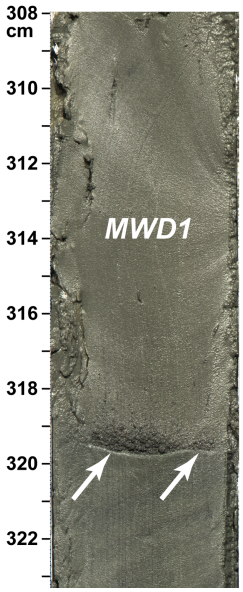

Fig. 5. Photography of the core Co1262, from ca. 308 to 323 cm depth, where the AD 472/512 tephra as thin, greyish band (arrow) underlies mass waste deposit MWD1 with a sandy base.

most of the existing records from Lake Ohrid apparently are disturbed at the Pleistocene/Holocene transition. In a record from nearby Lake Prespa, a first significant increase of organic matter occurred at the end of the Younger Dryas and the onset of the Holocene (Fig. 4). We assume that the increase of TOC between ca. 950 and 900 cm and the end of ice-rafted debris deposition at ca. 900 cm in core Co1262 can also be correlated with the onset of the Holocene. The peaks in TIC and Ca and the minimum in TOC around 800 cm depth in core Co1262 could correspond with the period 10 500–9500 cal yr BP, when similar fluctuations are observed at Lake Prespa (Fig. 4; Aufgebauer et al., 2012) and when a minimum in winter precipitation is reconstructed from a record at nearby Lake Maliq (Bordon et al., 2009). The radiocarbon age of the fish remains at 758 cm indicating a much older age (Table 1). Since reservoir effects of 1500 yr have been measured in several cores from Lake Ohrid (Wagner et al., 2008a; Vogel et al., 2010a), we can also assume that the fish remains are affected by a reservoir effect or that they are re-deposited. The first reliable chronological tie point is given by the peaks in K and Sr at 709 cm, which can be attributed to a significant occurrence of glass shards. The geochemical composition of the glass shards suggest that they originate from the Mercato eruption (Table 2, Fig. 6; cf. Damaschke et al., 2012), which has proposed maximum ages of 8890 cal yr BP (Santacroce et al., 2008) and recently dated (using charcoal from the base of the fallout deposits) at 8540 cal yr BP (Zanchetta et al., 2011). The minima in TIC and Ca and the maximum in K at ca. 660 cm depth are likely correlated with the 8.2 ka cooling event, as observed in other cores from lakes Ohrid and Prespa (Wagner et al., 2009, 2010; Vogel et al., 2010a; Aufgebauer et al., 2012). High TIC and Ca characterise the period after the 8.2 ka cooling event and are explained by warmer temperatures, higher carbonate precipitation and better carbonate preservation (Wagner et al., 2009, 2010; Vogel et al., 2010a; Aufgebauer et al., 2012). The mid-Holocene is chronologically well constrained by three radiocarbon ages between 574 and 514 cm depth, with ages between 5030 and 3510 cal yr BP (Table 1), and by the occurrence of the FL tephra at 517 cm depth with an age of 3370 ± 70 cal yr BP (Table 2, Figs. 4 and 6; Coltelli et al., 2000; Wagner et al., 2008a). The existing records indicate a second cooling/drying event around 4000 cal yr BP, however, this event is only poorly resolved in core Co1262. A significant decrease of TIC and Ca around ca. 2500 cal yr BP was observed in other cores from Lake Ohrid (Fig. 4), when an anthropogenic impact led to higher erosion in the catchment and increased the clastic matter input into Lake Ohrid (cf. Wagner et al., 2009, 2010; Vogel et al., 2010a). A similar pattern can be observed in core Co1262 at ca. 440 cm depth, where a terrestrial macrofossil remain yielded an age of 2190 cal yr BP (Table 1). Another independent chronological tie point comes from a tephra layer that appears as a thin greyish band just below MWD1 and corresponds to a Sr peak (Figs. 4 and 5). Geochemical identification of volcanic material from this horizon attributes the

Table 2. Major element glass composition of tephras and cryptotephras in core Co1262.

Tephra/Cryptotephra	Shards	SiO_2	TiO_2	Al_2O_3	FeO_{tot}	MnO	MgO	CaO	Na_2O	K_2O	P_2O_5	ClO	Tot. Alkali	Alk. Ratio
Co1262-320	1	47.77	1.14	19.35	7.96	0.12	2.5	10.39	4.95	4.94	0	0.88	9.89	1.00
(AD472/512)	2	48.04	1.13	20.2	7.72	0.38	1.44	8.19	6.39	5.42	0	1.1	11.81	0.85
	3	50.52	0.55	21.72	5.05	0.07	0.82	5.16	6.51	8.86	0	0.75	15.37	1.36
	4	50.49	0.7	21.77	5.22	0.13	0.99	5.96	4.81	9.19	0	0.75	14.00	1.91
	5	54.91	1.58	18.28	7.4	0.15	2.49	5.95	5.08	3.37	0.44	0.34	8.45	0.66
	6	47.72	1.02	20.36	7.75	0.14	2.35	9.81	5.94	3.99	0.15	0.77	9.93	0.67
	7	48.58	0.81	21.25	6.6	0.34	1.2	6.38	7.9	5.35	0.2	1.38	13.25	0.68
	8	48.48	0.8	20.91	7.33	0.17	1.19	7.72	6.48	5.68	0.09	1.16	12.16	0.88
	9	48.88	0.77	20.17	7.76	0.19	1.81	8.56	5.69	5.22	0	0.96	10.91	0.92
	10	48.06	1	20.87	7.08	0.42	1.4	7.76	6.91	5.43	0.07	0.99	12.34	0.79
Co1262-517	1	51.87	1.94	17.78	9.86	0.15	2.69	4.89	6.01	3.77	0.67	0.36	9.78	0.63
(FL)	2	53.84	1.78	19.37	7.47	0.24	1.85	4.6	6.77	3.42	0.37	0.29	10.19	0.51
	3	54.4	1.72	18.7	6.42	0.15	2.38	4.97	5.69	4.58	0.59	0.4	10.27	0.80
	4	53.96	1.89	17.41	8.18	0.23	2.83	5.45	5.58	3.62	0.46	0.38	9.2	0.65
	5	53.4	1.82	17.69	8.53	0.24	3.07	4.97	5.46	4.01	0.52	0.29	9.47	0.73
	6	55.25	1.8	18.1	7.31	0.33	2.23	4.36	6.03	3.91	0.39	0.28	9.94	0.65
	7	53.93	1.44	18.44	7.81	0	3.4	6.36	5.28	2.86	0.31	0.17	8.14	0.54
	8	53.87	1.5	17.87	7.94	0	3.48	6.24	5.54	3.01	0.35	0.2	8.55	0.54
	9	54.01	1.91	17.46	8.17	0.3	2.75	5.55	5.4	3.68	0.45	0.31	9.08	0.68
	10	53.36	1.74	18.26	7.62	0.27	3.37	5.82	5.73	3.15	0.35	0.33	8.88	0.55
	11	54.15	1.54	18.71	7.71	0.1	3.26	5.79	5.01	3.15	0.35	0.22	8.16	0.63
Co1262-709	1	51.87	1.94	17.78	9.86	0.15	2.69	4.89	6.01	3.77	0.67	0.36	9.78	0.63
(Mercato)	2	53.84	1.78	19.37	7.47	0.24	1.85	4.6	6.77	3.42	0.37	0.29	10.19	0.51
	3	54.4	1.72	18.7	6.42	0.15	2.38	4.97	5.69	4.58	0.59	0.4	10.27	0.80
	4	53.96	1.89	17.41	8.18	0.23	2.83	5.45	5.58	3.62	0.46	0.38	9.2	0.65
	5	53.4	1.82	17.69	8.53	0.24	3.07	4.97	5.46	4.01	0.52	0.29	9.47	0.73
	6	55.25	1.8	18.1	7.31	0.33	2.23	4.36	6.03	3.91	0.39	0.28	9.94	0.65
	7	53.93	1.44	18.44	7.81	0	3.4	6.36	5.28	2.86	0.31	0.17	8.14	0.54
	8	53.87	1.5	17.87	7.94	0	3.48	6.24	5.54	3.01	0.35	0.2	8.55	0.54
	9	54.01	1.91	17.46	8.17	0.3	2.75	5.55	5.4	3.68	0.45	0.31	9.08	0.68
	10	53.36	1.74	18.26	7.62	0.27	3.37	5.82	5.73	3.15	0.35	0.33	8.88	0.55
	11	54.15	1.54	18.71	7.71	0.1	3.26	5.79	5.01	3.15	0.35	0.22	8.16	0.63
	12	54.15	1.54	18.71	7.71	0.1	3.26	5.79	5.01	3.15	0.35	0.22	8.16	0.63

tephra to the AD 472/512 eruption of the Somma-Vesuvius (Table 2, Fig. 6; Wagner et al., 2008b; Sulpizio et al., 2010a; Vogel et al., 2010b). The geochemical differentiation between the AD 472 and AD 512 tephras is relatively easy, if the entire succession of the AD 472 eruption is preserved, because the composition of tephras from this event straddles the fields of phonolite, foidites and tephra-phonolites (Fig. 6; Santacroce et al., 2008). It becomes more difficult if only the final products of the AD 472 eruption are recognized, because they have a large compositional overlap with the AD 512 tephra (Sulpizio et al., 2010a, b). Volcanic ejecta from the AD 472 eruption were clearly identified in Lake Shkodra (Sulpizio et al., 2010b; Zanchetta et al., 2012), which is located ca. 160 km northwest of Lake Ohrid. In formerly studied cores from lakes Ohrid and Prespa, however, a mixture of AD 472 and AD 512 tephras was proposed (Vogel et al., 2010b; Damaschke et al., 2012). As the geochemical composition of the tephra at 320 cm depth in core Co1262 is similar to those previously found in lakes Ohrid and Prespa, we assume that it also includes the AD 512 deposits. The sandy horizon at the base of MWD1 is deposited directly above the AD 472/512 tephra. Calculating a mean sedimentation rate of ca. 1 mm yr^{-1} between the carbonate decline at ca. 440 cm depth (2200 cal yr BP) and the occurrence of the AD 472/512 tephra (1478/1438 cal yr BP) at 320 cm depth, we can assume that the mass movement occurred less than 20 yr after the deposition of the AD 472/512 tephra. Potential triggers for a mass movement include delta collapses, rockfalls, lake level changes, or earthquakes (e.g., Schnellmann et al., 2006; Girardclos et al., 2007). A delta collapse can be excluded, as there is no inlet close to the coring location and deltaic deposits cannot be observed in the seismic data (Figs. 2 and 3). The steep subaquatic slopes close to the Lini Peninsula could have promoted rockfalls, but typical rockfall structures, such as relatively fresh scarps onshore or subaquatic basin-marginal cones cannot be observed (cf.

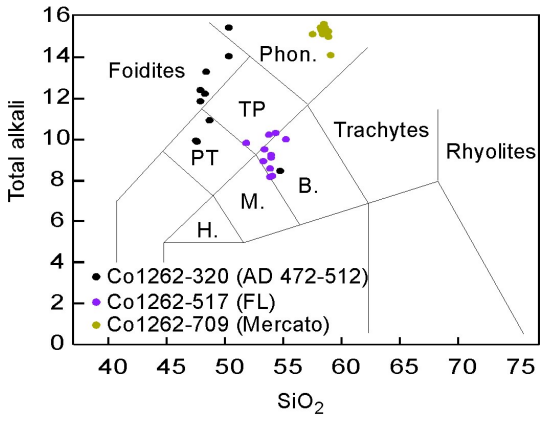

Fig. 6. Classification of tephras and cryptotephras recognised in core Co1262 from Lake Ohrid by means of the total alkali vs. silica diagram (TAS, Le Bas et al., 1986). The raw data of tephras and cryptotephras is given in Table 1.

Schnellmann et al., 2006; Figs. 1 and 2). The existing records from lakes Ohrid and Prespa or paleoclimatic reconstructions from the region do not indicate that the early 6th century AD was characterised by significant changes in lake level and hydrology (e.g., Wagner et al. 2009, 2010, 2012; Lindhorst et al., 2010; Vogel et al., 2010a; Leng et al., 2012). However, historical documents indicate that an earthquake destroyed the city of Lychnidus (Ohrid) in the early 6th century AD. Potential candidates for such an earthquake are the 518 AD earthquake, which according to some authors more affected the city of Scupi (Skopje; Aliaj et al., 2004; Ambraseys, 2009), or the 526 or 527 AD earthquake, which concentrated more on the Ohrid region (Ambrasyes, 2009; Reicherter et al., 2011). Although the bioturbated structure of the sediment core and the impossible differentiation between the AD 472 and AD 512 tephra do not allow a chronological discrimination between the two (or three) earthquakes, it is evident that MWD1 must have occurred during the early 6th century AD and is likely related to one of these earthquakes. An early 6th century AD age of MWD1 is confirmed by the patterns of TIC and Ca on top of it, which are again similar to those of former cores from Lake Ohrid. After low Ca between 121 and 100 cm depth, which would correspond to a period of ca. 200 yr based on a sedimentation rate of ca. 1 mm yr^{-1}, the increase of Ca and TIC can be correlated with the onset of the MWP, which culminated at 900–1000 AD in other cores from lakes Ohrid and Prespa (summarised in Wagner et al., 2010 and Aufgebauer et al., 2012; Fig. 4) and between 1000 and 1200 AD in the eastern Mediterranean (Kaniewski et al., 2011). The subsequent minimum of Ca and TIC correlates with the LIA (Wagner et al., 2009, 2010; Vogel et al., 2010a), and is confirmed by the age of macrofossil remains at 17 cm depth (140 cal yr BP, Table 1). Recent warming led to increasing Ca and TIC at the sediment surface.

5 Comparison with other sites

According to the chronological tie points and the patterns of geochemical fluctuations the Holocene sedimentation rates at the Lini site Co1262 are varying distinctly (Fig. 4) and are relatively high compared with other sites from the lake. After subtracting the mass wasting deposits in core Co1262, the Holocene sediments comprise almost 8 m, which is about twice as much as the Holocene sediment succession in the northeastern part of the lake (core Co1202, Fig. 1, Vogel et al., 2010a). In the southeastern part of the lake, the thickness of the Holocene sediment succession was similar (core Lz1120, Fig. 1, Wagner et al., 2009), but this coring location is close to an inlet. There is no significant inlet close to the site Co1262 and Lake Ohrid is an oligotrophic lake with relatively simple basin morphology. The significant variations in sedimentation rates and the overall high sedimentation rate suggest lake internal currents (Vogel et al., 2010c) and/or contourite drift as observed in Lake Prespa (Wagner et al., 2012) or other lakes (e.g., Girardclos et al., 2003; Gilli et al., 2005). Another reason for the varying but high sedimentation is probably due to the tectonic activity along the western margin of the lake. According to seismic data, the region around Lini Fault, which is one of the oldest faults in Lake Ohrid Basin, located offshore of Lini Peninsula is one of the most active areas. Half-grabens were developed within the hanging wall of related fault structures, creating depocentres that are filled with re-deposited material from the footwall. Seismic activity probably also induced the Udenisht Slide in the southwestern part of the lake (Fig. 1; Lindhorst et al., 2012). The chronological control of this slide is poor, but extrapolation of sedimentation rates of overlying sediment indicates that this slide is younger than 1500 yr and also probably associated with an early 6th century AD earthquake (Lindhorst et al., 2012). These observations strongly suggest that major earthquakes in Lake Ohrid triggered lacustrine slides and are confirmed by onshore information, which indicate that the morphology of the Ohrid basin is formed by frequent earthquakes of magnitudes between M 6.0 and 7.0 (Reicherter et al., 2011). Hence age estimation of these mass wasting deposits can be used as a proxy for estimating paleoseismicity. For example, the thick mass wasting deposit MWD2, which underlies core sequence Co1262, could originate from an older, Late Pleistocene earthquake. Most existing sediment records from Lake Ohrid spanning into the last glacial cycle have disturbed sedimentation at the Late Pleistocene/Holocene transition (Wagner et al., 2009; Vogel et al., 2010a), which might be related to high seismic activity. There are a number of other slides indicated in multichannel seismic sections Lindhorst et al. (2012), which suggest that a long paleoseismic record will become available once a deep drill core will be recovered from Lake Ohrid.

6 Conclusions

The Co1262 record shows the high potential of Lake Ohrid for paleoseismicity investigations, by combining seismic, sedimentological, climatic, tephrostratigraphic, and historical information. The most significant mass wasting deposit in core Co1262 is ca. 2 m thick and overlays a tephra, which is correlated with the AD 472/512 eruption of the Somma-Vesuvius. The exact age of the mass wasting deposit cannot be defined, because there is a geochemical overlap of the AD 472 and the AD 512 tephra and the sediments of Lake Ohrid are not annually laminated. However, the lack of apparent erosional discordance at the base of the mass wasting deposit and the small distance to the AD 472/512 tephra imply that the mass wasting deposit occurred in the early 6th century AD. This age is confirmed by the sediments, which overlay the mass wasting deposit and show characteristic variations related to the Medieval Warm Period and the Little Ice Age. Several potential triggers for this mass wasting event, such as delta collapses, rockfalls, or lake level changes can be excluded or are unlikely. More likely is a correlation with a historical earthquake, which destroyed the city of Lychnidus (Ohrid) in the early 6th century AD. According to historical documents, this earthquake could have occurred at 518 AD, 526 AD, or 527 AD. Within the framework of such uncertainties, core Co1262 is a very nice example of Holocene paleoseismicity studies. More data from other locations of the lake and similar examples from older periods will be needed to shed more light on the earthquake history of the lake.

Acknowledgements. The study was funded by the German Research Foundation (WA 2109/11) and by the International Continental Scientific Drilling Program (ICDP).

Edited by: K. Reicherter

References

Albrecht, C. and Wilke, T.: Ancient Lake Ohrid: biodiversity and evolution, Hydrobiology, 615, 103–140, 2008.

Aliaj, S., Adams, J., Halchuk, S., Sulstarova, E., Peci, V., and Muco, B.: Probabilistic Seismic Hazard Maps for Albania, 13th World Conference on Earthquake Engineering, Vancouver, BC, Canada, 2004.

Ambraseys, N.: Earthquakes in the Mediterranean and Middle East, Cambridge University Press, New York, 2009.

Ambraseys, N. and Jackson, J.: Seismicity and Associated Strain of Central Greece between 1890 and 1988, Geophys. J. Int., 101, 663–708, 1990.

Aufgebauer, A., Panagiotopoulos, K., Wagner, B., Schäbitz, F., Viehberg, F. A., Vogel, H., Zanchetta, G., Sulpizio, R., Leng, M. J., and Damaschke, M.: Climate and environmental change in the Balkans over the last 17 ka recorded in sediments, Quaternary Int., 274, 122–135, 2012.

Beck, C., Reyss, J.-L., Leclerc, F., Moreno, E., Feuillet, N., Barrier, L., Beauducel, F., Boudon, G., Clément, V., Deplus, C., Gallou, N., Lebrun, J.-F., Le Friant, A., Nercessian, A., Paterne, M., Pichot, T., and Vidal, C.: Identification of deep subaqueous coseismic scarps through specific coeval sedimentation in Lesser Antilles: implication for seismic hazard, Nat. Hazards Earth Syst. Sci., 12, 1755–1767, doi:10.5194/nhess-12-1755-2012, 2012.

Bordon, A., Peyron, O., Lézine, A.-M., Brewer, S., and Fouache, E.: Pollen-inferred Late-Glacial and Holocene climate in southern Balkans (Lake Maliq), Quaternary Int., 200, 19–30, 2009.

Burchfiel, B., Nakov, R., Dumurdzanov, N., Papanikolaou, D., Tzankov, T., Serafimovski, T., King, R., Kotzev, V., Todosov, A., and Nurce, B.: Evolution and Dynamics of the Cenozoic Tectonics of the South Balkan Extensional System, Geosphere, 4, 919–938, doi:10.1130/GES00169.1, 2008.

Caron, B., Sulpizio, R., Zanchetta, G., Siani, G., and Santacroce, R.: The Late Holocene to Pleistocene tephrostratigraphic record of Lake Ohrid (Albania), CR Acad. Sci., 342, 453–466, 2010.

Coltelli, M., Del Carlo, P., and Vezzoli, L.: Stratigraphic constrains for explosive activity in the past 100 ka at Etna volcano, Italy, Int. J. Earth Sci., 89, 665–677, 2000.

Damaschke, M., Sulpizio, R., Zanchetta, G., Wagner, B., Böhm, A., Nowaczyk, N., Rethemeyer, J., and Hilgers, A.: Tephrostratigraphic studies on a sediment core from Lake Prespa in the Balkans, Clim. Past Discuss., 8, 4443–4492, doi:10.5194/cpd-8-4443-2012, 2012.

EMSC: Europen Mediterranean Seismological Centre, available at: www.emsc-csem.org, last access: 18 December 2012.

Gilli, A., Anselmetti, F. S., Ariztegui, D., Beres, M., McKenzie, J. A., and Markgraf, V.: Seismic stratigraphy, buried beach ridges and contourite drifts: the Late Quaternary history of the closed Lago Cardiel basin, Argentina (49° S), Sedimentology, 52, 1–23, 2005.

Girardclos, S., Baster, I., Wildi, W., and Pugin, A.: Bottom-current and wind-pattern changes as indicated by Late-Glacial and Holocene sediments from western Lake Geneva (Switzerland), Eclogae Geol. Helv., 96, 39–48, 2003.

Girardclos, S., Schmidt, O. T., Sturm, M., Ariztegui, D., Pugin, A., and Anselmetti, F. S.: The 1996 AD delta collapse and large turbidite in Lake Brienz, Mar. Geol., 241, 137–154, 2007.

Hoffmann, N., Reicherter, K., Fernández-Steeger, T., and Grützner, C.: Evolution of ancient Lake Ohrid: a tectonic perspective, Biogeosciences, 7, 3377–3386, doi:10.5194/bg-7-3377-2010, 2010.

Kaniewski, D., Van Campo, E., Paulissen, E., Weiss, H., Bakker, J., Rossignol, I., and Van Lerberghe, K.: The medieval climate anomaly and the little Ice Age in coastal Syria inferred from pollen-derived palaeoclimatic patterns, Global Planet. Change, 78, 178–187, 2011.

Le Bas, M. J., Le Maitre, R. W., Streckeisen, A., and Zanettin, B.: A chemical classification of volcanic rocks based on the total alkali-silica diagram, J. Petrol., 27, 745–750, 1986.

Leng, M. J., Wagner, B., Aufgebauer, A., Panagiotopoulos, K., Vane, C., Snelling, A., Haidon, C., Woodley, E., Vogel, H., Zanchetta, G., Sulpizio, R., and Baneschi, I.: Understanding past climatic and hydrological variability in the Mediterranean from Lake Prespa sediment isotope and geochemical record over the last glacial cycle, Quaternary Sci. Rev., in press, 2012.

Lindhorst, K., Vogel, H., Krastel, S., Wagner, B., Hilgers, A., Zander, A., Schwenk, T., Wessels, M., and Daut, G.: Stratigraphic

analysis of lake level fluctuations in Lake Ohrid: an integration of high resolution hydro-acoustic data and sediment cores, Biogeosciences, 7, 3531–3548, doi:10.5194/bg-7-3531-2010, 2010.

Lindhorst, K., Gruen, M., Krastel, S., and Schwenk, T.: Hydroacoustic Analysis of Mass Wasting Deposits in Lake Ohrid (FYR Macedonia/Albania), Submarine Mass Movements and Their Consequences, 245–253, 2012.

Muço, B., Vaccari, F., Panza, G., and Kuka, N.: Seismic zonation in Albania using a deterministic approach, Tectonophysics, 344, 277–288, 2002.

Reicherter, K., Hoffmann, N., Lindhorst, K., Krastel, S., Fernandez-Steeger, T., Grützner, C., and Wiatr, T.: Active Basins and Neotectonics: Morphotectonics of the Lake Ohrid Basin (FYROM and Albania), Z. Dtsch. Ges. Geowiss., 162, 217–234, 2011.

Reimer, P. J., Baillie, M. G. L., Bard, E., Bayliss, A., Beck, J. W., Blackwell, P. G., Ramsey, C. B., Buck, C. E., Burr, G. S., Edwards, R. L., Friedrich, M., Grootes, P. M., Guilderson, T. P., Hajdas, I., Heaton, T. J., Hogg, A. G., Hughen, K. A., Kaiser, K. F., Kromer, B., McCormac, F. G., Manning, S. W., Reimer, R. W., Richards, D. A., Southon, J. R., Talamo, S., Turney, C. S. M., van der Plicht, J., and Weyhenmeyer, C. E.: IntCal09 and Marine09 Radiocarbon Age Calibration Curves, 0–50,000 Years cal BP, Radiocarbon, 51, 1111–1150, 2009.

Rethemeyer, J., Fülöp, R. H., Höfle, S., Wacker, L., Heinze, S., Hajdas, I., Patt, U., König, S., Stapper, B., and Dewald, A.: Status report on sample preparation facilities for 14C analysis at the new CologneAMS center, Nucl. Instrum. Meth. B, 294, 168–172, doi:10.1016/j.nimb.2012.02.012, 2013.

Santacroce, R., Cioni, R., Marianelli, P., Sbrana, A., Sulpizio, R., Zanchetta, G., Donahue, D., and Joron, J.-L.: Age and whole rock-glass compositions of proximal pyroclastics from the major esplosive eruption of Somma-Vesuvius: a review as a tool for distal tephrostratigraphy, J. Volcanol. Geoth. Res., 177, 1–18, 2008.

Schnellmann, M., Anselmetti, F. S., Giardini, D., McKenzie, J. A., and Ward, S.: Prehistoric earthquake history revealed by lacustrine slump deposits, Geology, 30, 1131–1134, 2002.

Schnellmann, M., Anselmetti, F. S., Giardini, D., and McKenzie, J. A.: Mass movement-induced fold-and-thrust belt structures in unconsolidated sediments in Lake Lucerne (Switzerland), Sedimentology, 52, 271–289, 2005.

Schnellmann, M., Anselmetti, F. S., Giardini, D., and McKenzie, J. A.: 15,000 Years of massmovement history in Lake Lucerne: Implications for seismic and tsunami hazards, Eclogae Geol. Helv., 99, 409–428, 2006.

Stankovic, S.: The Balkan Lake Ohrid and its living world, Monographiae Biologicae IX, edited by: Junk, W., Den Haag, The Netherlands, 1960.

Stuiver, M. and Reimer, P. J.: Extended (super 14) C data base and revised CALIB 3.0 (super 14) C age calibration program, 1993.

Suhadolc, P., Sandron, D., Fitzko, F., and Costa, G.: Seismic Ground Motion Estimates for the M6.1 Earthquake of July 26, 1963 at Skopje, Republic of Macedonia, Acta Geod. Geophys. Hu., 39, 319–326, 2004.

Sulpizio, R., Zanchetta, G., D'Orazio, M., Vogel, H., and Wagner, B.: Tephrostratigraphy and tephrochronology of lakes Ohrid and Prespa, Balkans, Biogeosciences, 7, 3273–3288, doi:10.5194/bg-7-3273-2010, 2010a.

Sulpizio, R., van Welden, A., Caron, B., and Zanchetta, G.: The Holocene tephrostratigraphic record of Lake Shkodra (Albania and Montenegro), J. Quaternary Sci., 25, 633–650, 2010b

Vogel, H., Wagner, B., Zanchetta, G., Sulpizio, R., and Rosén, P.: A paleoclimate record with tephrochronological age control for the last glacial-interglacial cycle from Lake Ohrid, Albania and Macedonia, J. Paleolimnol., 44, 295–310, 2010a.

Vogel, H., Zanchetta, G., Sulpizio, R., Wagner, B., and Nowaczyk, N.: A tephrostratigraphic record for the last glacial interglacial cycle from Lake Ohrid, Albania and Macedonia, J. Quaternary Sci., 25, 320–338, 2010b.

Vogel, H., Wessels, M., Albrecht, C., Stich, H.-B., and Wagner, B.: Spatial variability of recent sedimentation in Lake Ohrid (Albania/Macedonia), Biogeosciences, 7, 3333–3342, doi:10.5194/bg-7-3333-2010, 2010c.

Wagner, B., Reicherter, K., Daut, G., Wessels, M., Matzinger, A., Schwalb, A., Spirkovski, Z., and Sanxhaku, M.: The potential of Lake Ohrid for long-term palaeoenvironmental reconstructions, Palaeogeogr. Palaeocl., 259, 341–356, 2008a.

Wagner, B., Sulpizio, R., Zanchetta, G., Wulf, S., Wessels, M., and Daut, G.: The last 40 ka tephrostratigraphic record of Lake Ohrid, Albania and Macedonia: a very distal archive for ash dispersal from Italian volcanoes, J. Volcanol. Geoth. Res., 177, 71–80, 2008b.

Wagner, B., Lotter, A. F., Nowaczyk, N., Reed, J. M., Schwalb, A., Sulpizio, R., Valsecchi, V., Wessels, M., and Zanchetta, G.: A 40,000-year record of environmental change from ancient Lake Ohrid (Albania and Macedonia), J. Paleolimnol., 41, 407–430, 2009.

Wagner, B., Vogel, H., Zanchetta, G., and Sulpizio, R.: Environmental change within the Balkan region during the past ca. 50 ka recorded in the sediments from lakes Prespa and Ohrid, Biogeosciences, 7, 3187–3198, doi:10.5194/bg-7-3187-2010, 2010.

Wagner, B., Aufgebauer, A., Vogel, H., Zanchetta, G., Sulpizio, R., and Damaschke, M.: Late Pleistocene and Holocene contourite drift in Lake Prespa (Albania/F.Y.R. of Macedonia/Greece), Quaternary Int., 274, 259–272, 2012.

Zanchetta, G., Sulpizio, R., Roberts, N., Cioni, R., Eastwood, W. J., Siani, G., Caron, B., Paterne, M., and Santacroce, R.: Tephrostratigraphy, chronology and climatic events of the Mediterranean basin during the Holocene: an overview, Holocene, 21, 33–52, 2011.

Zanchetta, G., van Welden, A., Baneschi, I., Drysdale, R., Sadori, L., Roberts, N., Giardini, M., Beck, C., and Pascucci, V.: Multiproxy record for the last 4500 years from Lake Shkodra (Albania/Montenegro), J. Quaternary Sci., 27, 780–789, doi:10.1002/jqs.2563, 2012.

8 Discussion - Understanding sedimentary processes

In order to study modern and past sedimentary processes in lakes, sedimentologists can choose between several archives, such as outcrops, geomorphological features, sediment cores, or hydro-acoustic data (Cohen, 2003). Not all archives are suitable to resolve specific sedimentary problems or they are not available in every study area (cf. Cohen, 2003). The strengths, weaknesses and limits of data obtained from bedrock samples from the catchment, inlet streams, sediment cores, and hydro-acoustic surveys in the investigated study areas will be discussed below.

8.1 Surface sediment and catchment samples

To obtain information about the modern sediment composition of a lake, multiple spatially distributed short sediment cores (< 2 cm sample thickness) can be analyzed for their sedimentary properties, such as conducted at Lake El'gygytgyn (cf. chapter 2) and Lake Ohrid (Vogel et al., 2010a). Studies on surface sediments can yield crucial insights into lake-internal processes, such as current systems, nutrient and sediment distribution, productivity, and post-depositional re-organization of chemical compounds (cf. chapter 2, Vogel et al., 2010a). Inlet stream or bedrock samples from the catchment can be included into the analyses which can improve the knowledge about external influences, such as sediment, nutrient or OM supply by rivers or creeks, but also about probable source rock effects or weathering conditions in the catchment (cf. chapter 2). For example at Lake El'gygytgyn, the distribution of mafic rock related elements (Cr, Cu, Zn, V, Ni, Co) could be linked to basaltic rocks in southeastern parts of the catchment (cf. chapter 2). Moreover, the high correlation of acid related elements (Ba, Sr, AlO_3, Na_2O, Ca_2O, K_2O) to coarse grain-size fractions and feldspars imply cryogenic weathering in the catchment (cf. chapter 2).

Benefit of investigations on modern processes in a lake area is that the interpretation can be substantiated by simple observations. For example at Lake El'gygytgyn, the occurrence of a suspension cloud of silt-sized and clayey material focusing to the lake center was observed during field work in 2003 and explains a tongue of coarse-grained material in the surface sediments (cf. chapter 2). Moreover, observations from other, comparable lakes can also help to improve the understanding of sedimentary processes. For example a pronounced peak at around 100 µm in the grain-size distribution of Lake El'gygytgyn is probably linked to ice floe transportation and sediment supply onto the ice cover by rivers or creeks. Such a process was initially observed at Lake Baikal (Vologina et al., 2005) and subsequently confirmed for Lake El'gygytgyn for modern and past conditions (cf. chapters 2,3). Similarly, filtering of allochthonous clastic material and nutrients by extensive reed beds was observed in Lake Dojran (cf. chapter 6) and Lake Baiyangdian in North China (Wang et al., 2002).

Modern observations are commonly limited to some decades and also surface sediment samples only cover the last centuries. At Lake El'gygytgyn, 2 cm thick surface samples roughly represent the past 150 years (cf. chapter 2). Although sediment cores enable a cost-effective and rapid recovery of a continuous sediment sequence (Cohen, 2003), the recovery and analyses of multiple, spatially distributed

long sediment cores are often expensive and time consuming. However, individual sediment cores lack a perspective on spatial variability of sedimentary processes in a lake system (Cohen, 2003). This might result in misinterpretations, e.g. variations in sediment composition or grain-size distribution could be interpreted in terms of temporal variations in the paleoenvironmental or -climatologic settings at the lake, even though they are rather triggered by spatial variations.

8.2 Hydro-acoustic data

Hydro-acoustic surveys are a rapid and cost-effective approach to obtain spatial data about the sedimentation in lake systems. Information about the sediment architecture in a lake basin can help to detect undisturbed, horizontally bedded deposits in lacustrine sediment sequences, which are potential coring locations (cf. chapter 6, Niessen et al., 2007; Lindhorst et al., 2009; Aufgebauer et al., 2012). Furthermore, hydro-acoustic data can be used to differentiate between pelagic and event deposition. For example, the hydro-acoustic data from Lake Ohrid yield a high number of MWDs in the sediment successions (Lindhorst et al., 2012). Various MWDs are also reported on seismic data from El'gygytgyn (cf. chapter 5, Niessen et al., 2007). MWDs can be identified in hydro-acoustic data by hummocky reflectors indicating erosion processes (Lindhorst et al., 2010) or transparent or chaotic seismic areas (cf. chapters 5, 7). Transparent and chaotic areas in the hydro-acoustic data also mark three MWDs close to the Lini Peninsula in Lake Ohrid (cf. chapter 7). The upper about 2 m thick MWD was also observed in core Co1262 and a preliminary age model based on volcanostratigraphic tie points, radiocarbon dating and wiggle matching implied that the MWD was deposited in the 6^{th} century (cf. chapter 7). However, the vertical resolution of hydro-acoustic data is limited, e.g. to 1 m for Mini GI gun seismic and to 2 to 6 cm for high-resolution Inomar SES-2000 sub-bottom profiling equipment (cf. chapter 7, Wunderlich and Müller, 2003). Thus, very thin MWDs might not be displayed deeper in parts of the seismic profiles, where only Mini GI gun data is available. For example, less than 4 cm thick MWDs in the sediment sequence of core Co1262 (Lake Ohrid, cf. chapter 7) or various thin MWDs in the sediment sequence of Lake El'gygytgyn (Sauerbrey et al., 2013) are not displayed in the hydro-acoustic data (cf. chapter 5, 7).

Hydro-acoustic data is also frequently used to detect sediment structures that indicate lake-level fluctuations, such as clino-forms, down stepping wedges, as well as onlap, offlap and downlap structures (Hunt and Tucker, 1992; Abbott et al., 2000; Lindhorst et al., 2010; Wagner et al., 2012). Similar to the 2 m thick MWD close to the Lini Peninsula in Lake Ohrid, sediment structures indicating lake-level fluctuations in hydro-acoustic data can be linked to sediment data from cores. For example, in the sediment sequence of Lake Dojran, a hydro-acoustic reflector in 4.46 m sediment depth covers a lacustrine terrace in northern parts of the lake (cf. chapter 6). This indicates a higher lake-level and a rearrangement of the bathymetry with an enlarged lake surface area and wind fetch. Moreover, the reflector corresponds to a pronounced peak in the total sulfur (TS) content at 470 cm sediment depth (10 000 cal yr BP), which implies a distinct change in the redox conditions in the surface sediments and improved mixing conditions afterwards, likely triggered by the higher lake level and increased lake surface area (cf. chapter 6). Hence, hydro-acoustic data can be used to substantiate the interpretation of data obtained from a sediment core.

8.3 Sediment cores

Although, hydro-acoustic reflectors can be interpreted as probable changes in the lithology (Cohen, 2003), only sediment cores provide detailed insights into the composition of lacustrine deposits. Initial analyses of a sediment core commonly include a visual description, which can provide an important overview about the deposits and the sedimentary processes in the lake. Basic lithology data, such as sediment structure, texture, grain-size, and color can be used to determine sedimentary units, including MWDs (cf. chapter 7, and e.g. Sauerbrey et al., 2013), tephra layers (cf. chapter 7, and e.g. Damaschke et al., 2013), and pelagic sediments (cf. chapters 6, 7, and e.g. Melles et al., 2012). MWDs can be recognized by various sedimentary features, such as sorting, rounding, grading structures, or faulting (cf. chapter 7, Sauerbrey et al., 2013).

Volcanoclastic deposits can be identified by conspicuousness in grain-size compositions, color, and in the occurrence of glass shards (cf. chapter 7, Vogel et al., 2010c; Damaschke et al., 2013). However, ash deposits are frequently preserved as cryptotephra layers, which are difficult to detect as the ash particles are finely dispersed in the sediment (cf. chapter 7).

Sedimentary units representing normal pelagic sedimentation at lakes El'gygytgyn, Dojran and Ohrid may contain varying amounts of clastic material, endogenic calcite, OM and biogenic remains, such as diatoms, ostracodes or mollusks (cf. chapter 6, Melles et al., 2007; Wagner et al., 2009). Lithologic data from such horizons can give first insights into lake-internal environmental settings during the deposition. For example, laminated and bioturbated sedimentary units in the deposits of lakes El'gygytgyn (Melles et al., 2012), Ohrid (Wagner et al., 2009; Vogel et al., 2010b), and Dojran (cf. chapter 6) could be linked to different mixing conditions of the water column. Less intensive mixing, a stratified water column and low oxygen availability at the sediment/water interface are associated with laminated sequences, whereas intensive bioturbation implies improved mixing and sufficient oxygen supply to the bottom water.

Grain size and grain texture

Naked-eye grain-size and texture estimations can provide first information on the transport energy and transportation mechanism during the deposition. Coarse-grained deposits might indicate a low lake level with high transport energies, intensive wave activity, strong inflow, or strong lake-internal currents as observed at lakes Dojran (cf. chapter 6), El'gygytgyn (cf. chapter 2), or Prespa (Aufgebauer et al., 2012), or even fluvial influences. Moreover, the angularity of single grains and the sorting of the sediment can give crucial insights into the transport mechanism of clastic material. For example in the lowermost sequence of core Co1260 from Lake Dojran, poorly sorted material mainly consists of clay clasts and coarse silt with the sporadic occurrence of drop stones (cf. chapter 6). Firstly, this might indicate redeposition and a low lake level as the clay clasts were likely formed of old lacustrine sediments under subaerial conditions. Secondly, variable transport energies and/or additional transportation mechanism might be indicated by the overall poor sorting of the material. Ice floe transportation is implied by the occurrence of gravel- to pebble-sized drop stones. Thereby, the angular appearance of the drop stones at Lake Dojran might be related to a short transport distance in the catchment. Additional transportation

mechanism also includes eolian sediment supply directly into the lake or onto an ice cover which, however, could not be verified for sediments from Lake Dojran (cf. chapter 6). At Lake El'gygytgyn, sporadically occurring clay clasts are explained by eolian clastic sediment supply onto the ice cover, wherefrom the material moves through the ice along vertical conduits and might be compacted to 1 to 2 mm clasts (cf. chapter 3, and Melles et al., 2007).

More detailed information about the grain-size distribution can be obtained by granumoleric analyses with a laser particle analyzer. For example, the Saturn DigiSizer5200 which was used in these studies detects particles with diameters between 0.1 and 1000 µm. However, grain-diameters coarser than 600 µm might produce considerable errors during the measurement (cf. chapter 3), and air bubbles in a range of 100 to 500 µm within the transport liquid (demineralized and degassed water) may be identified as grains (cf. chapters 2, 3, and Loizeau et al., 1994). Since the Saturn DigiSizer5200 calculates the grain-size statistics from the average of three runs, errors caused by air bubbles can be identified by high standard deviations. Within the range 0.1 and 1000 µm, the Saturn DigiSizer5200 calculates 160 grain-size classes. This high resolution enables the reconstruction of multiple transport energies during the deposition, such as indicated by the polymodal grain-size patterns of interglacial samples from Lake El'gygytgyn (cf. chapters 2, 3).

In order to reconstruct transport energies and processes by using grain-size data, autochthonous matter, i.e. organic components, biogenic silica (SiO_2), endogenic calcite ($CaCO_3$), or vivianite ($Fe_3(PO_4)_2\,8\,H_2O$), have to be removed from the sample. For this purpose, multi-step pre-treatment procedures should be applied (cf. chapter 3). During the grain-size analyses for samples from ICDP site 5011-1 (Lake El'gygytgyn), the pre-treatment step to remove biogenic silica failed for a batch of 60 samples. The according samples yield significantly higher silt and lower clay contents (cf. Fig. 8.1), likely associated with the presence of diatoms with a diameter of around 20 µm which had been observed in the sediments of Lake El'gygytgyn (cf. Cremer and Wagner, 2003). Thus, each pre-treatment step should be evaluated by e.g. elemental analyses, Fourier-Transformed Infrared Sspectroscopy (FTIRS), X-Ray Diffraction (XRD), Scanning Electron Microscopy (SEM), or optical microscopy (cf. chapter 3), at least on representative samples in order to avoid systematical errors.

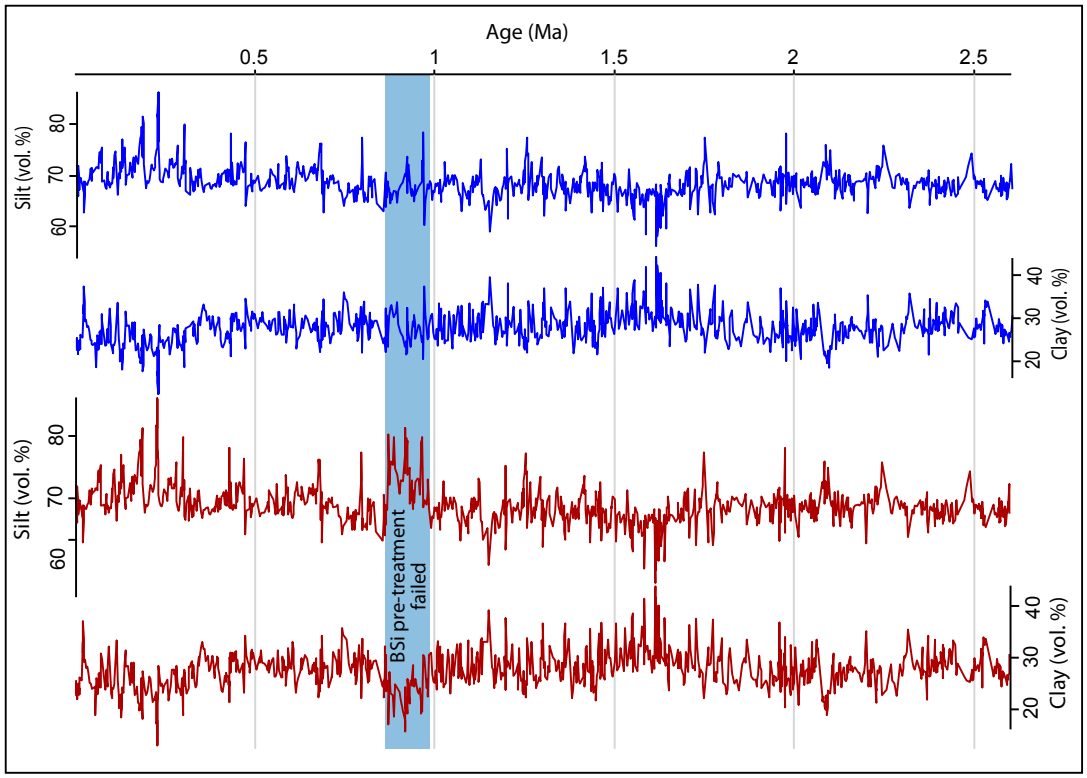

Figure 8.1: Blue: Silt and clay contents of ICDP core 5011-1 from Lake El'gygytgyn during the Quaternary. Red: Silt and clay content of the same sequence including the samples where for one sample batch the pre-treatment step to remove biogenic silica from the sediment failed (blue shaded area). The according samples yield noticeable higher silt and lower clay contents, which can be explained by a high abundance of diatoms in the samples

Inorganic geochemistry

Information about sediment properties can also be derived from inorganic geochemistry data. Inorganic geochemistry data can be obtained from powdered, discrete samples by ICP-OES or conventional XRF analyses (cf. chapter 2). Moreover, it can be obtained by XRF-scanning on split core halves (cf. chapters 6, 7). XRF- scanning is a rapid, non-destructive method to obtain high-resolution, semi-quantitative data about the elemental composition of a sediment succession (Jansen et al., 1998; Croudace et al., 2006; Rothwell et al., 2006). Inaccuracies in comparison to conventional XRF analyses are related to grain-size effects, variations in mineralogy, water content, porosity, and by the air path between the core and the X-ray detector (Jansen et al., 1998; Croudace et al., 2006). Using a combination of Cr and Mo X-ray tubes, elements with atomic numbers higher than 13 (Al) can be detected (Croudace et al., 2006). XRF data can be used to identify horizons with a special chemical composition such as tephra layers, cryptotephra layers, or MWDs (cf. chapter 7). For example, pronounced peaks in K, Sr, and Zr counts in the sediment sequence of Lake Ohrid correspond with the deposition of cryptotephra layers (cf. chapter 7 and Vogel et al., 2010c), as the chemical composition of the ash particles differs from the composition of the pelagic sediments. MWDs can also be identified by suspiciousness in clastic related elements (Al, K, Ti, Fe) in the XRF data (cf. chapters 6, 7, and Cohen, 2003). For example, in the sediment sequence Co1262 of Lake Ohrid the 2 m thick, homogenous MWD is characterized by stable K counts. In contrast, turbidites that are characterized by fining upward trends in the particle diameter (e.g. Bouma,

1962; Sauerbrey et al., 2013) can be identified in XRF data by decreasing or increasing trends due to grain-size effects. Grain-size effects on elemental compositions of lake sediments have been reported for example for Lake El'gygytgyn, where redundancy analyses (RDA) yield a high correlation of coarse silt to fine sand and K_2O, CaO, Sr, Ba, Na_2O, and Al_2O_3, and of medium silt to coarse silt to TiO_2, Fe_2O_3, Ni, and Co (cf. chapter 2).

In addition to the identification of event deposits, XRF scanning data can also yield high-resolution information about pelagic sediments and environmental conditions. Variations in the amount of clastic material as derived from Al, K, Ti or Fe counts can be explained by variations in erosional processes in the catchment area (cf. chapter 6) and/or by changes of the detrital input by rivers (Vogel et al., 2010b; Wennrich et al., 2013). Furthermore, Zr is widely used as an indicator for eolian input as it is regarded to originate from zirconium, a mineral relatively resistant against chemical and physical weathering (Müller et al., 2001). However, mutual dilution processes caused by variations of biogenic silica, endogenic calcite or OM contents can affect elemental concentrations as indicator for clastic sedimentation. For example at Lake Dojran, high K counts correspond to negligible contents of endogenic calcite and decreasing amounts of OM after 2 800 cal yr BP (cf. chapter 6). This might suggest that dilution processes could explain the high K counts. Independent data, such as $\delta_{13}C_{carb}$ can help to untangle such dilution processes. Increased clastic supply could be triggered by intensive erosion in the catchment, which might be at Lake Dojran reflected by low $\delta_{13}C_{carb}$ values due to enhanced supply of soil-derived CO_2 to the lake after 2 800 cal yr BP (cf. chapter 6).

Biogeochemical data

Chemical data from XRF scanning can also yield information about biological processes in a lake system. For example, productivity by diatoms can be derived from the Si/Ti ratio. The Si/Ti ratio represents the amount of biogenic silica in the sediments if grain-size effects can be excluded (cf. chapter 3, Melles et al., 2012; Wennrich et al., 2013). Whereas Ti is restricted to detrital sources, Si can be incorporated in biogenic silica and mineralogical components (cf. Melles et al., 2012; Wennrich et al., 2013). However, Si/Ti ratios can indicate incorrect BSi contents as high water contents reduce the count rates of XRF data, in particular for light elements such as Al and Si (cf. Tjallingii et al., 2007; Sprenk et al., 2013).

Information about primary productivity and the trophic status of a lake can also be derived from Ca as a component of authigenic-precipitated calcite. At lakes Ohrid and Dojran, the calcite content in the sediment is attributed to photosynthesis-induced inorganic precipitation (cf. chapters 6, 7, and Vogel et al., 2010b and references therein). Additional contributions to the calcite content are due to biogenic sources such as shell fragments or ostracod valves (cf. chapter 6, and Vogel et al., 2010b), and diagenetic siderite (Cohen, 2003; Aufgebauer et al., 2012). Ca can also be incorporated in detrital material (Cohen, 2003), possibly leading to misinterpretations of Ca profiles. A comparison of Ca records and total inorganic carbon (TIC) data, which is commonly available only in lower resolution, can yield the influence of detrital Ca. For example at Lake Ohrid, detrital supply has only negligible impact on Ca counts (cf. chapter 7, Fig. 4).

More detailed information about biological and chemical processes in a lake can be derived from biogeochemical data such as total organic carbon (TOC), the total nitrogen (TN), as well as from the total sulfur (TS) content. The TOC content is widely used as an indicator for amount of finely dispersed OM in the sediment (cf. chapters 6, 7, and Cohen, 2003), whereby OM in lake sediments only reflects a proportion of the biomass that sank to the lake floor as parts are degraded after burial (Cohen, 2003). At Lake Dojran, the TOC was determined on bulk dry sediment as well as on bulk dry samples that were pre-treated to remove $CaCO_3$ (cf. chapter 6). It turns out that the two methods yield partly different results and that both records should be interpreted cautiously. For example, the minimum in $CaCO_3$-adjusted TOC content during the 8.2-cooling event is not evident in the TOC data measured on the bulk samples. The minimum in $CaCO_3$-adjusted TOC content also corresponds to a minimum in the $CaCO_3$ content, which implies a relative enrichment of OM in the bulk sample. The $CaCO_3$-adjusted TOC content can also be calculated from TIC and TOC data, or water content variations should be taken into account as they are frequently related to the amount of OM in the sediment (e.g. chapter 6, 7, and Wagner et al., 2009).

The organic material can be of allochthonous and autochthonous origin (Cohen, 2003). At Lake Dojran for example, the deposition of OM is mainly triggered by lake-internal productivity, and external processes such as the formation of denser vegetation in the catchment area or enhanced erosion processes (cf. chapter 6). The relative proportion of allochthonous and autochthonous OM in the sediment can be estimated by TOC/TN ratios. Aquatic vegetation commonly exhibits low ratios between 4 and 10, and terrestrial plant material is characterized by values >20 (summarized by Leng et al., 2005). Lacustrine deposits with TOC/TN ratios between 10 and 20 suggest a mixture of both aquatic and terrestrial OM (Leng et al., 2005). However, the TOC/TN ratio can be altered by early diagenetic processes with a selective degradation of N in algae-derived OM (Meyers and Lallier-Vergès, 1999; Cohen, 2003). The interpretation of TOC/TN ratios can be even more complex as anaerobic utilization of OM produces CO_2, CH_4, and NH_4^+ (Meyers and Lallier-Vergès, 1999). Whereas CO_2 and CH_4 escape from the sediment, NH_4^+ can be absorbed by clay minerals, resulting in TOC/TN ratios <6 (Meyers and Ishiwatari, 1995). In order to avoid misinterpretation of TOC/TN records, other indicators for the origin of OM input such as isotope data from OM should be considered. At Lake Dojran, variations in $\delta^{13}C_{org}$ only partly agree with the $\delta_{13}C_{carb}$ record which imply that total dissolved carbon cannot be the only carbon pool for organic material in the sediments (cf. chapter 6). Moreover, variations in the $\delta^{13}C_{org}$ correspond to the TOC/TN ratio (cf. chapter 6). This might indicate that decomposition processes have only a minor impact on the TOC/TN ratio, and that variations in the isotopic composition of OM in the sediment are mainly triggered by changes in the allochthonous OM supply (cf. chapter 6).

The biogeochemical composition of lake sediments can also yield information about mixing conditions during the past. At Lake Dorjan, the TOC/TS ratio was used as an indicator for the oxygen supply to the bottom water and surface sediments (cf. chapter 6). Low TOC/TS ratios imply reducing conditions caused by depleted-oxygen availability in the bottom water and surface sediments (cf. chapter 6). Under anoxic conditions, sulfur supplied to a lake in form of inorganic sulfates and organic S-bearing compounds can be converted to H_2S by sulfur-reducing bacteria (Cohen, 2003). Subsequently, the hy-

drogen sulfides may react with iron to Fe-disulfides, or they form chemical compounds with OM (Cohen, 2003). At Lake Dojran, oxygen availability in the bottom waters and surface sediments as reflected by TOC/TS mainly depend on the thermal stratification of the water column during summertime, as mixing is supposed to occur during winter (cf. chapter 6).

8.4 Chronostratigraphy

In order to interpret past sedimentary processes in the context of paleoenvironmental or -climatological variability, a robust chronology for the analyzed sediment sequence has to be established. Age points in younger sediment sequences are mostly derived from radiocarbon dating methods as this method is somehow limited to ages <50 000 cal yr BP (e.g. Cohen, 2003, Reimer et al., 2013). For example at Lake Dojran, an age model for core Co1260 was calculated by using radiocarbon ages and cross correlation points to other lacustrine sediment sequences in the region (cf. chapter 6). It is crucial for age modeling of a sediment sequence to carefully consider whether the dated age is really correct. Errors may occur due to re-deposition of the dated material by post-sedimentary processes or during core opening, by contamination, by laboratory errors, or by systematic errors in the dating technique such as reservoir effects on radiocarbon ages (cf. chapter 6 and Cohen, 2003). Between each dating point, the age can be calculated by using a linear interpolation, a linear regression, a polynomial regression of higher degree, a cubic spline or a smooth spline function (e.g. Cohen, 2003; Blaauw, 2010). Thereby, the decision which interpolation method describes best the age of a sediment sequence should be based on the available dating points, their quality, and, in particular, on stratigraphic information such as MWDs or hiatuses, too. For example at Lake Dojran, a polynomial function of degree three describes best the variations in the sedimentation rate between the reliable age points (cf. chapter 6). A linear interpolation between the dating points could have also been conducted. However, this implies that changes in the sedimentation rate would occur at the specific depths of the age points which were not confirmed by stratigraphic information.

In core Co1262 from Lake Ohrid (chapter 7), the distribution of the age points is more complex and a smooth spline function can be applied to the data (cf. Fig. 8.2). Similar to core Co1260, stratigraphic information about the sediment sequence of core Co1262 are crucial for the establishment of the age model as MWDs were excluded prior to the age calculations (cf. Fig. 8.2). As the studies on core Co1262 focus on the deposition of the upper 2 m thick MWD no age model was presented in chapter 7 since the age of the MWD could be well defined by the occurrence of the cryptotephralayer AD 512/472 below the MWD.

Cross correlation to other records from the lake itself and the Balkan Region was conducted for core Co1260 from Lake Dojran (cf. chapter 6), and for core Co1262 from Lake Ohrid, too (Fig. 8-3, for discussion of the correlation points see chapter 7). Cross correlation can improve the quality of an age model, in particular during short-term climatic events such as the 8.2 cooling event when enhanced clastic sedimentation and/or reduced precipitation of endogenic calcite may significantly alter the sedimentation rate (cf. Fig. 8-3). However, cross correlation hampers the interpretation about timing and duration of climatic events.

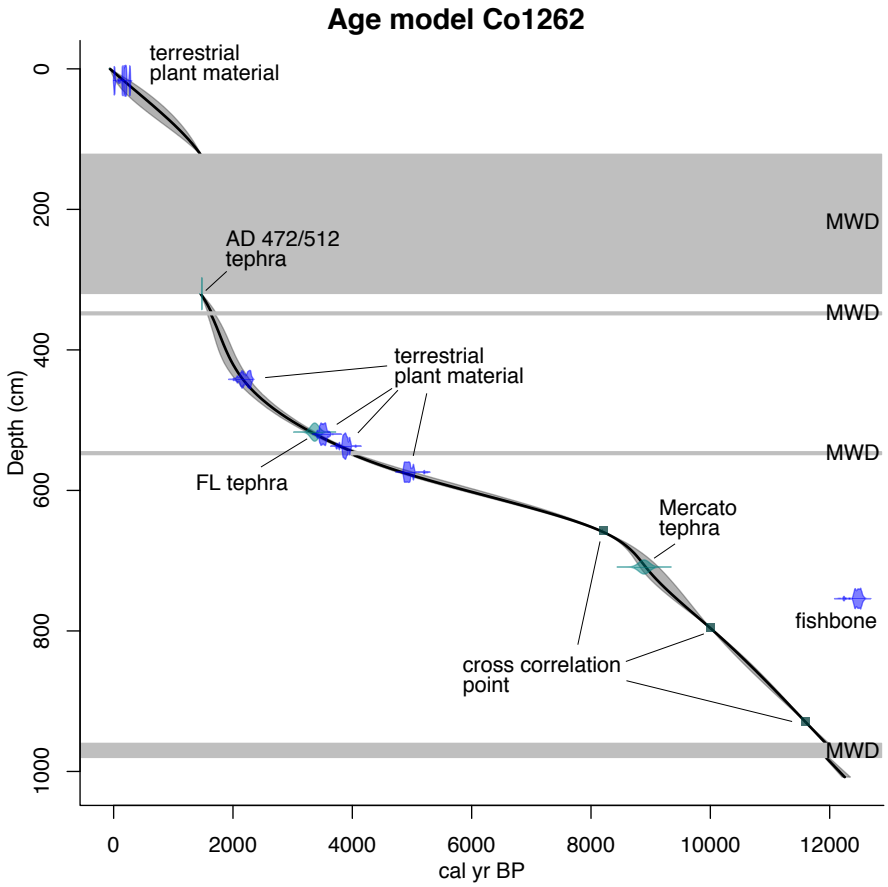

Figure 8.2: Age-depth model for Core 1262 from Lake Ohrid. Discussion of age points see chapter 7. Note that reservoir effects of up to 1 500 years were observed in surface sediments of Lake Ohrid (Wagner et al., 2008b) which imply that the radiocarbon age of the fishbone at 754 cm is likely too old. Purple: radiocarbon ages with most probable distribution of the ages ($2\,\sigma$ confidence level). Light green: tephra and cryptotephralayer including errors from the literature (cf. chapter 7). Dark green: cross correlation points to existing cores from the Balkan Region including other cores from Lake Ohrid. Grey bars: Observed MWDs in the sediment sequence that were not included into the age-depth modeling. The calibration of the radiocarbon ages bases on the IntCal 13.14C calibration curve (Reimer et al., 2013) and the age modeling with a smooth spline function (smoothing: 0.1) was conducted with the software Clam v.2.2. (Blaauw, 2010).

For the age model of core 5011-1 from Lake El'gygytgyn, major paleomagnetic reversals of the earth's magnetic field were used as chronological tie points (cf. chapter 4). Subsequently, stratigraphic parameters were synchronously tuned to Northern Hemisphere insolation variations and to the marine global benthic isotope stack LR04 (Lisiecki and Raymo, 2005). In chapter 3, a time series analysis was applied on grain-size data from core 5011-1 that were also used for tuning of the age model. Hence, the bulk spectrum of the grain-size data yields dominate oscillations on Milankovitch's eccentricity, obliquity and precession band (cf. chapter 3). In order to avoid this circular argument and to confirm Milankovitch's oscillation in the respective data, time series analyses could be performed on grain-size data versus composite depth. The resulting oscillation in meter could be recalculated into years by using the sedimentation rate derived from the tuned age model. However, conclusions about the relative dominance of the oscillations in the grain-size data during the Quaternary as shown by the evolutionary power spectrum were not affected by the circularity (cf. chapter 3).

8.5 Multivariate statistic methods

In chapters 2 and 3, the multivariate statistical methods Principal Component Analyses (PCA) and Redundancy Analyses (RDA) were applied to grain-size, geochemistry and mineralogical data in order to detect trends and dependencies in the data. PCA applied to geochemistry data from surface sediments from Lake El'gygytgyn yield three dominant clusters of elements (cf. chapter 2). The spatial distribution of these element clusters in the surface sediments, the inlet streams and the source rocks in the catchment yield crucial information about source rock effects, sediment supply and sediment redistribution in modern Lake El'gygytgyn. Subsequently, grain-size data were included and a RDA was carried out in order to detect grain-size effects on the elemental data which yield crucial information for the interpretation of downcore geochemical data (Wennrich et al., 2013).

In chapter 3, a PCA was applied to the volume frequency of each grain diameter measured by the laser particle analyzer in order to detect grain-size fractions that dominate the variations of the granumoleric data. Factor loadings of PC1 results yield the most important grain diameter (fractions) contributing to the grain-size distribution (cf. chapter 3, Fig. 4). Since variations in the grain-size data are primary attributed to environmental and climate variability in the catchment area, sample scores of PC1 were interpreted as climate dependent changes in the environmental settings at Lake El'gygytgyn (cf. chapter 3). High negative PC1 scores are associated to coarser sediments that were deposited during interglacial conditions. In contrast, high positive PC1 scores are linked to fine-grained deposits and to glacial climate conditions. Silt (medium silt) shows the weakest correlation to PC1 but high factor loading on PC2. Furthermore, silt does not show glacial-interglacial variability during the Quaternary (cf. chapter 3, Fig. 2,4). The strong correlation between PC2 and silt is likely not to be explained by geologic processes but rather by the horseshoe- (Kendall, 1971) or arch-effect (Gauch et al., 1977) which complicates the interpretation of PCA (chapter 2, Fig. 4). The artifact occurs if the analyzed data set is influenced by just one long gradient only (Swan, 1970; Gauch et al., 1977). Thereby, each variable (inhere: grain diameter) is successively replaced by the next one, resulting in an unimodal response to the gradient. However, if the data is affected by one gradient only, the variables should plot close to PC1 and do not show high correlations to further principal components (Gauch et al., 1977). According to Hill (1973), the arch is a result of the quadratic dependency of the second ordination axis on the first axis. Moreover, the PCA is a linear method by definition (Pearson, 1901; Hotelling, 1933) and variables with a large number of zero-values are interpreted to be similar. Thus, they yield low factor loadings on both PC1 and PC2 (Swan, 1970), such as also observed for very coarse and very fine grain diameters in Fig. 4 (chapter 3). These aspects result in two problems for the interpretation of the PCA. Firstly, a second gradient, reflected by PC2, is specified by the PCA although it is not present in the raw data. Secondly, the scaling of PC1 is disordered as the distance of samples and variables is not constant along this first component (Hill and Gauch, 1980). Hence, PCA analyses can be a useful tool to detect grain-size fractions that predominately alter the granumoleric distribution of the sediments, however, it requires a significant mathematic effort and the results should be validated by a comparison with the raw grain-size data. For example in chapter 3, this is confirmed by the strong correlation between mean grain-size and PC1 factor loadings ($R^2 = 0.93$).

9 Summary and Conclusion

Sedimentary processes in lakes El'gygytgyn (Far East Russian Artic), Dojran (Macedonia, Greece), and Ohrid (Macedonia, Albania) have been analyzed by using geophysical, sedimentary and statistical methods. The target of the individual studies presented in chapters 2 to 7 was to use the information about sedimentary processes for paleoenvironmental and paleoclimatological reconstructions. Conclusions from the obtained data drawn for the paleoenvironmental evolution of the lakes are presented in the individual chapters (chapters 2 to 7). In chapter 8, an evaluation of the used data sets and scientific approaches was conducted in order to discuss their potentials and limits.

Spatially distributed surface samples from lake sediments combined with samples from inlet streams and source rocks can provide crucial insights into modern deposition processes in a lake system. Information about allochthonous and autochthonous sediment supply as well as about redistribution processes in the lake improves the understanding of internal and external environmental factors that alter the sediment composition. This connection between these internal and external environmental settings and sedimentary processes is the key for paleoenvironmental and -climatological reconstruction. A profound understanding of modern conditions can improve the understanding of the history of a lake.

Hydro-acoustic surveys are a cost effective and rapid method and can yield crucial information about the sediment architecture. The obtained data can be very useful to detect horizontally bedded and undisturbed sediment sequences as potential coring locations. Moreover, hydro-acoustic data provides insights into the spatial distribution and morphostructure of the analyzed deposits indicating for example lake-level fluctuations, rearrangements of the bathymetry, erosional processes, or Mass Wasting Deposits (MWDs). However, hydro-acoustic data usually lacks an independent chronology and the vertical resolution is limited.

In order to obtain detailed information about the development and history of a lake, a sediment core should be analyzed. Basic sedimentary properties, such as grain-size as indicator for the transport energy, or the color and water content which are frequently linked to variations in the organic matter content, can already provide a first overview about the sedimentary processes and environmental settings during the deposition. More detailed information about clastic, organic and nutrient sediment supply as well as about in-lake productivity can be derived from inorganic and organic geochemistry data. However, particularly inorganic geochemistry data derived from XRF-scanning is frequently affected by mutual dilution which complicates a paleoenvironmental or paleoclimatological interpretation.

A robust chronology can be established by using tephrostratigraphic information, radiocarbon dating for younger sediments, and for example paleomagnetic tie points for older deposits. Age models can be improved by cross correlation or wiggle matching. However, this can hamper a subsequent interpretation about the duration or oscillations of climatic events. Age-depth model calculations shall be conducted considering probable systematic or laboratory errors in the dating method and stratigraphic information, such as hiatuses, MWDs, or changes in the sedimentation rate.

Statistic methods, such as Time-Series Analyses, Principal Component Analyses (PCA) or Redundancy Analyses (RDA) can be a helpful tool to detect patterns and trends in large data sets. However, results of such mathematical approaches should be evaluated by a comparison with the raw data. It was demonstrated that statistic calculations can provide results or mathematic artifacts that are not present in the original data. For example, PCA analyses on grain-size data imply the dependency of the data on a second gradient that is not present in the data. Moreover, the mathematic approach itself can hamper the interpretation of the results, for example as shown for core 5011-1 from Lake El'gygytgyn, where a tuned age model was used for Time Series Analysis.

In summary, various data sets and scientific or mathematical approaches can be used to study sedimentary processes in lakes as a basis for subsequent paleoenvironmental and paleoclimatological interpretations. It has been demonstrated that each data set and mathematic approach has its own limits and potentials. Thus, in dependency on the scientific question and capabilities, a selection of the proposed methods should be conducted.

10 References

Abbott, M. B., Finney, B. P., Edwards, M. E., and Kelts, K. R.: Lake-Level Reconstruction and Paleohydrology of Birch Lake, Central Alaska, Based on Seismic Reflection Profiles and Core Transects, Quaternary Research, 53, 154-166, 10.1006/qres.1999.2112, 2000.

ACIA: Impacts of a Warming Arctic - Arctic Climate Impact Assessment, Cambridge and New York, Cambridge University Press, 144 pp., 2004.

Aufgebauer, A., Panagiotopoulos, K., Wagner, B., Schäbitz, F., Viehberg, F. A., Vogel, H., Zanchetta, G., Sulpizio, R., Leng, M. J., and Damaschke, M.: Climate and environmental change in the Balkans over the last 17 ka recorded in sediments from Lake Prespa (Albania/F.Y.R. of Macedonia/Greece), Quaternary International, 274, 122-135, 10.1016/j.quaint.2012.02.015, 2012.

Axford, Y., Briner, J. P., Cooke, C. A., Francis, D. R., Michelutti, N., Miller, G. H., Smol, J. P., Thomas, E. K., Wilson, C. R., and Wolfe, A. P.: Recent changes in a remote Arctic lake are unique within the past 200,000 years, Proceedings of the National Academy of Sciences, 106, 18443-18446, 10.1073/pnas.0907094106, 2009.

Backman, J., Moran, K., McInroy, D., and IODP Expedition 302 Scientists: Arctic Coring Expedition (ACEX): Paleooceanographic and tectonic evolution of the central Artic Ocean, IODP Preliminary Reports, 302, 2005.

Blaauw, M.: Methods and code for 'classical' age-modelling of radiocarbon sequences, Quaternary Geochronology, 5, 512-518, 10.1016/j.quageo.2010.01.002, 2010.

Bouma, A. H.: Sedimentology of some Flysch deposits, a graphic approach to facies interpretation, Elsevier, Amsterdam, 1962.

Brigham-Grette, J., Melles, M., and Minyuk, P.: Overview and significance of a 250 ka paleoclimate record from El'gygytgyn Crater Lake, NE Russia, Journal of Paleolimnology, 37, 1-16, 2007.

Brigham-Grette, J., Melles, M., Minyuk, P., Andreev, A., Tarasov, P., DeConto, R., Koenig, S., Nowaczyk, N., Wennrich, V., Rosén, P., Haltia, E., Cook, T., Gebhardt, C., Meyer-Jacob, C., Snyder, J., and Herzschuh, U.: Pliocene Warmth, Polar Amplification, and Stepped Pleistocene Cooling Recorded in NE Arctic Russia, Science, 340, 1421-1427, 10.1126/science.1233137, 2013.

Caron, B., Sulpizio, R., Zanchetta, G., Siani, G., and Santacroce, R.: The Late Holocene to Pleistocene tephrostratigraphic record of Lake Ohrid (Albania), Comptes Rendus Geoscience, 342, 453-466, 10.1016/j.crte.2010.03.007, 2010.

Cohen, A. S.: Paleolimnology: The History and Evolution of Lake Systems, Oxford University Press, Oxford, 2003.

Cremer, H. and Wagner, B.: The diatom flora in the ultra-oligotrophic Lake EI'gygytgyn, Chukotka, Polar Biology, 26, 105-114, 10.1007/s00300-002-0445-0, 2003.

Croudace, I. W., Rindby, A., and Rothwell, R. G.: ITRAX: description and evaluation of a new multi-function X-ray core scanner, New Techniques in Sediment Core Analysis, 267, 51-63, 2006.

Cvijic, J.: L'ancien Lac Egéen, Annales de Géographie, 20, 233-259, 1911.

Damaschke, M., Sulpizio, R., Zanchetta, G., Wagner, B., Böhm, A., Nowaczyk, N., Rethemeyer, J., and Hilgers, A.: Tephrostratigraphic studies on a sediment core from Lake Prespa in the Balkans, Climate of the Past, 9, 267-287, 10.5194/cp-9-267-2013, 2013.

Dietz, R. S. and McHone, J. F.: El'gygytgyn: Probably the world largest meteorite crater, Geology, 4, 391-392, 1977.

Fedorov, G. and Kupolov, A.: Gas Mercury Survey in the El'gygytgyn Crater, in: The Expedition El'gygytgyn Lake 2003 (Siberian Arctic), edited by: Melles, M., Minyuk, P., Brigham-Grette, J., and Juschus, O., Reports on polar and marine research, AWI, Bremerhaven, 69-70, 2005.

Fedorov, G., Nolan, M., Brigham-Grette, J., Bolshiyanov, D., Schwamborn, G., and Juschus, O.: Preliminary estimation of Lake El'gygytgyn water balance and sediment income, Climate of the Past, 9, 1455-1465, 10.5194/cp-9-1455-2013, 2013.

Gauch, H. G., Whittaker, R. H., and Wentworth, T. R.: A comparative study of reciprocal averaging and other ordination techniques, Journal of Ecology, 65, 157-174, 1977.

Giorgi, F. and Lionello, P.: Climate change projections for the Mediterranean region, Global and Planetary Change, 63, 90-104, 10.1016/j.gloplacha.2007.09.005, 2008.

Glushkova, O. Y. and Smirnov, V. N.: Pliocene to Holocene geomorphic evolution and paleogeography of the El'gygytgyn Lake region, NE Russia, Journal of Paleolimnology, 37, 37-47, 10.1007/s10933-006-9021-x, 2007.

Griffiths, H. I., Reed, J. M., Leng, M. J., Ryan, S., and Petkovski, S.: The recent palaeoecology and conservation status of Balkan Lake Dojran, Biological Conservation, 104, 35-49, 2002.

Gurov, E. P., Gurova, E. P., and Rakitskaia, R. B.: Stishovite and coesite in shock-metamorphosed rocks of the El'gygytgyn crater in Chukotka, Akademiia Nauk SSSR Doklady, 248, 213-216, 1979.

Hill, M. O.: Reciprocal Averaging: An Eigenvector Method of Ordination, Journal of Ecology, 61, 237-249, 1973.

Hill, M. O. and Gauch, H. G.: Detrended correspondence analysis: an improved ordination technique, Vegetation, 42, 47-58, 1980.

Hoffmann, N., Reicherter, K., Fernàndez-Steeger, T., and Grützner, C.: Evolution of ancient Lake Ohrid: a tectonic perspective, Biogeosciences, 7, 3377-3386, 10.5194/bg-7-3377-2010, 2010.

Hotelling, H.: Analysis of a complex statistical variables into principal Components, Journal of Education and Psychology, 24, 417-441, 498-520, 1933.

Hunt, D. and Tucker, M. E.: Stranded parasequences and the forced regressive wedge systems tract: deposition during base-level fall, Sedimentary Geology, 81, 1-9, 10.1016/0037-0738(92)90052-S, 1992.

Jansen, J. H. F., Van der Gaast, S. J., Koster, B., and Vaars, A. J.: CORTEX, a shipboard XRF-scanner for element analyses in split sediment cores, Marine Geology, 151, 143-153, 10.1016/S0025-3227(98)00074-7, 1998.

Kendall, D. G.: Seriation from abundance matrices, in: Mathematics in the archeological and history siences, edited by: Hodson, F. R., Kendall, D. G., and Tautu, P., Edinburgh University Press, 215-252, 1971.

Layer, P. W.: Argon-40/argon-39 age of the El'gygytgyn impact event, Chukotka, Russia, Meteoritics & Planetary Science, 35, 591-599, 2000.

Leng, M. J., Metcalfe, S., and Davies, S.: Investigating Late Holocene Climate Variability in Central Mexico using Carbon Isotope Ratios in Organic Materials and Oxygen Isotope Ratios from Diatom Silica within Lacustrine Sediments, Journal of Paleolimnology, 34, 413-431, 10.1007/s10933-005-6748-8, 2005.

Leng, M. J., Baneschi, I., Zanchetta, G., Jex, C. N., Wagner, B., and Vogel, H.: Late Quaternary palaeoenvironmental reconstruction from Lakes Ohrid and Prespa (Macedonia/Albania border) using stable isotopes, Biogeosciences, 7, 3109-3122, 10.5194/bg-7-3109-2010, 2010.

Lindhorst, K., Krastel, S., Schwenk, T., Kurschat, S., Daut, G., Wessels, M., and Wagner, B.: Seismic investigations of ancient Lake Ohrid (Macedonia/Albania): a pre-site survey for the SCOPSCO ICDP-drilling campaign, EGU General Assembly, Vienna, Austria, 19-24 April 2009, 2009.

Lindhorst, K., Vogel, H., Krastel, S., Wagner, B., Hilgers, A., Zander, A., Schwenk, T., Wessels, M., and Daut, G.: Stratigraphic analysis of lake level fluctuations in Lake Ohrid: an integration of high resolution hydro-acoustic data and sediment cores, Biogeosciences, 7, 3531-3548, 10.5194/bg-7-3531-2010, 2010.

Lindhorst, K., Gruen, M., Krastel, S., and Schwenk, T.: Hydroacoustic Analysis of Mass Wasting Deposits in Lake Ohrid (FYR Macedonia/Albania), in: Submarine Mass Movements and Their Consequences, Springer Netherlands, 245-253, 2012.

Lindhorst, K., Krastel, S., Reicherter, K., Stripp, M., Wagner, B., and Schwenk, T.: Sedimentary and tectonic evolution of Lake Ohrid (Macedonia/Albania), Basin Research, in press.

Lisiecki, L. E. and Raymo, M. E.: A Pliocene-Pleistocene stack of 57 globally distributed benthic δ^{18}O records, Paleoceanography, 20, PA1003, 10.1029/2004pa001071, 2005.

Loizeau, J.-L., Arbouille, D., Santiago, S., and Vernet, J.-P.: Evaluation of a wide range laser diffraction grain-size analyzer for use with sediments, Sedimentology, 41, 353-361, 1994.

Magny, M., de Beaulieu, J.-L., Drescher-Schneider, R., Vannière, B., Walter-Simonnet, A.-V., Miras, Y., Millet, L., Bossuet, G., Peyron, O., Brugiapaglia, E., and Leroux, A.: Holocene climate changes in the central Mediterranean as recorded by lake-level fluctuations at Lake Accesa (Tuscany, Italy), Quaternary Science Reviews, 26, 1736-1758, 10.1016/j.quascirev.2007.04.014, 2007.

Manley, R., Spirovska, M., and Andovska, S.: Water balance model of Lake Dojran, BALWOIS, 2008.

Matzinger, A., Jordanoski, M., Veljanoska-Sarafiloska, E., Sturm, M., Müller, B., and Wüest, A.: Is Lake Prespa Jeopardizing the Ecosystem of Ancient Lake Ohrid?, Hydrobiologia, 553, 89-109, 10.1007/s10750-005-6427-9, 2006.

Matzinger, A., Schmid, M., Veljanoska-Sarafiloska, E., Patceva, S., Guseska, D., Wagner, B., Müller, B., Sturm, M., and Wüest, A.: Eutrophication of ancient Lake Ohrid: Global warming amplifies detrimental effects of increased nutrient inputs, Limnology and Oceanography, 52, 338-353, 2007.

Melles, M., Brigham-Grette, J., Glushkova, O. Y., Minyuk, P. S., Nowaczyk, N. R., and Hubberten, H. W.: Sedimentary geochemistry of core PG1351 from Lake El'gygytgyn - a sensitive record of climate variability in the East Siberian Arctic during the past three glacial-interglacial cycles, Journal of Paleolimnology, 37, 89-104, 10.1007/s10933-006-9025-6, 2007.

Melles, M., Brigham-Grette, J., Minyuk, P., Koeberl, C., Andreev, A., Cook, T., Fedorov, G., Gebhardt, C., Haltia-Hovi, E., Kukkonen, M., Nowaczyk, N., Schwamborn, G., Wennrich, V., and and the El'gygytgyn Scientific Party: The Lake El'gygytgyn Scientific Drilling Project - Conquering Arctic Challenges through Continental Drilling, Scientific Drill., 11, 29-40, 2011.

Melles, M., Brigham-Grette, J., Minyuk, P., Nowaczyk, N., Wennrich, V., Deconto, R., Andersen, P., Andreev, A. A., Coletti, A., Cook, T., Haltia-Hovi, E., Kukkonen, M., Lozhkin, A., Rosén, P., Tarasov, P., Vogel, H., and Wagner, B.: 2.8 Million Years of Artic Climate Change from Lake El'gygytgyn, NE Russia, Science, 337, 315-320, 10.1126/science.1222135, 2012.

Meyers, P. and Lallier-Vergés, E.: Lacustrine Sedimentary Organic Matter Records of Late Quaternary Paleoclimates, Journal of Paleolimnology, 21, 345-372, 10.1023/A:1008073732192, 1999.

Meyers, P. A. and Ishiwatari, R.: Organic matter accumulation records in lake sediments, in: Physics and Chemistry of Lakes., edited by: Lerman, A., Imboden, D. M., and Gat, J. R., pringereVerlag Berlin, Heidelberg, New York, 279-328., 1995.

Moran, K., Backman, J., Brinkhuis, H., Clemens, S. C., Cronin, T., Dickens, G. R., Eynaud, F. d. r., Gattacceca, J. r. m., Jakobsson, M., Jordan, R. W., Kaminski, M., King, J., Koc, N., Krylov, A., Martinez, N., Matthiessen, J., McInroy, D., Moore, T. C., Onodera, J., O'Regan, M., Pälike, H., Rea, B., Rio, D., Sakamoto, T., Smith, D. C., Stein, R., St John, K., Suto, I., Suzuki, N., Takahashi, K., Watanabe, M., Yamamoto, M., Farrell, J., Frank, M., Kubik, P., Jokat, W., and Kristoffersen, Y.: The Cenozoic palaeoenvironment of the Arctic Ocean, Nature, 441, 601-605, 2006.

Mottaghy, D., Schwamborn, G., and Rath, V.: Past climate changes and permafrost depth at the Lake El'gygytgyn site: implications from data and thermal modeling, Climate of the Past, 9, 119-133, 10.5194/cp-9-119-2013, 2013.

Müller, J., Oberhänsli, H., Melles, M., Schwab, M., Rachold, V., and Hubberten, H. W.: Late Pliocene sedimentation in Lake Baikal: implications for climatic and tectonic change in SE Siberia, Palaeogeography, Palaeoclimatology, Palaeoecology, 174, 305-326, 10.1016/S0031-0182(01)00320-0, 2001.

NGRIP-members: High-resolution record of Northern Hemisphere climate extending into the last interglacial period, Nature, 431, 147-151, 10.1038/nature02805, 2004.

Niessen, F., Gebhardt, A. C., Kopsch, C., and Wagner, B.: Seismic investigation of the El'gygytgyn impact crater lake (Central Chukotka, NE Siberia): preliminary results, Journal of Paleolimnology, 37, 49-63, 10.1007/s10933-006-9022-9, 2007.

Nolan, M. and Brigham-Grette, J.: Basic hydrology, limnology, and meteorology of modern Lake El'gygytgyn, Siberia, Journal of Paleolimnology, 37, 17-35, 10.1007/s10933-006-9020-y, 2007.

Nolan, M., Cassano, E. N., and Cassano, J. J.: Synoptic climatology and recent climate trends at Lake El'gygytgyn, Climate of the Past, 9, 1271-1286, 10.5194/cp-9-1271-2013, 2013.

Pearson, K.: On lines and planes of closest fit to system of points and space, Philosophical Magazine, 6, 559-572, 1901.

Pienitz, R., Melles, M., and Zolitschka, B.: Results of recent sediment drilling activities in deep crater lakes, Pages News, 3, 117-118, 2009.

Reimer, P. J., Bard, E., Bayliss, A., Beck, J. W., Blackwell, P. G., Bronk Ramsey, C., Buck, C. E., Cheng, H., Edwards, R. L., Friedrich, M., Grootes, P. M., Guilderson, T. P., Haflidason, H., Hajdas, I., Hatté, C., Heaton, T. J., Hoffmann, D. L., Hogg, A. G., Hughen, K. A., Kaiser, K. F., Kromer, B., Manning, S. W., Niu, M., Reimer, R. W., Richards, D. A., Scott, E. M., Southon, J. R., Staff, R. A., Turney, C. S. M., and van der Plicht, J.: IntCal13 and Marine13 Radiocarbon Age Calibration Curves 0-50,000 Years cal BP, Radiocarbon, 55, 2013.

Rothwell, R. G., Hoogakker, B., Thomson, J., Croudace, I. W., and Frenz, M.: Turbidite emplacement on the southern Balearic Abyssal Plain (western Mediterranean Sea) during Marine Isotope Stages 1-3: an application of ITRAX XRF scanning of sediment cores to lithostratigraphic analysis, Geological Society, London, Special Publications, 267, 79-98, 10.1144/gsl.sp.2006.267.01.06, 2006.

Sauerbrey, M. A., Juschus, O., Gebhardt, A. C., Wennrich, V., Nowaczyk, N. R., and Melles, M.: Mass movement deposits in the 3.6 Ma sediment record of Lake El'gygytgyn, Far East Russian Arctic, Climate of the Past, 9, 1949-1967, 10.5194/cp-9-1949-2013, 2013.

Serreze, M. and Francis, J.: The Artic Amplification Debate, Climatic Change, 76, 241-264, 2006.

Sotiria, K. and Petkovski, S.: Lake Doiran - An overview of the current situation, Greek Biotope/Wetland Centre (EKBY), Society for the Investigation and Conservation of Biodiversity and the Sustainable Development of Natural Ecosystems (BIOECO), Thermi, 117, 2004.

Sprenk, D., Weber, M. E., Kuhn, G., Rosén, P., Frank, M., Molina-Kescher, M., Liebetrau, V., and Röhling, H. G.: Southern Ocean bioproductivity during the last glacial cycle - new detection method and decadal-scale insight from the Scotia Sea, Geological Society, London, Special Publications, 381, 10.1144/sp381.17, 2013.

Stankovic, S.: Sur les particularités limnologiques des lacs égéens, Verhandlungen der internationalen Vereinigung für theoretische und angewandte Limnologie, 5, 138-146, 1931.

Stankovic, S.: The Balkan Lake Ohrid and its Living World, Monographiae Biologicae, Dr. W. Junk, Amsterdam, 1960.

Stojanov, R. and Micevski, E.: Geology of Lake Doiran and its surrounding, Contributions of the Macedonian Academy of Sciences and Arts, Section of Biological and Medical Sciences, 10, 37-52 (in Macedonian with English abstract), 1989.

Sulpizio, R., Zanchetta, G., D'Orazio, M., Vogel, H., and Wagner, B.: Tephrostratigraphy and tephrochronology of lakes Ohrid and Prespa, Balkans, Biogeosciences, 7, 3273-3288, 10.5194/bg-7-3273-2010, 2010.

Swan, J. M. A.: An Examination of some ordination problems by use of simulated vegetation data, Ecology, 51, 89-102, 1970.

Thiede, J., Winkler, A., Wolf-Welling, T., Eldholm, O., Myhre, A., Baumann, K.-H., Henrich, R., and Stein, R.: Late Cenozoic history of the Polar North Atlantic: results from ocean drilling, Quaternary Science Reviews, 17, 185-208, 1998.

Tjallingii, R., Röhl, U., Kölling, M., and Bickert, T.: Influence of the water content on X-ray fluorescence core-scanning measurements in soft marine sediments, Geochemistry, Geophysics, Geosystems, 8, Q02004, 10.1029/2006GC001393, 2007.

Vogel, H., Wessels, M., Albrecht, C., Stich, H. B., and Wagner, B.: Spatial variability of recent sedimentation in Lake Ohrid (Albania/Macedonia), Biogeosciences, 7, 3333-3342, 10.5194/bg-7-3333-2010, 2010a.

Vogel, H., Wagner, B., Zanchetta, G., Sulpizio, R., and Rosén, P.: A paleoclimate record with tephrochronological age control for the last glacial-interglacial cycle from Lake Ohrid, Albania and Macedonia, Journal of Paleolimnology, 44, 295-310, 10.1007/s10933-009-9404-x, 2010b.

Vogel, H., Zanchetta, G., Sulpizio, R., Wagner, B., and Nowaczyk, N.: A tephrostratigraphic record for the last glacial-interglacial cycle from Lake Ohrid, Albania and Macedonia, Journal of Quaternary Science, 25, 320-338, 10.1002/jqs.1311, 2010c.

Vologina, E., Granin, N., Francus, P., Lomonosova, T., Kalashinkova, I., and Granina, L.: Ice transport of sand-silt material in southern lake Baikal, Russian Geology and Geophysics, 46, 186-192, 2005.

Wagner, B., Sulpizio, R., Zanchetta, G., Wulf, S., Wessels, M., Daut, G., and Nowaczyk, N.: The last 40 ka tephrostratigraphic record of Lake Ohrid, Albania and Macedonia: a very distal archive for ash dispersal from Italian volcanoes, Journal of Volcanology and Geothermal Research, 177, 71-80, 10.1016/j.jvolgeores.2007.08.018, 2008a.

Wagner, B., Reicherter, K., Daut, G., Wessels, M., Matzinger, A., Schwalb, A., Spirkovski, Z., and Sanxhaku, M.: The potential of Lake Ohrid for long-term palaeoenvironmental reconstructions, Palaeogeography, Palaeoclimatology, Palaeoecology, 259, 341-356, 10.1016/j.palaeo.2007.10.015, 2008b.

Wagner, B., Lotter, A. F., Nowaczyk, N., Reed, J. M., Schwalb, A., Sulpizio, R., Valsecchi, V., Wessels, M., and Zanchetta, G.: A 40,000-year record of environmental change from ancient Lake Ohrid (Albania and Macedonia), Journal of Paleolimnology, 41, 407-430, 10.1007/s10933-008-9234-2, 2009.

Wagner, B., Vogel, H., Zanchetta, G., and Sulpizio, R.: Environmental change within the Balkan region during the past ca. 50 ka recorded in the sediments from lakes Prespa and Ohrid, Biogeosciences, 7, 3187-3198, 10.5194/bg-7-3187-2010, 2010.

Wagner, B. and Wilke, T.: Preface "Evolutionary and geological history of the Balkan lakes Ohrid and Prespa", Biogeosciences, 8, 995-998, 10.5194/bg-8-995-2011, 2011.

Wagner, B., Aufgebauer, A., Vogel, H., Zanchetta, G., Sulpizio, R., and Damaschke, M.: Late Pleistocene and Holocene contourite drift in Lake Prespa (Albania/F.Y.R. of Macedonia/Greece), Quaternary International, 274, 112-121, 10.1016/j.quaint.2012.02.016, 2012.

Wang, W., Wang, D., and Yin, C.: A Field Study on the Hydrochemistry of Land/Inland Water Ecotones with Reed Domination, Acta hydrochimica et hydrobiologica, 30, 117-127, 2002.

Watzin, M., Puka, V., and Naumoski, T.: Lake Ohrid and its Watershed. State of the Environment Report. Lake Ohrid Conservation Project, Tirana, Albania and Ohrid, Macedonia, 2002.

Wennrich, V., Minyuk, P. S., Borkhodoev, V. Y., Francke, A., Ritter, B., Nowaczyk, N., Sauerbrey, M. A., Brigham-Grette, J., and Melles, M.: Pliocene to Pleistocene climate and environmental history of Lake El'gygytgyn, Far East Russian Arctic, based on high-resolution inorganic geochemistry data, Climate of the Past Discussion., 9, 5899-5940, 10.5194/cpd-9-5899-2013, 2013.

Wunderlich, J. and Müller, S.: High-resolution sub-bottom profiling using parametric acoustics, International Ocean Systems, 7, 6-11, 2003.

Zacharias, I., Bertachas, I., Skoulikidis, N., and Koussouris, T.: Greek Lakes: Limnological overview, Lakes & Reservoirs: Research & Management, 7, 55-62, 10.1046/j.1440-1770.2002.00171.x, 2002.

Zech, R., Huang, Y., Zech, M., Tarozo, R., and Zech, W.: High carbon sequestration in Siberian permafrost loess-paleosols during glacials, Climate of the Past, 7, 501-509, 10.5194/cp-7-501-2011, 2011.

11 Paper Contributions

Francke, A., Wagner, B., Leng, M. J., and Rethemeyer, J.: A Late Glacial to Holocene record of environmental change from Lake Dojran (Macedonia, Greece), Climate of the Past, 9, 481-498, 10.5194/cp-9-481-2013, 2013

A. Francke participated in the fieldwork and conducted the laboratory work for the geochemical and sedimentary data at the University of Cologne. The isotope analyses were carried out by A. Francke at the NERC Isotope Geochemistry Laboratory at the British Geological Survey (BGS) in Nottingham under the guidance of M. Leng. A. Francke wrote the text with contributions from all co-authors. Overall, A. Francke contributed 80% to the paper.

Francke, A., Wennrich, V., Sauerbrey, M., Juschus, O., Melles, M., and Brigham-Grette, J.: Multivariate statistic and time series analyses of grain-size data in quaternary sediments of Lake El'gygytgyn, NE Russia, Climate of the Past, 9, 2459-2470, 10.5194/cp-9-2459-2013, 2013.

A. Francke evaluated and conducted the pre-treatment steps for the grain-size analyses and carried out the grain-size measurements with the assistance of students. The data processing and the statistic calculations were done by A. Francke. The text was written by A. Francke with contributions from V. Wennrich, M. Sauerbrey and M. Melles. Overall, A. Francke contributed 80% to the paper.

Wagner, B., **Francke, A.**, Sulpizio, R., Zanchetta, G., Lindhorst, K., Krastel, S., Vogel, H., Rethemeyer, J., Daut, G., Grazhdani, A., Lushaj, B., and Trajanovski, S.: Possible earthquake trigger for 6^{th} century mass wasting deposit at Lake Ohrid (Macedonia/Albania), Climate of the Past, 8, 2069-2078, 10.5194/cp-8-2069-2012, 2012.

A. Francke participated in the fieldwork at the lake and conducted the sedimentary and biogeochemical laboratory work. The text was written by B. Wagner. A. Francke provided comments on the text and Figures 4 and 5. Overall, A. Francke contributed 50% to the paper.

Wennrich, V., **Francke, A.**, Dehnert, A., Juschus, O., Leipe, T., Vogt, C., Brigham-Grette, J., Minyuk, P. S., Melles, M., and El'gygytgyn Science, P.: Modern sedimentation patterns in Lake El'gygytgyn, NE Russia, derived from surface sediment and inlet streams samples, Climate of the Past, 9, 135-148, 10.5194/cp-9-135-2013, 2013.

A. Francke conducted the grain-size analyses of the surface sediments and carried out the data processing and statistical calculations. A first draft for the text as well as Figures 2, 4, 5 and 6 were provided by A. Francke. The published text was written by V. Wennrich. Overall, A. Francke contributed 60% to the paper.

Gebhardt, A. C., **Francke, A.**, Kück, J., Sauerbrey, M., Niessen, F., Wennrich, V., and Melles, M.: Petrophysical characterization of the lacustrine sediment succession drilled in Lake El'gygytgyn, Far East Russian Arctic, Climate of the Past, 9, 1933-1947, 10.5194/cp-9-1933-2013, 2013.

The paper and preliminary work partly bases on grain-size data that was provided by A. Francke. In addition, A. Francke participated on the scientific discussion about the publication and contributed with 15% to the paper.

Nowaczyk, N., Haltia-Hovi, E., Ulbricht, D., Wennrich, R., Sauerbrey, M., Rosén, P., Vogel, H., **Francke, A.**, Meyer-Jacob, C., Andreev, A. A., and Lozhkin, A.: Chronolgy of Lake El'gygytgyn sediments - a combined magnetostratigraphic, palaeoclimatic and orbital tuning study based on multi-parameter analyses, Climate of the Past, 9, 2413-2432, doi:10.5194/cp-9-2413-2013, 2013.

The age model of ICDP core 5011-1 from Lake El'gygytgyn bases on paleomagnetic dating and tuning of several proxies to orbital parameters. A. Francke conducted the analyses, data processing and calculation of the Principal Component Analyses of the grain-size data. Overall, A. Francke contributed with 10% to the paper.

12 Erklärung

Ich versichere, dass ich die von mir vorgelegte Dissertation selbständig angefertigt, die benutzten Quellen und Hilfsmittel vollständig angegeben und die Stellen der Arbeit - einschließlich Tabellen, Karten und Abbildungen -, die anderen Werken im Wortlaut oder dem Sinn nach entnommen sind, in jedem Einzelfall als Entlehnung kenntlich gemacht habe; dass diese Dissertation noch keiner anderen Fakultät oder Universität zur Prüfung vorgelegen hat; dass sie - abgesehen von unten angegebenen Teilpublikationen - noch nicht veröffentlicht worden ist, sowie, dass ich eine solche Veröffentlichung vor Abschluss des Promotionsverfahrens nicht vornehmen werde. Die Bestimmungen der Promotionsordnung sind mir bekannt.

Die von mir vorgelegte Dissertation ist von PD Dr. Bernd Wagner betreut worden.

Folgende Teilpublikationen liegen vor:

Francke, A., Wagner, B., Leng, M. J., and Rethemeyer, J. (2013): A Late Glacial to Holocene record of environmental change from Lake Dojran (Macedonia, Greece), Climate of the Past, 9, 481-498, 10.5194/cp-9-481-2013,2013.

Francke, A., Wennrich, V., Sauerbrey, M., Juschus, O., Melles, M., and Brigham-Grette, J.: Multivariate statistic and time series analyses of grain-size data in quaternary sediments of Lake El'gygytgyn, NE Russia, Climate of the Past, 9, 2459-2470, 10.5194/cp-9-2459-2013, 2013.

Wagner, B., **Francke, A.**, Sulpizio, R., Zanchetta, G., Lindhorst, K., Krastel, S., Vogel, H., Rethemeyer, J., Daut, G., Grazhdani, A., Lushaj, B., and Trajanovski, S.: Possible earthquake trigger for 6^{th} century mass wasting deposit at Lake Ohrid (Macedonia/Albania), Climate of the Past, 8, 2069-2078, 10.5194/cp-8-2069-2012, 2012.

Wennrich, V., **Francke, A.**, Dehnert, A., Juschus, O., Leipe, T., Vogt, C., Brigham-Grette, J., Minyuk, P. S., Melles, M., and El'gygytgyn Science, P.: Modern sedimentation patterns in Lake El'gygytgyn, NE Russia, derived from surface sediment and inlet streams samples, Climate of the Past, 9, 135-148, 10.5194/cp-9-135-2013, 2013.

Gebhardt, A. C., **Francke, A.**, Kück, J., Sauerbrey, M., Niessen, F., Wennrich, V., and Melles, M.: Petrophysical characterization of the lacustrine sediment succession drilled in Lake El'gygytgyn, Far East Russian Arctic, Climate of the Past, 9, 1933-1947, 10.5194/cp-9-1933-2013, 2013.

Nowaczyk, N., Haltia-Hovi, E., Ulbricht, D., Wennrich, R., Sauerbrey, M., Rosén, P., Vogel, H., **Francke, A.,** Meyer-Jacob, C., Andreev, A. A., and Lozhkin, A.: Chronolgy of Lake El'gygytgyn sediments - a combined magnetostratigraphic, palaeoclimatic and orbital tuning study based on multi-parameter analyses, Climate of the Past, 9, 2413-2432, doi:10.5194/cp-9-2413-2013, 2013.

Köln, den 10.02.14